Characterisation of Fission Yeast DNA Replication Origins

Thesis presented for the degree of

Doctor of Philosophy

University of London

by Christian Heichinger

Cell Cycle Laboratory

Cancer Research UK

44 Lincoln's Inn Fields, London

Supervisor: Dr. Paul Nurse

September, 2005

UMI Number: U592046

All rights reserved

INFORMATION TO ALL USERS
The quality of this reproduction is dependent upon the quality of the copy submitted.

In the unlikely event that the author did not send a complete manuscript
and there are missing pages, these will be noted. Also, if material had to be removed,
a note will indicate the deletion.

UMI U592046
Published by ProQuest LLC 2013. Copyright in the Dissertation held by the Author.
Microform Edition © ProQuest LLC.
All rights reserved. This work is protected against
unauthorized copying under Title 17, United States Code.

ProQuest LLC
789 East Eisenhower Parkway
P.O. Box 1346
Ann Arbor, MI 48106-1346

Abstract

In many eukaryotic organisms the chromosomal origins of DNA replication (ORIs) are not characterised by a clearly defined consensus sequence. In this thesis using the fission yeast, for the first time I have carried out a genome-wide analysis to identify such ORIs during the mitotic and meiotic cell cycles.

The data can be summarised as follows: a total of 401 ORIs were identified which were used 29 percent of the time during mitotic S-phase and were spaced every 31 kilobases (kb) on average. The same ORIs were used during pre-meiotic S-phase although with lower efficiency in most chromosomal regions. A further 503 potential ORIs were used less efficiently at eight percent of the time during mitotic S-phase. This totals 904 ORIs which were distributed at an average inter-origin distance of 14 kilobases (kb) throughout 12.5 megabases (Mb) of the three chromosomes of fission yeast. These data support the idea of a continuum of ORI activity. The 401 efficient ORI loci contained A+T-rich regions located between genes, and these intergenic regions were typically larger than average. ORIs were not defined by a strict sequence consensus but the presence of AT-hook binding sequences. When the initiation factors Cdc18 and Cdt1 were over-expressed, regions of DNA containing particularly efficient ORIs with exceptionally large AT-hook binding domains became over-amplified, suggesting that interactions between these factors and efficient ORIs may be important for the mechanism ensuring that an ORI only fires once in each S-phase.

Acknowledgements

First, I would like to thank Paul Nurse for being everything you could wish for in a supervisor, and for reminding me that things always take longer in reality. He gave me the privilege to enjoy the perfect study environment in his laboratory where I met so many nice and interesting colleagues during those four years, as well as the opportunity to collaborate with other people and groups which I greatly enjoyed.

I would like to thank Jacky Hayles, the heart and soul of the lab, who would always listen and help, for all her support especially with my less than perfect genetics skills. I would like to thank everybody in the Cell Cycle laboratory, past and present for their team spirit especially my friends Klaus Leonhard, Stefania Castagnetti and Damien Hermand collectively known as "Bay 2" as well as Oliver Harris, for the fun times we enjoyed together. A special thank you also goes to Rafael Carazo-Salas who would always be there for advice, for his friendship, great discussions, and for going through the hardship of reading the draft of this thesis. I would like to thank Bela Novak, who I had the privilege to spend a short but very enjoyable time with as a colleague, for being a great listener no matter how big or small the problem. Thank you also to my colleagues in the New York laboratory, especially to Atanas Kaykov and Janni Petersen, for their friendship and for making me laugh, you are wonderful!

Finally, thank you to Juerg Bähler and his group in the Sanger Institute, for a perfect collaboration and support throughout the period of my PhD studies.

This PhD was funded by a studentship from Cancer Research UK, and supported by the Rockefeller University.

This thesis is dedicated to my partner Geoff
for his support, trust and love.

TABLE OF CONTENTS

TABLES AND FIGURES

List of Abbreviations:

adenine (A)
anaphase promoting complex/cyclosome (APC/C)
autonomously replicating sequence (ARS)
base pairs (bp)
Cell Cycle Laboratory (CCL)
cell division cycle (cdc)
cyclin-dependent kinase (CDK)
cyclin-dependent kinase inhibitor (CDKi)
cytosine (C)
DNA synthesis phase (S phase)
DNA unwinding element (DUE)
double strand break (DSB)
experimental (Exp)
guanine (G)
hydroxyurea (HU)
kilobase (kb)
maturation promoting factor (MPF)
megabase (Mb)
minichromosome maintenance protein (MCM)
mitotic phase (M phase)
origin of DNA replication initiation (ORI)
origin recognition complex (ORC)
pre-initiation complex (pre-IC)
pre-replicative complex (pre-RC)
proliferating cell nuclear antigen (PCNA)
reference (Ref)
replication initiation point (RIP)
ribosomal DNA (rDNA)
S phase cyclin-dependent kinases (S-CDKs)
thiamine (T)
two-dimensional (2D)

Publication arising from this Thesis:

Heichinger, C., Penkett, C., Bahler, J. and Nurse, P. Genome Wide Characterisation of Fission Yeast DNA Replication Origins. Manuscript submitted.

Notes on Collaborative Work:

This study was done in collaboration with Juerg Baehler in the Fission Yeast Functional Genomics Group, who provided the microarrays and the technical Know How. This thesis consists entirely of my own work. Chris Penkett and Juan Mata contributed technical advice and scripts for normalisation and processing of microarray raw data. Aengus Stewart from CRUK provided some help with the bioinformatics analysis and Gavin Burns from the Sanger Centre provided initial help with microarray experiments.

Chapter I

General Introduction

1 General Introduction

The eukaryotic cell cycle consists of two major events: S phase, during which chromosomal DNA is synthesised and duplicated; and M phase or mitosis, where replicated chromosomes are segregated equally into two daughter cells. These two events are often separated by **G**ap phases, called G_1 and G_2. The eukaryotic cell cycle is thus characterised by the process that a cell has to go through in order to divide into two equal daughter cells. This process happens in an ordered progression from G_1-S-G_2-M, but the proportion of time different cell types spend within each phase varies. To avoid genome instability, it is essential that the DNA is fully replicated during S phase before it is segregated at mitosis. To achieve this goal, eukaryotic cells have evolved multiple controls and checkpoints, among which the most fundamental ones have been evolutionarily conserved from yeast to humans (reviewed in (Nyberg et al., 2002; Chen and Sanchez, 2004; Takeda and Dutta, 2005)). Two types of checkpoints are active or can be triggered during the cell cycle, ones that act globally and ensure the order of S and M phase and ones that act within S phase to ensure error free and complete rounds of DNA replication. Much effort has been devoted to the identification and characterisation of molecules involved in DNA replication, in particular in the onset or initiation of DNA replication. The work presented in this thesis was carried out using the unicellular fission yeast *Schizosaccharomyces pombe*, which has proved a particularly useful model system in the identification and characterisation of molecules implicated in the cell cycle

of eukaryotes. In this chapter, I will give a general overview of the major components involved in cell cycle regulation of S phase in eukaryotes. Thereafter, I will focus on fission yeast DNA replication and S phase regulation in more detail, but will also refer to work in other organisms for comparative purposes before presenting the major aims of this thesis.

1.1 Cell Cycle Control of S phase in eukaryotes: Overview

1.1.1 Cyclin Dependent Kinases and Cyclins

Cyclin **d**ependent **k**inases (CDKs) play a central role in the regulation of the eukaryotic cell cycle. These were first identified in genetic screens of mutant yeast cells which continued to increase in cell size in the absence of cell division, which is a characteristic of the *cdc* (**c**ell **d**ivision **c**ycle) phenotype (Bonatti et al., 1972). The CDK *cdc2* was first isolated in the budding yeast *Saccharomyces cerevisiae* where it is known as *cdc28* (Hartwell et al., 1974) and in fission yeast (Nurse et al., 1976). It was shown in fission and in budding yeast that Cdc2/28 was required in both at the G_1/S transition for commitment to the cell cycle and the G_2/M transition for control of mitosis (Hartwell et al., 1974; Nurse and Thuriaux, 1980; Nurse and Bissett, 1981). Complementation studies showed that the budding yeast *cdc28* as well as the human *cdc2* homologue could complement for temperature sensitive mutations of *cdc2* in fission yeast (Beach et al., 1982; Lee and Nurse, 1987). *Cdc2* was identified as a component of the **M**aturation **P**romoting **F**actor (MPF) in the frog *Xenopus laevis* (Dunphy et al., 1988; Gautier et al., 1988). MPF was first discovered in the frog *Rana pipiens* as a cytoplasmic factor of mature oocytes that could induce first meiotic division in G_2-arrested immature oocytes (Masui

and Markert, 1971; Smith and Ecker, 1971). MPF was later shown to act as mitotic inducer in somatic cells (Sunkara et al., 1979; Kishimoto et al., 1982). *Cdc2* homologues were also discovered in starfish and hepatoma cells of rats (Labbe et al., 1988; Langan et al., 1989). Together, these findings indicated that the major regulatory functions of *cdc2* had been evolutionarily conserved and established *cdc2* as one of the master regulators of the eukaryotic cell cycle. Higher eukaryotes have evolved several core CDKs which are used at different stages of the cell cycle. The *cdc2* homologue is also commonly known as *cdk1* and is the key regulator for the onset of mitosis (reviewed in (Doree and Hunt, 2002). The cell cycle in fission yeast and budding yeast is driven by only one core CDK, Cdc2/Cdc28 which provides the switch between S phase and M phase. This switch is managed by the association of Cdc2/Cdc28 with regulatory subunits called cyclins (reviewed in (Humphrey and Pearce, 2005)). Cyclins are proteins that are regulated by periodic accumulation and destruction during the cell cycle (reviewed in (Murray, 2004)). CDK activity is generally low during G_1 phase and an increase in activity brings about onset of S phase. A further increase in CDK activity brings about onset of mitosis. Several controls are in place to ensure that cells do not enter S phase or M phase prematurely. **M**itotic **CDK** activity (M-CDK) is destroyed after metaphase in mitosis by proteolysis of cyclins via a multi-subunit protease, called the proteasome (Coux et al., 1996; Baumeister et al., 1998). This degradation is facilitated by the cell cycle regulated ubiquitin ligase, the **A**naphase **P**romoting **C**omplex / **C**yclosome (APC/C) (reviewed in (Rape and Kirschner, 2004; Castro et al., 2005)) and is essential for exit

from mitosis (reviewed in (Bosl and Li, 2005)). Regulation of CDKs is further achieved by their phosphorylation via different protein kinases and inhibition by proteins classified as CDK inhibitors (CDKi). For instance, in fission yeast CDK activity is inhibited by various mechanisms in different stages of the cell cycle (Hayles and Nurse, 1995; Sveiczer et al., 2000). During G_1, the cell cycle regulated CDKi Rum1 (for **R**eplication **u**ncoupled from **m**itosis) accumulates (Benito et al., 1998) and specifically inhibits CDK activity by association with any residual or newly synthesised CDK complex (Correa-Bordes and Nurse, 1995; Correa-Bordes et al., 1997). This regulation prevents entry into mitosis if cells are delayed or arrested in G_1. During S phase, Rum1 is degraded by proteolysis (Correa-Bordes et al., 1997; Benito et al., 1998) and CDK activity is kept relatively low by inhibitory tyrosine phosphorylation (Y-15) through the kinases Wee1 (Featherstone and Russell, 1991; Parker et al., 1992) and Mik1 (Lundgren et al., 1991), which prevents pre-mature entry into mitosis. Progression into mitosis requires high CDK activity which is achieved by de-phosphorylation of the CDK through the Cdc25 phosphatase (Fantes, 1979; Russell and Nurse, 1986; Gould and Nurse, 1989; Moreno et al., 1989; Moreno et al., 1990).

Here I have given a basic introduction to cell cycle regulation which is very complex and involves a network of positive and negative regulators. Mathematical and computational methods are now used in an attempt to integrate all the molecules that are involved and have been identified in order to develop cell cycle models (Sveiczer et al., 2000; Sveiczer et al., 2004; Fuss et al., 2005).

1.1.2 S phase regulation of CDK substrates

Eukaryotic cells initiate DNA replication from multiple sites throughout the genome, called **O**rigins of DNA **R**eplication **I**nitiation (ORIs). This implies that initiation events across the genome must be co-ordinated in order for the whole genome to be replicated only once during each cell cycle. This is managed by CDKs, which also co-ordinate onset of mitosis and the integration of S phase and M phase into an orderly cell cycle progression. This prevents onset of S before M and the return to M from G1 before DNA replication in S has occurred. When this regulation is compromised, re-replication of DNA within the same cell cycle (endo-reduplication), or at the other extreme segregation of unreplicated chromosomes can be the consequence.

The cell prevents endo-reduplication of DNA by regulating at least three different ATP-dependent protein complexes, which are substrates of CDKs (reviewed in (Kelly and Brown, 2000; Bell and Dutta, 2002; Blow and Dutta, 2005; Takeda and Dutta, 2005)): the replication initiator called **O**rigin **R**ecognition **C**omplex (ORC); the **pre-R**eplicative **C**omplex (pre-RC) (Diffley et al., 1994) which includes the replication initiation factors Cdc6 and Cdt1 and the **M**ini**C**hromosome **M**aintenance protein complex (MCM(2-7)). ORC is a hexameric protein complex which associates with chromatin at DNA sequences where replication starts, termed **O**rigins of DNA **R**eplication **I**nitiation (ORIs) (reviewed in (Bell and Dutta, 2002)). It was first discovered in a footprinting assay for proteins that bound to a conserved sequence within the budding yeast ORI *ARS1* in vitro (Bell and Stillman, 1992) and this footprint was also confirmed in vivo (Diffley and

Cocker, 1992). Further footprinting assays showed that the region in *ARS1* where ORC associated was extended in G_1 compared with G_2 and that this change defined an ORI to be either in the "pre-replicative" state which appears near the end of mitosis and persists through G_1 or the post-replicative state adopted after entry into S phase (Diffley et al., 1994). This identified the multi-protein pre-RC that assembled at ORIs upon exit from mitosis. The formation of pre-RCs on ORIs makes DNA competent for DNA replication and ORIs are said to be in the licensed state in contrast to the unlicensed state when ORIs are not associated with pre-RCs and incompetent for DNA replication such as occurs during G_2 phase of the cell cycle (reviewed in (Nishitani and Lygerou, 2002; Nishitani and Lygerou, 2004)). Pre-RCs subsequently recruit the replication machinery. The sequential assembly of the multi protein pre-RC is highly conserved from yeast to humans (reviewed in (Bell and Dutta, 2002; Gerbi et al., 2002; Mendez and Stillman, 2003; DePamphilis, 2005)). This involves the recruitment of the replication initiation factors Cdc6 and Cdt1 to ORC, which are both required to load the MCM2-7 complex onto ORIs. In addition, a protein called Noc3 has been identified as part of the pre-RC in budding yeast, where it is essential for the interaction between ORC and cdc6 (Zhang et al., 2002). The assembly of the pre-RC can only occur in a certain window during the cell cycle, during which CDK activity is low and APC/C activity is high, this normally only occurs between late mitosis and early G_1 phase (Diffley et al., 1995; Diffley, 2004). The activation of ORIs on the other hand can only take place when CDK activity is present. This places the pre-RC at S phase onset.

Previous studies in yeast, *Xenopus*, the fruit fly *Drosophila melanogaster* and mammals suggest that one or more of the six ORC subunits undergoes cell cycle dependent modifications in form of phosphorylation by the S phase CDK and ubiquitination (reviewed in (Bell and Dutta, 2002; DePamphilis, 2005; Stillman, 2005)). These modifications potentially restrict the ability of ORC to initiate pre-RC assembly to early G_1 of the cell cycle and this cell cycle regulated process was termed "The ORC Cycle" (DePamphilis, 2003). In budding yeast, ORC seems to be stably associated with chromatin throughout the cell cycle (Diffley et al., 1995). This contrasts with mammalian cells where there is evidence that the Orc1 subunit is selectively destabilised during S phase, released from chromatin and only restored during the subsequent G_1 phase (Li and DePamphilis, 2002; DePamphilis, 2003). In proliferating cells in the embryo of *Drosophila* Orc1 protein levels are dependent on G_1 specific transcription and Orc1 accumulates in late G_1/S phase (Asano and Wharton, 1999). In somatic cells of *Drosophila*, Orc1 has been suggested to be selectively ubiquitinated during mitosis and degraded by the APC/Fzr system (Araki et al., 2003) in the background of strong constitutive transcription. In *Xenopus* an in vitro system of extracts made from unfertilised eggs, which are naturally arrested in meiotic metaphase II, have been used to address questions surrounding cell cycle regulation (reviewed in (Philpott and Yew, 2005)). These extracts can be released into the mitotic cell cycle by mimicking fertilisation. Upon addition of either sperm or somatic cell chromatin lacking functional ORC, endogenous ORC from egg extracts rapidly

associates with the chromatin and DNA replication is initiated. However, the affinity of ORC for DNA changes upon binding of the MCM2-7 complex (reviewed in (DePamphilis, 2005)). In sperm chromatin the subunits Orc1 and Orc2 become salt sensitive indicating that they become destabilised (Rowles et al., 1999), in somatic cell chromatin the effect is more severe and the Orc1/2/4 subunits have been shown to dissociate from chromatin upon S phase entry (Sun et al., 2002). CDK1/cyclin dependent phosphorylation has been observed on one or more ORC subunits of yeast, *Xenopus* and mammals at some stage between S to M phase and there is some evidence from mammals that during this period further assembly of the pre-RC is blocked (reviewed in (DePamphilis, 2005)). Together, these modifications have the potential to render ORC inactive during the S, G_2 and M phases and may prevent re-initiation of DNA replication during the cell cycle.

The initiation factor *cdc6* was initially identified in budding yeast in a screen for *cdc* mutants that failed to undergo S phase (Hereford and Hartwell, 1974). The fission yeast homologue of *cdc6* is called *cdc18* and was identified in a mutant screen for genes that when mutated cause cell cycle defects (Nasmyth and Nurse, 1981). Cdc6 has a central role in regulating S phase onset in eukaryotes, as it is essential to assemble and maintain the pre-RC until onset of S phase (reviewed in (Bell and Dutta, 2002)). Thereafter, it is negatively regulated by CDKs to prevent re-initiation within the same cell cycle from existing pre-RCs. Phosphorylated Cdc6/Cdc18 is exported from the nucleus in vertebrate cells (Saha et al., 1998; Petersen et al., 1999; Pelizon et al., 2000; Delmolino et al., 2001) or

degraded in fission yeast (Brown et al., 1997; Jallepalli and Kelly, 1997; Kominami and Toda, 1997; Jallepalli et al., 1998) and budding yeast (Drury et al., 1997; Elsasser et al., 1999; Drury et al., 2000; Perkins et al., 2001). There is evidence that some Cdc6 remains on DNA throughout the cell cycle in mammalian cells but phosphorylation is thought to inactivate the chromatin bound fraction by an as yet unresolved mechanism (Coverley et al., 2000; Mendez and Stillman, 2000; Biermann et al., 2002; Coverley et al., 2002; Alexandrow and Hamlin, 2004).

The *cdt1* gene was first identified in fission yeast as a target of *cdc10* transcriptional regulation (Hofmann and Beach, 1994). Cdt1 was later found to be an important eukaryotic replication initiation factor which is required together with Cdc6 for loading of MCMs onto chromatin (Nishitani et al., 2000). CDK phosphorylation targets Cdt1 for degradation during S phase in mammalian cells (Liu et al., 2004; Sugimoto et al., 2004) and fission yeast ((Nishitani et al., 2000), D. Hermand, personal communication) or nuclear export in budding yeast (Tanaka and Diffley, 2002).

MCM genes were identified in screens for factors that confer plasmid maintenance, cell cycle progression and chromosome missegregation (reviewed in (Dutta and Bell, 1997)). MCM is a heterohexameric protein complex which binds to chromatin at the M/G_1 transition in an ORC and Cdc6 dependent manner (Aparicio et al., 1997; Donovan et al., 1997; Liang and Stillman, 1997; Tanaka et al., 1997; Young and Tye, 1997; Feng et al., 2000) to form the pre-RC. It is still unclear whether the MCM2-7 complex functions as a replicative helicase but current data from

different systems suggests that it is involved both in initiation and in elongation of DNA synthesis (reviewed in (Forsburg, 2004)). In budding yeast, MCMs are exported from the nucleus into the cytoplasm in G_2 and M phases and it has been speculated that CDK phosphorylation is involved in this process (Labib et al., 1999; Nguyen et al., 2000). In other species, MCMs have been shown to be constitutively nuclear and are primarily regulated by dissociation from chromatin after onset of S phase (Madine et al., 1995; Schulte et al., 1995; Fujita et al., 1996; Okishio et al., 1996; Su and O'Farrell, 1997; Weinreich and Stillman, 1999; Kearsey et al., 2000). *Xenopus* Mcm4 and human Mcm2/4 are phosphorylated by CDK during S phase this probably decreases the affinity of MCMs for chromatin (Coue et al., 1996; Hendrickson et al., 1996; Fujita et al., 1998) and may also inhibit helicase activity in the human MCM complex (Ishimi et al., 2000; Ishimi and Komamura-Kohno, 2001).

1.2 DNA replication and S phase control in Fission Yeast

A diagrammatic representation of the fission yeast cell cycle is shown in Figure 1. Cells spend the majority of time in G_2 phase (~0.75 of a cell cycle) (Mitchison, 1970) which is the main time window for cell growth in fission yeast. Once cells have reached a critical size, they can enter mitosis (reviewed in (Forsburg and Nurse, 1991)) and segregate their chromosomes into two daughter nuclei. After nuclei have divided and separated in mitosis the cell goes through a very short G_1 phase (0.08 of a cell cycle) (Nasmyth et al., 1979). This does not provide enough time for cytokinesis before S phase. Instead, septation occurs during S phase followed by symmetrical cell division in late S phase and early G_2. S phase

is also relatively short in fission yeast. It was experimentally determined to last about 0.1 of a cell cycle (Mitchison and Creanor, 1971; Nasmyth et al., 1979). Under normal circumstances, different Cdc2-cyclin complexes operate at the G_1/S (Cig2, Cig1, Puc1) and the G_2/M (Cdc13) transitions in fission yeast (Fisher and Nurse, 1995; Martin-Castellanos et al., 2000). However, it has been shown that the mitotic B type cyclin Cdc13 can regulate both, M and S phase in the absence of the G_1/S phase cyclins (Fisher and Nurse, 1996). From these findings in fission yeast, the so-called "quantitative model" for regulation of cell cycle progression was developed and proposed (Stern and Nurse, 1996). This model suggests that low levels of Cdc2-cyclin activity can promote DNA replication whereas higher Cdc2-cyclin activity is essential for cells to progress into mitosis and that these periodic changes in CDK activity are dependent on cell cycle regulation of cyclin levels. The "qualitative model" on the other hand suggests that different cyclins have either S phase or M phase promoting abilities and thus are able to provide different functionality to the CDK perhaps by modulating its substrate specificity or location within the cell (Miller and Cross, 2001; Moore et al., 2003). This model is supported by recent findings in budding yeast which proposed that the Cdk1-Clb2 complex provides high kinase activity required for mitotic CDK targets whereas the lower Cdk1-Clb5 activity is sufficient to activate S phase specific targets (Loog and Morgan, 2005). However, the two models are not necessarily mutually exclusive. For instance, it is possible that fission yeast operates according to the qualitative model under normal

circumstances but switches to the quantitative model as a backup mechanism if different cyclin functionality is lost.

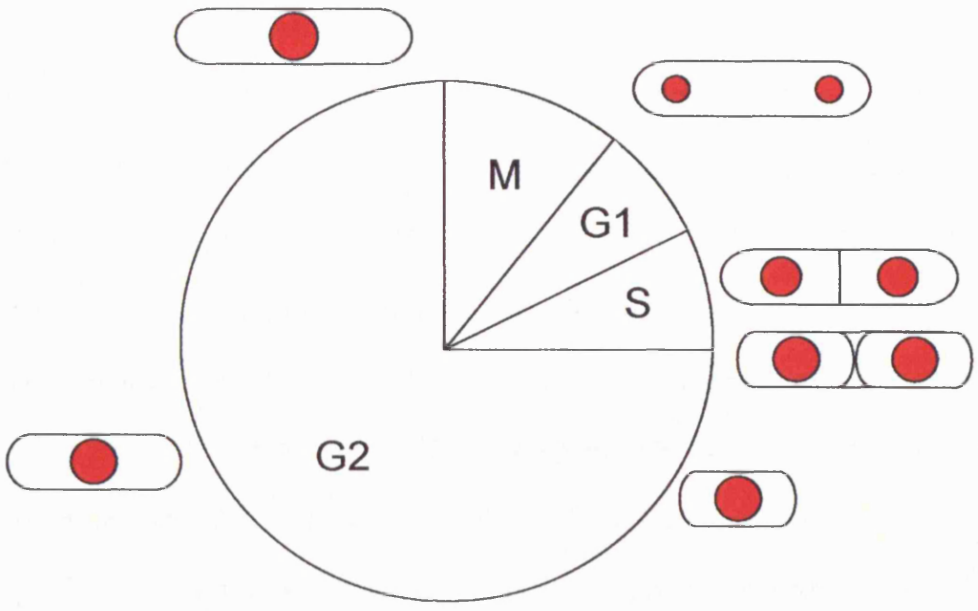

Figure 1: Schematic Representation of the Fission Yeast Cell Cycle

1.2.1 Origins of DNA replication Initiation and ORC

The initial model of regulation of DNA synthesis was based on bacteria, drawn up by Francois Jacob and Sydney Brenner in 1962 (Jacob and Brenner, 1963). This model suggested that a replicon contains two genetic elements, the structural gene that encodes the initiator protein which acts on the DNA sequence called replicator (ORI). This model was later confirmed in *E. coli* (Yasuda and Hirota, 1977; Chakraborty et al., 1982) and both the initiator and the replicator were found to be highly conserved in bacteria (Fujita et al., 1989). On the basis of the bacterial model, eukaryotic ORIs were first identified in budding yeast as chromosomal fragments that promoted high frequency of transformation and extrachromosomal maintenance of plasmid DNA [(**A**utonomously

Replicating **S**equence (ARS)] (Stinchcomb et al., 1979). A common DNA sequence was identified that was required for ARS activity on plasmids and ORI activity in the chromosomal context (Celniker et al., 1984; Marahrens and Stillman, 1992), which indicated that eukaryotic replicons consisted of a conserved replicator sequence similar to bacterial replicons. However, studies in other eukaryotic model systems including fission yeast have since shown that such a conserved replicator sequence appears to be unique to budding yeast at least so far (reviewed in (Cvetic and Walter, 2005). Despite this lack of a conserved replicator, the eukaryotic initiator protein or ORC has been found to be highly conserved in yeasts and metazoans (Gavin et al., 1995; Bell and Dutta, 2002).

The deficiency of a common consensus sequence has made it difficult to identify ORIs in other eukaryotes and hence to define and specify the DNA sequence that is required for replication initiation. Figure 2 contrasts and compares the major features of ORIs in different eukaryotic model systems. Genetic dissection of ARS elements in budding yeast revealed an essential sequence of 100 to 200 bp organised into several domains, which contribute synergistically to overall ARS activity (Broach et al., 1983; Kearsey, 1984; Marahrens and Stillman, 1992; Newlon and Theis, 1993). Efficient ORC binding requires an 11 bp ARS consensus sequence (ACS) 5'(A/T)TTTA(T/C)(A/G)TTT(A/T)3' (Rowley et al., 1994; Rowley et al., 1995), common to all budding yeast ORIs and the adjacent B1 element rich in non-conserved AT sequences (Newlon and Theis, 1993). Additional domains may act as enhancers of ORI activity, such as a B3 element which binds the transcription factor Abf1 in the genetically

characterised ARS1 (Diffley and Stillman, 1989; Diffley et al., 1994). The B2 element in ARS1 consists of A+T-rich sequences, which have been suggested to function as a **D**NA **u**nwinding **e**lement (DUE) (Newlon and Theis, 1993) and/or associate with components of the pre-RC via a degenerate **A**RS **C**onsensus **S**equence (ACS) (Wilmes and Bell, 2002). Different combinations of these B elements were identified in other ARS sequences (Newlon and Theis, 1993).

Plasmid transformation assays were also employed to identify fission yeast ARS elements (Sakaguchi and Yamamoto, 1982; Maundrell et al., 1985; Wright et al., 1986; Johnston and Barker, 1987; Maundrell et al., 1988; Olsson et al., 1993; Caddle and Calos, 1994; Dubey et al., 1994; Wohlgemuth et al., 1994; Clyne and Kelly, 1995; Clyne and Kelly, 1997), many of which have since been shown to be active in their chromosomal context (summarised in (Segurado et al., 2003)). Genetic dissection of ARS elements in fission yeast showed that relatively large DNA sequences of 500 – 1000 bp were required for ORI activity compared with the small 100 – 200 bp required in budding yeast (Clyne and Kelly, 1995; Dubey et al., 1996; Kim and Huberman, 1998; Okuno et al., 1999). ORIs in fission yeast are generally more A+T-rich than those in budding yeast (Raghuraman et al., 2001) and do not share a consensus sequence which is critical for ORC binding in budding yeast. The six homologous subunits of the ORC complex (SpOrc1 to SpOrc6 or Orp1 to Orp6) have been identified in fission yeast and so far SpOrc1/2/4/5 have been found to be essential for DNA replication (Gavin et al., 1995; Muzi-Falconi and Kelly, 1995; Grallert and Nurse, 1996; Leatherwood et al., 1996; Ishiai et al.,

1997; Chuang and Kelly, 1999; Lygerou and Nurse, 1999; Moon et al., 1999). Whilst fission yeast ORC seems to be associated with ORIs at all stages of the cell cycle, the SpOrc2 subunit is a phosphoprotein which becomes phosphorylated first in S phase and reaches a maximum phosphorylation level in G_2/ M (Lygerou and Nurse, 1999; Vas et al., 2001; Wuarin et al., 2002), a process that is reversed during the M to G_1 transition (Lygerou and Nurse, 1999). It is possible that this contributes to regulation of pre-RC formation on ORIs and prevents re-initiation during S, G_2 and M. The most striking feature of fission yeast ORC is found in the SpOrc4 subunit which is characterised by the presence of nine AT-hook motifs at the N-terminus (Chuang and Kelly, 1999; Chuang et al., 2002), these motifs are commonly found in non-histone chromosomal proteins called **H**igh **M**obility **G**roup **I** proteins (HMG-I) (Maher and Nathans, 1996; Reeves, 2001). Genetic analysis and footprinting assays of ARS elements revealed that fission yeast ORIs generally consist of two SpOrc4 binding sites marked by degenerate asymmetric A+T-rich sequences, other functional domains that do not bind ORC but may also contribute to overall ORI activity (Kong and DePamphilis, 2001; Lee et al., 2001; Takahashi and Masukata, 2001; Kong and DePamphilis, 2002; Takahashi et al., 2003). This indicates that fission yeast ORIs generally function as compound ORIs, which may require multiple initiator and replicator molecules to bring about a single initiation event. Co-operative binding of ORC molecules may be essential for efficient activation of ORIs as deletion of one A+T-rich element can reduce ORI activity (Okuno et al., 1999; Takahashi et al., 2003).

Metazoan ORIs are more similar to fission yeast than budding yeast ORIs both with respect to size and to their dispersed modular organisation. Research into metazoan ORIs has focused on genetic and biochemical analysis of a small number of ORIs that can initiate DNA replication in *cis* at ectopic chromosomal locations (reviewed in (Aladjem and Fanning, 2004)). Like fission yeast ORIs, they seem to lack any sequence consensus, contain A+T-rich sequences and are often under regulation by *cis* and *trans* acting elements. Well studied examples of *cis* acting elements which both acts as enhancers in their chromosomal context include the locus-control region (LCR) in the human beta globin locus that is involved in the regulation of globin gene expression (Aladjem and Fanning, 2004) and a structural element of A+T-rich sequences which is thought to function as a DUE in the c-myc ORI (Liu et al., 2003). ORI elements in metazoan systems can be classified as either localised initiation events or initiation zones (Gilbert, 2001). For instance, the human lamin B2 locus consists of a single defined initiation event, whereas multiple potential initiation sites are located in close proximity over a 55 kb region in the Chinese hamster ovary DHFR locus (Vaughn et al., 1990; Dijkwel et al., 1994; Dijkwel and Hamlin, 1995; Dijkwel et al., 2002). Initiation zones were also found in fission yeast (Dubey et al., 1994) and *Drosophila* (Ina et al., 2001). The fission yeast ura4 locus has been well characterised and consists of three distinct initiation events within a ~ 5 kb long region (Kim et al., 2001). Like in fission yeast (Chuang and Kelly, 1999) and budding yeast (Lee and Bell, 1997), ORC in metazoan cells typically associates with asymmetric A+T-rich regions in the chromosomal

context (reviewed in (Aladjem and Fanning, 2004) but so far no or little specific affinity of metazoan ORC for these sequences has been shown in vitro (Vashee et al., 2003; Remus et al., 2004). Interestingly, fission yeast ORC targets and competes for the same A+T-rich sequences as *Xenopus* ORC in *Xenopus* egg extract (Kong et al., 2003) and the same sequences also bind human ORC (Vashee et al., 2003). AT-hook motifs are unique to ORC in fission yeast and it has been speculated that HMG-I proteins may functionally substitute for AT-hook motifs and target ORC to ORIs in metazoan cells (Chuang and Kelly, 1999).

An interesting feature of eukaryotic ORIs is that only a subset of ORIs is used in every cell cycle. A wide range of efficiencies has been observed in fission yeast ORIs (Gomez and Antequera, 1999; Segurado et al., 2003). The most efficient fission yeast ORI identified so far is ars2004, but even this shows some passive replication from adjacent ORIs in its chromosomal context (Okuno et al., 1997). In the hamster DHFR locus, initiation sites are distributed at frequent intervals but used with very different efficiencies (Dijkwel et al., 2002). The most efficient eukaryotic ORIs have been identified in budding yeast (~90 % efficiency) (Friedman et al., 1997; Yamashita et al., 1997). One possible explanation for reduced ORI efficiency is ORI interference (Dubey et al., 1994). This has been observed in the well characterised fission yeast ORI locus upstream of the ura4 gene on Chromosome Three, where deletion of one of the three ORIs within the ~5 kb cluster resulted in higher efficiency of ORI utilisation of neighbouring ORIs (Dubey et al., 1994). The parameters that govern which ORI is chosen in each cell cycle are not clear. Relative AT-content

and the size of A+T-rich regions have been shown to influence ORI specification in fission yeast (Segurado et al., 2003; Dai et al., 2005) and may also influence ORI efficiency. A replication enhancer within the ura4 ORI locus in fission yeast has been found to affect ORI efficiency (Kim et al., 2001; Antunes et al., 2003), which could be explained by positive interactions between *cis* and/or *trans* acting transcription elements and DNA replication factors (see section 1.3).

The length of S phase can vary considerably during different stages of development. For instance, the normal replication program can be overridden by developmental regulation in preblastula embryos of *Xenopus* and *Drosophila* (reviewed in (Gilbert, 2001)). DNA replication initiates apparently randomly from any genomic locus at high efficiency, this reduces the length of S phase compared with somatic cells, where ORIs are spaced further apart and used at lower efficiencies. Current experimental data suggests that ORC molecules in fission yeast and other eukaryotic cells are generally restricted to one to two molecules for each potential ORI (reviewed in (DePamphilis, 2005)). However, cells in embryos contain 10^5 times more ORC molecules than somatic cells, this could lead to promiscuous binding of ORC to DNA sequences that are normally not used as ORIs in somatic cells (Hyrien and Mechali, 1993). This hypothesis is supported by data from *Drosophila* where increasing ORC to DNA ratios correlate with an increase in unspecific binding to DNA (Remus et al., 2004).

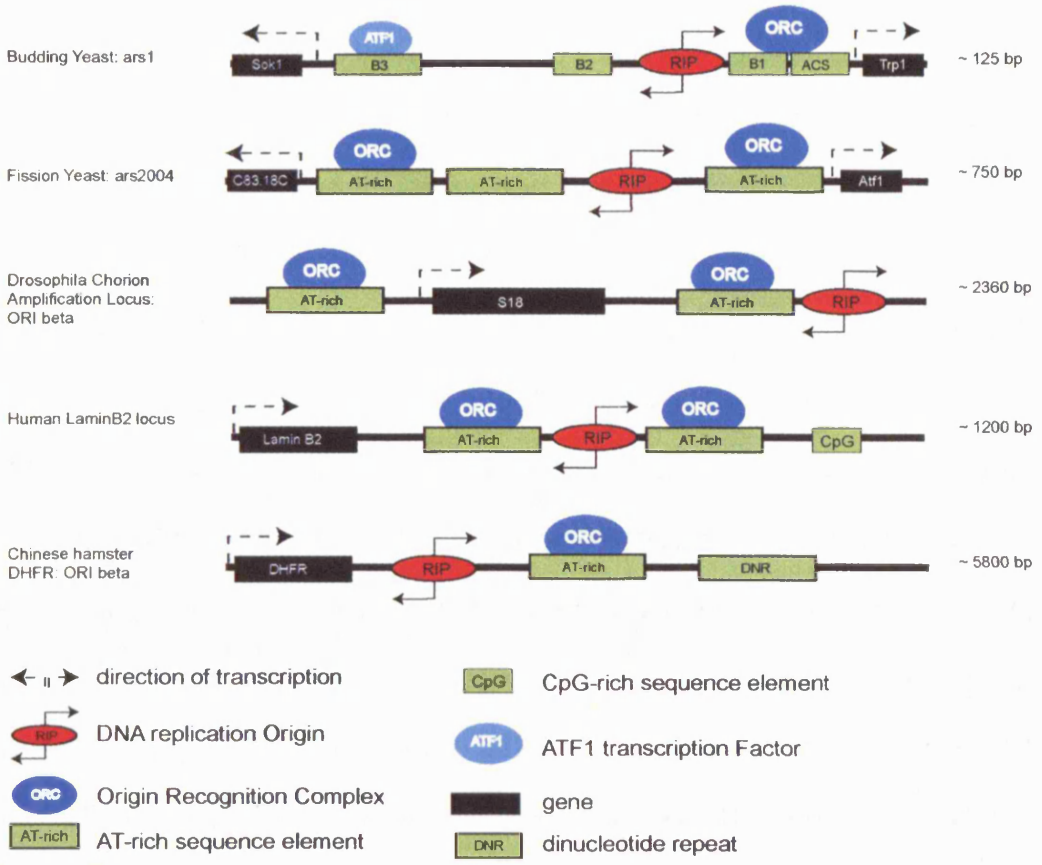

Figure 2: Summary of the structure of eukaryotic DNA Replication Origins

1.2.2 Assembly and Regulation of the pre-replicative Complex

Cdc18 is the fission yeast homologue of *cdc6* and has been shown to be essential for DNA replication (Nasmyth and Nurse, 1981; Kelly et al., 1993). Cdc18 levels are cell cycle regulated by transcription and proteolysis and peak at the G_1/S transition at the onset of S phase (Nishitani and Nurse, 1995; Baum et al., 1998). Expression is regulated by the Cdc10/Res1/Res2 transcription complex which is first active as cells enter mitosis and specifically promotes transcription of Cdc18, Cdt1 and other genes required for progression and execution of S phase (Kelly et al., 1993; Hofmann and Beach, 1994; Baum et al., 1998). Cdc2 dependent

phosphorylation as cells enter S phase, targets Cdc18 for ubiquitin-mediated degradation (Kominami and Toda, 1997).

Cdt1 (**C**dc10-**d**ependent **t**ranscript 1) is also periodically expressed through the cell cycle and peaks from mitotic exit to onset of S phase (Nishitani et al., 2000). Both Cdc18 and Cdt1 are loaded independently of each other onto chromatin during exit from mitosis (Nishitani et al., 2000). Cdt1 was shown to physically interact with the Cdc18 carboxyl terminus, which identified Cdt1 as a partner of Cdc18 (Nishitani et al., 2000). When Cdc18 or Cdt1 expression from an inducible promoter was switched off at the G_2/M transition, cells could complete mitosis as expected, but failed to initiate subsequent DNA replication. In these cells, association of the Mcm4 fission yeast homologue, Cdc21, which is essential for pre-RC formation at exit from mitosis, was compromised (Nishitani et al., 2000). Loss of Cdc21 localisation to chromatin in the absence of Cdc18 was also observed in a nuclear localisation assay (Kearsey et al., 2000). These data in fission yeast suggest that Cdc18/Cdc6 is required together with Cdt1 for the recruitment of the MCM complex and pre-RC formation. This is supported by observations in other eukaryotic systems (reviewed in (Bell and Dutta, 2002; Forsburg, 2004)).

All six MCM subunits have been conserved in fission yeast and were identified by genetic screens or sequence homology (reviewed in (Kearsey and Labib, 1998)). They form a hetero-hexamer and have the potential to bind and hydrolyse ATP (Adachi et al., 1997). Their association with chromatin is cell cycle regulated, and the complex binds ORIs in an ORC, Cdc18 and Cdt1-dependent manner at the exit from

mitosis and remain on chromatin until S phase (Grallert and Nurse, 1996; Ogawa et al., 1999; Kearsey et al., 2000; Nishitani et al., 2000). In vitro reconstitution experiments for fission yeast, budding yeast and mammalian MCM proteins have shown that they can form different stable complexes of either a catalytic or regulatory nature (Ishimi, 1997; You et al., 1999; Lee and Hurwitz, 2000; Schwacha and Bell, 2001). In fission yeast, the Mcm4/6/7 trimer can confer highly processive helicase activity when incubated with single stranded T-rich tails in forked DNA substrate and is thought to act as a catalytic subunit (Lee and Hurwitz, 2001), whereas Mcm2 and the Mcm3/5 complex interfere with the assembly of the catalytic complex and are thought to negatively regulate helicase activity (Lee and Hurwitz, 2000). It is interesting that ATPase and thus helicase activity of the catalytic domain in fission yeast (Lee and Hurwitz, 2001) and mammalian MCMs (You et al., 2003) is activated upon incubation with T-rich single stranded DNA. Considering this data it is possible that activation of the eukaryotic MCM helicase may be dependent on binding to A+T-rich ORI sequences in vivo. This is consistent with recent observations in budding yeast where Mcm4/6/7 was preferentially activated by *ARS1* sequences in vitro (Biswas-Fiss et al., 2005).

1.2.3 Activation of pre-RCs

Assembly of pre-RCs at ORIs is essential but not sufficient for initiation of DNA synthesis. This requires the assembly of additional conserved proteins on pre-RCs to form what is also known as the **pre**-Initiation **C**omplex (pre-IC) (Zou and Stillman, 1998). The assembly and activation of the pre-IC is governed by the activity of CDKs and the **D**bf4 **D**ependent

Kinases (DDKs) (Johnston et al., 2000), Cdc2 (Cdk1) and Hsk1 (Cdc7) in fission yeast (Masai et al., 1995; Brown and Kelly, 1998). In budding yeast, this assembly takes place throughout S phase in a temporal sequence dependent on the time of ORI activation (Aparicio et al., 1999; Zou and Stillman, 2000), in contrast to pre-RC assembly which occurs in a strict time window at the exit from mitosis. This temporal pattern is governed by the association of the protein Cdc45 with pre-RCs at ORIs, a factor that is essential and pivotal for the transition to DNA replication but not for the assembly of the pre-RC. The pre-RC has been shown to be stable in the absence of Cdc45 in budding yeast (Hopwood and Dalton, 1996; Owens et al., 1997). Cdc45 loading precedes the unwinding of DNA at ORIs before the recruitment of replicative polymerases. Unwinding of DNA around ORI sequences is also referred to as "ORI firing". Homologues of Cdc45 have also been identified and characterised in fission yeast, *Drosophila*, *Xenopus* and human cells (Mimura and Takisawa, 1998; Miyake and Yamashita, 1998; Kukimoto et al., 1999; Loebel et al., 2000). Chromatin immunoprecipitation from Xenopus egg extracts showed that Cdc45 forms a tight complex with MCM2-7, that helicase activity in vitro in this complex is dependent on the association with Cdc45 (Masuda et al., 2003; Pacek and Walter, 2004) and that loading of DNA polymerases α and ε, replication protein A (RPA) and cell proliferating nuclear antigen (PCNA) onto chromatin requires Cdc45 (Mimura and Takisawa, 1998; Mimura et al., 2000). In budding yeast Cdc45 genetically and physically interacts with MCM proteins (Hopwood and Dalton, 1996; Zou and Stillman, 1998; Zou and Stillman, 2000) and it

has been suggested that Cdc45 moves with the replication fork together with MCMs in the elongation step (Aparicio et al., 1997; Tercero et al., 2000). These data indicate that Cdc45 has a conserved function as a mediator between the pre-RC and the replication machinery. Association of Cdc45 with the pre-RC is stimulated by Cdc23/Mcm10 in fission yeast (Nasmyth and Nurse, 1981; Aves et al., 1998; Uchiyama et al., 2001; Gregan et al., 2003; Yang et al., 2005), and a requirement of Mcm10 for loading of Cdc45 has also been suggested in budding yeast (Sawyer et al., 2004) as well as in *Xenopus* in vitro studies (Wohlschlegel et al., 2002). This indicates that this function of Cdc23/Mcm10 has also been conserved in eukaryotes. Cdc23/Mcm10 has been shown to be constitutively bound to chromatin in fission yeast (Gregan et al., 2003) and budding yeast (Homesley et al., 2000) in contrast to studies in human HeLa cells and Xenopus egg extracts which indicate that binding is periodic (Izumi et al., 2000; Izumi et al., 2001; Wohlschlegel et al., 2002; Izumi et al., 2004). It has been suggested that this may be the consequence of a difference in interaction partners of Cdc23/Mcm10 on chromatin (Gregan et al., 2003). Cdc45 function depends on several other initiation factors that have been identified in recent years. Dpb11, which was originally identified in budding yeast, and Cut5, its fission yeast homologue, were found to be essential for DNA replication (Saka and Yanagida, 1993; Araki et al., 1995; McFarlane et al., 1997). Subsequently their role as a loading factor for DNA polymerases ε and α was established in budding yeast (Masumoto et al., 2000). This process is facilitated by the formation of a complex with Sld2 a protein that is

controlled by CDK phosphorylation (Masumoto et al., 2002). Homologues of Dpb11/Cut5 have also been identified in higher eukaryotes and seem to be involved either in loading of polymerases and/or Cdc45 (reviewed in (Takeda and Dutta, 2005)). In budding yeast and fission yeast, Cdc45 loading onto chromatin is dependent on the interaction with a factor called Sld3 which is loaded probably via association with MCM proteins (Kamimura et al., 2001; Nakajima and Masukata, 2002; Yamada et al., 2004). Sld3 has not yet been identified in higher eukaryotes. The multi-protein GINS (**G**o-**I**chi-**N**i-**S**an, 5-1-2-3 in Japanese) complex was first identified in budding yeast and consists of four conserved proteins (Sld5, Psf1, Psf2, and Psf3) (Kubota et al., 2003). A homologous complex has also been identified in *Xenopus* (Takayama et al., 2003). GINS is required for Cdc45 and polymerase loading and possibly replication elongation, but it is currently unclear which subunits of the complex are essential.

The DDK Hsk1/Cdc7 associates with chromatin at ORIs during S phase and contributes to activation of the pre-IC and ORI firing by phosphorylation of the Mcm2-7 complex in fission yeast (Brown and Kelly, 1998; Takeda et al., 1999; Takeda et al., 2001) and other eukaryotes (Lei et al., 1997; Kumagai et al., 1999; Jares and Blow, 2000; Kihara et al., 2000). In budding yeast this requires prior activation of CDK (Nougarede et al., 2000) in contrast to *Xenopus* where it has been shown that DDK is required prior to CDK activity (Jares and Blow, 2000). Further studies will be essential to clarify this point.

Ars2004 is a well characterised fission yeast ORI and has been shown to consist of two A+T-rich sequences which are separated by ~500

nucleotides (nt) and associate with ORC in vivo (Takahashi et al., 2003). This study suggested that either a single ORC molecule or two ORC molecules could contribute to this footprint. The model for fission yeast pre-RC formation and activation which I am presenting here (Figure 3) is based on the latter possibility: ORC is constitutively bound to DNA throughout the cell cycle and I speculate that at least two ORC complexes are bound to each ORI. An increase in CDK activity during S phase results in Orc2 phosphorylation which may interfere with the maintenance and/or re-assembly of pre-RCs (also referred to as re-licensing) perhaps by interfering with association of Cdc18 with ORC on chromatin and as a consequence re-initiation. In addition, the licensing factors Cdc18 and Cdt1 are phosphorylated by Cdc2 and degraded which also prevents re-initiation in G_2 and during M. In late M phase when Cdc2 activity is destroyed by the APC/C, ORC becomes dephosphorylated and Cdc18 and Cdt1 associate with ORCs at ORIs and form pre-RC complexes by loading the Mcm2-7 complex. This may require the concerted action of pre-RCs from two ORC binding sites perhaps facilitated by *cis* and *trans* acting molecules in the vicinity. ORI firing occurs after loading of Cdc45 and associated proteins, which recruit replicative DNA polymerases, and requires the phosphorylation of the Mcm2-7 complex by the Hsk1/cdc7-Dfp1/Dbf4 dependent kinase.

1.2.4 Checkpoint Pathways in Fission Yeast

The eukaryotic cell has evolved safeguards to make sure that all DNA is replicated and that damaged DNA is repaired before cells enter mitosis. Two checkpoint pathways (reviewed in (Nyberg et al., 2002; Bartek et al.,

2004; Cobb et al., 2004)) can be distinguished, which monitor the integrity of DNA and have been conserved from yeast to humans (Chen and Sanchez, 2004)). In fission yeast, these are characterised by the protein kinases Chk1 and Cds1 (Chk2) (Boddy et al., 1998; Lindsay et al., 1998). Both pathways are dependent on activation of the protein kinase Rad3 (=ATM/ATR homologue), which is downstream of other checkpoint proteins that may interact with DNA replication intermediates from unreplicated DNA and damaged DNA structure. The Cds1-dependent checkpoint is activated during S phase in response to replication stress and DNA damage (Lindsay et al., 1998; Brondello et al., 1999). The Chk1 pathway provides extra time for DNA repair and is mainly active in G_2, but has been shown to be activated during S phase if the function of Cds1 is compromised (Walworth et al., 1993; Brondello et al., 1999). The Cds1 pathway is activated upon addition of the drug hydroxyurea (HU), which results in dNTP depletion and accumulation of stalled replication forks. Studies in budding yeast have suggested that this checkpoint inhibits activation of ORIs which replicate late during S phase (Santocanale and Diffley, 1998; Yabuki et al., 2002). Once HU is removed, cells recover and DNA replication proceeds in an apparently normal fashion. Both Chk1 and Cds1 phosphorylate Cdc25 in the presence of DNA damage or replication blocks thereby inhibiting Cdc2 and entry into mitosis (Zeng et al., 1998; Furnari et al., 1999). In addition, Wee1 and Mik1 which are potent Cdc2 (Cdk1) inhibitors are upregulated by phosphorylation and this may contribute to the DNA damage checkpoint (O'Connell et al., 1997; Baber-Furnari et al., 2000; Raleigh and O'Connell, 2000).

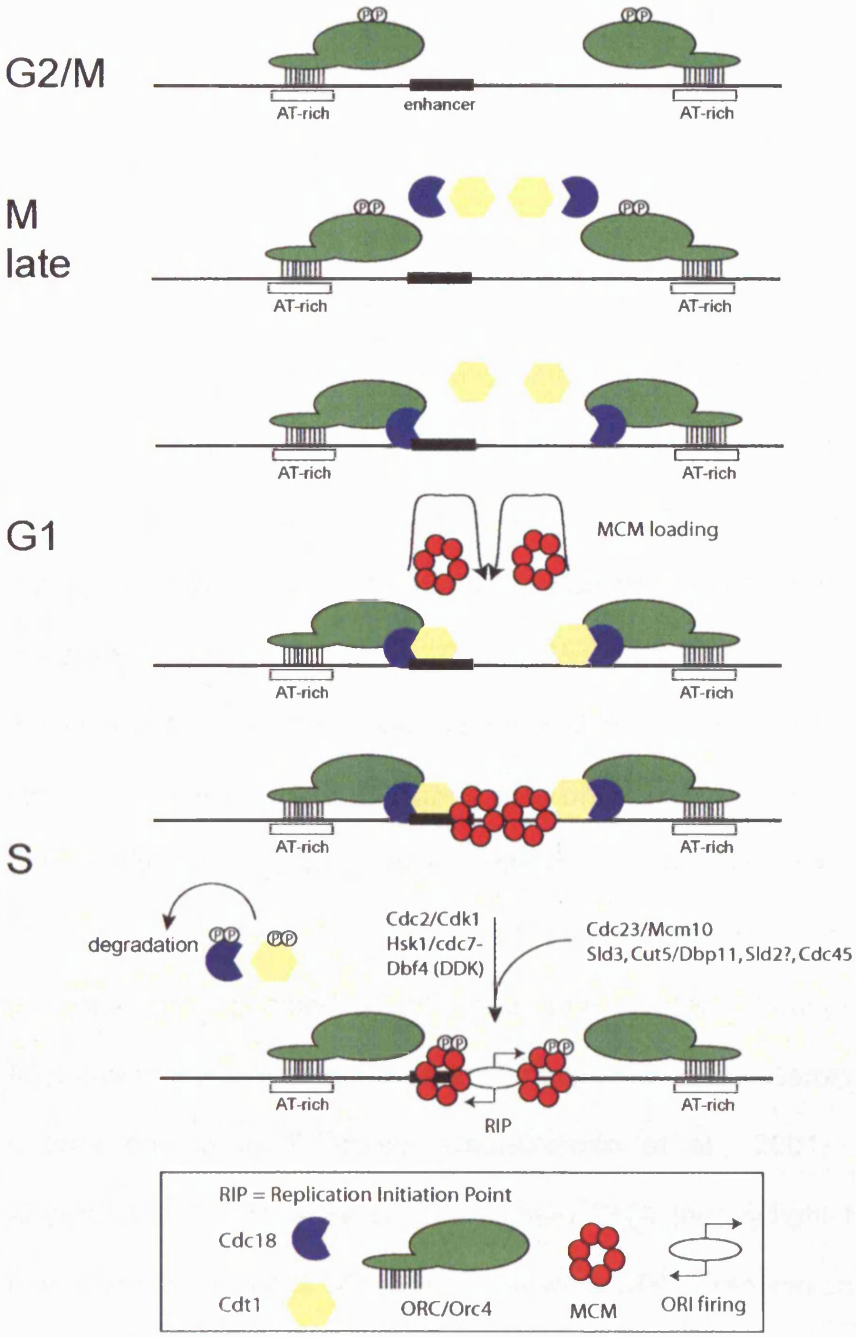

Figure 3: Formation of the pre-RC and Transition to pre-IC
Pre-RC Formation (Model): (G_2/M) Two ORC molecules are constitutively associated with a fission yeast ORI and CDK mediated phosphorylation may inhibit pre-RC assembly. (M late) CDK activity is destroyed by APC/C degradation, ORC becomes dephosphorylated, Cdc18 and Cdt1 associate with chromatin/ORC at ORIs to form a pre-RC complex by loading Mcm2-7 in G_1. Efficient Mcm2-7 loading may require two pre-RCs/ORI. ORIs are now licensed for DNA replication, Cdc45 is loaded onto the pre-RC during S phase and recruits replicative polymerases. The Mcm2-7 complex is phosphorylated by the Hsk1/cdc7-Dfp1/Dbf4 dependent kinase and DNA replication is initiated.Cdt1 and Cdc18 dissociate from chromatin and are degraded to prevent re-licensing.

1.3 Genomic Views of Eukaryotic DNA Replication

The sequencing of eukaryotic genomes has made genome-wide analysis of DNA replication possible and data are now available from budding yeast, fission yeast, fly and human cells (reviewed in (Kearsey, 2002; Newlon and Theis, 2002; McCune and Donaldson, 2003; Antequera, 2004; Donaldson, 2005; Macalpine and Bell, 2005)). The first studies of this nature were carried out in budding yeast. Microarrays were used in three different experimental approaches to identify ORIs and assess replication timing across the 16 chromosomes of the 13.5 **M**ega**b**ase (Mb) genome (Raghuraman et al., 2001; Wyrick et al., 2001; Yabuki et al., 2002). The first approach was an adaptation from the Meselson and Stahl experiment (Meselson and Stahl, 1958) of semi-conservative replication of DNA. Cells were grown in heavy isotope (^{13}C and ^{15}N) and synchronously released into DNA replication in medium containing light isotope. The two fractions of replicated (light) and unreplicated (heavy) DNA were fluorescently labelled and separately hybridised to microarray chips during a time course in S phase (Raghuraman et al., 2001). The relative abundance of replicated to unreplicated DNA (heavy/light ratio) through time identified regions of the genome where DNA replication initiated and hence ORIs, and it also allowed assessment of the temporal activation of ORIs during S phase. Using this approach, 332 ORIs were identified across the budding yeast genome. In the second study, chromatin from a synchronous population of replicating cells was immunoprecipitated (ChIP) using antibodies to MCMs (Mcm3, Mcm4, Mcm7) and ORCs (Orc1 and Orc1-6 complex) which were likely to bind specifically to ORI

sequences (Meselson and Stahl, 1958; Wyrick et al., 2001). The immunoprecipitated DNA was hybridised to microarray chips (ChIP/CHIP) and 429 binding sites, termed pro-ARSs were identified that co-precipitated with all the proteins mentioned. This method had the advantage that the location of pre-RCs could be identified but the disadvantage that replication timing could not be addressed. Also, not all pre-RCs have the potential to act as active ORIs, thus leading to false positives in ORI identification. The expected overlap between putative ORIs (regions with pre-RCs) and active ORIs was around 80 %. These two analyses were complemented by a third approach, which was based on the monitoring of the increase of DNA content from 1C to 2C on microarrays during a synchronous S phase and termed the monitoring method (Yabuki et al., 2002). 260 potential replication origins were identified across the genome, 112 of which were also active in the presence of HU, which suggests that they are activated early during S phase. A comparison between the different ORI identification/mapping techniques showed that a common set of 168 ORIs was identified which co-localised in all three approaches (Macalpine and Bell, 2005).

The 13.8 Mb genome sequence of fission yeast is distributed over three chromosomes and was published in 2002 (Wood et al., 2002). There are currently no results from microarray analyses on fission yeast DNA replication. However, relative A+T-richness was identified as a marker for ORIs and used in a bioinformatic algorithm to map 384 A+T-rich islands, 90 % of which were expected to co-localise with active ORIs (Segurado et al., 2003). ORIs in budding yeast and fission yeast have been exclusively

found in intergenic regions (Gomez and Antequera, 1999; Segurado et al., 2003; Dai et al., 2005), which suggests that gene expression interferes with DNA replication (Wyrick et al., 2001). Budding yeast ORIs preferentially localise to large intergenic regions (Wyrick et al., 2001), which may also apply to fission yeast ORIs (Segurado et al., 2003). In contrast to budding yeast (Macalpine and Bell, 2005), fission yeast ORIs favour intergenic regions that are flanked by two **5' UnTranslated Regions** (5'UTRs) that consist of promoters (Gomez and Antequera, 1999; Segurado et al., 2003). This suggested there could be a mechanistic relationship between DNA replication and transcription (Gomez and Antequera, 1999). Numerous examples from different eukaryotic systems indicate that the processes of DNA replication and transcription are functionally linked (reviewed in (Gilbert, 2002; Antequera, 2004; Cvetic and Walter, 2005)). Mammalian DNA replication frequently initiates upstream from promoters which consist of CpG-rich islands and were also found to be associated with ORC proteins (Delgado et al., 1998; Antequera and Bird, 1999; Ladenburger et al., 2002; Antequera, 2003). It has also been suggested in mammals that genes that are actively transcribed are replicated early in S phase (Hatton et al., 1988). Several microarray analyses that focused on the replication timing of human chromosomes confirmed these results for large transcription and replication domains (White et al., 2004; Woodfine et al., 2004; Donaldson, 2005; Jeon et al., 2005; Woodfine et al., 2005). In addition, microarray analysis of DNA replication in *Drosophila* chromosomes identified a correlation between the time of replication and the probability that a gene

is expressed (Schubeler et al., 2002; MacAlpine et al., 2004). This contrasts with findings from budding yeast where no such genome-wide correlation could be found (Raghuraman et al., 2001) but instead an interference between pre-RC formation and transcription of neighbouring genes during G_1 has been reported in a mathematical analysis which was carried out on the basis of microarray data (Alter and Golub, 2004). ORIs in budding yeast are activated throughout S phase in a temporal program (Friedman et al., 1997; Yamashita et al., 1997; Raghuraman et al., 2001; Wyrick et al., 2001; Yabuki et al., 2002). ORIs that fire at onset of S phase are classified as early ORIs, ones that fire towards the end of S phase as late ORIs. Centromeres in fission yeast and budding yeast are replicated early and telomeres late (Friedman et al., 1996; Raghuraman et al., 2001; Yabuki et al., 2002). A similar temporal program of ORI firing has been suggested in fission yeast (Kim and Huberman, 2001; Kim et al., 2003), indicating differential control of ORI activation in regions proximal to centromeric and telomeric heterochromatin. However, the number of ORIs analysed in fission yeast was small and the data used to assess replication timing in both studies was not clear. Further investigation is essential to verify these results in fission yeast.

In human cells, gene-rich euchromatin generally replicates early whereas gene-poor heterochromatin is replicated late in S phase (Woodfine et al., 2004; Woodfine et al., 2005). A picture emerges where the specification and the activity of ORIs are influenced by a combination of primary sequence determinants and epigenetic factors, probably involving nuclear positioning and acetylation state of the chromatin as well

as availability of nucleotide pools (Gilbert, 2001; Gilbert, 2001; Mechali, 2001; Melendy and Li, 2001; Gerbi and Bielinsky, 2002; Gilbert, 2002; Gilbert, 2002; Vogelauer et al., 2002; Anglana et al., 2003; Aladjem and Fanning, 2004; Antequera, 2004; Schwob, 2004). It has been suggested in *Xenopus* that these epigenetic factors become established in G_1 of the cell cycle after licensing of ORIs by pre-RCs when a temporal and spatial program for replication is put in place (Dimitrova and Gilbert, 1999). Experiments using a cell-free system of hamster nuclei in *Xenopus* egg extracts identified two stages that influence the subsequent DNA replication program in S phase: the timing decision point (TDP) and the origin decision point (ODP) (Dimitrova and Gilbert, 1999; Okuno et al., 2001; Li et al., 2003). According to these studies, the TDP determines the temporal sequence in which ORIs are activated during S phase and occurs about one to two hours after pre-RC formation, this coincides with chromatin remodelling in the nascent nucleus and is staged prior to the ODP (Gilbert, 2001; Li et al., 2001; Gilbert, 2002). The ODP was defined as the time at which a subset of ORIs is selected in a particular cell cycle (Wu and Gilbert, 1996; Wu and Gilbert, 1997; Okuno et al., 2001; Li et al., 2003). The ODP will have an impact on ORI efficiency, which depends on the pattern of ORI utilisation. The TDP may also affect ORI efficiency, because ORIs that are activated late during S phase may be inefficient due to passive replication from adjacent more efficient ORIs. Only the TDP has been shown to be associated with chromatin remodelling and to restrict early ORIs to euchromatic chromosome domains. The significance of the ODP in global selection of ORIs and the molecules involved in the

ODP and cell cycle regulated ORI selection are currently unknown. Neither ODP nor TDP seem to be required to regulate DNA replication and it has been speculated that these events are important for integration of replication with other chromosomal functions during development (Wu et al., 1998; Gilbert, 2001; Gilbert, 2002; Gilbert, 2002).

1.4 Endo-reduplication in Eukaryotes

Fission yeast is unusual amongst eukaryotes in that re-replication can be efficiently induced by multiple mechanisms, making it a valuable resource for the study into S phase regulation. This control is centred on the CDK Cdc2-Cdc13 and the major replication licensing factors Cdc18 and Cdt1 (Nishitani and Nurse, 1995; Fisher and Nurse, 1996; Nishitani et al., 2000; Yanow et al., 2001). CDK activity can be de-regulated by uncoupling S phase from mitosis in different mutant backgrounds. High Cdc2-Cdc13 activity is essential for cells to enter mitosis and to prevent re-licensing by inactivation of pre-RC components through phosphorylation. Several mutant alleles of Cdc2 and Cdc13 have been identified, which interfere with the normal dependency of S phase upon completion of mitosis resulting in repeated rounds of S phase without intervening mitosis and in the generation of polyploid cells (Broek et al., 1991; Hayles et al., 1994). If Cdc13 is removed, cells carry out rounds of re-replication with DNA contents of 64C and more (Hayles et al., 1994; Fisher and Nurse, 1996). Re-replication occurs approximately with the same periodicity as in a normal cell cycle, but without an intervening mitosis (Hayles et al., 1994). CDK activity can also be de-regulated by overexpression of the CDK inhibitor Rum1, which depletes cells of mitotic kinase activity thereby

preventing mitosis and promoting repeated rounds of DNA replication (Moreno and Nurse, 1994; Correa-Bordes and Nurse, 1995). Accumulation of up to 32C DNA in a single cell nucleus is the consequence. The overexpression of the licensing factor Cdc18 also results in repeated rounds of S phase in the absence of mitosis, this does not require ongoing protein synthesis of *cdc18* (Nishitani and Nurse, 1995). This results in DNA contents of up to 32C in a single cell nucleus. When Cdc18 is co-overexpressed with Cdt1, this effect is enhanced and DNA contents of up to 64C can accumulate in some cells (Yanow et al., 2001). It was found that re-replication in this background was due to re-licensing of ORIs, i.e. re-assembly of the pre-RC on ORIs which was not limited to S phase but could equally occur during G_2, promoting illegitimate firing of ORIs. Similarly, it has been shown that in *Xenopus* egg extract, the addition of recombinant Cdt1 to G_2 nuclei which were depleted of Cdt1 but not Cdc6, licenses DNA for new rounds of DNA synthesis (Maiorano et al., 2005). In fission yeast endoreplication can also be induced in cells with an Orc2 mutant allele that reduces binding of Cdc13 to ORIs (Wuarin et al., 2002), which indicates that this is an essential step in the control of the pre-RC (Cdc18/Cdt1) by CDK. These studies emphasise that Cdc18 is a crucial regulator for ORI licensing that is ectopically triggered when Cdc18 is overexpressed.

Re-replication occurs as a natural phenomenon in polyploid plant, arthropod and mammalian cells as well as in the selective amplification of genes during development (reviewed in (Edgar and Orr-Weaver, 2001; Tower, 2004; Claycomb and Orr-Weaver, 2005)). For instance, in

Drosophila repeated firing of one or more ORIs interspersed in eggshell (chorion) gene clusters results in up to ~60fold amplification of the DNA organised into an onion skin structure (Spradling, 1981; Delidakis and Kafatos, 1989; Claycomb et al., 2004). The increase in gene dosage provides large amounts of protein required in a small time-window during development. The process of gene amplification is a clear deviation from the "once per cell cycle" dogma for DNA replication initiation and there is increasing evidence that regulatory factors similar to those involved in inducing re-replication in fission yeast are responsible for controlled endoreduplication in metazoans (reviewed in (Tower, 2004; Claycomb and Orr-Weaver, 2005; Lilly and Duronio, 2005)). These have been mainly studied using the chorion gene amplification as an experimental system. Chorion amplification requires Orc2, CyclinE, Orc1, Dbf4, Cdt1, Mcm6 and several transcription factors which are essential for G_1/S transition. For instance, Cdt1 is essential for amplification and localises to the amplifying chorion gene loci, which is dependent on Orc2 (Whittaker et al., 2000).

Metazoans have evolved an additional safeguard to prevent re-replication, a protein called Geminin (McGarry and Kirschner, 1998), which is a negative regulator of Cdt1 and has not been found in budding or fission yeast. Geminin is low in G_1, accumulates during S and G_2, and forms a complex with Cdt1 as cells enter S phase to prevent loading of Mcm2-7 and re-licensing of ORIs (McGarry and Kirschner, 1998; Quinn et al., 2001; Tada et al., 2001; Mihaylov et al., 2002; Wohlschlegel et al., 2002; Cook et al., 2004; Maiorano et al., 2004). It is ubiquitinated by the APC/C and degraded during mitosis (McGarry and Kirschner, 1998;

Nishitani et al., 2001; Wohlschlegel et al., 2002). Inhibition of Geminin results in re-replication of DNA in *Drosophila* and mammalian cells mediated by accumulation of Cdt1 activity (Mihaylov et al., 2002; Melixetian and Helin, 2004; Zhu et al., 2004) which is analogous to the effect of Cdt1 overexpression in fission yeast (Nishitani et al., 2000). Interestingly, in Geminin mutants more intense overamplification is observed and ectopic amplifying loci appear (Tower, 2004). Considering the data from fission yeast, this identifies Geminin and Cdt1 as a crucial negative regulator for endoreplication in a normal cell cycle but as a positive regulator for developmentally regulated overamplification in an endocycle. Geminin has frequently been implicated in metazoan development (Kroll et al., 1998; Del Bene et al., 2004; Luo and Kessel, 2004). Hence, it may be that metazoans require additional mechanisms to co-ordinate DNA replication and cell proliferation during development, which might explain why no homologues of Geminin have been identified in the yeasts. Another essential complex that has been recognized to bind to *cis* acting sequences in the *Drosophila* chorion amplification locus (Beall et al., 2002) consists of the proteins Myb (**my**elo**b**lastosis), Mip130, Mip120, Mip40 and Caf1p55 (Peters et al., 1987). Mutants of these proteins reduce amplification probably by interference with their interaction with ORC on chromatin (Beall et al., 2002) and it has been speculated that Myb supports site-specific initiation at amplifying loci (Beall et al., 2004). Myb has been shown to interact with **h**istone **a**cetyl **t**ransferases (HATs) and **h**istone **d**eacetylase **c**omplexes (HDACs), indicating that chromatin remodelling plays a role in gene amplification. Involvement of HDACs in

developmental gene amplification is further supported by findings that a mutation in the HDAC gene rpd3 could lead to hyperacetylation across the genome thereby affecting acetylation patterns at ORIs and changing Orc2 distribution on chromatin and that this could as a consequence interfere with locus specific DNA amplification in the chorion amplification locus of *Drosophila* follicle cells (Aggarwal and Calvi, 2004).

In addition to *trans* acting regulators, several *cis* acting elements have been identified that are essential for efficient chorion amplification (Delidakis and Kafatos, 1989; Orr-Weaver et al., 1989). The ACE3 (**A**mplification **C**ontrol **E**lement, Chromosome **Three**) is a 320 bp long region which is highly conserved among four different *Drosophila* species and is required for high levels of amplification together with four distinct **A**mplification **E**nhancing **R**egions (AERs) and the actual replication origin, called ORI-ß (Tower, 2004). ACE3 has been shown to bind the Myb complex and both ACE3 and ORI-ß associate with ORC in vivo at A+T-rich sequences ((Austin et al., 1999; Tower, 2004) and references therein). The region also consists of additional ORIs which are used at lower frequency than ORI-ß. Amplification from ACE3 and ORI-ß is extremely sensitive to position effects and it has been suggested that positive interactions between transcription and DNA replication are required for developmental gene amplification (Lu and Tower, 1997). It is interesting that the structure of the chorion amplification locus resembles the ORI structure of the initiation zone seen in the mammalian DHFR locus (Linskens and Huberman, 1990; DePamphilis, 1999). This locus also contains multiple redundant ORIs which are stimulated by

transcriptional activity from the DHFR promoter (Saha et al., 2004). ORI ß within the hamster DHFR locus can also confer over-amplification (Milbrandt et al., 1981; Anachkova and Hamlin, 1989). This suggests that regulation and organisation of mammalian ORIs are similar to those found in the amplifying systems in *Drosophila* and it remains to be seen whether this similarity is also found in amplifying ORIs of the fission yeast Cdc18/Cdt1 re-replication systems (see Chapters IV and V).

1.5 Meiotic Cell Cycle Controls in Fission Yeast

Fission yeast cells become committed to go through the cell cycle in late G_1. Before this point (known as Start) the cell is able to undergo either of two different developmental programmes: the mitotic cell cycle or the meiotic cell cycle. The meiotic cell cycle is characterised by sexual development and the formation of spores. Haploid spores are produced either from a diploid cell or a zygote, the product of conjugation (Esposito and Klapholz, 1981; Yamamoto et al., 1997). In meiosis, two nuclear divisions take place but only one S phase occurs prior to the first nuclear division and is termed pre-meiotic S phase. Pre-meiotic S phase is followed by high levels of homologous recombination not seen in mitosis and is essential for introducing genetic diversity (Kleckner, 1996; Yamamoto et al., 1997; Fox and Smith, 1998). Interestingly, the time cells spend in pre-meiotic S phase is two to five times longer than mitotic S phase ((Williamson et al., 1983; Collins and Newlon, 1994) and references therein).

In fission yeast, this specialised cell cycle programme is achieved through differences in regulation compared with the mitotic cell cycle and

also involves meiosis specific proteins (reviewed in (Okayama et al., 1996; Murakami and Nurse, 2000; Marston and Amon, 2004)). Exit from G_1 into meiosis requires both nitrogen starvation and M or P factor pheromone, which together inhibit the activity of Cdc2 (Stern and Nurse, 1997; Yamaguchi et al., 1997; Kitamura et al., 1998; Stern and Nurse, 1998). The onset of S phase seems to be regulated by the same core DNA replication initiation proteins as in mitosis, including Cdc2, Cdc18, Mcm2, Mcm4, Mcm6 and Orp1, and reduced activity of these proteins prevent completion of DNA replication (Iino et al., 1995; Murakami and Nurse, 2001; Lindner et al., 2002). In addition, the Cds1 dependent checkpoint is activated in the presence of HU and cells arrest with no obvious DNA replication (Murakami and Nurse, 1999; Tonami et al., 2005). In fission yeast, it is currently unclear what mechanisms prevent a second round of S phase between first and second nuclear division, but data from *Xenopus* suggest that CDK activity is upregulated in this time window (Nakajo et al., 2000). This is consistent with the absence of fission yeast Mcm4 on chromatin during this period (Lindner et al., 2002).

It has been speculated that processes during replication may be directly linked to subsequent stages of recombination in meiosis. The formation of double strand breaks for recombination in pre-meiotic S phase in budding yeast is dependent on replication, but there is no correlation between the position of ORIs and double strand breaks (Borde et al., 2000). In fission yeast, it has been reported that the frequency of integration by homologous recombination at ORIs during mitotic S-phase was up to 50-fold higher than in other genomic regions, suggesting that

there could be a similar coupling mechanism in pre-meiotic S phase (Segurado et al., 2002). However, it has recently been shown that double strand break formation can take place without DNA replication if the S phase checkpoint is absent, indicating that replication and recombination in fission yeast is linked by checkpoint controls (Murakami and Nurse, 2001; Tonami et al., 2005).

1.6 Summary of Aims

The principle aim of my thesis was the genome-wide characterisation of ORIs in the fission yeast *Schizosaccharomyces pombe*, which included:

- The genome-wide mapping of ORIs in the mitotic and meiotic cell cycles, using microarray technology.
- Characterisation of ORI features in the mitotic and meiotic cell cycles in particular the efficiency of ORI utilisation.
- A comparative analysis between features that are similar or different in ORIs during the mitotic and meiotic cell cycles
- Bioinformatic analysis of ORIs including the search for consensus sequences.
- Genome-wide characterisation of DNA amplification in different fission yeast re-replication systems when CDK activity is inhibited or replication initiation factors are over-expressed.

Chapter II

Genome Wide Identification of DNA replication Origins in the Mitotic and Meiotic Cell Cycle

2 Genome Wide Identification of DNA replication Origins in the Mitotic and Meiotic Cell Cycle

2.1 Introduction

There is only limited information concerning the whole genomic organisation of ORIs in eukaryotes. Budding yeast is the only eukaryote where between 260 and 429 ORIs have been mapped on a genomic level using microarray approaches (reviewed in (Macalpine and Bell, 2005)). A much smaller number of ORIs has been studied in metazoan organisms where the complexity of genomes and ORIs has made it difficult to identify potential ORI sequences. A subset of 62 early firing ORIs was recently identified in *Drosophila* (MacAlpine et al., 2004). Some DNA replication timing profiles from microarrays are also available from human cells, but ORIs have not been mapped on a genome-wide level (Woodfine et al., 2004; Woodfine et al., 2005).

ORIs have been studied in the context of the mitotic cell cycle but little is known about ORI usage in the meiotic cell cycle. The only data available stems from a study restricted to six ORIs on Chromosome Six of budding yeast (Collins and Newlon, 1994). This study concluded that ORI position was generally the same in the mitotic and meiotic cell cycles.

Fission yeast ORIs are more complex than budding yeast ORIs and structurally more similar to metazoan ORIs. A subset of ~45 fission yeast ORIs has been physically mapped (Gomez and Antequera, 1999; Segurado et al., 2003). Genome-wide characterisation of ORIs is essential to enhance our understanding of the structure and function of eukaryotic

ORIs. The first aim of this chapter was to identify ORIs across the fission yeast genome to construct a physical map of ORIs used during S phase of the mitotic cell cycle. The second aim was to map the locations of ORIs in pre-meiotic S phase and to compare ORI position and usage during mitotic and meiotic DNA replication.

2.2 Results

2.2.1 Evaluation of Microarrays for Origin Mapping

The technique of microarray analysis has been used in post genomic projects for whole genome mapping of ORIs in *S. cerevisiae* and to map a subset of 62 ORIs in *Drosophila* (MacAlpine et al., 2004). Different experimental approaches for microarray analysis of DNA replication and identification of ORIs have been described. I decided to evaluate the monitoring method which was successfully applied for genome-wide identification of ORIs in *S. cerevisiae* (Yabuki et al., 2002). The increase in signal ratio from one to twofold is monitored using microarrays as the copy number of DNA sequences increases from 1C (unreplicated) to 2C (fully replicated) during a synchronous S phase of the cell cycle in a large population of cells. The principle of this approach is outlined in Figure 4. Experimental DNA (replicating) and reference DNA (unreplicated) are differentially labelled using the two colour assay and co-hybridised to microarrays. DNA sequences proximal to ORIs will be replicated first (red) and these sequences will be more abundant than sequences that are distal to ORIs (green). At the same time, signals will increase with time at probes where the replication fork passes through. Hence, hybridisation signals will reflect the relative abundance of DNA sequences. This should

result in a DNA replication profile similar to the one shown in the plot in Figure 4. Peaks should correspond to areas where DNA replication starts and therefore mark the positions of ORIs as indicated.

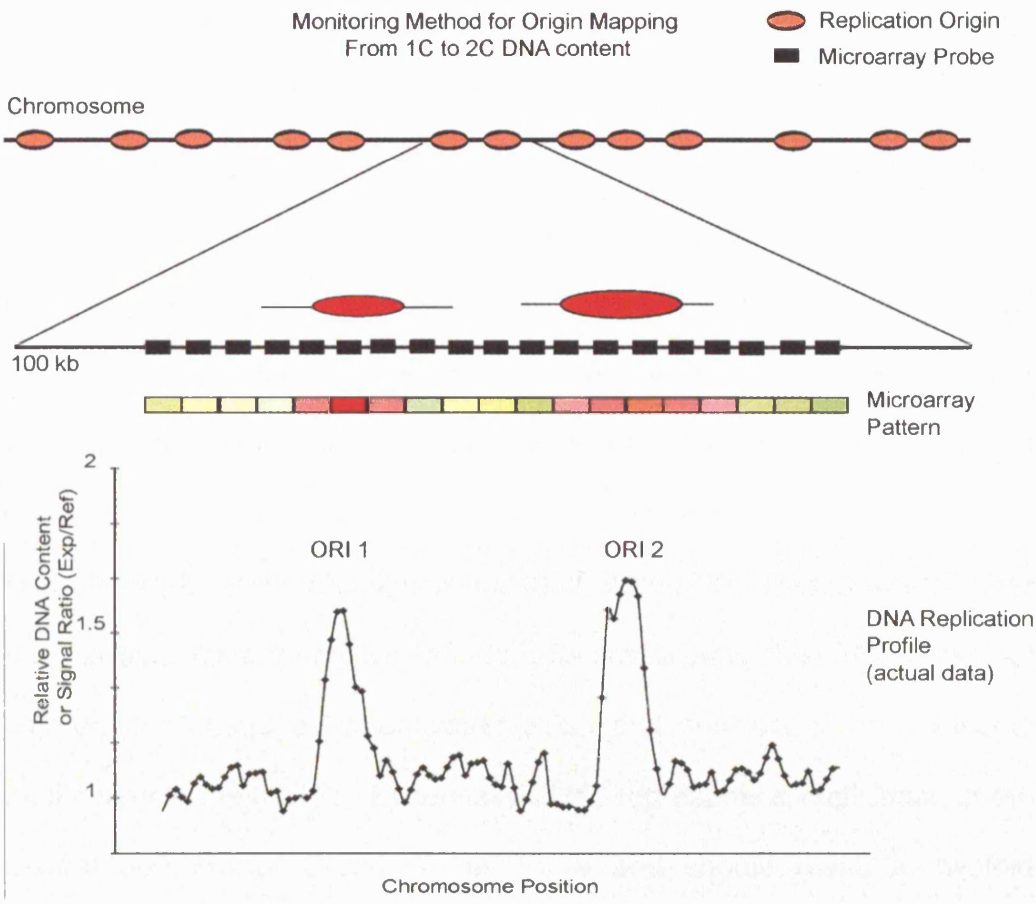

Figure 4: Monitoring Method for ORI Mapping

Top diagram: Schematic distribution of ORIs on a chromosome and the distribution of microarray probes across two ORIs in a 100 kb region (not drawn to scale)

Middle diagram: Microarray pattern of probes as a result of monitoring DNA replication; green probes correspond to DNA sequences that are unreplicated (or bulk replication), red probes to DNA sequences that are more abundant (replicated).

Bottom diagram: Translation of the microarray pattern into relative signal ratios between experimental (replicating) and reference (unreplicated) DNA.

Traditionally microarrays have been employed in gene expression studies to observe increases in the abundance of transcripts of twofold and above. For the monitoring method to work, the microarrays (see Materials and Methods) had to be sensitive enough to follow changes in signal ratios between one and two fold. The preparation of transcripts for microarray hybridisation results in a relatively high signal to noise ratio. This is because cDNA has to be synthesised during the labelling procedure which introduces some variability in the relative abundance of a particular sequence dependent on the efficiency of the reverse transcription. A much smaller signal to noise ratio has been observed when labelled DNA is hybridised to microarrays. Small increases in signal ratios between one and two could be distinguished in previous studies (Yabuki et al., 2002; Macalpine and Bell, 2005). To assess whether our microarrays were sensitive enough for monitoring less than twofold differences, I used a fission yeast strain that consists of an additional minichromosome (CH16). Essentially CH16 represents a duplication of the central 500 Mb of Chromosome Three and should result in twofold increases in signal ratios on the microarrays. A genetic cross was carried out to incorporate the temperature sensitive cdc25-22 allele into the minichromosome strain. Upon temperature shift to the restrictive temperature of 36.5 °C, the cdc25-22^{ts} allele blocked cells in G_2 of the cell cycle with a 2C DNA content. DNA from G_2 blocked cells lacking CH16 was used as a reference for differential hybridisation to microarrays. Two types of microarrays were evaluated: ORF microarrays, covering the coding regions of the fission yeast genome, and intergenic microarrays,

covering all non-coding regions. The result of this analysis is illustrated in Figure 5A/B. Both the intergenic and the ORF microarrays were sensitive enough to map the duplicated region, highlighted in red in Figure 5A. Figure 5B gives a more detailed view of the signal ratios from the ORF microarray across Chromosome Three. The average signal ratio for the minichromosome CH16 co-ordinates was 1.8 on ORF and intergenic microarrays and was reproducible in two experimental repeats. This signal ratio was 20 % short of the expected signal ratio of two for a duplicated region, and further analysis and discussion of this point is presented in Chapter III. However this experiment established the high sensitivity of the microarrays and the reproducibility of the microarray signals, which was considered to be sufficient to detect significant increases in the abundance of replicated DNA sequences. I thus decided to use both the ORF and intergenic microarrays and the monitoring method for genome-wide mapping of fission yeast ORIs.

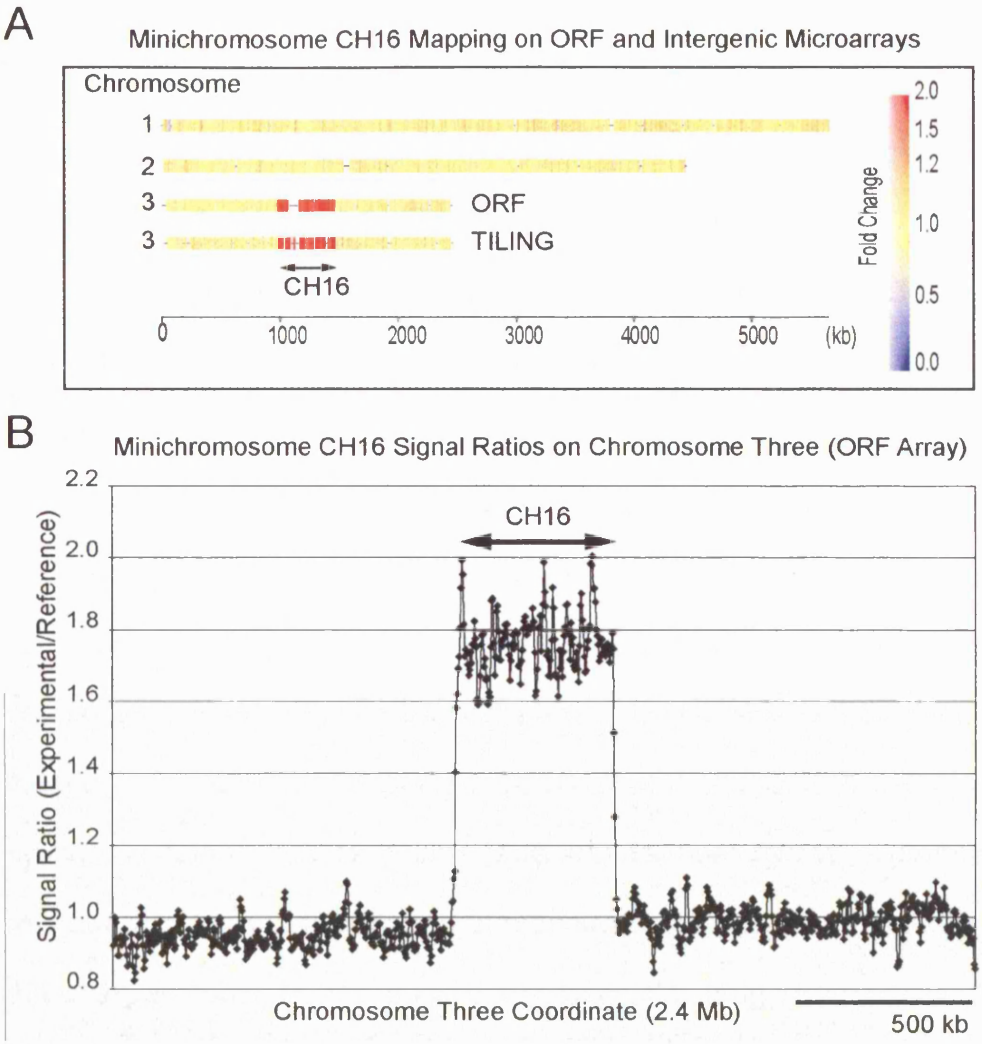

Figure 5: Evaluation of Microarrays for ORI Mapping
Signal ratios were calculated as the average of three neighbouring ratios (moving average). The Minichromosome CH16 strain HM248 (Niwa et al., 1989) was crossed with cdc25-22^{ts}. Cells were grown exponentially and blocked in G_2 by temperature shift from 25°C to 36.5°C for 3.5h and harvested. DNA from a cdc25-22^{ts} strain lacking CH16 was used as a reference for differential hybridisation to microarrays. The area to which CH16 maps is shown in red in (A) and exhibits signal ratios around 1.8fold (B).

2.2.2 ORI mapping in mitotic S phase

To identify ORIs during the mitotic cell cycle, cells were synchronised using the temperature sensitive cdc25-22 mutant strain that blocks cells in the G_2 phase of the cell cycle at the restrictive temperature of 36.5 °C. Cells were released from G_2 by shifting the temperature to 25 °C after 3.5 hours (Figure 6A). These cells entered a highly synchronous S phase after completing mitosis and G_1 of the cell cycle (Figure 6B(left panel) and Figure 6D). Two different experimental approaches were used to map ORIs. In the first approach DNA samples were taken at 5 to 10 minute intervals during S phase. This experiment will be referred to as the time course experiment (Figure 6B, left panel). First a pilot experiment was carried out to establish experimental conditions and assess the level of synchrony during the time course. This was followed by two experimental repeats. A total of 54 ORF and intergenic microarrays was used for the three experiments. In the second approach the drug hydroxyurea (HU) was added to cells before release from G_2. HU is an inhibitor of ribonucleotide reductase, which leads to depletion of the dNTP pool in cells. Replication forks stall several kilobases away from the initiation point thus confining DNA synthesis to the vicinity of ORIs (Pasero et al., 2002). The result is a cell cycle block in early S phase without a noticeable increase in DNA content (Figure 6B, right panel). This HU block was reversible and cells completed DNA replication after HU wash out at 120 minutes into the block. This is indicated by a shift of the FACS peak from 1C (cells accumulate due to cell division starting at 90 minutes) to 2C DNA content. This experiment will be referred to as the HU experiment. Again a

pilot study was initially conducted and three experimental repeats were used for further analysis. A total of 29 microarrays was used for this experiment. DNA from samples taken in either experiment was differentially hybridised to the microarrays. Unreplicated DNA from G_2 blocked cells served as a reference sample in both types of experiment. For the time course experiment, raw signals from microarrays were normalised (Lyne et al., 2003) and scaled on the basis of factors obtained from a logistic curve derived from the flow cytometry profile during the time course (Figure 6C). The relative DNA content was plotted as a function of time for each probe and a sigmoid regression was fitted. An example of the regression analysis for the probes that map to the previously characterised ORI ars2004 is shown in Figure 7. This demonstrates that the shape of the regression changes and is dependent on whether a segment is replicated earlier (shift to left) or later (shift to right) during S phase. The time at which 50 % of each probe along the chromosomes became replicated was determined from the regression analysis. The results from two experimental repeats were averaged and a replication profile of time versus chromosome position was plotted.

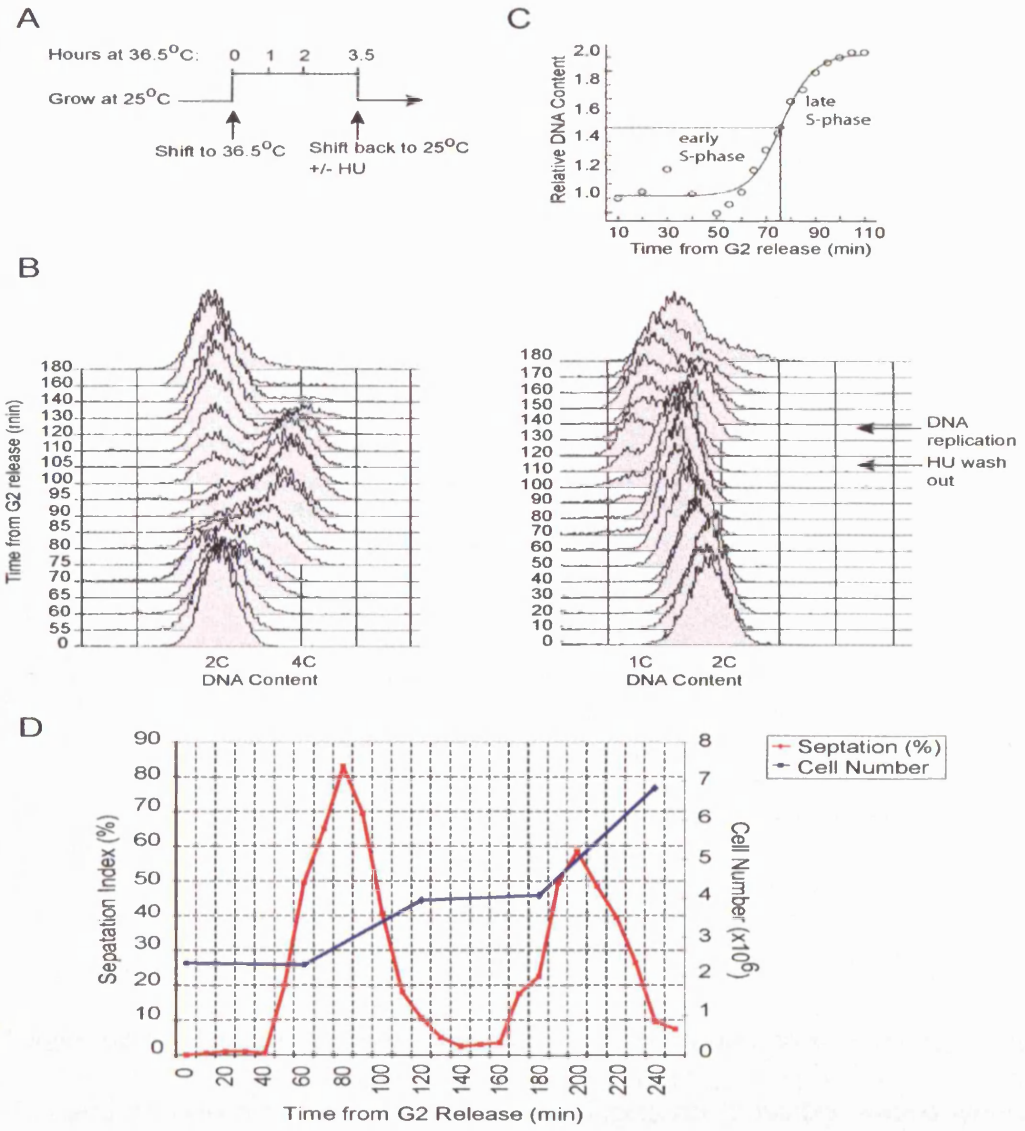

Figure 6: Synchronising Cells in Mitotic S phase

(A) Cdc25-22^{ts} block/release experiment (see text/Methods). (B) Cell cycle profile of a synchronous mitotic S phase with (left panel) or without(right panel) HU. To measure DNA content by flow cytometry analysis, samples were taken at release (time 0) and at 5 minute intervals throughout S phase in the time course experiment. DNA content increases from 2C to 4C. For the HU experiment, samples were taken every 10 minutes for analysis of DNA content. HU was washed out after 120 minutes into the block. Cell division in fission yeast occurs in early G_2 phase after DNA replication. Division in both experiments follows the peak of septation (D) around 90 minutes from G_2 release. The peaks shift to the left as cells divide. (C) Replication kinetics of a synchronous culture. Signals from (B) were converted to relative DNA content, a logistic curve was plotted and used for scaling of microarray signals at respective timepoints during S phase. DNA replication took place between 55 and 100 minutes after release. The time at which half the DNA was replicated (as indicated) was determined for each probe to construct a replication profile (see figure 4). (D) Septation index and Cell Number. The peak of septation with 80 % at 80 minutes in the first cell cycle precedes doubling of cell number and gives an estimate of cell synchrony.

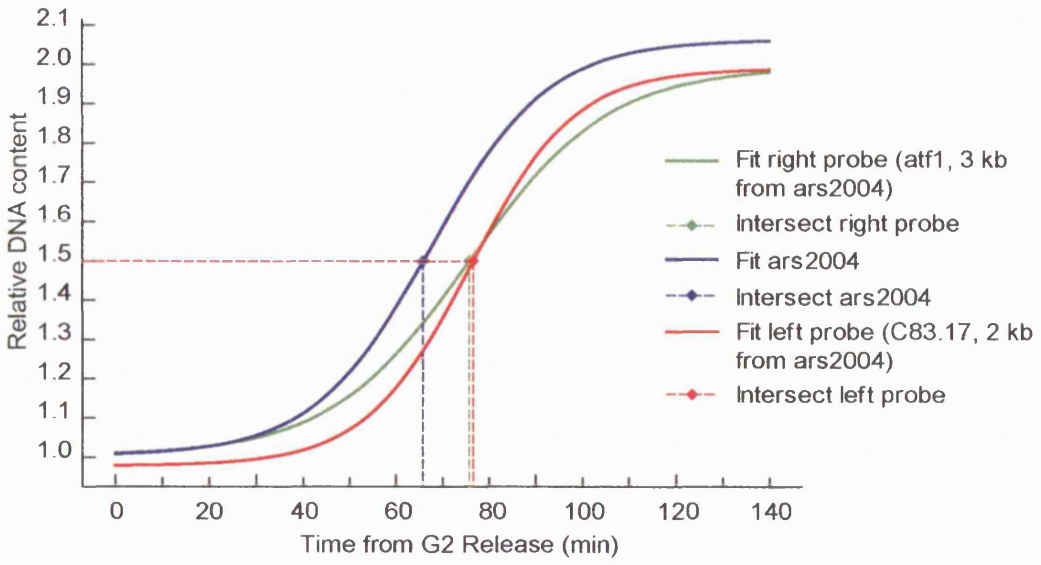

Figure 7: Regression Analysis for determining Replication Timing of ORI2004
The relative DNA content for the DNA segment corresponding to each microarray probe was plotted as a function of time during synchronous progression through S phase. The central probe for ars2004 and two adjacent probes (left and right to central probe) are shown. Analysis of these plots identified the time point at which each segment became 50 % replicated.

Replication profiles for all three chromosomes are shown in Figure 8. Peaks on the profile indicate regions along the chromosome that replicate first and therefore the location of ORIs, troughs are possibly places where replication forks meet, which are replicated at a later stage during S phase. Peaks were considered to correspond to ORIs only if they replicated at least three minutes faster (calculated from averaged time course data) than adjacent regions and were reproducible in both experimental repeats. This threshold was defined as a percentage of the total time it took for DNA replication. The bulk of DNA was replicated within 12 minutes as calculated from the replication profiles in Figure 8. A three minute time difference thus corresponds to a 25 % difference in timing. In addition peaks were only considered if they were clearly defined

in both experimental repeats. Using these strict cutoff criteria, it was expected that some ORIs were overlooked. However, this strategy was important to avoid the identification of false positives. For the HU experiment, a single time point 90 minutes after release from G_2 was analysed for ORI mapping. This experiment allowed mapping of ORIs at a higher resolution, as fork migration was much reduced. ORIs were only mapped if a peak was described by at least three contiguous probes that showed a hybridisation ratio above 1.1 (see Methods). This meant that this stretch of DNA sequence was at least 10 % more abundant than flanking sequences. The results of the HU experiment for all three chromosomes are shown in Figure 9. The signal ratio from the 90 minute time point was plotted against chromosome position. A typical 300 kb region for both experiments is shown in Figure 10A/B. Results were highly reproducible as demonstrated in Figure 10A, which shows a triplicate repeat of the HU data. Here nine ORIs from defined peaks were identified as well as a region of ~30 kb that was significantly above the threshold, but did not present distinct peaks. The overlay of the two experiments (Figure 10C) shows that the nine ORIs identified in the HU experiment are all marked by peaks in the replication profile of the time course. In addition, the 30 kb region now resolves into three independent peaks in the replication profile resulting in a final score of 12 ORIs for the 300 kb region. Combining the data sets of the two experimental approaches, a total of 401 peaks were detected that were reproducible and above the defined threshold. An additional 503 peaks that were clearly defined by at least five contiguous probes but with signal ratios below 1.1 were

identified in the HU experiment. These peaks were reproducible in the three experimental repeats and I concluded that they mostly correspond to inefficient initiation events (Figure 37A and Figure 39). Because it was not certain that they were all ORIs, they were excluded from further analysis at this stage, but I will consider them further later in the Results. 308 or 77 % of peaks were identified in both, the time course and the HU experiment. The remaining 93 peaks were clearly observed in the time course experiment but showed no signal increases in the HU experiment that qualified the threshold criteria. A complete ORI map is shown in Figure 11. A comprehensive annotated list of ORIs can be found in the Appendix.

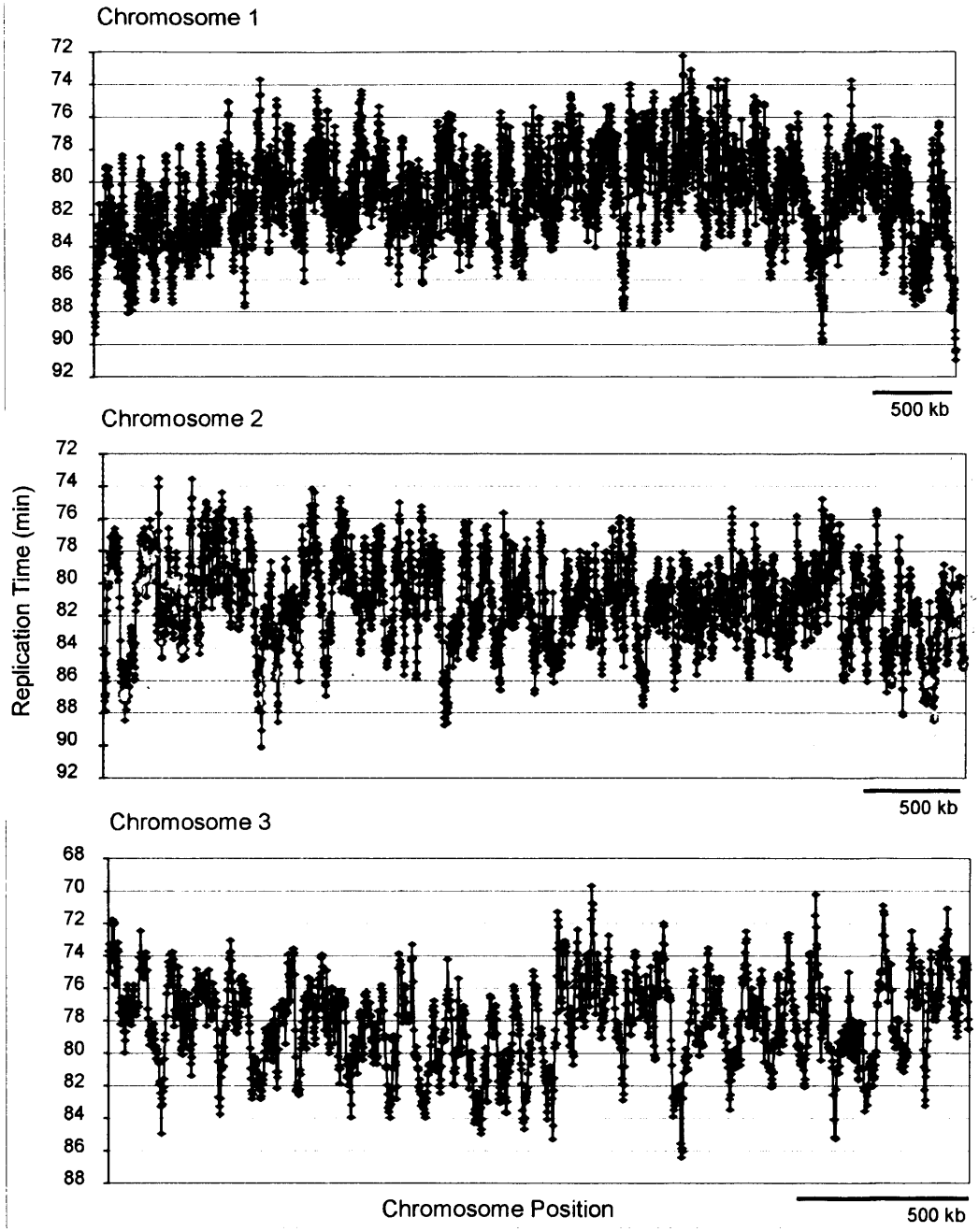

Figure 8: Genome Wide DNA Replication Timing Profiles
The time at which 50 % of each probe was replicated was plotted against chromosome position for the three fission yeast chromosomes. Peaks are regions that replicate early during S phase and are markers for ORIs. Troughs are possibly places were replication forks meet and mark areas between active ORIs. The chromosomal regions covered on the plots are as follows: Chr1 (~5.6 Mb), Chr2 (~4.5 Mb), Chr3 (~2.4 Mb).

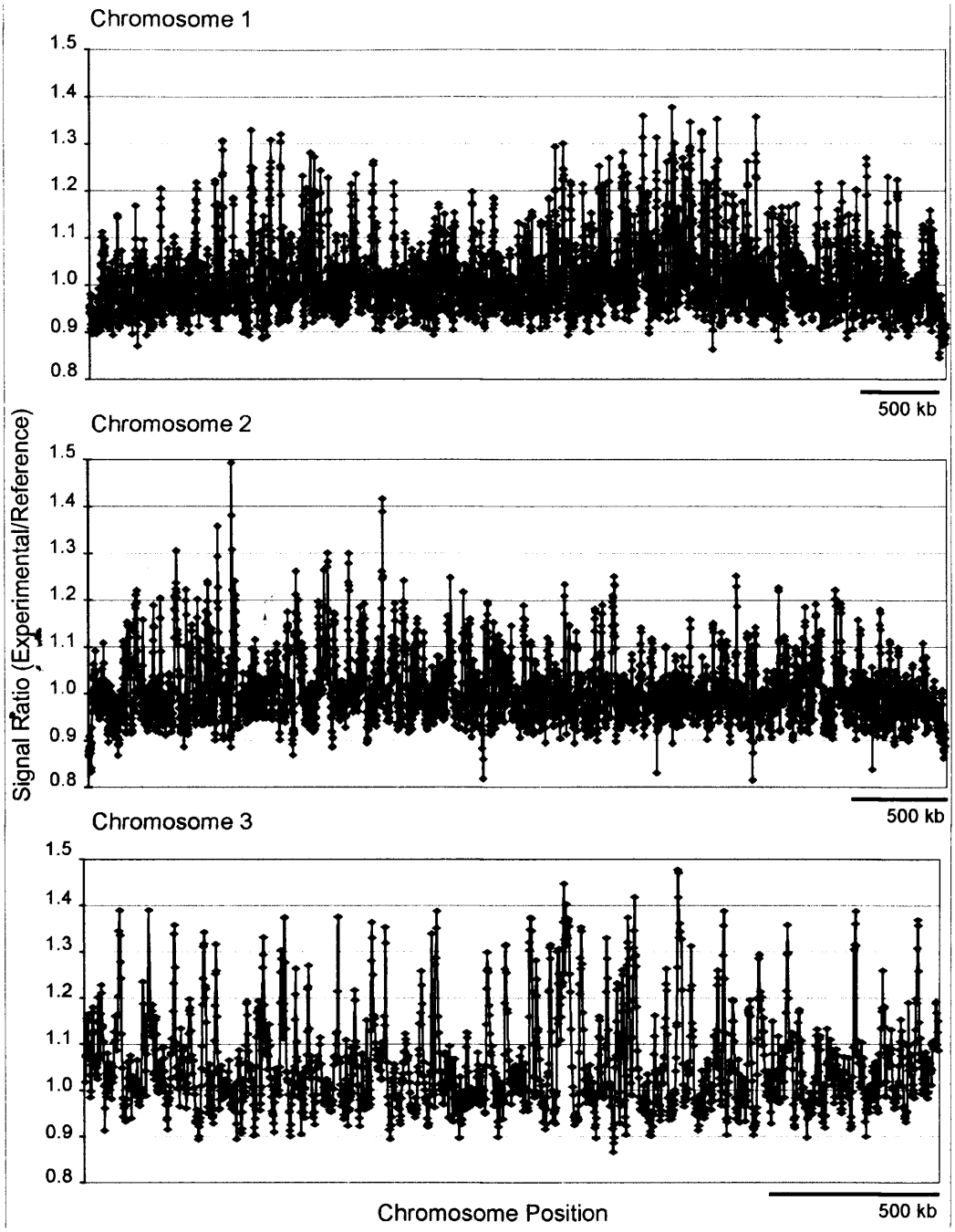

Figure 9: Genome Wide DNA Replication Profiles
The normalised signal ratios from the 90min time point were plotted against chromosome position for the three fission yeast chromosomes. Signal ratios around 1 indicate that there is no DNA replication in this region. Peaks appear in areas where DNA is replicated and are markers of ORIs.

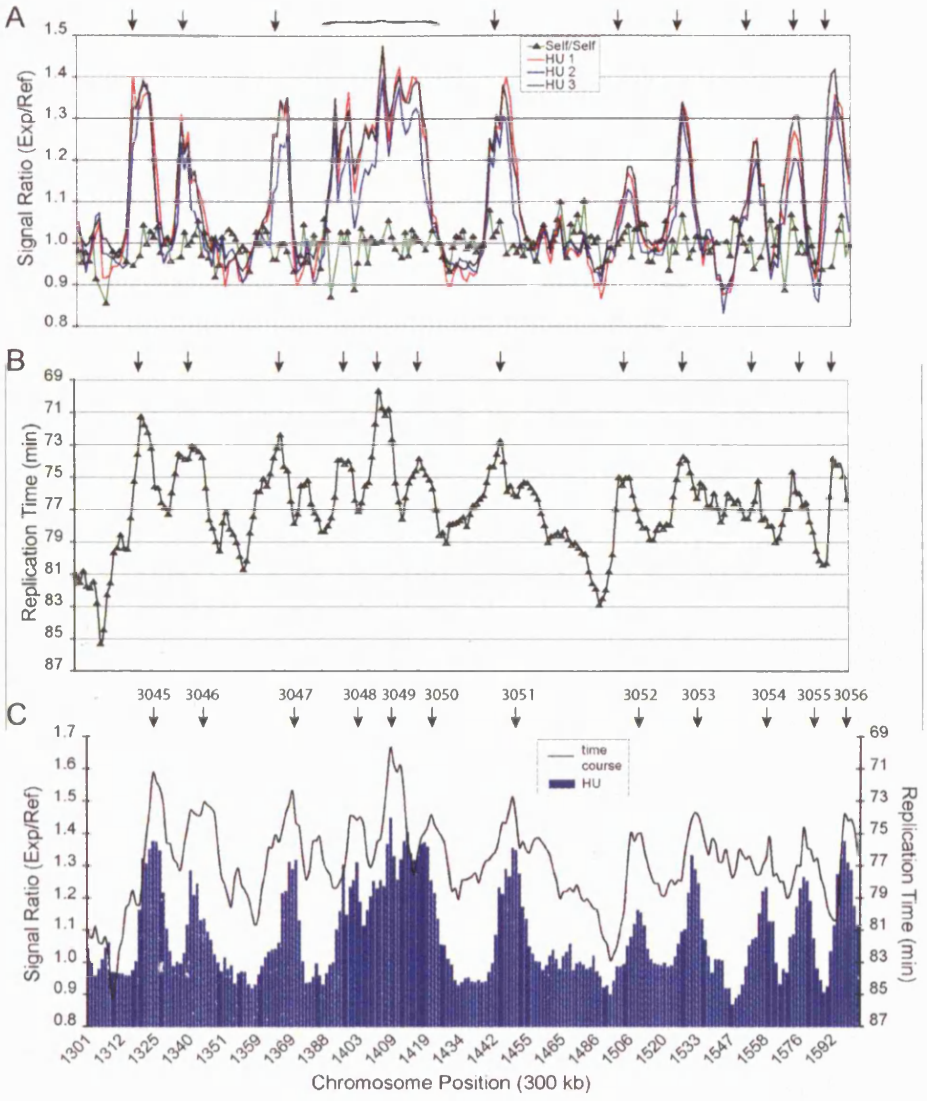

Figure 10: Mapping Origins of DNA Replication in Mitosis
(A) Replication profile of a 300 kb region of Chromosome Three in triplicate for the HU experiment. DNA extracted from G_2 blocked cells (2C, reference) and cells at 90 minutes into the HU block (2C – 4C, experimental) was differentially labelled with dCTP-Cy3 or dCTP-Cy5 as described in Methods and co-hybridised to ORF and intergenic microarrays. The signal obtained for each probe was normalised and plotted against chromosome position. The centre of peaks defines the area that is most replicated and therefore marks the position of ORIs (arrows). The bracket indicates the position of an initiation zone. The green line (signal ratios around 1) corresponds to data from a self/self hybridisation (control of unreplicated vs. unreplicated G_2 blocked DNA). (B) Replication timing profile for the time course experiment of the same region as in (A). DNA was extracted from cells at 5 to 10 minute intervals during S phase, differentially labelled and co-hybridised with G_2 DNA as in (A). Microarray signals were scaled and normalised and the time at which 50 % of each probe was replicated was determined (as described in Methods) and plotted against chromosome position. Centres of peaks indicate probes that replicate first, which mark ORIs (arrows).(C) Overlay of averaged signal of HU experiments (A) and averaged signal of the time course experiments (B). Arrows indicate the position of ORIs. For complete ORI maps of all three chromosomes see Appendix.

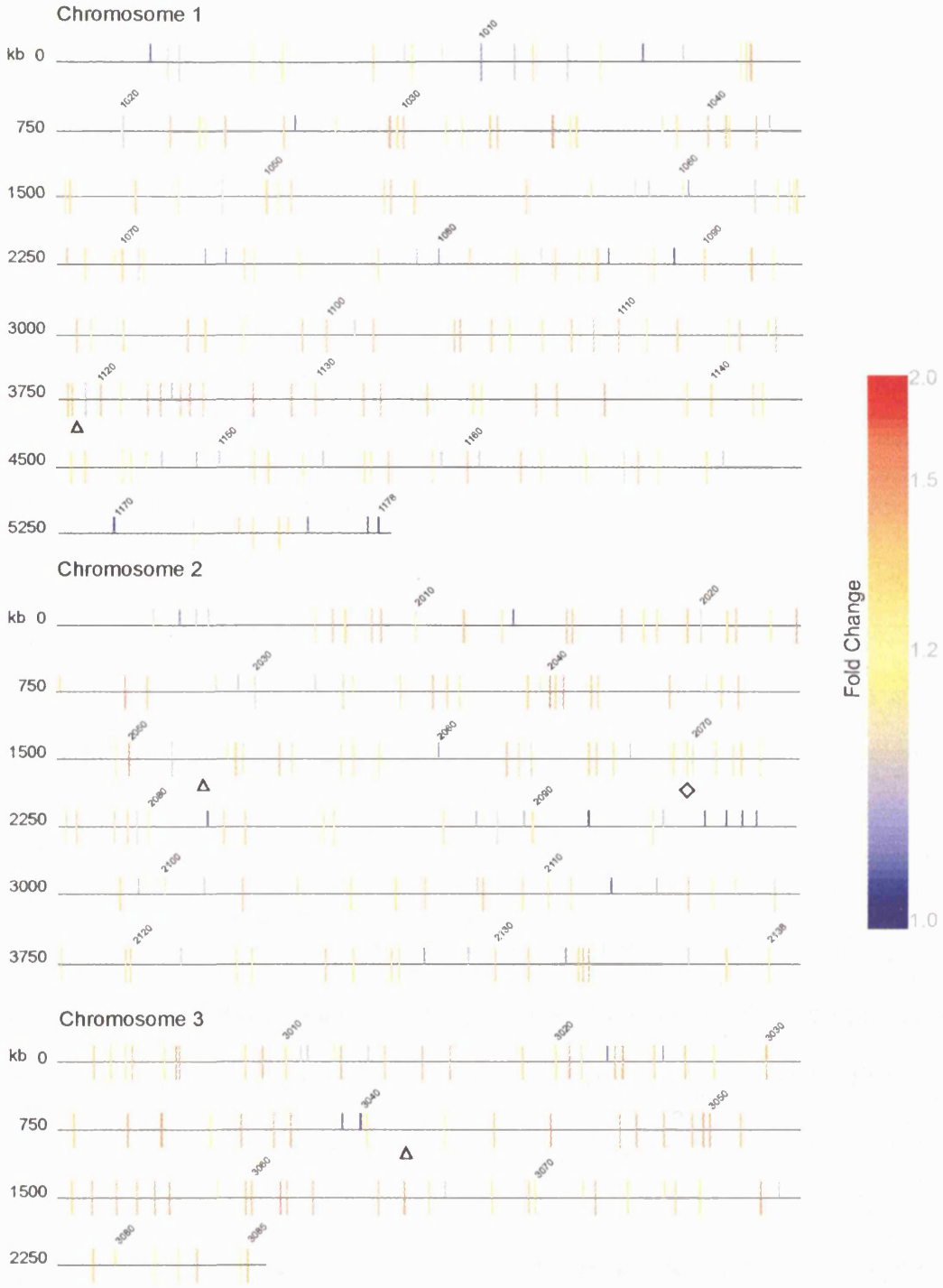

Figure 11: Whole Genome Origin Map of Fission Yeast
ORIs from the time course experiments are outlined above the line, ORIs from the HU experiment below the line. The chromosome position is indicated on the left of the diagram. The colour code on the right of the diagram indicates the average signal ratio obtained for ORIs from the 90 minute time point in HU. The centromeres are marked by a triangle (Δ), the mating type locus by a square (◊).

To validate the mapping data I checked whether 35 ORIs previously characterised by two dimensional neutral/neutral agarose gel electrophoresis analysis (2D-gel analysis) (for example of 2D-gel Southern blot see Figure 24) had been identified on the microarrays (Gomez and Antequera, 1999; Segurado et al., 2003). Thirty-two out of the 35 (89%) 2D-gel ORIs co-localised with ORIs from the present analysis. The three ORIs 2067, 2080 and 2096 (Segurado et al., 2003) not identified, were defined by small peaks indicative of weak ORI activity and were found amongst the 503 weak peaks. Interference with closely spaced ORIs could have reduced the signal ratios obtained for ORI2080 and ORI2096, which are both flanked by nearby ORIs on the replication profiles. I also checked for the presence of pARS747, pARS744, pARS745, pARS772, pARS767 and pARS727 (Maundrell et al., 1988), which were initially identified by a screen for autonomously replicating sequences (ARS). These are small genomic DNA fragments that confer high frequency of transformation when cloned into a plasmid lacking an ORI sequence, which suggests that these fragments have ORI function. pARS747 was not considered since it maps to subtelomeric regions poorly covered by the microarrays. Three of the pARS fragments, pARS744, pARS772 and pARS767 (see Figure 12A) were identified in the present analysis. pARS727 and pARS745 did not show significant signal peaks, but pARS745 is found amongst the 503 peaks with a signal ratio below 1.1. The DNA sequence of pARS727 has been shown to be passively replicated from adjacent ORIs in its genomic context (Kim and Huberman, 2001), which is consistent with the absence of an ORI on the replication

profiles. A+T-rich island 1156, shown to be negative for ORI activity by 2D-gel analysis was identified as an active ORI in both the time course and HU experiments as shown in Figure 12B. The mean difference in the chromosomal position of ORIs mapped in this study and corresponding ORIs mapped by 2D-gel analysis was 1.36 kb (Table 1). I can conclude that our experimental approach for ORI mapping was effective in identifying almost 90 % of previously characterised ORIs.

I then compared our ORI data with results from an earlier genome-wide bioinformatic analysis (Segurado et al., 2003). This analysis suggested that ORIs in fission yeast are defined by A+T-rich islands that have at least 72 % AT content across a 1000 bp window. 384 A+T-rich islands were identified exclusively in intergenic regions, a subset of which was confirmed via 2D-gel analysis to consist of active ORIs. Of these 384 putative ORIs, 324 mapped to regions in the genome covered by the microarrays. Some of these were very close together and so grouped into 296 distinct ORI regions (see Methods), of which 257 or 87 % co-localized with microarray ORIs. Examples of ORIs identified in both experimental approaches are shown in the replication profiles of three chromosomal regions in Figure 12. These plots show 24 ORIs of which 19 co-localised with A+T-rich islands. The mean difference of the chromosomal position between the corresponding ORIs in the two data sets was 1.56 kb. Only 10 ORIs out of the 257 matches showed differences greater than 5 kb. Of the 144 ORIs (401 minus 257) which were not predicted by the bioinformatic approach, the majority (113 ORIs) mapped to regions with AT contents of 72 % or above using a 500 bp window, which is an AT

content that is above the intergenic average of 69.4 % (Dai et al., 2005). Many of these ORIs would have been missed due to the stringent cutoff criteria employed in the bioinformatic analysis, where A+T-rich islands were defined by AT levels at or above 72% in a 1000 bp sliding window. This leaves only 31 ORIs, which map to intergenic regions with AT contents below 72 %, 16 of which were active in the presence of HU. It has been recently shown that intergenic regions in fission yeast can be active in a plasmid maintenance assay if they consist of AT levels above 70 % (Dai et al., 2005) which included 20 of the 31 ORIs. The remaining 11 ORIs had AT levels which normally do not promote ORI activity, yet 7 of them were also active in the presence of HU. I conclude that the comparison with the bioinformatic analysis shows that AT richness is a good predictor for ORI activity, although the threshold of a window size of 1000 bp for a 72 % AT richness may have been too large.

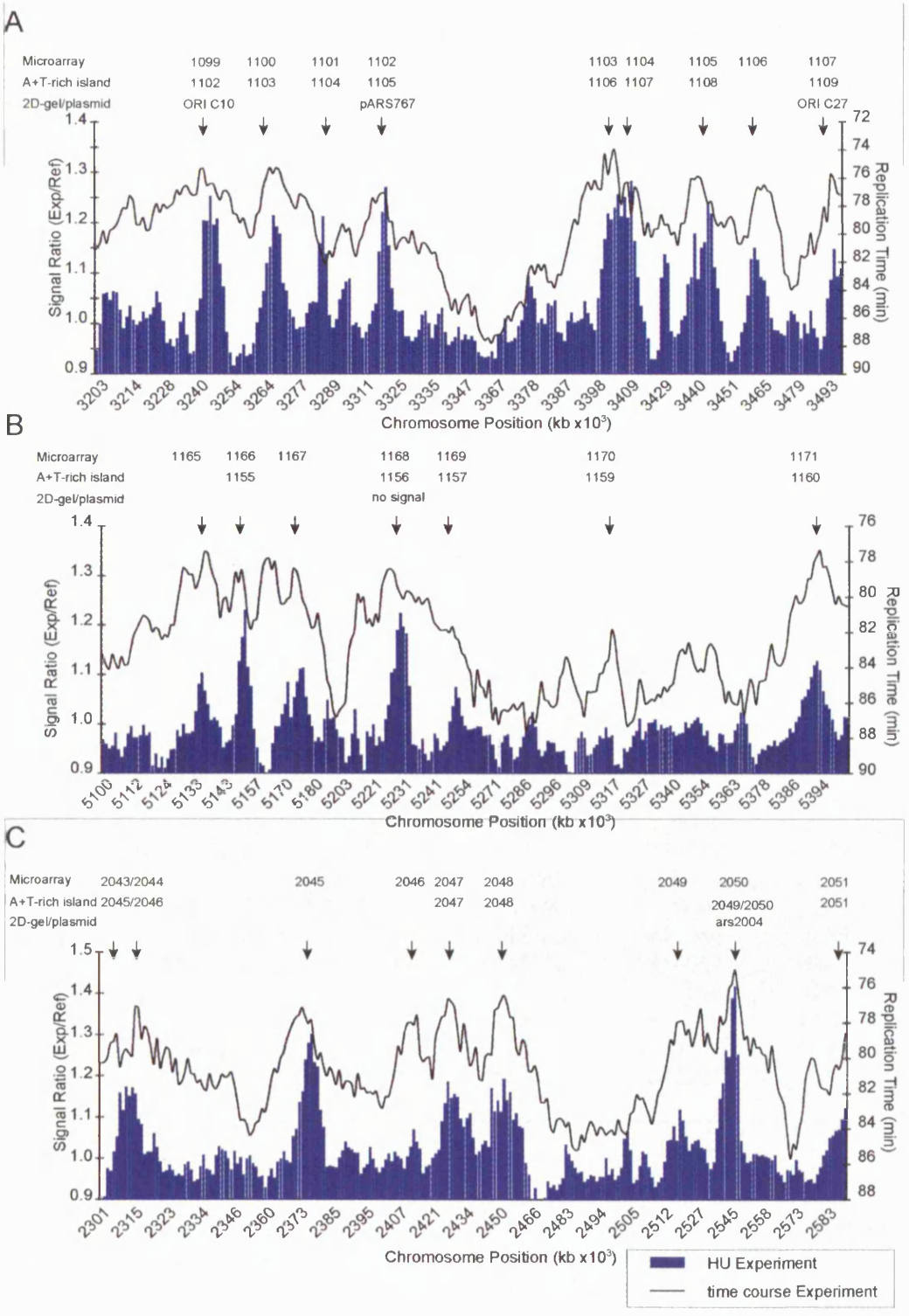

Figure 12: Co-localisation of previously identified ORIs and Microarray ORIs
The location of ORIs in two different 300 kb regions of Chromosome One (A/B) and a 300 kb region on Chromosome Two (C) is indicated with arrows. The published name for ORIs that were identified previously, either by 2D-gel analysis or plasmid maintenance assays and/or the bioinformatic analysis (A+T-rich island), is indicated. Microarray ORI1168 corresponds to A+T-rich island 1156, which did not show a signal by 2D-gel analysis.

Chromo-some	Microarray Name	2D-gel Name	2D gel Map Position (bp)	Microarray Map Position (bp)	Δ Map Position (bp)
I	ORI1002	AT1015	112691	113896	-1205
I	ORI1006	AT1024	326263	326001	-263
I	ORI1018	ORI12	715023	713564	-1460
I	ORI1027	AT1041	1027173	1021911	-5262
I	ORI1030	ARS1	1096418	1095332	-1086
I	ORI1063	ORI18/ORIJ	2228454	2230761	-2307
I	ORI1075	RIP1	2440400	2442981	-2582
I	ORI1095	ORI76	3060754	3060522	-232
I	ORI1099	ORI C10	3246134	3245826	-308
I	ORI1107	ORI c27	3498495	3496579	-1916
I	ORI1131	ORI19	4066594	4064746	-1848
I	ORI1136	PCR1	4248917	4248673	-244
I	ORI1162	ORI22	5019371	5019237	-134
I	ORI1163	AT1153	5040652	5041297	-645
II	ORI2012	AT2022	448400	448811	-411
II	ORI2018	AT2026	603402	606100	-2698
II	ORI2039	AT2041	1255510	1255476	-34
II	ORI2042	ORI C7	1278257	1280407	-2150
II	ORI2050	ars2004	1546335	1546892	-557
II	ORI2068	ORI75	2118076	2117792	-284
II	ORI2073	AT2072	2187624	2188311	-688
II	ORI2091	Tug1	2791938	2794668	-2731
II	ORI2092	Rum1	2800977	2799811	-1166
III	ORI3006	ars3003	119903	119903	0
III	ORI3007	ars3002/3004	123489	123154	-336
III	ORI3049	AT3043	1411604	1410248	-1356
III	ORI3050	AT3044	1417525	1418087	-562
III	ORI3061	AT3053	1719140	1721086	-1946
III	ORI3064	ORI C11	1823251	1818815	-4436
III	ORI3065	nmt1	1841649	1843891	-2242
III	ORI3066	AT3058	1867575	1868681	-1107

Table 1: Comparison of 2D-gel and Microarray mapped ORIs
ORI position is given in bp counted from the left arm of each chromosome. 2D-gel data from the following publications was used: (Gomez and Antequera, 1999; Segurado et al., 2003). Only ORIs that were covered by the microarrays were considered. The analysis does not include ORIs that were mapped by plasmid maintenance assays only (pARSs) and ORIs that were shown to be negative for ORI activity by 2D-gel analysis.

2.2.3 ORI mapping in pre-meiotic S phase

Very little is known about the ORI firing program in eukaryotic cells in pre-meiotic S phase and there is currently no data available from fission yeast. In this organism, pre-meiotic S phase follows conjugation of two haploids and is itself followed both by high levels of recombination and a different pattern of chromosomal segregation, which distinguishes it from mitotic S phase. To investigate whether changes in ORIs might contribute to these differences, ORIs were mapped during pre-meiotic S phase. First, cells were synchronised using the temperature sensitive pat1-114 diploid mutant strain (Mata et al., 2002). Nitrogen starved cells accumulated in the G_1 phase of the cell cycle, and entered a highly synchronous meiosis upon temperature shift to 34 °C (Figure 13). Cells were released into pre-meiotic S phase either in the presence or absence of HU and replication profiles were constructed as described for mitotic S phase in 2.2.2. The results for Chromosome Three from the time course and the HU experiment are shown in Figure 14A/B. A 300 kb region from Chromosome Three is shown in Figure 14C. Peaks on the two profiles co-localised and seven ORIs could be identified. Next, the results from the mitotic and meiotic time course experiments were compared to identify any differences in ORI firing patterns (Figure 15). Again, peaks on the two profiles co-localised, which means that all seven ORIs mapped in meiosis are also active in mitosis. However, the mitotic ORI3034 was not identified on the meiotic profiles, which suggests that this is silent or very inefficiently used during pre-meiotic DNA replication.

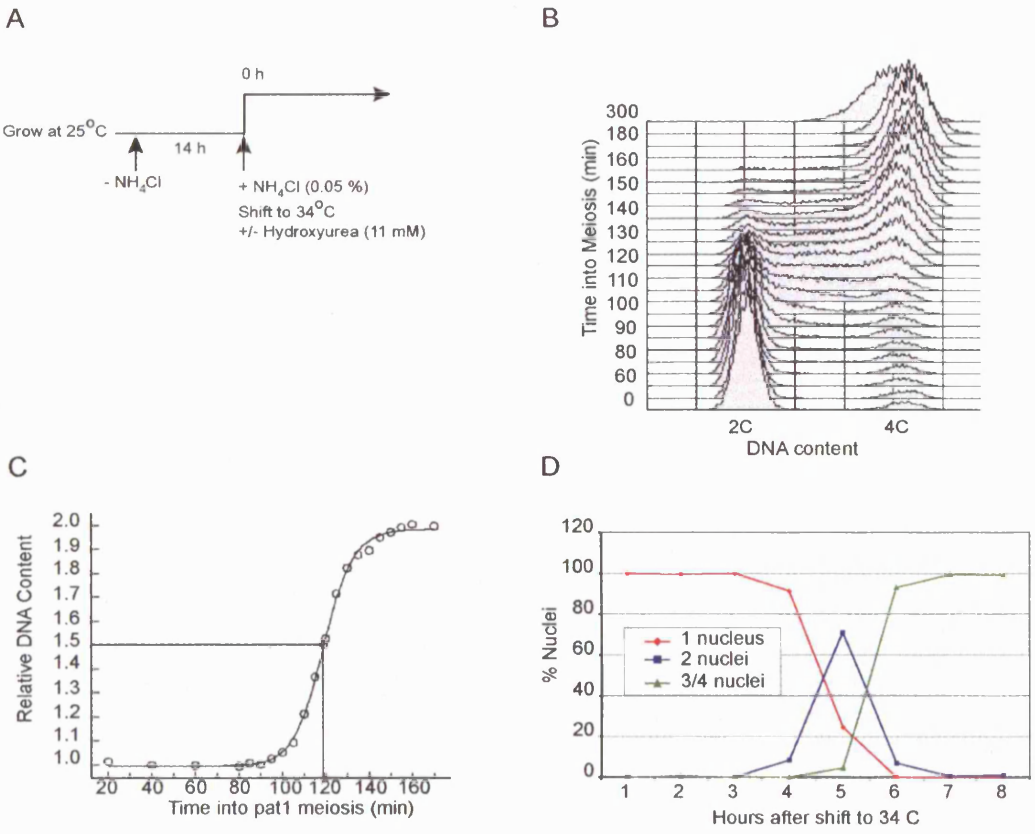

Figure 13: Synchronising Cells in Pre-meiotic S phase.
(A) Synchronising cells in meiosis with pat1-114^{ts}. Temperature sensitive pat-114 diploid cells grown to exponential phase were starved of nitrogen (NH_4Cl) overnight to accumulate cells in G_1 of the cell cycle. Nitrogen was added back to the medium and the temperature was shifted to 34 °C in the presence or absence of 11mM HU. This induces cells to go into a synchronous meiosis. (B) Cell cycle profile of a synchronous meiotic S phase. Samples for flow cytometry analysis were taken at five minute intervals throughout S phase and analysed for increase in DNA content from 2C to 4C. (C) Replication kinetics of a synchronous culture. Signals from (B) were converted to relative DNA content and a logistic curve was plotted and used for scaling microarray signals at respective timepoints during pre-meiotic S phase. DNA replication takes place between ~ 90 and 160 minutes after temperature shift. The time at which half the DNA was replicated (as indicated) was determined for each probe to construct a replication profile (Figure 14A). (D) The percentage of cells containing one nucleus, two nuclei and three or four nuclei were determined during the first eight hours after temperature shift to 34 °C. The sharpness of transition from uninucleate cells to binucleate cells (first meiotic division) and cells with four nuclei (second meiotic division) gives an estimate of cell synchrony.

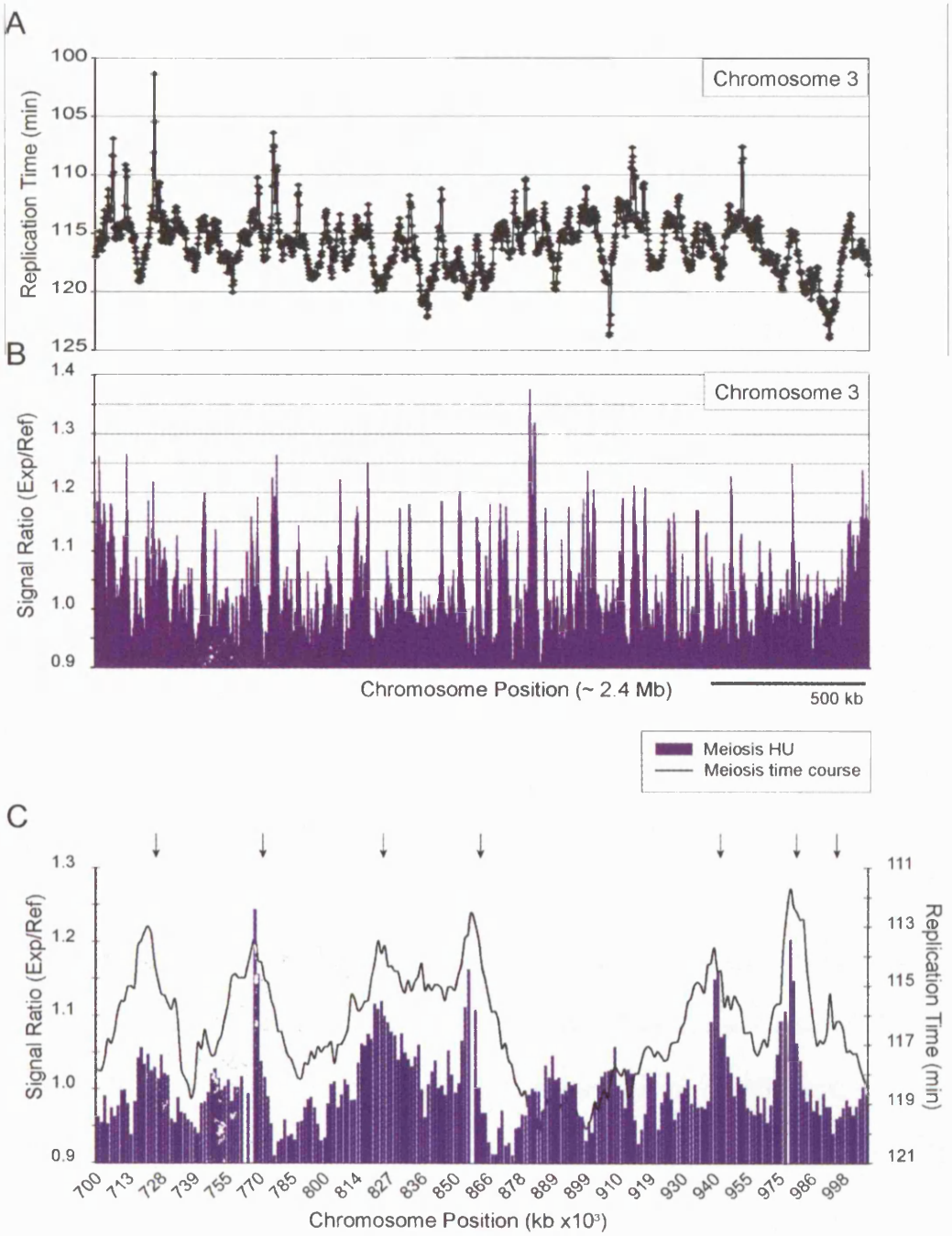

Figure 14: Mapping of ORIs in Meiosis.
(A) DNA replication timing profile of Chromosome 3 from the time course experiment. For further details see mitotic profile (Figure 8). (B) DNA replication profile of Chromosome 3 from the HU experiment. For further details see mitotic profile (Figure 9). (C) Comparison of replication profiles in meiosis with and without HU (300 kb, Chromosome 3). Overlay of averaged signal of HU experiments and averaged signal of the time course experiments. Arrows indicate position of ORIs. Gaps in the HU profile represent probes that were eliminated during data analysis.

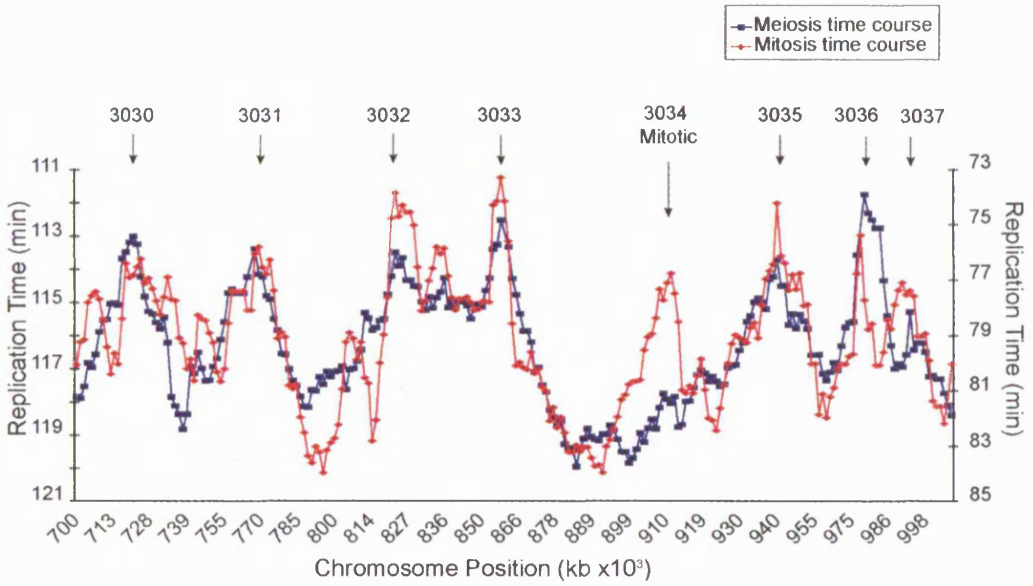

Figure 15: The same ORIs are used in pre-meiotic S phase and mitotic S phase.
Mitotic and meiotic DNA replication timing profiles from the time course experiments are compared (300 kb). The arrows indicate positions of ORIs. ORI3034 was not mapped in meiosis.

I only found four more ORIs (around 1 %) across the genome, ORI1106, 1121, 2078 and 3037, which behaved in a similar way and were not detected in the meiotic time course. In contrast, all ORIs used in meiosis were identified in mitosis and no additional ORIs were mapped in the meiotic time course. A summary with the number of mitotic and meiotic ORIs is shown in Table 2. I conclude that ORIs used in meiosis and mitosis are essentially identical.

Chromosome	Mitotic ORIs	Meiotic ORIs
One	178	176
Two	138	137
Three	85	83
Total	401	396

Table 2: Summary of ORIs identified in Meiosis and Mitosis

2.3 Discussion

In this chapter I describe the identification of 401 ORIs in the mitotic cell cycle, 77 % of which were also active in the presence of the ribonucleotide inhibitor HU. This is a significantly larger proportion than reported in budding yeast, where only 45 % of ORIs were shown to be active in HU (Yabuki et al., 2002). This could mean that a smaller number of ORIs is affected by the intra S phase checkpoint in fission yeast. Alternatively our microarrays may have been more sensitive towards small increases in DNA content. A small peak could also be distinguished on the HU replication profiles for the 23 % of ORIs that were identified in the time course experiment only (found amongst the 503 weak peaks), although these peaks did not qualify the stringent threshold criteria for ORI mapping. It is therefore possible that most fission yeast ORIs show some activity in the presence of HU.

384 putative ORIs were identified in a previous genome-wide bioinformatic analysis (Segurado et al., 2003), which is similar to the number identified in the present study. After discounting ORIs in areas that were not or poorly covered by the microarrays I found that 87 % co-localised with ORIs identified in the microarray analysis. Similarly, 89 % of ORIs from 2D-gel analysis mapped to ORIs in the microarray analysis. This means that I managed to identify close to 90 % of previously characterised ORIs all within an average range of 1.6 kb of their published map position. This underlines the high efficiency and accuracy of the monitoring method in combination with the microarrays used for ORI mapping.

ORI1168 corresponds to an ORI that has been shown not to be active by 2D gel analysis (Segurado et al., 2003). This difference could be due to changes in ORI behaviour under different growth conditions. Cells were grown at 25 °C in minimal medium for the microarray analysis but at 32 °C and rich medium for the 2D-gel analysis. Potentially the addition of HU could lead to activation of otherwise silent ORIs and the identification of false positives. However, the ORI in question is active in both the time course and the HU experiment which argues against this possibility. One criticism of the monitoring method used in this study (Figure 4) is that the increase in copy number and therefore the difference in abundance of a particular sequence is measured rather than replicated DNA itself. This could cause mapping of false positives, for instance in areas where recombination intermediates accumulate. However, recombination events in the mitotic cell cycle are relatively infrequent and should therefore not lead to a significant increase in the abundance of a particular DNA sequence. Even in meiosis, where recombination occurs at a much higher frequency, a recombination frequency in excess of 10 % in a particular locus is considered exceptional. The potential caveats of the monitoring method are outweighed by the advantages. First there is no need for labelling of DNA in vivo, which could interfere with the normal DNA replication program and cause artefacts. Second the monitoring method has been shown to be the most reliable in mapping ORIs in budding yeast (Macalpine and Bell, 2005) and thus likely to identify the least false positives compared with in vivo labelling and Chromatin Immunoprecipitation/Microarray hybridisation (ChIP CHIP) techniques.

Two of the previously identified pARS elements were not amongst the 401 ORIs mapped in this analysis and they are found in areas of the genome where no silencing effects should interfere with ORI activity. This indicates that a significant number of pARS elements may not be active in their native chromosomal context which is consistent with results from previous studies in budding yeast (Brewer and Fangman, 1991). It is possible that a subset of these account for the 13 % of A+T-rich islands which I did not identify as active ORIs on the replication profiles. This suggests that other factors apart from relative AT contents play a role in the definition of fission yeast ORIs. Additional parameters that can influence differential specification of pARS elements will be discussed in Chapters III and IV.

The number of ORIs I identified in fission yeast is similar to the number found in budding yeast, which has a genome of similar size. Between 250 and 430 ORIs were identified in budding yeast by microarray analysis indicating that a similar number of ORIs is required in the two yeasts for timely completion of mitotic S phase. I did not find any significant differences between the position of ORIs when I compared the replication profiles in the meiotic and mitotic cell cycle. This is consistent with previously published results in budding yeast (Collins and Newlon, 1994). I conclude that high levels of recombination and differential patterns of chromosome segregation in the meiotic cell cycle have no influence on the positions chosen for DNA replication initiation during pre-meiotic S phase. Differences in ORI utilisation between mitotic and pre-meiotic S phase are further discussed in chapters III and IV.

In conclusion, I identified 401 peaks on mitotic replication profiles that co-localise with 396 peaks in the meiotic replication profiles. These peaks are likely to mark the position of ORIs as verified by data from 2D-gel analysis. An additional 503 weak but distinct peaks were reproducible in the HU experiments and mostly co-localise in mitosis and meiosis. These are likely to represent inefficient initiation events. Therefore, I have shown on a genomic scale that ORIs used in the mitotic and pre-meiotic S phase are virtually identical in fission yeast.

Chapter III

Characteristics of DNA replication Origins in the Mitotic and pre-Meiotic S phases

3 Characteristics of DNA replication Origins in the Mitotic and pre-Meiotic S phases

3.1 Introduction

Eukaryotic genomes are very complex and this seems to be reflected also in the diversity of their ORI structure which has made it difficult to identify common features in their sequence. ORIs have been shown to generally map to intergenic regions and introns where AT contents are above genome average (reviewed in (Gilbert, 2001; Aladjem and Fanning, 2004)). The size of sequences that can confer ORI activity in ectopic chromosomal loci and on plasmids varies extensively within and between eukaryotic genomes from 100 bp in budding yeast to around eight kb in metazoans and in terms of distribution of initiation events, localised ORIs are distinguished from initiation zones (Gilbert, 2001).

ORI activation in S phase follows a temporal program in eukaryotes and ORIs are activated throughout S phase. How often an ORI is chosen in an average cell population is expressed by its efficiency. A large range of efficiencies from just about detectable and close to 100 % has been observed (DePamphilis, 1993; Friedman et al., 1997; Okuno et al., 1997; Yamashita et al., 1997; Gomez and Antequera, 1999; Segurado et al., 2003). Budding yeast ORIs are generally very efficient in comparison with metazoan ORIs which may be due to the presence of a well defined consensus sequence in the yeast. How ORIs are specified and chosen is currently unclear, but ORI distribution seems to be random across genomes. However, a regular interorigin distance must be achieved in

each cell cycle to prevent unreplicated gaps at the end of S phase, a fact known as the random completion problem (Hyrien et al., 2003). One way to prevent unreplicated gaps is to speed up replication towards the end of S phase. This could be achieved either by firing of additional ORIs or increase in replication fork velocity. It has been shown that increase in ORI frequency is used to reduce the length of S phase in early *Xenopus* and *Drosophila* embryos (Shinomiya and Ina, 1991; Blow et al., 2001). In contrast, replication fork velocities seem to remain constant.

In fission yeast, ORIs are on average ~800 bp in size (Clyne and Kelly, 1995; Dubey et al., 1996; Kim and Huberman, 1998; Okuno et al., 1999). Results from 2D-gel analysis and bioinformatic analysis suggest that ORIs map to intergenic regions and prefer to localise in intergenic regions that are flanked by two 5' untranslated regions (5' UTRs) (Gomez and Antequera, 1999; Segurado et al., 2003). In the previous chapter, I have shown that ORI choice in the mitotic and meiotic cell cycle is almost identical. However, the time required for DNA replication in pre-meiotic S phase is considerably longer than in the mitotic cell cycle. It is currently not clear what contributes to the increased length of S phase in meiosis (Collins and Newlon, 1994). The number of ORIs used in a particular cell cycle, the staggering of ORI firing during S phase and differences in replication fork velocities could all lead to an increase in replication time. Data from 2D-gel analysis of a small number of budding yeast ORIs suggested that ORI efficiencies are almost identical in meiosis and mitosis (Collins and Newlon, 1994). There is currently no data with respect to ORI utilisation in pre-meiotic S phase in fission yeast or metazoan cells.

The aim of this chapter was to characterise and compare features of ORIs on a whole genome level in the mitotic and the meiotic DNA replication program. This included analyses of ORIs in terms of their distribution, replication timing, genomic context, efficiency and replication fork velocity.

3.2 Results

3.2.1 Distribution and Context of ORIs

The distribution of the 401 ORIs identified in the previous chapter was determined across the three fission yeast chromosomes and the whole genome. As shown in Figure 16A, the mean interorigin distance was similar on all 3 chromosomes, 31 kb on Chromosome One, 32 kb on Chromosome Two and 29 kb on Chromosome Three, but there is a difference in the distribution of ORIs among chromosomes. Chromosomes One and Two have a higher percentage of ORIs spaced within 20 kb intervals than Chromosome Three. This is surprising as Chromosome Three has a slightly higher average density of ORIs. A greater degree of ORI clustering on Chromosomes One and Two and a more even distribution on Chromosome Three could be responsible. The average interorigin distance across the genome was 31 kb but a considerable range between 3.2 kb and 114.3 kb was observed (Figure 16B), which indicates that ORIs are randomly distributed across the genome rather than at regular intervals. Figure 16B also shows a comparison of ORI distribution from this study and the distribution of putative ORIs from the bioinformatic analysis. The mean interorigin distances were similar in the two studies, the small difference can be explained by the number of ORIs

analysed (401 vs. 384). However, the peak of interorigin distance in the bioinformatic analysis was between 10 and 20 kb in contrast to 20 and 30 kb in the present analysis. There was also a 0 kb peak in the bioinformatic analysis, which was due to ORIs that cluster. Some of these differences could be explained by the limit in resolution for distinguishing two closely spaced ORIs. To address this, a subset of 41 A+T-rich clusters including all A+T-rich islands within 5 kb of each other was compared with the mapping data of microarray ORIs. Thirteen of these were not mapped at all in the microarray analysis. Of the remaining 28, nine could be identified as unique ORIs, the other 19 mapped to regions with two or more A+T-rich islands. The frequency of ORIs that co-localised with only one A+T-rich island increased once A+T-rich islands were more than 5 kb apart. Only twelve ORIs with interorigin distances below 5 kb could be identified across the genome and the smallest interorigin distance was 3.2 kb. These data indicate that replication forks of ORIs that were spaced close together merged in the HU and the time-course experiments and suggests that the resolution to distinguish ORIs in clusters was around 5 kb in the microarray analysis.

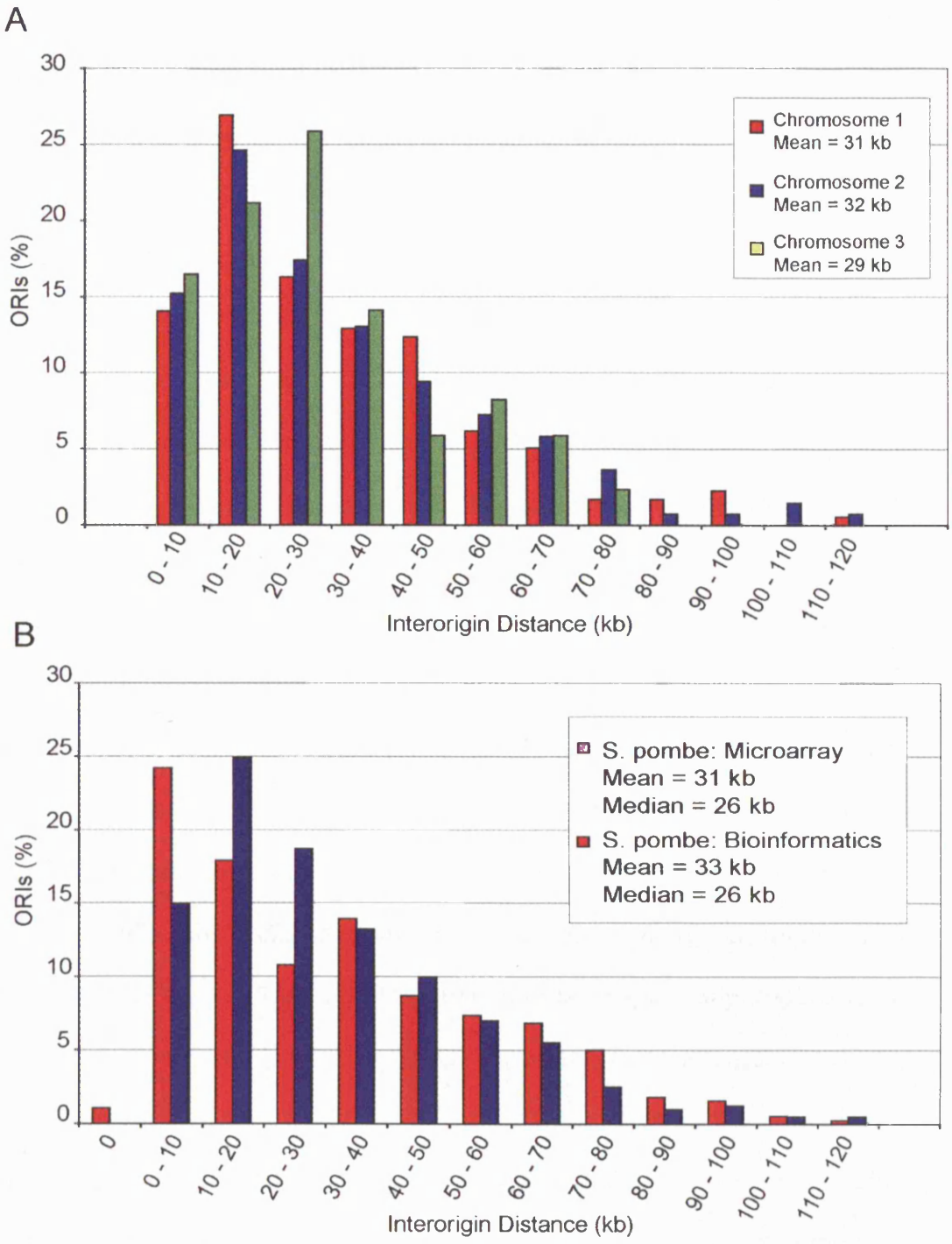

Figure 16: Distribution of Interorigin Distances in Fission Yeast.
Histogram showing (A) the inter-origin distances for the three chromosomes and (B) a genome-wide comparison of inter-origin distances for 401 ORIs from the present analysis and 384 ORIs from the bioinformatic analysis at 10 kb intervals.

Next a genome-wide analysis of the intergenic context of ORIs was performed. As mentioned in Chapter Two, the average difference in map position between A+T-rich islands and microarray ORIs was 1.56 kb. Given that 87 % of ORIs co-localised with A+T-rich islands, a subset of 272 A+T-rich islands (these 272 map to the 257 ORI regions which I defined in the previous Chapter 2.2.2) identified in the bioinformatic approach (Segurado et al., 2003) that co-localised with microarray ORIs was analysed for intergenic context. The result of this analysis is summarised in Table 3. 37 % (46 % expected) of ORIs were located between genes transcribed in tandem orientation, 54 % (27 % expected) were found between divergent and 9 % (27 % expected) between convergent transcription units. This suggests a preference for ORIs to localise in intergenic regions that are flanked by promoters in two 5' UTRs. However, the mean intergenic size, which is 1335 bp for divergent, 988 bp for tandem and 552 bp for convergent intergenic regions (Figure 17A), was typically much smaller than the mean size of intergenic regions that consist of ORIs, 2325 bp, 2023 bp and 2018 bp respectively (Figure 17B). This indicates that ORIs preferentially localise in large intergenic regions, independent of their ORI context. The discrepancy was most notable in convergent regions and least so in divergent regions. It should be noted that only 23 AT-rich islands/ORIs mapped to convergent intergenic regions (8 %), which could contribute to sudden changes in their distribution pattern (Figure 17B). To account for the size bias in the calculation of ORI frequencies, regions below 1200 bp in the observed and expected frequencies were excluded. This is a size that can easily

accommodate an average fission yeast ORI of 800 bp. 77 % of ORIs qualified this criterion which resulted in ratios of 34 % tandem (46 % expected), 58 % divergent (46 % expected) and 8 % convergent (8 % expected) and left a 12 % bias for ORIs to map between divergent transcription units. Almost all ORIs (95 %) map to intergenic regions which are bigger than 800 bp although this subset included fewer than 50 % of total intergenic regions (Table 4). I conclude that there is a strong preference of ORIs for large intergenic regions, and that it is this feature which is largely responsible for the excess of ORIs in divergent gene regions and the deficit in convergent gene regions.

INTERGENIC CONTEXT	NUMBER OF AT-RICH ISLANDS	% AT-RICH ISLANDS [EXPECTED]	MEAN INTERGENIC SIZE AT-RICH ISLAND	MEAN INTERGENIC SIZE GENOME
Divergent	148	54 [27]	2325	1335
Convergent	23	9 [27]	2018	552
Tandem	101	37 [46]	2023	988

Table 3: Summary of Intergenic Context of ORIs
A subset of 272 AT-rich islands that co-localised with 257 ORIs was analysed for intergenic context. The expected and observed frequencies of AT-rich islands in intergenic regions between divergent, convergent and tandemly transcribed genes were determined. The expected frequencies were calculated from the actual frequencies of intergenic contexts within the whole fission yeast genome and would apply if ORIs in AT-rich islands were evenly distributed across intergenic regions with different intergenic contexts. The mean intergenic size for the 272 intergenic regions consisting of AT-rich islands was calculated for each intergenic context and compared with the average intergenic size of 5018 intergenic regions.

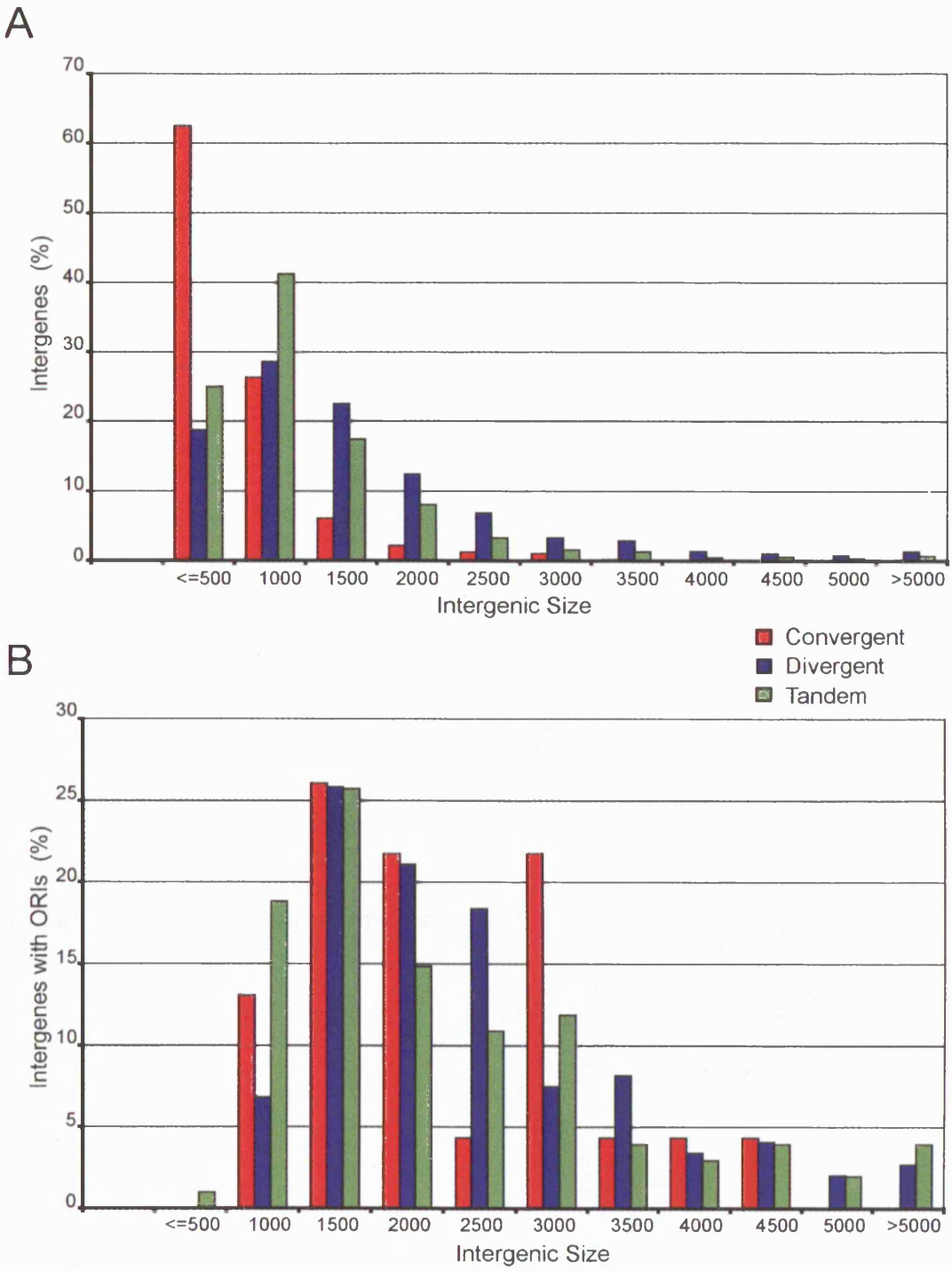

Figure 17: ORIs preferentially localise to large intergenic Regions
Histogram showing the distribution of intergenic size for the three different intergenic contexts (convergent/divergent/tandem) for all 5018 *S. pombe* intergenic regions (A) and the 272 *S. pombe* intergenic regions that consist of AT-rich islands/ORIs (B).

> = Intergenic Size Cutoff Value	Intergenic Regions that qualify Cutoff (%)	Intergenic Regions that consist of ORIs and qualify Cutoff (%)
0 (All)	100	100
500	67	100
600	58	99
700	50	97
800	44	95
900	38	91
1000	33	88
1100	29	86
1200	24	77
1300	22	73
1400	19	68
1500	17	62
1600	15	59
1700	13	55
1800	12	52
1900	11	48
2000	10	43
2500	6	29

Table 4: ORIs mostly map to Intergenic Regions which are bigger than 800 bp
The number of intergenic regions that are bigger than cutoff values given in the first column were calculated for the total number of intergenic regions (second column) and intergenic regions that consist of ORIs (third column).

3.2.2 Replication Timing Program in Mitosis and Meiosis

3.2.2.1 Replication Time and Time of ORI firing in mitosis and meiosis

The time of ORI activation during S phase was determined from the replication timing profiles for 401 mitotic and 396 meiotic ORIs (see Methods). A list of activation times for all ORIs is enclosed in the Appendix. To compare the time of ORI activation in meiosis and mitosis, the respective time at which the first ORI was activated was used to mark the start of S phase (= time zero). A histogram of the distribution of ORI firing during mitotic and meiotic S phase is shown in Figure 18.

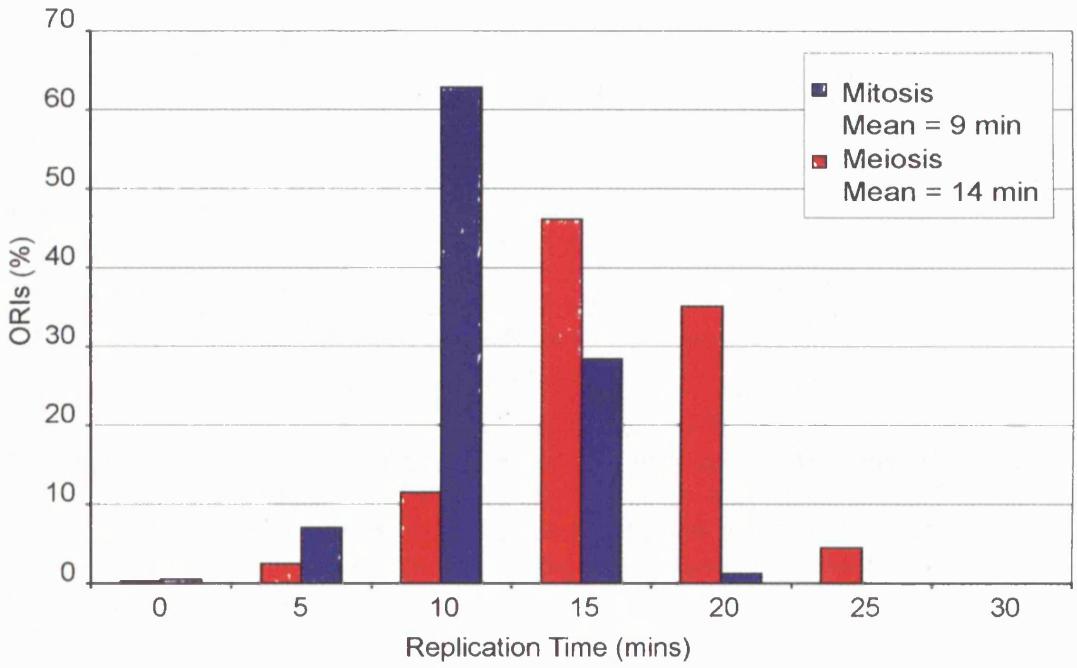

Figure 18: Comparison of ORI Activation Time during Mitotic and Meiotic S phase
The time at which the first ORI fired was determined to be time zero. The time at which ORIs are activated in S phase was calculated for meiosis and mitosis and a histogram of the distribution was plotted.

The distribution demonstrates that ORIs fire throughout S phase in mitosis and meiosis. ORI activation in meiosis took place over a slightly longer

period of time indicating that ORI firing is more staggered in meiotic S phase. The bulk of ORIs was activated around mid S phase both in meiosis and mitosis, although more ORIs were activated in the second half of S phase in meiosis than was the case in mitosis. The results of this analysis are summarised in Table 5. The time between activation of the first ORI and the last ORI was 18 minutes in mitosis and 22 minutes in meiosis. Mid S phase was determined from the average time of ORI activation to be 9 minutes in mitosis and 12 minutes in meiosis. The total time for completion of S phase was 24 minutes in mitosis and 32 minutes in meiosis. The significance of this data will be discussed later in this chapter.

	Mitosis	Meiosis	Δ Time (min) Meiosis/Mitosis
Time between earliest and latest ORI	18	22	4
Time for completion of S phase	24	32	8
Δ Time (min) ORIs/S phase	6	10	

Table 5: Comparison of ORI Activation Time and Time of DNA Replication in S phase
The difference between the activation time of the earliest and the latest ORI was determined for 401 ORIs in mitosis and 396 ORIs in meiosis. The average time for completion of S phase was determined by subtracting the time of replication of the earliest probe from the latest probe. All replication timing data is based on the time point when 50 % of the respective region was replicated.

Next I examined the timing of replication of different chromosomal regions during S phase. The histogram in Figure 19A/B shows the distribution of ORI activation of the three chromosomes in mitosis and meiosis respectively. Chromosomes One and Two replicated at the same time

both in meiosis and mitosis, Chromosome Three replicated on average 3 minutes earlier in mitosis and 4 minutes earlier in meiosis than Chromosomes One and Two. The left arm of Chromosome Two replicated 2 minutes earlier than the right arm in mitosis and 4 minutes earlier in meiosis (data not shown). These are small differences in timing, although it should be remembered that the overall length of mitotic S phase in fission yeast is only about 20 minutes (Mitchison and Creanor, 1971). A subset of 93 or 23 % of ORIs were not replicated to a significant level in the HU experiment and on average these replicated three minutes later than other ORIs as shown in Figure 20. ORIs in subtelomeric regions frequently replicated up to nine minutes later than average in mitosis and meiosis, examples of which include ORIs 1177 and 1178 on Chromosome One. In contrast, some ORIs close to the centromere were activated nine minutes earlier than average in mitosis, such as ORIs 1117 and 1118. A similar pattern of ORI activation around the centromeres was observed in meiosis, although ORIs generally replicated at mid S phase rather than at onset of S phase in these regions. Three ORIs (2069 – 2071) that map to or adjacent to the mating type locus replicated early in the first half during meiotic and mitotic S phase Figure 21. ORI2068 (pARS756) which maps close to the mat1 mating type cassette replicated late in mitosis, but early in meiosis (results not shown). The **r**eplication **f**ork **b**arrier (RFB) distal to the mating type locus, which is essential for mating type switching, is marked by a sharp decrease in signal in the time course experiment Figure 21, indicating that this region is replicated late in S phase. It should also be mentioned that although the subtelomeric regions were typically

ones that replicated towards the end of S phase both in mitosis and meiosis, there were regions within the chromosomes which were replicated at even later stages, presumably passively, since no ORIs could be identified in these regions.

A

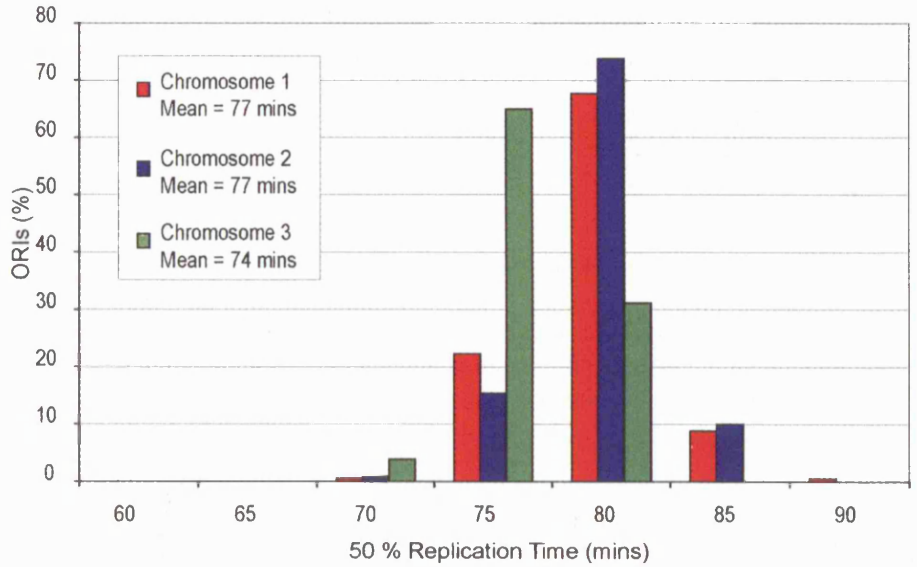

B

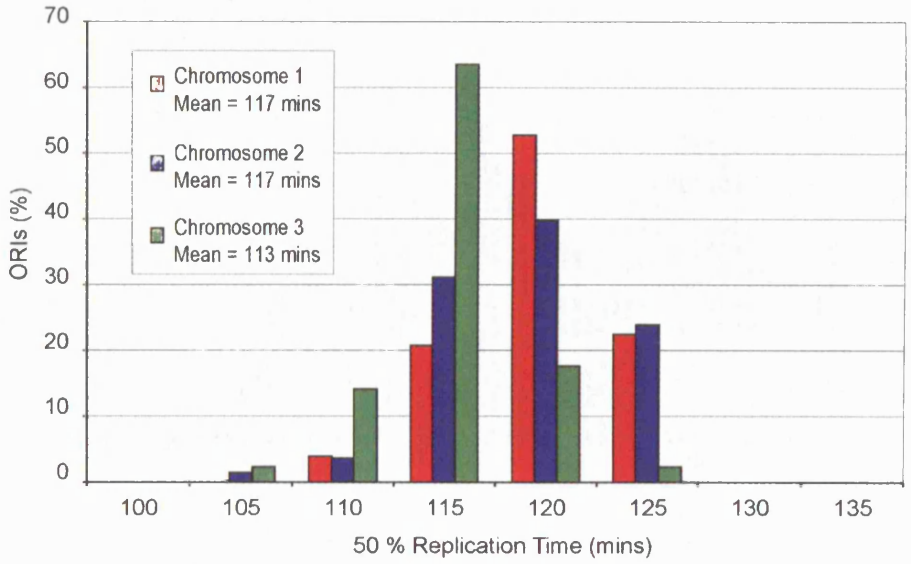

Figure 19: Replication Timing of Chromosomes in Mitosis and Meiosis
The 50 % Replication time for ORIs was determined for the three chromosomes from the replication timing profiles and the distribution was plotted as a histogram for mitosis (A) and meiosis (B).

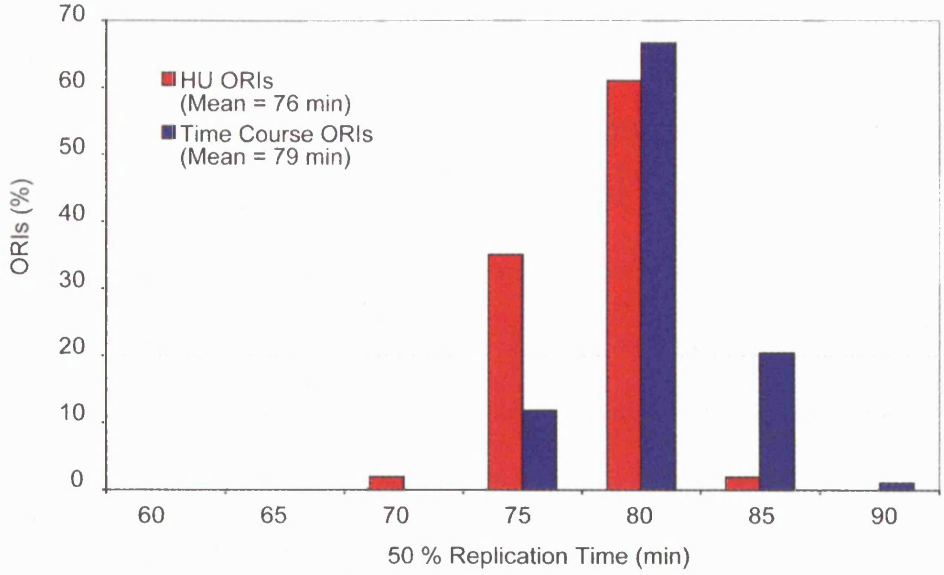

Figure 20: Time of ORI Activation in Mitosis
The time at which ORIs fire during S phase from ORIs mapped in the HU experiment and from ORIs mapped in the time course experiment only was determined and a histogram with a comparison of the distribution was plotted at five minute intervals.

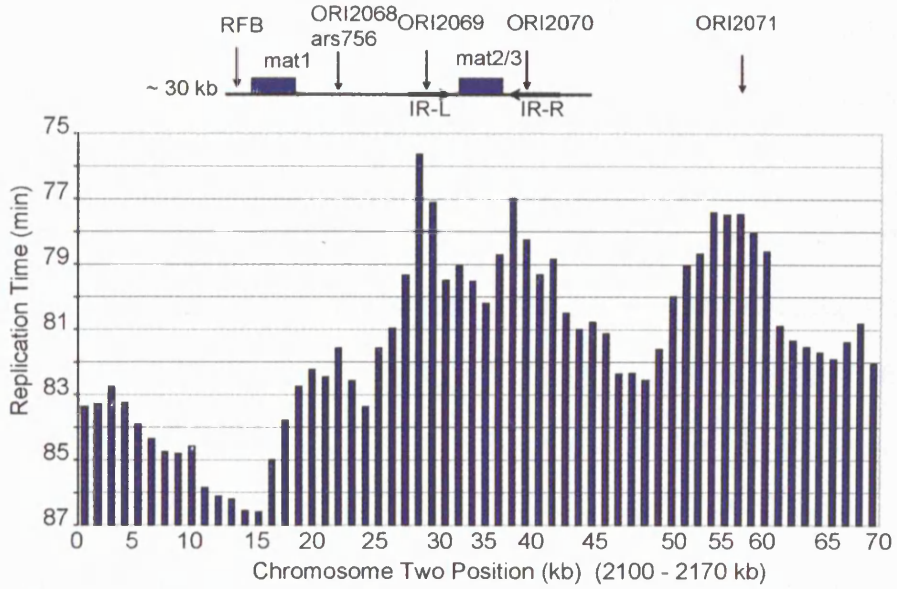

RFB: Replication Fork Barrier/Block Site
IR-L/R: Inverted Repeats
mat1, mat2/3: mating type cassettes

Figure 21: Replication of the Mating Type Locus in Mitosis
The mitotic replication profile from the time course experiment of the 50 kb region containing the ~20 kb Mating Type Locus on Chromosome Two of fission yeast is shown. The position of features of the mating type locus is indicated. The three ORIs identified in the mating type locus as well as the replication fork block site are marked by arrows.

3.2.2.2 Early and Late domain structure in mitosis and meiosis

To assess patterns of replication timing, regions of similar replication timing and regions that differed significantly in replication timing from adjacent areas were identified. A Perl script (Woodfine et al., 2004) was used to assess the optimal segmentation across the three chromosomes, which delineates the replication timing pattern observed by visual inspection. Data from the average of two experimental repeats was used for this analysis. An example of this analysis is shown in Figure 22 for the mitotic replication timing data of the entire Chromosome Two. The replication timing of ORIs on Chromosome Two correlated well with the domain structure delineated by the computational analysis (data not shown) and suggested that this analysis could be used to systematically identify large scale differences in replication timing within and between the three chromosomes. Relatively small domains from around 40 kb and larger domains of up to 800 kb of early and late replicating DNA could be detected. The late domains were typically small; most of these did not contain ORIs and hence were presumably passively replicated. This indicates that they correspond to places where replication forks meet rather than true (actively) late replicating domains. There were only two larger late domains, both of which consisted of active ORIs (Figure 22, indicated by arrows). The rest of the chromosome was replicated at a similar time during S phase between 79 and 82 minutes. The difference between the earliest domain (77.5 mins) and the latest domain next to the left telomere (85.5min) was only 8 minutes. This indicates that the time of

DNA replication is relatively evenly distributed across Chromosome Two in mitosis.

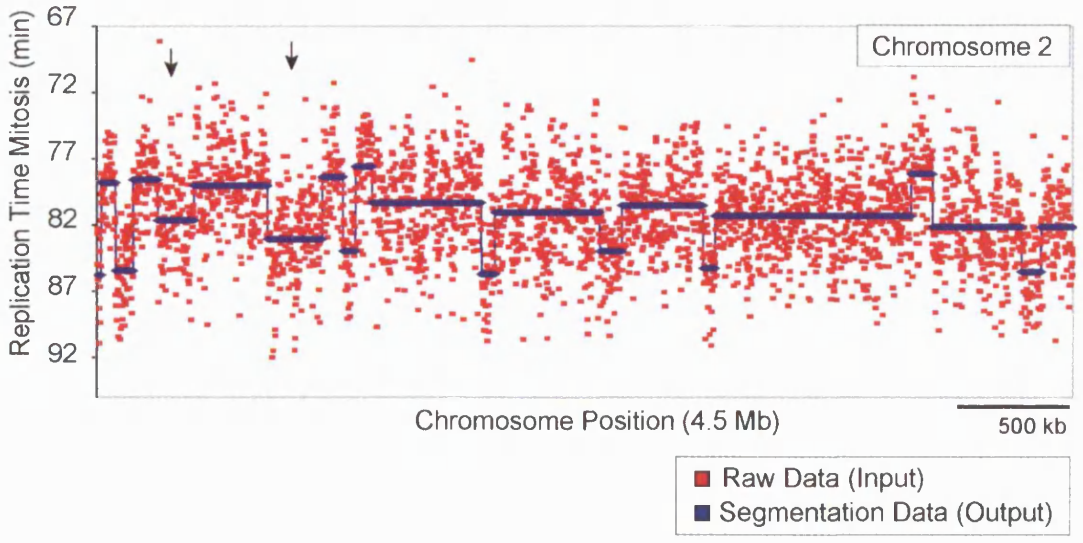

Figure 22: Segmentation Analysis for Replication Timing
Analysis showing the optimal segmentation of replication timing data on Chromosome Two. The raw data (red) is superimposed with the segmentation data (blue). The two arrows indicate late replicating domains, which contain ORIs.

A comparison of segmentation patterns for meiosis and mitosis of all three chromosomes is shown in Figure 23. Again very few segments of late replication that consist of ORIs were identified. The most significant segment of ~800 kb that replicates later than adjacent regions in meiosis and in mitosis was found on Chromosome One next to the telomere on the left arm (indicated by arrow). This segment replicated five minutes later than the adjacent region to the right and four minutes earlier than the subtelomeric region to the left in mitosis. Replication times in mitosis were on average very similar across the three chromosomes, most segments being replicated within four minutes. The two subtelomeric regions on

Chromosome One were replicated at a similar time in mitosis and meiosis. The subtelomeric region on the right arm of Chromosome Two replicated four minutes earlier than the left subtelomeric region both in mitosis and meiosis. There are no subtelomeric regions shown for Chromosome Three, as the two telomeres are flanked by repetitive rDNA gene sequences, which were not represented by microarray probes. The segmentation pattern in mitosis and meiosis was similar for all three chromosomes. However the time difference between the earliest and latest replicating segments which was eight minutes in mitosis was about twice as long i.e. 15 minutes in meiosis. Three chromosomal regions were identified, which show a significant difference in replication timing patterns between meiosis and mitosis: One on the left arm of Chromosome Two and one on the proximal and distal ends of Chromosome Three (indicated by curly bracket). The region on Chromosome Two consists of three early segments in meiosis and two segments in mitosis, but is replicated typically earlier in meiosis than in mitosis with respect to adjacent segments to the right. This could contribute to and is consistent with the difference in replication time of ORIs between the left arm and the right arm of Chromosome Two identified earlier in this chapter, which was greater in meiosis (four mins) than in mitosis (two mins). Interestingly, one of the early replicating segments in this region included the centromere and another one the mating type genes. The two regions identified on Chromosome Three both flank rDNA genes. It is possible that differential regulation of rDNA genes in meiosis influences replication timing in these regions. The correlation between replication timing of ORIs in meiosis and

mitosis was 55 % which also indicates that there are differences in replication timing programs in the two cell cycles. Gene densities and the time of replication of chromosomal segments show a positive correlation in human genomes (Woodfine et al., 2004). The gene densities on Chromosomes One and Two in fission yeast are similar, 1/2483 bp and 1/2457 bp respectively, but significantly lower on Chromosome Three, 1/2790 (Wood et al., 2002), suggesting a negative correlation between replication time and gene density on a whole chromosome level in fission yeast. The late replicating segments identified here comprise average gene densities and were found to be neither particularly gene poor nor gene rich. Centromeres on Chromosomes One and Two were located in early replicating segments, the centromere on Chromosome Three replicated around mid S phase. However, the coverage of the peri-centromeric region on Chromosome Three was poor. This could have influenced the timing ratios in this particular segment. There was no significant correlation in mitosis or meiosis between the GC content of DNA and the timing of DNA replication.

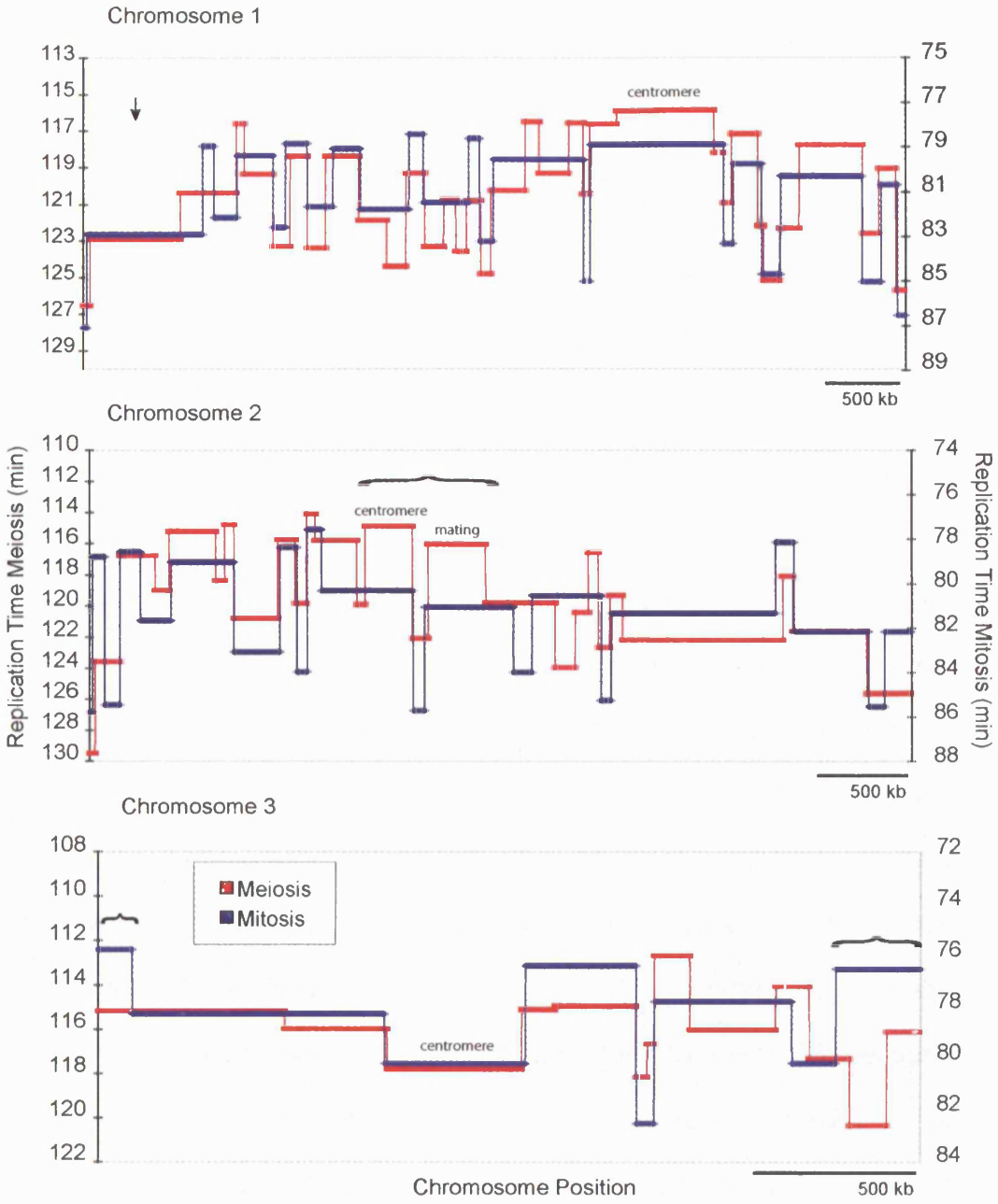

Figure 23: Segmentation of Replication Timing in Meiosis and Mitosis
Segmentation analysis of replication timing data was carried out for all three chromosomes in meiosis and mitosis respectively. The comparison of segmentation patterns in meiosis and mitosis for each chromosome is shown. The arrow indicates a late replicating region on Chromosome One and the curly brackets indicate domains that show significant differences during mitotic and pre-meiotic S phase.

3.2.3 ORI efficiency in Mitosis and Meiosis

Eukaryotic genomes consist of an excess of potential ORIs hence not all ORIs are used for timely completion of DNA replication in S phase (Newlon et al., 1993). In fission yeast, only a subset of ORIs is activated in every cell cycle and dependent on the frequency of usage, ORIs show varying degrees of efficiency as can be determined from signal ratios on Southern blots derived from 2D-gel analysis. The signal ratios obtained from the replication profiles of HU blocked cells were extremely reproducible (Figure 10A and Methods) and could be used to address the distribution of ORI efficiency on a genome-wide level. ORIs used efficiently would be fired in most cell cycles and exhibit a high signal ratio in the HU experiments, whilst ORIs used inefficiently would exhibit a low ratio provided that signal ratios reflect relative ORI efficiency. To validate this approach these estimates of ORI efficiency were compared with data from 19 ORIs previously analysed by 2D-gels (Segurado et al., 2003). Two of the 2D-gel ORIs were excluded from this comparison: First, the data of the false positive result (see Chapter Two) for ORI1156, because there was evidence of broken replication intermediates on the 2D-gel as could be judged from small Y-arcs below the major Y-arc (Kalejta and Hamlin, 1996). This could have reduced the signal from the bubble arc. Second ORI2055, which was located within the centromere on Chromosome Two and was not covered on the microarrays. An example of a Southern blot of one of the 2D-gels is shown in Figure 24A. These gels allow a comparison of signal intensity in the bubble arc, reflecting ORI utilisation in that region with the Y arc reflecting passive replication

through that region (see Methods). The ratio gives an estimate of the efficiency of DNA replication. These two sets of data were highly correlated (88 %) as demonstrated in Figure 24B. In addition to the 2D-gel comparison, a verification of the microarray data was carried out with results from a single molecule analysis (Patel et al., 2005). This study used DNA combing to assess the efficiency of ORIs (Sivakumar et al., 2004). The experimental parameters were analogous to the HU experiment in the microarray analysis. Single molecules of DNA were stretched on glass slides and replication intermediates emanating from ORIs were visualised. FISH was used to assess the abundance of intermediates from 15 ORIs mapping to two different areas on Chromosome Three. Nine of these were distributed over a 217 kb region including the ura4 locus and six over a 212 kb region around the nmt1 locus. The results of this comparison are summarised in Table 6 and Figure 25. The correlation between the two datasets was 92 % and therefore highly significant. Together these two comparisons indicated that the microarray analysis could be used to systematically determine efficiency of ORI utilisation across the fission yeast genome.

A

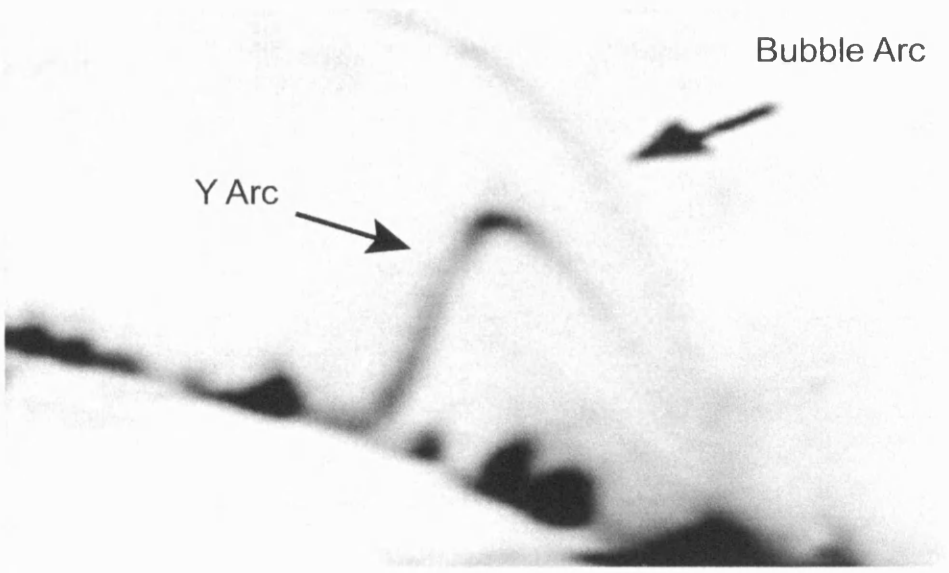

B

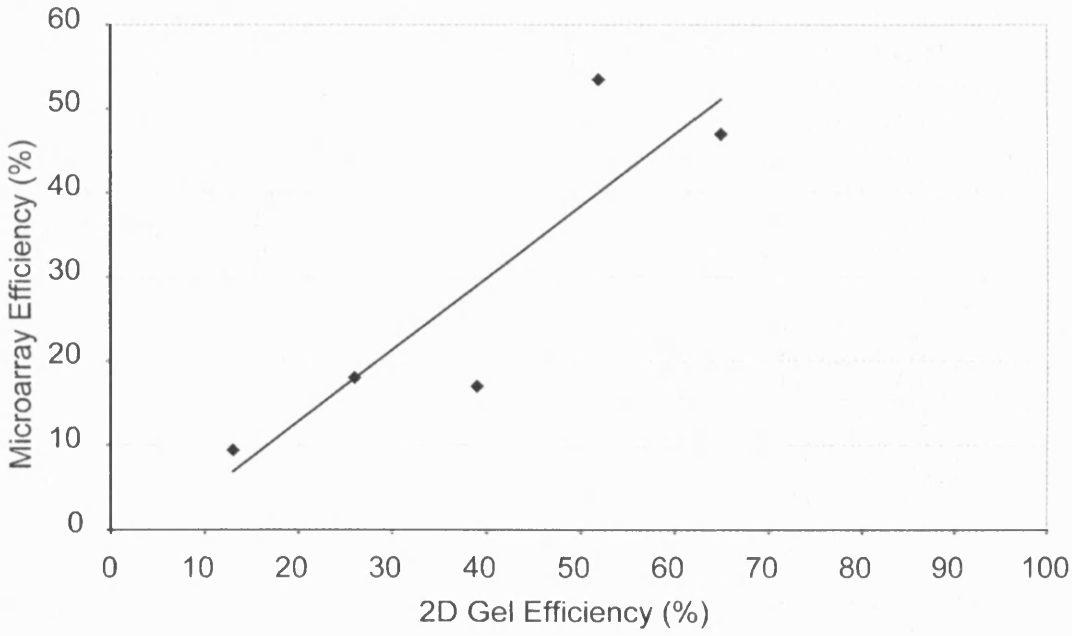

Figure 24: ORI Efficiencies from 2D-gel and Microarray Analysis correlate
(A) Example of a Southern blot from 2D-gel analysis. ORI efficiency was determined for 19 ORIs (Segurado et al., 2003) by calculating the ratio of the signal from the bubble arc and the total signal from the Y-arc and bubble arc (see also Methods). (B) The 2D-gel efficiency data was binned into five groups and plotted against ORI efficiency determined from the signal ratios of the HU experiments (see Methods). The correlation between the two data sets was 88 %.

ORI-Nr. Single Molecule Analysis	ORI-Nr. Microarray	Single Molecule Efficiency	Microarray Efficiency
3002	3001	34	37
3002.2	3002	14	26
3003	3004	32	45
3004/5	3006/7	71	64
3005.3/3005.5	3008	27	29
3006	3009	53	52
3007	3010	31	31
3008/9	3011/3012	22	27
3055	3064	43	42
3056	3065 (cluster)	29	25
3057	3065	50	52
3058	3066	15	27
3059	3068	59	46
3060	3072	50	48
Total		38	39

Table 6: Comparison of Single Molecule and Microarray ORI Efficiencies
ORI Efficiency was derived from 15 ORIs in two regions of Chromosome Three from Single Molecule Analysis (Patel et al., 2005) and the present study. The table shows a comparison of the two data sets. Efficiencies were added up if ORIs clustered and two ORI numbers were stated on one line. For the cluster around ORI3065, two peaks could be distinguished on the microarrays and the corresponding efficiencies were determined for ORI3056 and ORI3057 of the single molecule analysis. ORI efficiencies given are adjusted values (+17%); see text.

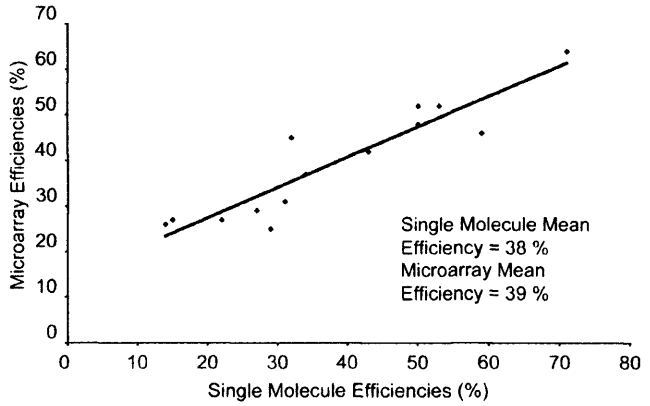

Figure 25: ORI Efficiency in Single Molecule and Microarray Analysis
ORI efficiencies from Table 6 from Microarray Analysis were plotted against ORI efficiencies from Single Molecule Analysis (Patel et al., 2005) resulting in a correlation graph. The correlation between the two datasets was 92 %.

However, the presence of HU could cause ORIs that fired later in S phase to have less extensive bubbles compared with those firing early in S phase because of depletion of deoxyribonucleotides within the cell. If such depletion occurred and reduced bubble size, then this could distort the estimates of ORI efficiency. To asses this, the peak width was used to estimate bubble length from the mitotic replication profile of the HU experiment (see Methods). As shown in Figure 26, fork elongation for ORIs firing in the first half of S phase was 12.3 kb, not significantly different from the 10.9 kb estimated for ORIs that fire in the second half of S phase. A similar pattern of fork elongation was seen on the meiotic replication profiles (Figure 28). There was no significant correlation between the signal ratio from the microarrays and the bubble size (16 %) and no correlation between replication timing and bubble size (10 %). Together, these data established that the signal ratio observed in HU can be used to measure the efficiency of utilisation of those ORIs that fire in HU.

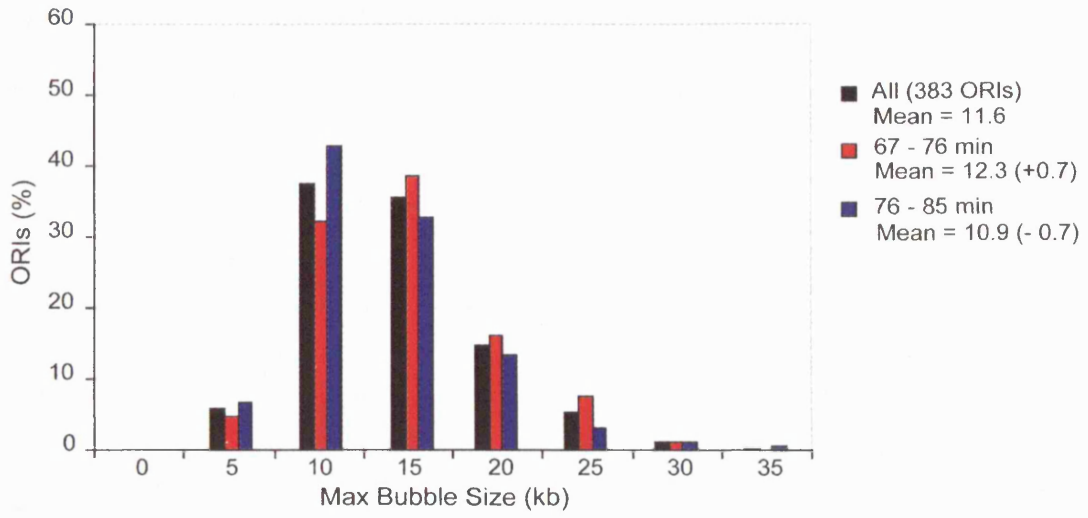

Figure 26: Replication Fork Elongation in early and late firing ORIs
The average width of peaks on the replication profile from the HU experiment in mitosis (Figure 10) was measured to determine the distance of fork elongation. Fork elongation for all ORIs was 11.6 kb on average. Fork elongation for ORIs that fire in first half of S phase (67 – 76 min) was 12.3 kb, in second half of S phase 10.9 kb. 383 ORIs were analysed in total. The 18 ORIs not included in this analysis map to peri-centromeric regions (8), subtelomeric regions (7) and clusters of ORIs (3), where objective measurements were not possible.

It also had to be verified that the majority of cells had reached the time of ORI activation by 90 minutes from G_2 release otherwise overall signal ratios would be reduced. This was the time in the HU experiment when cells for DNA extraction were harvested (see Chapter Two). A time course experiment in the presence of HU was carried out. DNA samples from cells harvested 75, 90 and 120 minutes after G_2 release were analysed on microarrays. As can be seen in Figure 27, signal ratios increase from 75 minutes (green line) to 90 minutes (red line) where the majority of peaks reach the maximum signal ratio. Peaks generally decrease slightly from 90 to 120 minutes (blue line). This could be due to cells starting to leak through the HU block, which may change the distribution of signal ratios in

the central region of the peak. This data suggests that the 90 minute time point is the time of optimal synchrony during an HU block and also indicates that the signal at the peak is fully saturated at this time point.

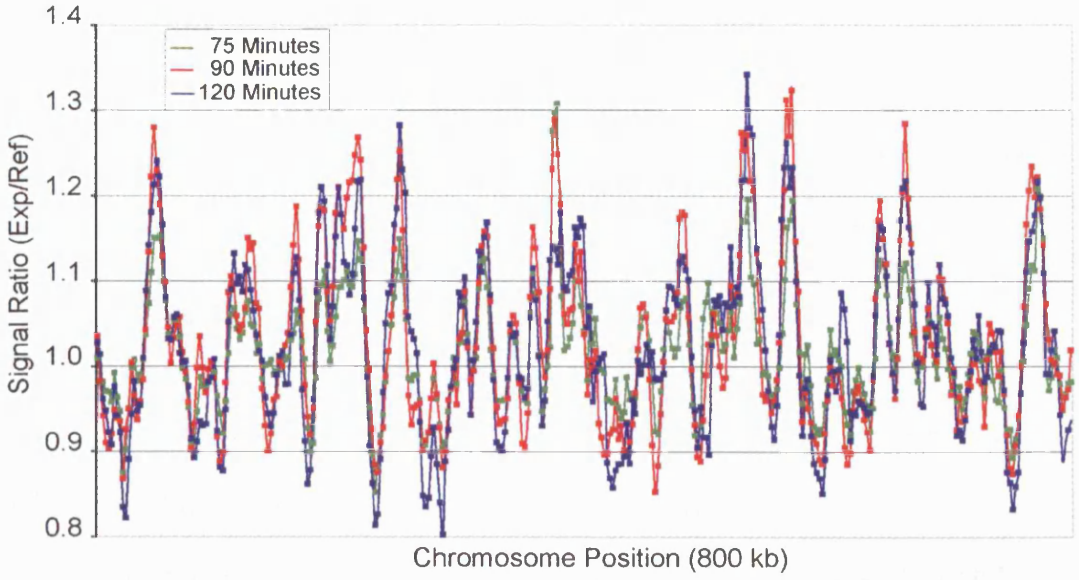

Figure 27: HU Signals are saturated by 90 Minutes into the HU Block
A 800 kb region from Chromosome Three of one HU experiment is shown, comparing signal ratios at 75, 90 and 120 mins from G2 release.

Next the total signal increase on microarrays from 0 to 90 minutes was determined for Chromosome Three to see whether this was sufficient to saturate the central probe within each peak. Five percent of DNA was replicated, which translates into 122.5 kb of replicated DNA (2450 kb x 5%). Considering the 85 ORIs identified on Chromosome Three, this meant that on average 1.44 kb of DNA (122.5 kb / 85 ORIs) around each ORI was replicated if every ORI was used at 100 % efficiency. However, ORIs are not used at 100 % efficiency, as shown previously by 2D-gel analysis. An average ORI efficiency of 27 % was determined from 21

ORIs previously characterised by 2D-gel analysis. Therefore the amount of replicated DNA will be about three times 1.44 kb that is 4.3 kb. The average interprobe distance on Chromosome Three was 1.3 kb, consequently the central probe that maps to the ORI should be fully replicated and the signal saturated by 90 minutes into the S phase block. Together these findings are consistent with data from single molecule analysis of replication bubbles in fission yeast after HU block. These studies showed that labelled replication intermediates from ORIs were 10 – 24 kb in size under the same experimental conditions (Kaykov, A, unpublished data). It can be reasoned that these comparisons confirm that the signal ratios from the microarray data of the HU experiment could be used to estimate relative ORI efficiencies across the genome.

Using this approach, the efficiency of ORI usage in both the mitotic and meiotic S phase was estimated from the maximum signals within each peak corresponding to ORIs mapped in Chapter Two. In meiosis signal ratios were generally lower than in mitosis (Figure 28), suggesting that ORIs did not fire at the same efficiency as in mitosis.

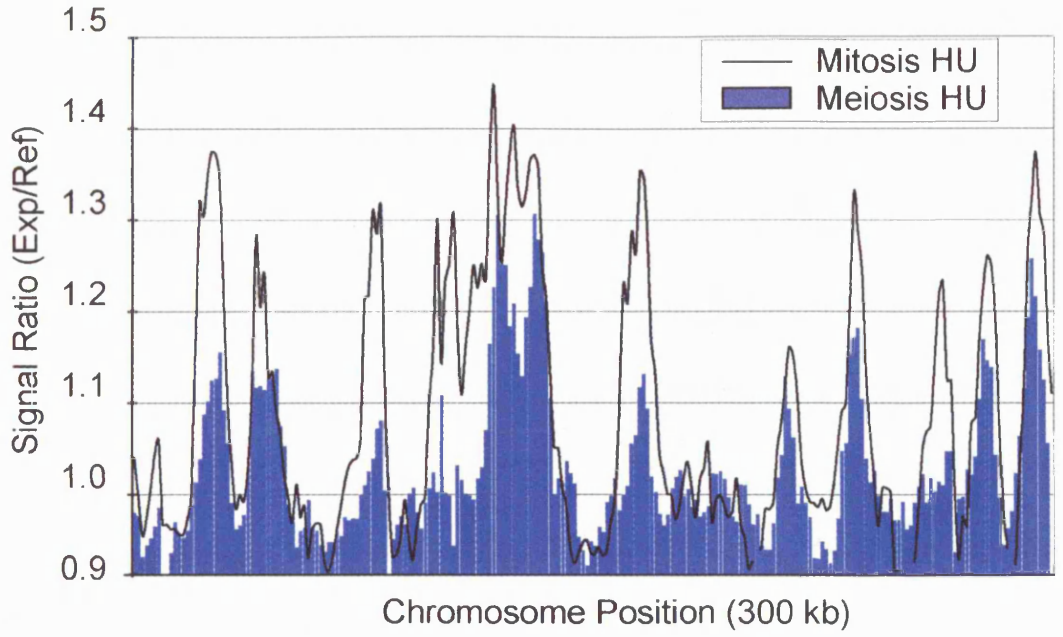

Figure 28: ORIs show higher signal ratios in Mitosis than Meiosis in HU
Overlay of the HU experiment in Mitosis and Meiosis. A 300 kb region on chromosome Three is shown.

The average ORI efficiency was calculated to be 24 % in mitosis and 13 % in meiosis. This indicated that only around half the ORIs were used in a particular meiotic S phase compared with mitotic S phase. However, the relative ORI efficiency calculated from the microarray data does not necessarily show absolute levels. The minichromosome experiment in Chapter Two showed that average signal ratios in the duplicated regions were 20 % short of the expected signal ratio. This shortfall could be due to loss of the minichromosome CH16 during the experiment. Previous studies showed that CH16 was lost in 0.2 % of cells in a wild type background (Niwa et al., 1989). However, the cdc25-22^{ts} allele could elevate mitotic loss. To assess this, mitotic loss of wild type CH16 and cdc25-22^{ts} CH16 were compared using the red/white half-sectoring colony assay (see Methods). As summarised in Table 7 mitotic loss was 0.2 % in

a wildtype background and increased to 3.4 % in a cdc25-22^{ts} background at the permissive temperature of 25 °C. Minichromosome loss was slightly less (2.7 %) if cells were blocked for 3.5 h at restrictive temperature (36.5 °C) after plating. This meant that only around three percent of the 20 % shortfall in signal could be due to minichromosome loss.

Strain/Condition	Colony number	Number of red Colonies	% mitotic loss
CH16 at 25°C	1565	3	0.2
Cdc25-22 CH16 grown at 25°C	1557	54	3.4
Cdc25-22 CH16 blocked for 3.5 h at 36.5°C	1298	35	2.7

Table 7: Mitotic stability and minichromosome CH16 loss
Mitotic stability of the minichromosome CH16 was assessed in a wild type and cdc25-22^{ts} background using the red/white colony assay. Colonies that lose the minichromosome and therefore the adenine marker turn red on selective media.

The remaining 17 % signal loss could not be explained experimentally. I assumed that this signal loss was linear between ratios of 1.0 to 2.0, and efficiency values were adjusted accordingly. To validate this approach, the effect on the efficiency correlation with the 19 ORIs from the 2D-gel data was investigated. As can be seen from the correlation graph in Figure 29A, the efficiencies from microarray ORIs were typically lower than efficiencies from 2D-gel data. The adjustment of microarray ORI efficiencies did not change the correlation significantly (86%), but at the same time moved the absolute value closer to the efficiencies determined by 2D-gel analysis (Figure 29B).

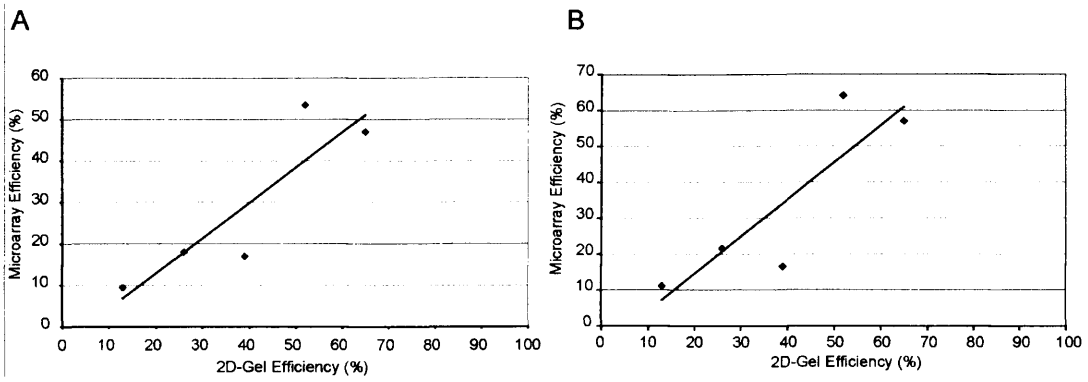

Figure 29: Adjustment of Efficiencies maintains Correlation with 2D-gel Data

Two probes corresponding to ORI sequences of ars2004 and ars2003 were also present on the microarray. Both showed significant increase in signal ratios in the HU experiments. Ars2004 was shown to be a very efficient ORI by 2D-gel analysis. The signal ratio of the bubble arc from 2D-gel blots was 58 %, which compared with an efficiency of 51 % in mitosis and 59 % in meiosis after adjustment of microarray efficiency values. Together these analyses suggested that the 17 % signal shortfall was linear and subsequently efficiencies were adjusted accordingly. This resulted in an average ORI efficiency of 29 % in mitosis (24/0.83) and 16 % in meiosis (13/0.83). A distribution of ORI efficiencies in meiosis and mitosis is shown in Figure 30. Both, the mitotic and meiotic efficiency data follow a similar normal distribution with a skew towards high efficiency values. The frequency of ORIs in the low efficiency ranges was influenced by the threshold criteria used for ORI mapping in mitosis and would be expected to be higher if very inefficient ORIs had been mapped in this analysis. Next the distribution of efficiencies on each of the three chromosomes was determined for mitosis and meiosis. The efficiency

distributions in mitosis are shown in Figure 31. Chromosomes One and Two showed similar distributions. However, Chromosome Three had a very different distribution pattern with more ORIs in higher efficiency ranges. A similar pattern was observed in meiosis. The average efficiency for Chromosome One was 28 % in mitosis and 16 % in meiosis, for Chromosome Two 25 % and 16 % and for Chromosome Three 36 % and 20 %. Another significant difference in average ORI efficiency was observed between the right arm and the left arm of Chromosome Two, 22 % and 29 % in mitosis and 15 and 20 % in meiosis. Within chromosomes, large domains of efficient and inefficient ORIs can be distinguished (Figure 9). This includes two ~1.3 Mb clusters of efficient ORIs on Chromosome One and two smaller ~500 kb clusters of efficient ORIs on the left arm of Chromosome Two. Efficiencies in these clusters are typically between 25 and 50 %. This indicates that ORI efficiencies can vary over large regions within chromosomes and between chromosomes, a pattern that was reproducible in meiotic and mitotic S phase.

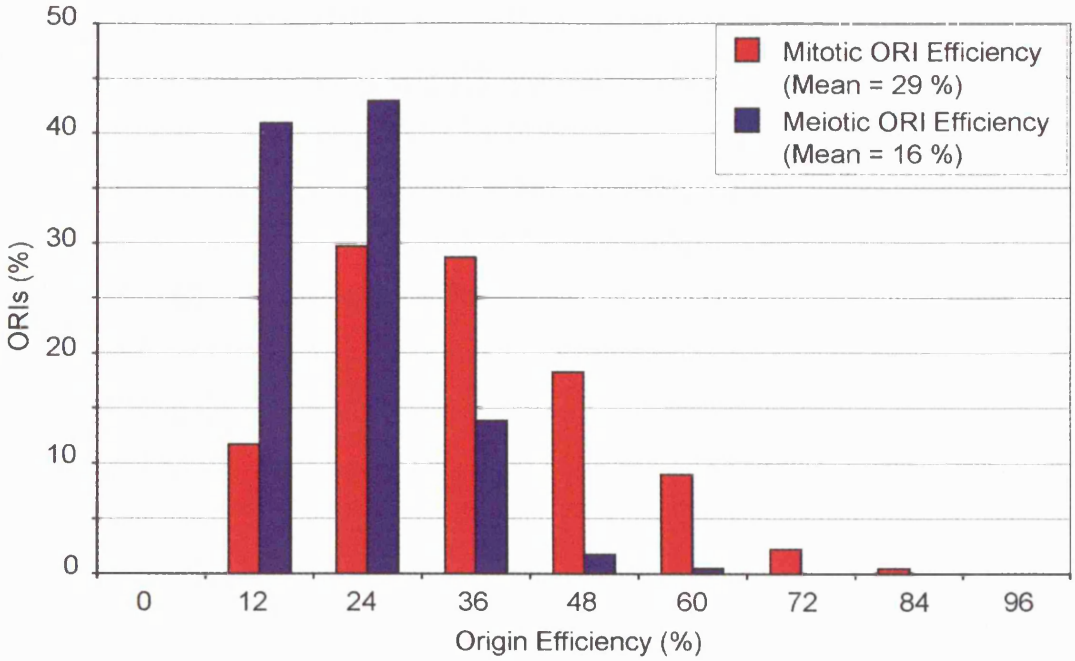

Figure 30: ORIs are less efficient in Meiosis than Mitosis
ORI efficiency is higher in mitosis than in meiosis. The signal ratio from the most replicated probe within each ORI was used to determine the efficiency of 401/396 ORIs in mitosis and meiosis. The mean ORI efficiencies for each data set are indicated.

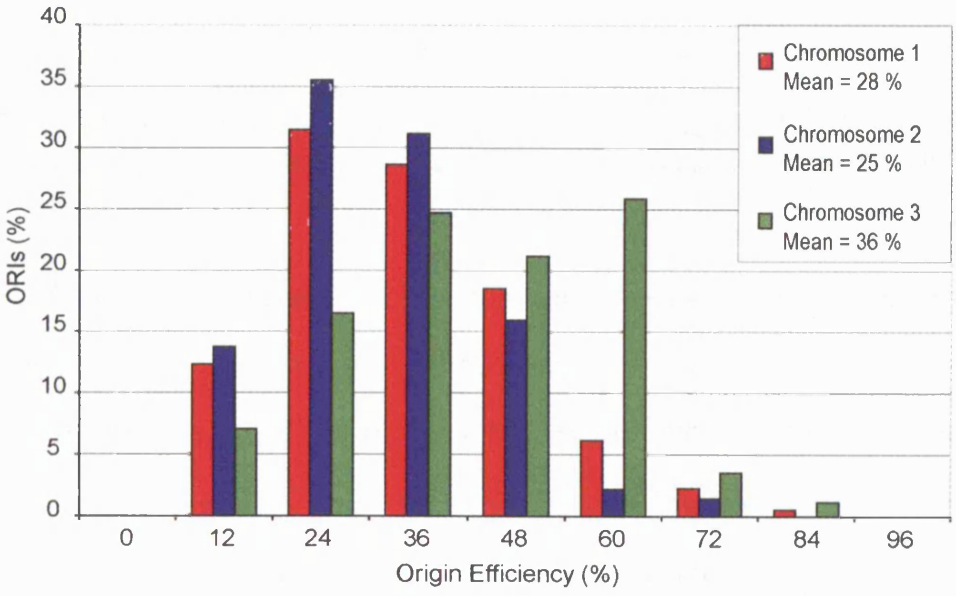

Figure 31: Distribution of ORI Efficiencies across Chromosomes varies
The frequency of ORI efficiencies in 12 % steps was determined for each chromosome and the corresponding distribution was plotted as a histogram.

To determine any correlation between replication timing and ORI efficiency, the efficiency of ORI utilisation was plotted as a function of time of replication during S phase (Figure 32). This showed a correlation of 60 %, indicating that ORIs which fire early in S phase tend to be efficient, whilst those that fire late are inefficient.

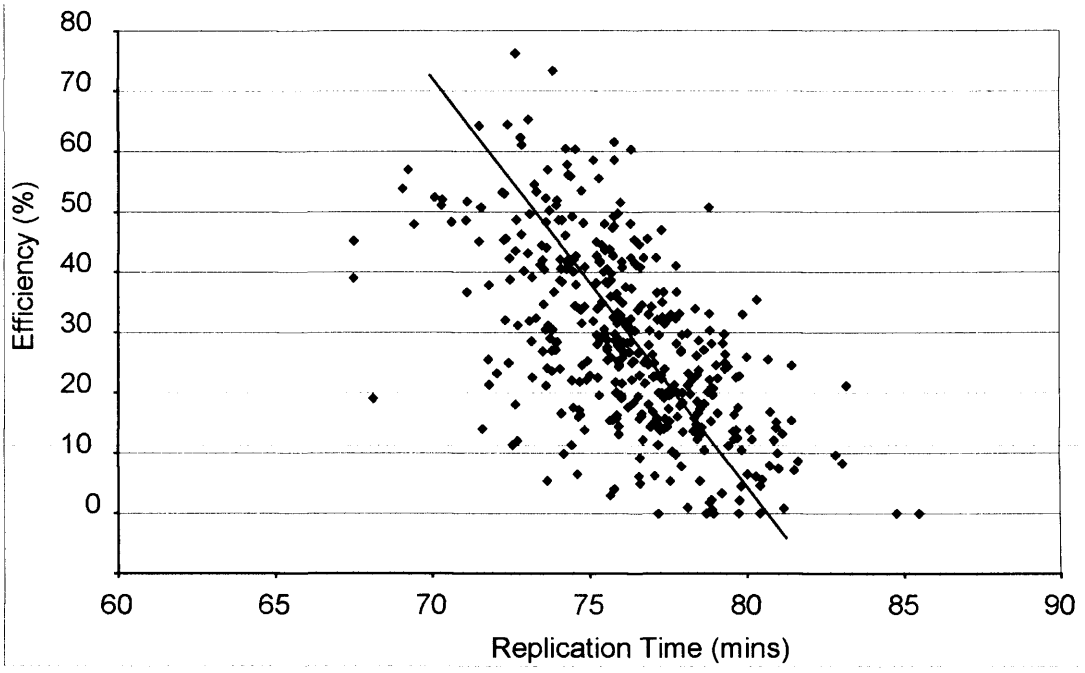

Figure 32: Origin Efficiency and Time of Replication show a negative Correlation
ORI efficiency in mitosis was plotted against time of ORI replication in mitosis for 401 ORIs. The correlation was 60 %.

ORI efficiencies in the mitotic and meiotic S phases showed a correlation of 49 %, indicating differential control in ORI usage in the two types of cell cycle. To investigate this further, ORIs that were utilised at least two times more efficiently in pre-meiotic S phase than in mitotic S phase were identified, by comparing their efficiencies with their respective S phase averages. When their chromosomal locations were mapped, many of these ORIs used more efficiently in pre-meiotic S phase were found to map to three regions: within 600 kb of telomeres, near the mating

type region, and within a 750 kb segment located in the centre of Chromosome One (Figure 33). The same areas were generally devoid of efficient ORIs in mitosis. There is also a pattern of repression of ORI efficiency in meiosis compared with mitosis (Figure 34). For instance, an increased frequency of ORIs that were 0.4 times as efficient in meiosis were distributed over the right arm of Chromosome Two (as indicated), which is also poor in efficient ORIs in mitosis. Only two meiotically repressed ORIs were found within 600 kb of telomeres in regions where ORIs were generally induced in meiosis.

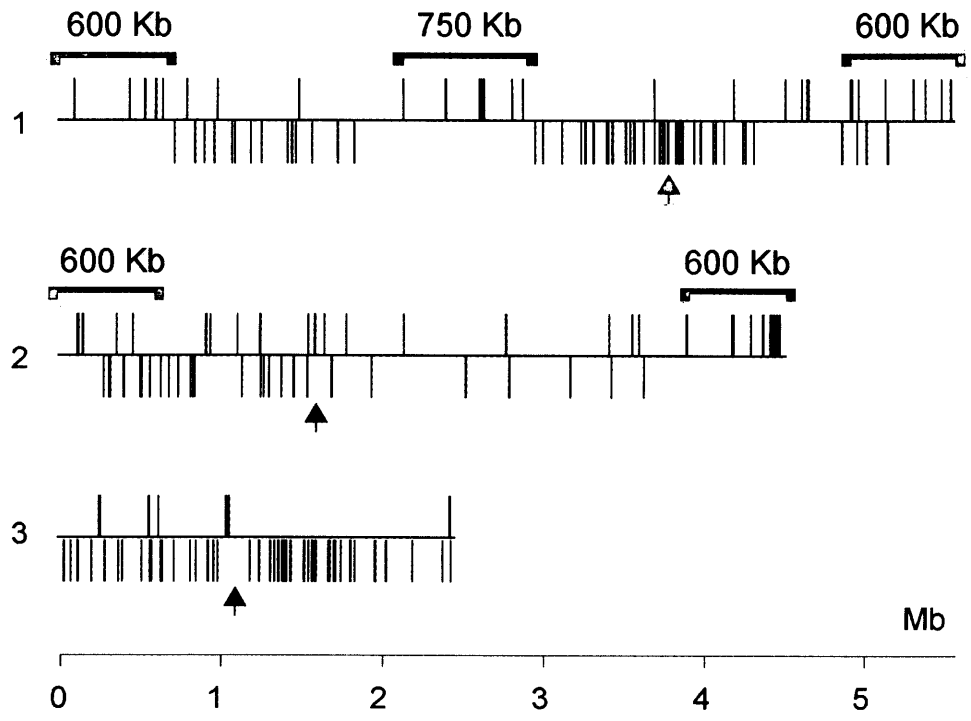

Figure 33: Comparison of ORI induction in meiosis and efficient ORIs in mitosis
ORIs that are at least twofold induced in meiosis correspond to black lines on the upper half of each chromosome. ORIs that are more than 35 % efficient in mitosis are shown on the bottom half. The position of centromeres is marked with arrows.

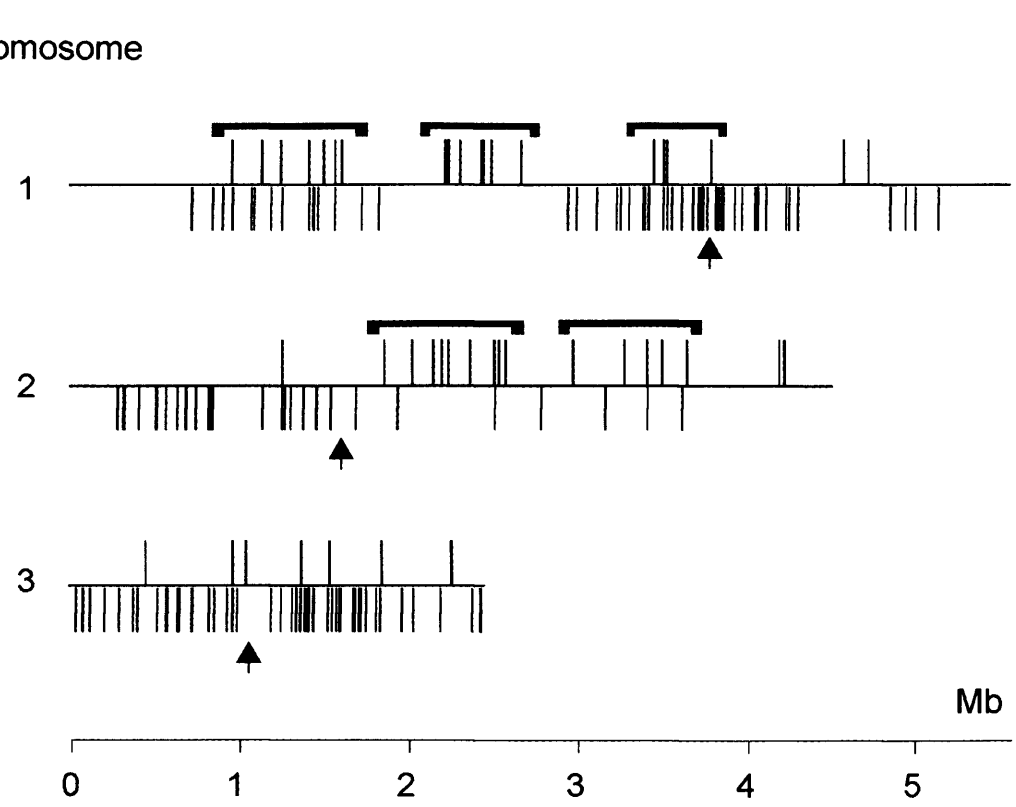

Figure 34: Comparison of ORI repression in meiosis and efficient ORIs in mitosis
ORIs that are repressed by more than half (0.4) in meiosis compared with the relative efficiency in mitosis are shown on upper half of chromosomes (black lines), ORIs that are more than 35 % efficient in mitosis are shown in bottom half. The position of centromeres is marked with arrows.

3.2.4 Replication Fork Velocities, ORI utilisation and S phase duration

The replication fork velocity can be estimated from the gradient of the peaks on the replication timing profiles in the time course experiments (Raghuraman et al., 2001). An example of the principle is shown in Figure 35 for two ORIs. Only replication forks of clearly demarcated ORIs where replication forks did not merge on the replication profiles were included in this analysis. This analysis was applied to a subset of replication forks from 31 mitotic ORIs (62 forks) and 38 meiotic ORIs (76 forks). A comparison of the distribution of replication fork velocity in mitosis and

meiosis is shown in Figure 36. A broad range of replication fork velocities was observed from 1.4 kb/min to 5.5 kb/min. This heterogeneity in fork velocities was not just confined to replication forks that emanated from different ORIs, but there were also a number of ORIs where the leftward and rightward forks had different slopes (Figure 35). The mean replication fork velocity was 2.8 kb/min in mitosis and 3.3 kb/min in meiosis. However, cells were grown at 25 °C in the mitotic time course compared with 34 °C in meiosis, which could account for the 0.5 kb/min increase in replication fork velocity in meiosis. These results indicate that the average replication fork velocity is essentially similar in meiosis and mitosis. In terms of distribution, fork velocities in meiosis show a greater deviation from the mean (meiosis : mitosis = 0.8 : 0.5) and a larger range (meiosis : mitosis = 4.1 : 2.6), which results in a flatter and wider distribution. This indicates that replication fork velocities generally exhibit a greater variance in pre-meiotic S phase.

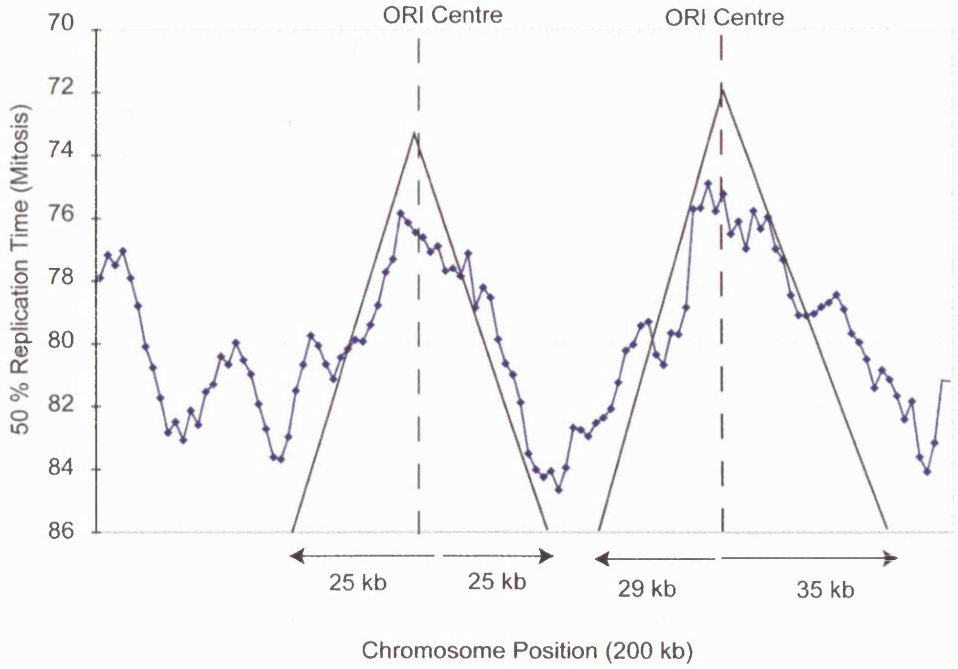

Figure 35: Principle for Estimation of Replication Fork Velocity
The centre of ORIs is marked with a dashed line. Two trend lines were fitted for each peak to determine the gradients corresponding to replication fork velocities (distance travelled/time (kb/min)).

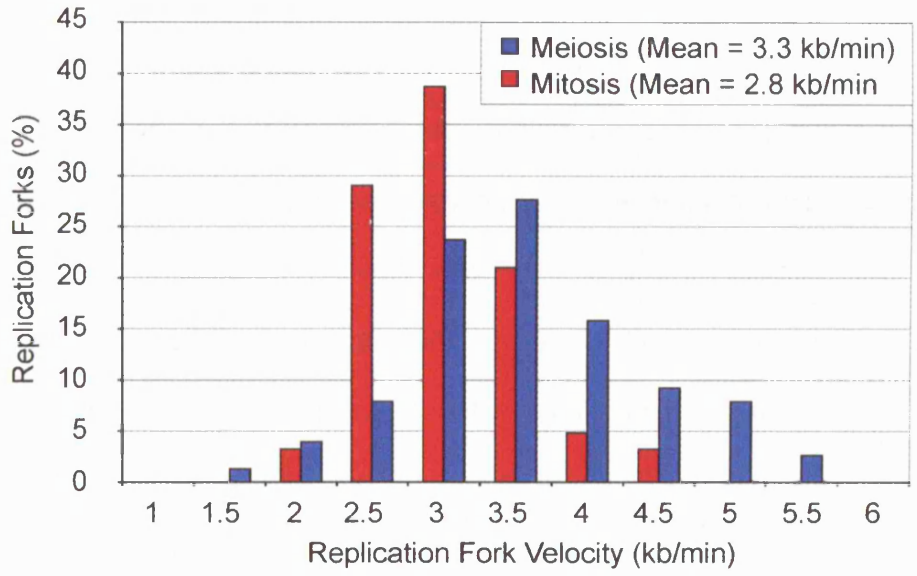

Figure 36: Replication Fork Velocities are similar in Meiosis and Mitosis
A histogram with the distribution of the replication fork velocities in Mitosis and Meiosis is shown. Replication fork velocity was measured from 62 mitotic replication forks and 76 meiotic replication forks and the % frequency in 0.5 kb steps was determined.

The data obtained for ORI efficiency and replication fork velocity were used to calculate and compare the theoretical length of S phase in mitosis and meiosis as shown in Table 8. Provided the firing of all ORIs occurred at the beginning of S phase (obviously an oversimplification), an ORI efficiency of 29 % in mitosis would result in 116 active ORIs per cell cycle. These would replicate 650 kb/minute at a replication fork velocity of 2.8 kb/min and therefore take 19 minutes to replicate the whole genome of 12.5 Mb (1.2 Mb rDNA repeat and centromere cores not included). In meiosis, the same calculation for 16 % or 64 active ORIs and a replication fork velocity of 3.3 kb/min results in an S phase length of 30 minutes, about 60 % longer than mitosis. The differences in theoretical lengths of S phases in mitosis and meiosis calculated here are consistent with replication timing measured from the time course data earlier in this chapter (Table 5). However it is not possible to compare absolute duration of S phases in meiosis and mitosis, as the level of synchrony is likely to be different and could not be measured accurately in the two experimental systems. The time between activation of the earliest and the latest ORI was 22 minutes in meiosis and 18 minutes in mitosis, the time for completion of S phase calculated from the time when the last ORI was activated took six minutes in mitosis and ten minutes in meiosis. This means that it took four minutes longer for all ORIs to be activated and four minutes longer to complete S phase from the latest initiation event in meiosis. Together this data suggests that a combination of staggering of ORIs and decreased ORI efficiencies are the two main contributors to increased length of S phase in meiosis.

	% ORI Efficiency	Active ORIs/ Cell Cycle	Replication Fork Velocity (kb/min)	S Phase duration in 12.5 Mb Genome (min)
Mitosis	29	116	2.8	19
Meiosis	16	63	3.3	30

Table 8: Calculation of S phase Duration in Mitosis and Meiosis

The caveat with the calculation in Table 8 is that the 116 ORIs used in mitosis would have to be evenly spaced in order to complete S phase in the ~20 minutes available. But in fact ORI spacing ranges from 3.2 kb to 114.3 kb. A 114.3 kb gap could only be filled if the efficiency of the two ORIs flanking this region was particularly high, i.e. if they were used in almost every cell cycle or if efficient ORIs cluster in the flanking regions. To investigate this further, a region with large interorigin distances was chosen to see whether it consisted of particularly high ORI efficiencies or unusual ORI firing patterns/clusters. Overlays of the time course and the HU replication profiles of this region is shown in Figure 37. Three ORIs were mapped in the 140 kb region on Chromosome Two (as indicated with filled squares/ORI names), one of which (ORI2060) in the time course experiment only. The two ORIs flanking the 140 kb region (ORI2059 and 2061) were identified in both experiments and showed efficiencies between 10 and 20 %. ORI2061 was in a group with two other closely spaced ORIs about 10 kb apart, which were also relatively weak in HU (10 – 15 % efficiency). Interestingly an additional six distinct peaks were identified in the HU experiment located between ORI2059 and 2061, a

subset of the 503 less efficient ORIs mentioned in Chapter Two. The pattern from the time course experiment also suggested late ORI activity in this region, although it was difficult to distinguish clearly defined peaks. Small peaks were relatively evenly spaced at distances between 10 – 15 kb and the average efficiency of these peaks was low at 8 %.

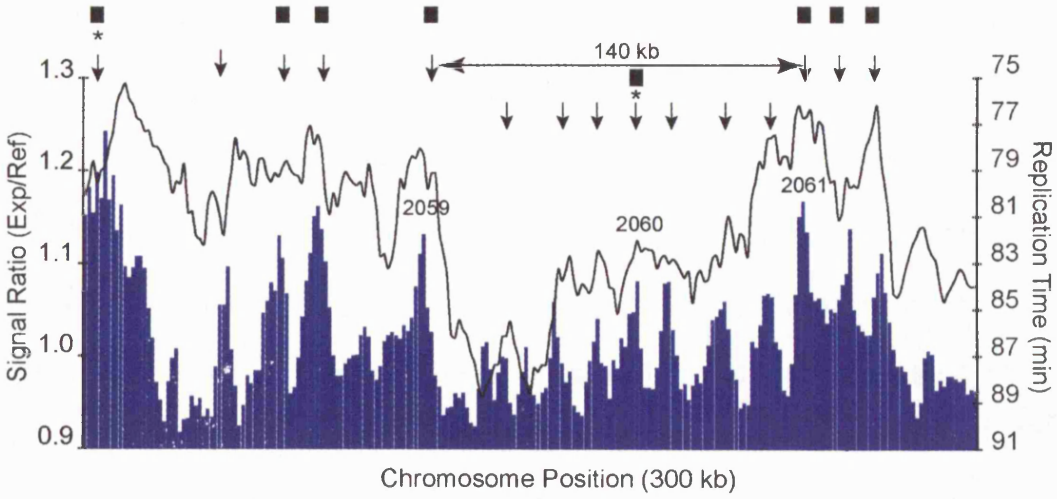

Figure 37: Characterisation of large interorigin Spaces
An overlay of HU and time course experiment over a 300 kb region of Chromosome Two. ORIs that were mapped in the microarray analysis are indicated as a filled square, ORIs mapped in the bioinformatic analysis by a star. The arrows indicate peaks on the replication profiles.

The distribution pattern of peaks across the three chromosomes and the whole genome is shown in Figure 38A/B. The distribution of the 904 peaks identified in the HU experiment including the 401 more efficient ORIs was similar across the three chromosomes at 13 – 14 kb (Figure 38A). The majority of peaks (~75 %) were spaced between 5 and 20 kb apart, the median was 12 kb, the mean 14 kb across the genome (Figure 38B). The average efficiency of the 503 additional peaks was low at 8 % (40 active

ORIs/cell cycle) compared with the average efficiency of 29 % for the 401 ORIs identified (116 active ORIs/cell cycle). This means that an average 74 % of replication was accomplished by a subset of 401 ORIs with 29 % efficiency and the remaining 26 % by a subset of the 503 weak ORIs. In conclusion the data suggests that replication initiation events in the fission yeast are relatively evenly spaced at 5 – 15 kb intervals, although more than 50 % of these are used at efficiencies below 10 %. However, these small peaks could be due to background noise. To investigate this, peaks in three experimental repeats were inspected visually. This showed that even small peaks with signal ratios below 1.1 times were extremely reproducible across the genome, an example of the 300 kb region from Figure 37A is shown in Figure 39. The possibility that these peaks could be due to dye bias in the labelling reaction with preferential incorporation of dyes in AT residues compared with GC residues can be discounted by the processing of data in the microarray analysis (see Methods). Also peaks are described by both, probes that map to intergenic regions and have high AT contents and probes that map to genes with relatively low AT contents. This should interfere with the formation of a clear peak if there was any dye bias, but the peaks are frequently distributed over an excess of six probes. Together this data suggested that it was unlikely those small peaks were due to background noise and that they were instead the result of weak but significant DNA replication initiation events.

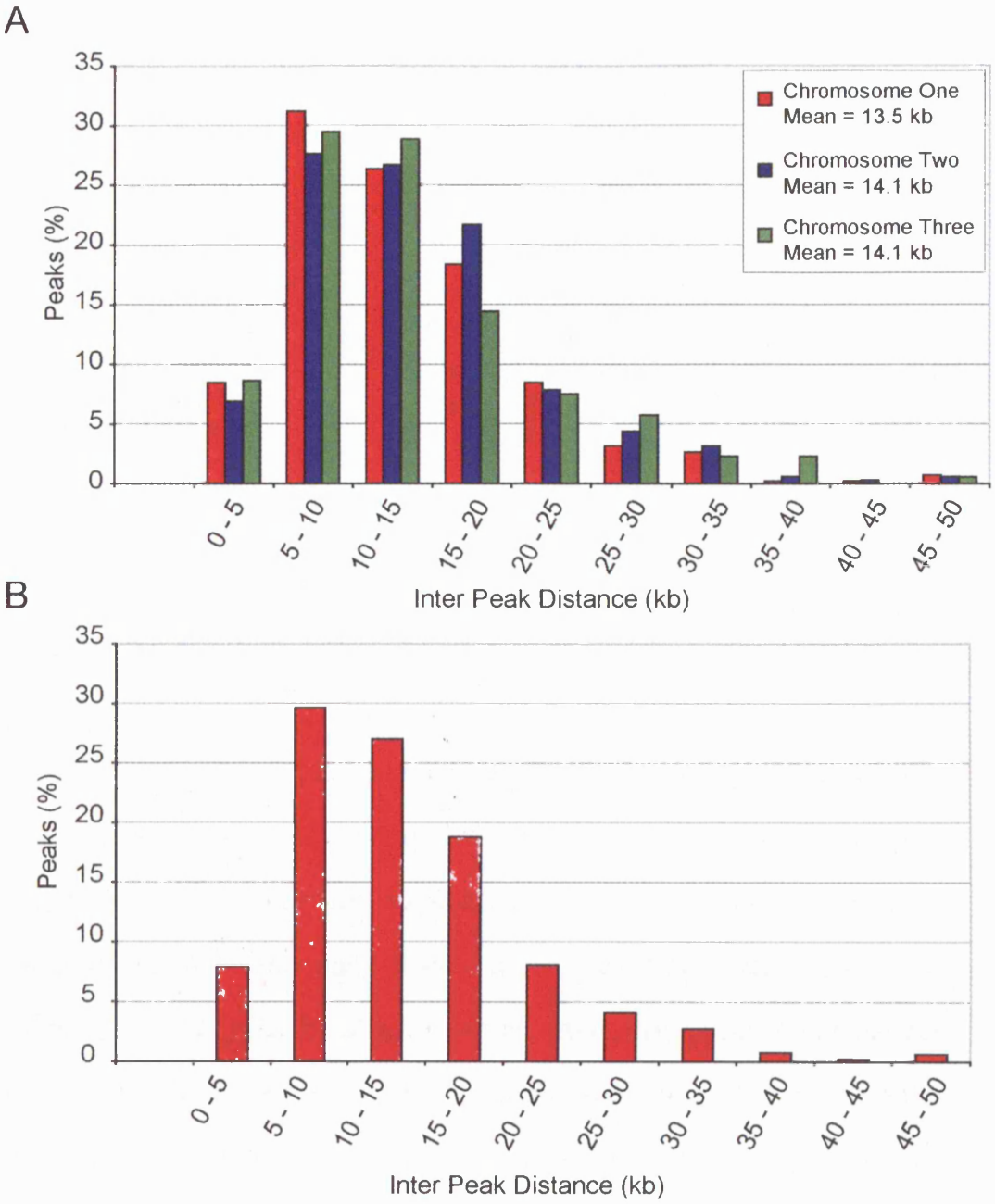

Figure 38: Peaks on Replication Profiles are spaced at 5 – 15 kb intervals
Inter peak distances were determined between the central map position of the 904 peaks identified on the replication profile of the HU experiment for (A) individual chromosomes and (B) genome-wide.

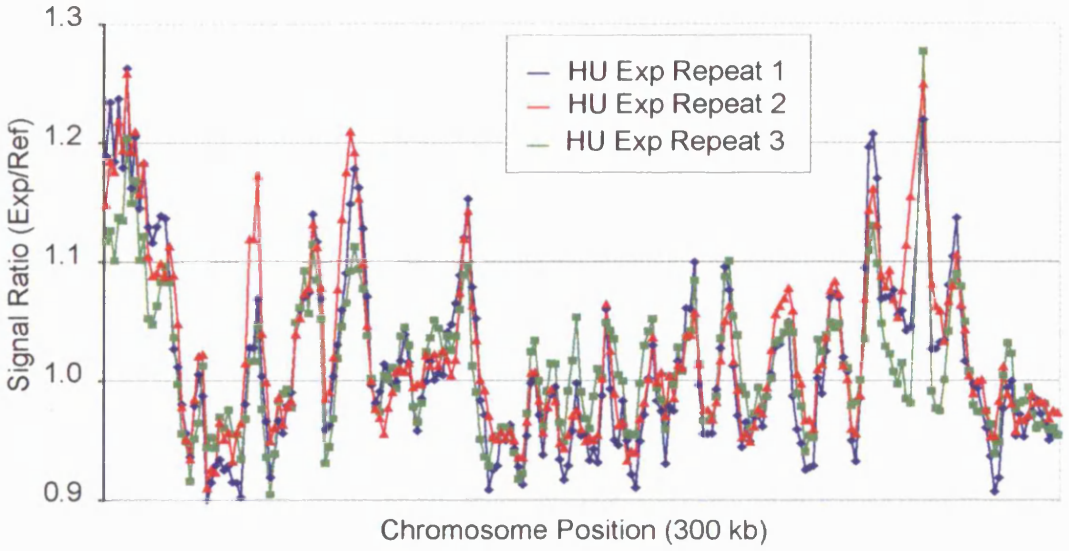

Figure 39: Small Peaks co-localise in the three Experimental Repeats
Replication profiles of a triplicate repeat of the HU experiment; the same 300 kb region is shown as in Figure 37A.

One caveat in this analysis was that the addition of HU could have affected the pattern of ORI firing because of slowing down replication fork migration, which could lead to additional initiation events in intergenic regions that were normally silent, which has been demonstrated in mammalian cells recently (Anglana et al., 2003). However, a comparison of the time course (no HU) and HU experiments suggests that the small peaks correspond to initiation events in late S phase, although peaks on the replication profiles of the time course could not always be clearly distinguished (Figure 37). High AT content is a good marker for a region to act as an ORI (Segurado et al., 2003). The relative AT content was determined for all peaks within the two regions as shown in Table 9. Apart from one peak, all had AT contents above 70 %. The average AT content for the small peaks not mapped as ORIs was 72 %, which is above the intergenic average of 69 % (Dai et al., 2005). Two of these peaks with AT-

contents of 74 % on Chromosome Two (indicated with a star) co-localised with A+T-rich islands identified in the bioinformatic analysis. This suggested that the estimate of 87 % A+T-rich islands from the bioinformatic analysis that were identified as active ORIs in the present analysis in Chapter Two was conservative. In fact including the 503 weak peaks in addition to the 401 ORIs in the comparison, a total of 281 A+T-rich islands (95 %) could be identified on the replication profiles in the HU experiment.

Position (bp)	Chromosome	ORI Number	AT content
1808000	2	2059	75
1833000	2		69
1836000	2		71
1845000	2		71
1858000	2		72
1870000	2	2060*	76
1880000	2		71
1895000	2		72
1918000	2		74
1929000	2		72
1941000	2	2061	76
1857000	1	1055	74
1865000	1		73
1886000	1		73
1896000	1	*	74
1901000	1		72
1921000	1		74
1928000	1		72
1934000	1		71
1938000	1		72
1949000	1	*	74
1963000	1		72
1974000	1	1056*	76

Table 9: AT contents at small Peaks are typically above 70 %
The AT-content was determined around peaks that map to regions of large interorigin spaces shown in Figure 37. A 500 bp window and 50 bp step was used to determine AT content (see Methods).

In conclusion, the data suggest that small peaks on the replication profile of the HU experiments represent weak initiation events. The majority of these are possibly used to bridge unreplicated gaps in the chromosomes that remain towards completion of S phase between two significant or efficient ORIs. Occasional differences in the location of the small peaks between meiosis and mitosis suggest that any region that has above average AT-content could be chosen stochastically dependent on the position of unreplicated gaps, which may vary according to the developmental program. Such a stochastic model has been suggested in fission yeast (Dai et al., 2005). In that study 26 intergenic regions within a 60 kb region were cloned into plasmids either as monomers and/or dimers to identify sequences that could confer ORI activity in an extrachromosomal context. To see whether potential ORI sequences identified in this analysis could act as ORIs in their chromosomal context, the sequences were mapped to corresponding probes on the microarrays. The result of this analysis is shown in Table 10 and Figure 40. Fourteen of the 26 intergenic regions showed some ARS activity on plasmids (Table 10, $5^{th}/6^{th}$ column). Seven intergenic regions that had ARS activity mapped to a distinct peak on the replication profiles (Table 10, column "Array Peak" and Figure 40, large arrows). The other seven intergenic regions mapped within these peaks (small arrows) but could not be distinguished as separate initiation events on the microarrays. The relative transformation efficiencies did not always correspond well to the ORI efficiencies observed (Table 10, compare column 5/6 and 9). For instance the intergenic region between the genes mex67/C1921.04C had a very

high transformation efficiency of 320 but only a 12 % ORI efficiency, in contrast to Ucp3/fnx1 with an efficiency of 59 and 19 % respectively. There was a better correlation in terms of percentage AT content as well as intergenic length (Table 10, columns 2/3/4 and 9). In general, regions that had less than 71 % AT content in a 500 bp window did not show ORI or ARS activity (Table 10, column 4 and 5/6/9). Two ORIs (ORI2079 and 2080) were identified in this region in Chapter Two and co-localised with areas that show strong ARS activity. Five more small but distinct peaks co-localised (large arrows), which did not qualify the threshold for ORI mapping. The fact that small peaks on the microarray replication profile map to sequences that confer ARS activity in plasmids suggests that these peaks correspond to weak initiation events. This confirms the conclusion from the previous analyses that the fission yeast genome consists of many weak initiation events that are relatively evenly distributed at 10 – 15 kb intervals. In summary, the data presented here together with the data from (Dai et al., 2005) strongly argues for a stochastic model of DNA replication initiation in fission yeast.

Intergenic Region	Length (bp)	AT interg enic (%)	AT 500 bp window (%)	ARS activit y* (mono mer)	ARS activit y* (dime r)	Array ORI	Array Peak	Array Efficien cy (%)
rpl3701/rad60	870	68.74	71	0	0		N	0
Rad60/mex67	201	72.64	71.2	0	0		N	0
Mex67/1921.04c	956	73.43	76.4	320	ND	NA	1	12
C1921.04c/ape1	2,102	65.70	67.8	0	0.3		N	0
Ape1/pvg3	1010	67.72	68.8	0	0		N	0
Pvg3/SPBC1921.07c	843	68.21	71.4	0	0.4		N	0
SPBC1921.07c/hob1	808	68.19	69.4	0	0		N	0
Hob1/C21D10.11c	510	65.29	66.6	0	0		N	2
C21D10.11c/C21D10.10	308	77.60	71.2	0	209	NA	2	5
C21D10.10/C21D10.09c	1,093	67.25	69	0	0		N	0
C21D10.09c/C21D10.08c	553	72.88	73.4	0	128	2079	3	22
C21D10.08c/C21D10.07	84	71.43	66.2	0	0		N	3.4
C21D10.07/C21D10.06c	2,153	69.02	74	94	ND		4	8
C21D10.06c/ucp3	639	72.93	73.6	0	58		N	13
Ucp3/fnx1	3,194	70.95	77.8	59	ND	2080	N	19
fnx1/glo1	773	71.93	72.4	0	61	2080	5	21
glo1/C21D10.02	884	69.23	71	0	58	2080	N	21
C21D10.02/pst1	1,197	67.25	74	91	ND	2080	N	6.5
Pst1/C12C2.09c	957	68.03	71.6	0	69		N	0
C12C2.09c/C12C2.08	329	71.43	69.6	0	0		N	0
C12C2.08/C12C2.07c	1,704	67.72	69.4	0	1.7	NA	6	5
C12C2.07c/C12C2.06	250	71.20	65.6	0	0		N	0
C12C2.06/C12C2.05c	314	68.15	68.4	0	0		N	0
C12C2.05c/C12C2.04	575	72.87	74.4	0	74	NA	7	3
C12C2.04/C12C2.14c	1,505	66.18	69.2	0	0		N	0
C12C2.14c/C12C2.03c	1,573	65.48	68.4	0	0		N	0

Table 10: Comparison of ARS and ORI activity of 26 Intergenic Regions
This table shows a comparison between the ARS activity of 26 intergenic regions as determined by a transformation efficiency assay (Dai et al., 2005) and ORI activity from microarray analysis. Grey shading = ARS & ORI activity; Red shading = false negatives; green shading = false positives. No shading = no ARS & ORI activity. The number given in the Array Peak column corresponds to the number of the peak on the replication profiles as indicated in Figure 40.

(*ARS*, autonomously replicating sequence; ND, not determined.**ARS* activity is the number of transformants obtained with a plasmid containing the intergenic region, expressed as a percentage of the number of transformants obtained with an identical amount of the control plasmid pRC20 containing *ars1* (100%). The activities of intergenic regions 4 and 6, while low, were 10 and 12 times the background activity, respectively.)

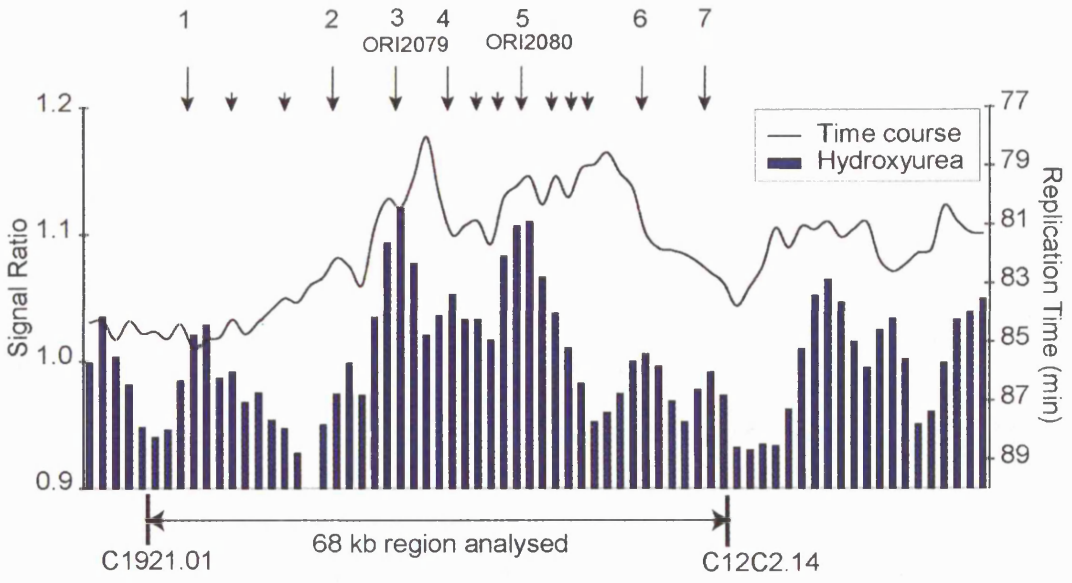

Figure 40: Peaks on the replication profiles co-localise with ARS activity
An overlay of the time course and HU experiments for a 100 kb region from Chromosome Two is shown. A 68 kb region (as indicated) previously analysed for ARS activity on plasmids (Dai et al., 2005), was analysed for ORI activity. Distinct peaks on the replication profiles are indicated with large arrows and correspond to probes that show ARS activity. The small arrows correspond to probes with ARS activity that could not be mapped to distinct peaks. The numbers were used to indicate which ARS sequences correspond to which probes on the microarrays (see Table 10, column "Array Peak").

At a 16 % ORI efficiency in meiosis, about 63 ORIs will be active in any particular cell cycle (1/200kb). This roughly corresponds to the estimated number of 50 – 150 double strand breaks (DSBs) and 50 meiotic recombination events in fission yeast ((Cervantes et al., 2000) and references therein). The best characterised meiotic DNA break site is Mbs1 close to the ura1 locus on Chromosome One. It has been shown that Mbs1 is broken at a 10.8 % efficiency (Young et al., 2002), which can be translated to 40 % efficiency according to a DSB repair model (Szostak et al., 1983). Interestingly, the two ORIs flanking this break site are used at 16 % and 23 % efficiencies. Mbs1 maps to a large intergenic region (7.2 kb) with AT contents of up to 79.4 %. These genetic

markers normally confer strong ORI activity. However, no significant signal was detected on the replication profiles, indicating that this region is usually replicated passively from adjacent ORIs.

3.3 Discussion

In this Chapter I characterised the structure and organisation of ORIs as well as differences in ORI usage in meiosis and mitosis, both in space and time.

The average inter-origin distance of 31 kb for the 401 ORIs identified in Chapter Two is similar to that of budding yeast (Figure 41) and follows a similar distribution.

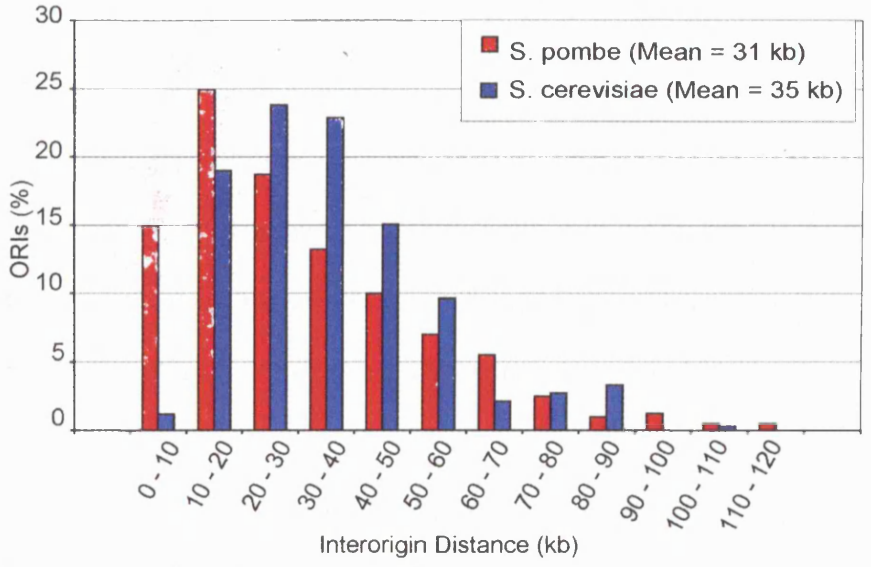

Figure 41: Comparison of Interorigin Distance in Fission Yeast and Budding Yeast
Histogram of the distribution of fission yeast and budding yeast inter-origin distance (Raghuraman et al., 2001).

However, when the additional 503 peaks identified in the replication profiles of the HU experiment are included in this comparison, a significant

difference results, as shown in Figure 42. This difference is not only restricted to the average inter-origin spacing which is reduced to 14 kb (904 peaks) from 31 kb (401 ORIs) but also marks a significant change in the distribution pattern. More than 80 % of peaks are spaced within 20 kb distances. This pattern suggests that initiation events in fission yeast are more clustered than in budding yeast. Alternatively it could be that the change in distribution is simply a consequence of the number of ORIs identified, which may vary dependent on differences of threshold values applied for ORI mapping and differences in experimental techniques. The distribution pattern and spacing of the 904 peaks is more similar to one seen in *Xenopus* sperm nuclei (Figure 42B). Here the distance between replication eyes was measured on combed DNA molecules from sperm nuclei incubated in *Xenopus* egg extracts in vitro (Marheineke and Hyrien, 2004). In this system, DNA replication initiates at around 10 kb intervals at very high efficiencies and hence the time of S phase is much reduced (20mins) compared with somatic cells and very similar to the mitotic S phase length in fission yeast. Although the 904 peaks on the replication profiles exhibit a much reduced efficiency compared with the Xenopus system and replication fork velocities vary (fission yeast : *Xenopus* = 2.8 kb/min : 1.2 kb/min), the comparison indicates that replication initiation events can potentially occur at high density at 10 – 15 kb intervals across eukaryotic genomes. It could be that this is a common feature of fission yeast and metazoan cells and used to regulate the length of S phase by modulating site-specific initiation dependent on the developmental program of the cell. Dense clusters of ORIs could also be identified in

fission yeast, which resulted in high signal ratios across an extended region on the HU replication profiles. These were reminiscent of initiation zones in metazoans, such as the 52 kb initiation zone in the human ß globin locus (Biamonti et al., 2003).

A

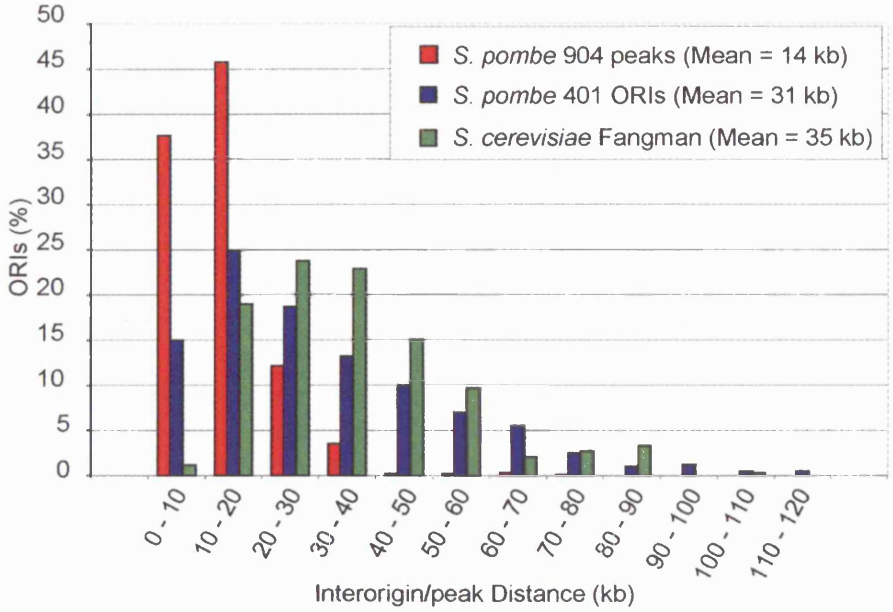

B

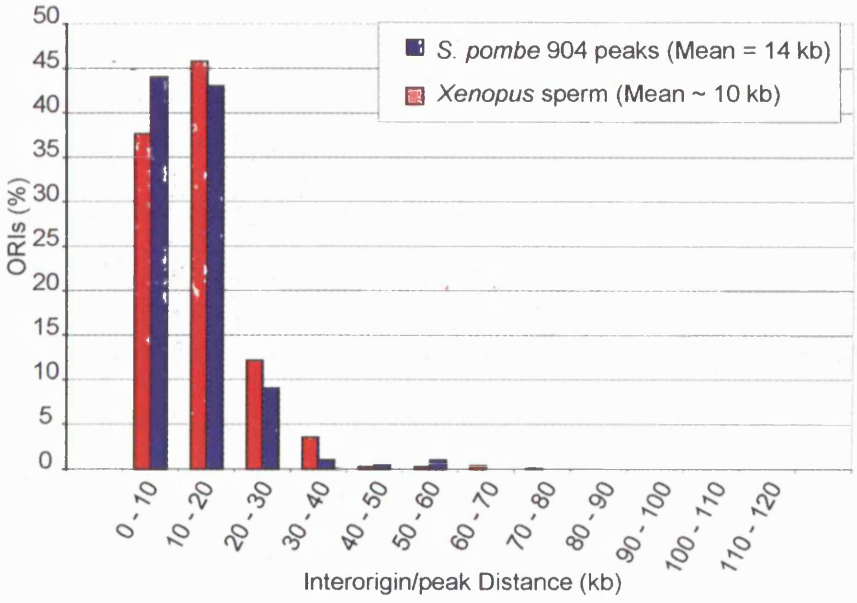

Figure 42: Interorigin Distances in Fission Yeast, Budding Yeast and Xenopus sperm
The distance between the centre (A) of the 401 ORIs mapped in Chapter Two and the 904 peaks identified in the HU experiment and the 332 ORIs mapped in budding yeast (Raghuraman et al., 2001) was determined and plotted as a histogram. The distance between the centre of (B) 904 peaks as in (A) and replication eyes from 5 – 10 Mb of chromosomal DNA in *Xenopus* (Marheineke and Hyrien, 2004).

Fission yeast ORIs were confirmed to localise to intergenic regions as shown previously (Segurado et al., 2003). This suggests a spatial separation between transcription and replication initiation due to negative interference. For instance, transcription may interfere with the assembly of pre-RCs as has been suggested in budding yeast (Nieduszynski et al., 2005). I showed that the minimum intergenic size to accommodate an ORI is around 800 bp consistent with previous estimates of the average size of fission yeast ORIs. ORIs prefer to localise between large intergenic regions with an average size of 2.2 kb in length between the starts and stops of coding regions, and these tend to be found between divergently transcribed genes. This size requirement may be necessary to comfortably accommodate the approximately 1 kb ORI sequence as well as 5' and 3' UTRs and promoter regions. The average 5' and 3' UTRs in fission yeast are 170 and 320 bp respectively (N. Peat, unpublished data). Dependent on the intergenic context, an extra 300 – 500 bp are required if ORIs interfere with these region. Less space would be necessary for two 5' UTRs in divergent intergenic regions than 5' and 3'UTRs in tandem and convergent regions, which might explain some of the bias of ORIs to preferentially localise between divergent transcription units. In addition, transcription and replication initiation could be functionally linked and share cis- and trans acting elements. This would cause evolutionary pressure for A+T-rich islands, the genetic markers for ORIs, to localise upstream of promoters and CpG islands as has been previously shown in mammalian cells (Delgado et al., 1998; Antequera and Bird, 1999). This in turn could result in a preference for ORIs to localise between divergent

transcription units as has been shown in fission yeast (Gomez and Antequera, 1999). In contrast to fission yeast, budding yeast ORIs are enriched at convergent transcripts (Macalpine and Bell, 2005) arguing against a positive interaction between regulators of transcription and DNA replication in eukaryotes. Intergenic regions in fission yeast and human cells are much larger than in budding yeast (Lander et al., 2001; Wood et al., 2002). The small intergenic regions in budding yeast may have forced a less complex ORI structure reminiscent of viral and bacterial ORIs which resulted either in the maintenance or the evolution of a consensus sequence that supports specific and relatively strong interactions with ORC. As a consequence these ORIs may not require interaction with trans acting regulators for their specification.

ORIs in fission yeast fire throughout S phase in meiosis and mitosis but the majority of ORIs is activated in mid S phase. The time between the first and the last replication initiation event in meiosis is four minutes longer than in mitosis, which suggests that ORI activation is more staggered than in mitosis. There are small differences in replication timing between chromosomes of up to four minutes. This is consistent with observations in budding yeast and mammalian cells (Raghuraman et al., 2001; Yabuki et al., 2002; Woodfine et al., 2004; Woodfine et al., 2005). Heterochromatic regions appear to be differentially regulated in terms of activation timing; telomeres replicate late, peri-centromeric regions as well as the mating type locus replicate early during S phase which has been observed in previous studies (Kim and Huberman, 2001; Kim et al., 2003). A comparison of timing domain structures in mitosis and meiosis showed

that the centromere and mating type locus on Chromosome Two as well as regions around rDNA repeats on Chromosome Three are differentially regulated. Centromeres and telomeres are re-localised from the spindle pole body to the cell cortex after pre-meiotic S phase in fission yeast. It is possible that nuclear positioning influences the replication timing in these regions in meiosis. The differential regulation of ORI activation in heterochromatic regions is also seen in metazoan cells where epigenetic factors are thought to be involved (reviewed in (Antequera, 2004)). The heterochromatic regions in fission yeast seem very few and well defined, which offers an opportunity to dissect the molecular basis of this phenomenon in future studies.

The efficiency of ORI firing each S phase varies considerably from around 70 % to less than 10 %. There is a good correlation of ORI efficiency with time of replication. A similar correlation between efficiency and timing could be observed on Chromosome Six of budding yeast (Figure 43) using 2D-gel analysis (Friedman et al., 1997).

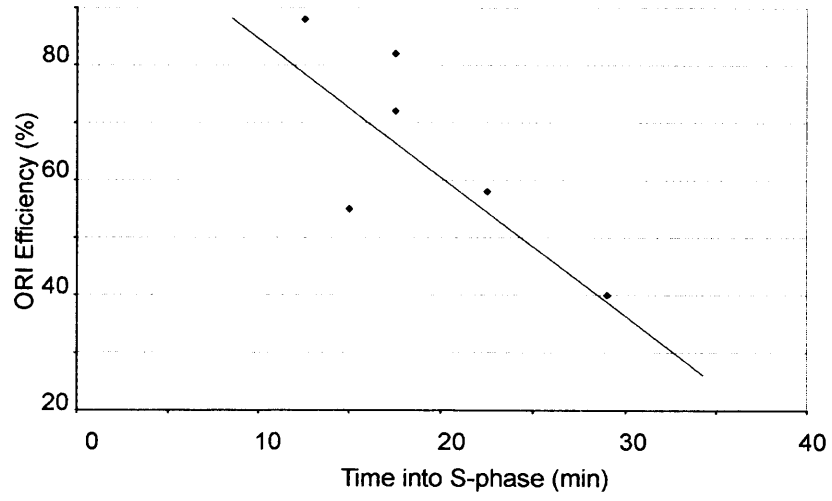

Figure 43: Replication Timing and ORI efficiency correlate in Budding Yeast

ORIs that are activated late in S phase generally show low efficiencies in HU, but fork migration distances from late ORIs are similar to ones in early ORIs. This indicates that late ORIs are generally not inhibited by the addition of HU. Perhaps un-surprisingly, those ORIs which are most efficient and are used every two to three cell cycles, fire early in S phase, whilst those used every ten cell cycles fire late. Late ORIs are presumably inefficient due to passive replication from adjacent early ORIs. Thus a large part of the temporal program in S phase can be explained by ORI efficiency. For instance, the right arm of Chromosome Two is poor in efficient ORIs which could explain its later replication than the rest of the genome. Similarly, Chromosome Three has typically higher efficiency than Chromosomes One and Two in meiosis and mitosis of up to 11 % and thus replicates three to four minutes earlier. The pattern of ORI efficiencies in mitosis shows an even distribution of efficient ORIs across Chromosome Three but clusters of efficient and inefficient ORIs on Chromosomes One and Two. Chromosome Three has a lower gene density than the other chromosomes and intergenic regions are on average about 100 bp bigger as a consequence. The observed pattern may be a result of interference of high gene density with ORI specification and/or efficiency due to a positive correlation with intergenic size. However, although fission yeast ORIs preferentially map to large intergenic regions, the correlation of efficiency and intergenic size was only 20 % in mitosis. This suggests that large intergenic regions are essential for specification of ORIs but that the absolute size of an

intergenic region has only a minor impact on the efficiency of ORIs. In budding yeast, addition of HU has been shown to activate the intra S phase checkpoint, which inhibits activation of late firing ORIs (Santocanale and Diffley, 1998). A similar effect on ORI firing has been suggested in *Drosophila*, where 62 ORIs that are active in the presence of HU have been mapped on the left arm of Chromosome Two recently, using microarray analysis (MacAlpine et al., 2004). It is currently unclear whether and how many late ORIs are inhibited by this checkpoint in fission yeast (Kim and Huberman, 2001). Perhaps the identification of true late firing ORIs by 2D-gel analysis is difficult, due to low efficiencies of these ORIs. To address this issue in the future, a fission yeast strain that lacks the gene rad3 essential for the activation of the intra S phase checkpoint could be used. If the rad3 dependent checkpoint does inhibit the activation of efficient late ORIs, these ORIs should be activated early in S phase in the HU experiment and hence show significant signal increases in the presence of HU.

The efficiency at which ORIs are utilised during mitotic and pre-meiotic S phase is different, at 29 % for mitotic S phase and 16 % for pre-meiotic S phase. Because fork velocity is similar at 2.8 kb/min and 3.3 kb/min respectively, differing efficiencies mean that the minimum length for S phase assuming synchronous ORI firing at S phase onset is 19 mins and 30 mins. This is consistent with the differences in replication timing observed on the replication timing profiles, 24 minutes in mitosis and 32 minutes in meiosis. I conclude that the combination of staggering of ORI firing and decreased ORI efficiency seem to be the main contributors to

the increased length of pre-meiotic S phase. Genome-wide analysis of ORI efficiency also allowed a comparison of relative ORI usage in mitotic and pre-meiotic S phases. Around 50 % of ORIs were differentially regulated in meiosis and mitosis, which is a significantly larger proportion than previously suggested for a subset of budding yeast ORIs (1/6 or ~15 %). However, this discrepancy might be due to the small number of ORIs analysed in the budding yeast study (Collins and Newlon, 1994). Interestingly, many ORIs that were induced in pre-meiotic S phase localised 600 kb proximal to telomeres on Chromosomes One and Two and to a 750 kb region in the centre of Chromosome One. This suggests that ORIs in these regions are subject to a position effect, which could be a consequence of epigenetic factors modulating the chromatin environment differentially in the two types of cell cycle. For instance, a shift in histone acetylation levels in the vicinity of ORIs could result in changes of ORI activation time and hence ORI utilisation (Vogelauer et al., 2002; Antequera, 2004). Consistent with this, extended regions near telomeres have been shown to be repressed by various *Clr* silencing proteins (*Clr1* zinc finger protein, *Clr4* methyltransferase and *Clr3* HDAC), and become transcriptionally activated during meiosis (Mata et al., 2002; Hansen et al., 2005).

The number of ORIs active in any particular S phase very roughly corresponds to the 50 meiotic recombination events in fission yeast (Munz et al., 1989). However, on the replication profiles, the best mapped meiotic DNA break site Mbs1 is not associated with strong ORI activity which suggests that ORIs are spatially separated from sites of prominent double

strand breaks. This could be explained by the fact that recombination in fission yeast, although linked to DSB formation, has been shown to occur between 20 and 50 kb away from the break ((Cervantes et al., 2000) and references therein). It is thus possible that the actual recombination event which follows DSB formation co-localises with the ORI. It has recently been suggested that the sequence of pre-meiotic S phase and the occurrence of DSBs in fission yeast is coupled by DNA replication checkpoint proteins (Tonami et al., 2005). Proteins associated with the replication fork presumably activate the checkpoint, but this does not clarify whether there is a functional link between ORI activation and introduction of a DSB. As shown here the majority of ORIs in fission yeast fire in the presence of HU from onset to mid S phase and a coupling between DNA replication and DSB formation could happen at this early stage, before the mutant block points used in previous studies, as has been suggested (Murakami and Nurse, 2001). Clearly, more work is needed to present conclusive evidence for the dependence of recombination on ORI utilisation during pre-meiotic DNA replication in fission yeast.

The distribution of inter-origin distances observed for the 401 ORIs identified in Chapter Two together with the uneven distribution of efficiencies within and between chromosomes suggests a stochastic model of ORI firing across the fission yeast genome. This could result in large unreplicated gaps at the end of S phase, which would cause genome instability and segregation defects of chromosomes in the subsequent mitosis. Somehow cells provide the means to cope with this

problem. The data from the replication profiles indicates that 503 additional initiation events, which typically appear in late S phase, but did not qualify the strict threshold for ORI mapping in our analysis are distributed between more efficient ORIs across the fission yeast genome. Such weak peaks were particularly common between significant ORIs that were spaced at considerable distances. They co-localise with A+T-rich islands which have above average intergenic AT-contents and with regions that have been shown to exhibit ARS activity in a plasmid context. Of the 904 peaks that were identified on the replication profiles, more than 50 % are used in less than $1/10^{th}$ of cell cycles. Hence the bulk of DNA (~74 %) is replicated from the 401 relatively efficient ORIs that could be identified in Chapter Two of this analysis. I suggest that distinct small peaks on the replication profiles represent weak ORIs and that fission yeast can activate ORIs in late S phase in 5 – 15 kb intervals from most intergenic regions that have AT-contents around 72 %. This is probably essential to replicate gaps towards the end of S phase that had not been passively replicated from significant adjacent ORIs. Our analysis suggests that the microarrays used were sensitive enough to map weak initiation events and could therefore provide a useful tool to address the random completion problem (Hyrien et al., 2003) on a whole genome level in future studies.

Chapter IV

Genome wide Characterisation of DNA Amplification

4 Genome wide Characterisation of DNA Amplification

4.1 Introduction

Two types of situation can lead to endo-reduplication in fission yeast. In the first the G_2/M CDK, Cdc2/Cdc13, is inactivated. This can be done either by switching off (s/o) *cdc13* expression in a strain which has the *cdc13* gene controlled by the *nmt1* promoter, or by overexpression (o/e) of Rum1, which is thought to act by binding to the Cdc2/Cdc13 complex and inhibits the kinase activity (Correa-Bordes and Nurse, 1995). In the second situation, DNA synthesis initiation factors are somewhat overexpressed. Higher levels of the initiation factor Cdc18 generated by expression of the *cdc18* gene under the *nmt1* promoter are sufficient to induce DNA synthesis but the effects of Cdc18 o/e are much enhanced if Cdt1, a second initiation factor is also overexpressed (Yanow et al., 2001). It has been suggested that o/e of Cdc18 leads to incomplete rounds of re-replication of the genome (Nishitani and Nurse, 1995; Yanow et al., 2001). Conversely, complete rounds of re-replication are thought to occur in a *cdc13* s/o background (Fisher and Nurse, 1996). The aim of this chapter is to gain insights into the mechanism of re-replication, by observing differences in the mode of ORI firing in the above mentioned re-replication systems.

4.2 Results

4.2.1 Comparison of Re-replication Profiles in different Endo-Reduplicating Systems

A *cdc13* s/o strain was used to deplete cells of Cdc13 (see Methods). Cells grown to early exponential phase were starved of nitrogen overnight. This led cells to arrest in G_1 and results in a semi-synchronous cell culture inducing efficient re-replication upon re-addition of nitrogen. After eight hours of induction, the average DNA content per cell had increased from 2C to 32C (Figure 44A). DNA from these cells was differentially hybridised to microarrays with unreplicated DNA obtained from G_1 arrested cells. Microarray analysis demonstrated that the signal ratio averaged around one, which indicated that the entire genome was equally amplified (Figure 45, green graph). I conclude that in this type of endo-reduplication all ORIs were used equally effectively.

Next nmt1-Cdc18 was o/e either by its own or co-o/e together with Cdt1 (see Methods). Full induction of the nmt1 promoter occurs approximately 15h after removing thiamine from the culture medium. Cells accumulated an 8C DNA content after 21 h without thiamine in a Cdc18 o/e strain (Figure 44B) and up to a 32C DNA content in the case of co-o/e of Cdc18 and Cdt1 from G_2 phase of the cell cycle (Figure 44C). When Cdc18 was o/e, replication profiles showed that 13 regions became amplified (Figure 45, blue graph). The same regions were also amplified when Cdt1 was overexpressed in addition, but to a greater extent (Figure 45, red graph). Regions 5 and 12 were found to be over-amplified around threefold above the rest of the genome (Figure 45, red graph), which

corresponds to a DNA content of up to 96C at genome-wide amplification levels of 32C (see Figure 44C). It should be noted that the efficiency of re-replication in experimental repeats varied in the Cdc18 o/e and Cdc18/Cdt1 co-o/e systems and the levels shown in the flow cytometry profiles of Figure 44B/C are the maximum levels achieved in one particular experimental repeat. However, the degree of amplification and thus signal ratios were similar in experimental repeats as demonstrated in Figure 46. In the three experimental repeats of the Cdc18/Cdt1 co-o/e experiments, experiment one showed the least efficient re-replication, followed by experiments two and three (Figure 46A, left to right). The majority of cells did not accumulate DNA contents above 4C in experiment one, but more than 50 % of cells accumulated DNA contents in excess of 8C in experiments two and three. Despite this difference in re-replication efficiency, the same regions were over-amplified to a similar extent in all three experiments (Figure 46B). Similar results were obtained for the Cdc18 o/e experiment (compare Figure 48 Chromosome Three, blue line with Figure 50C, black line).

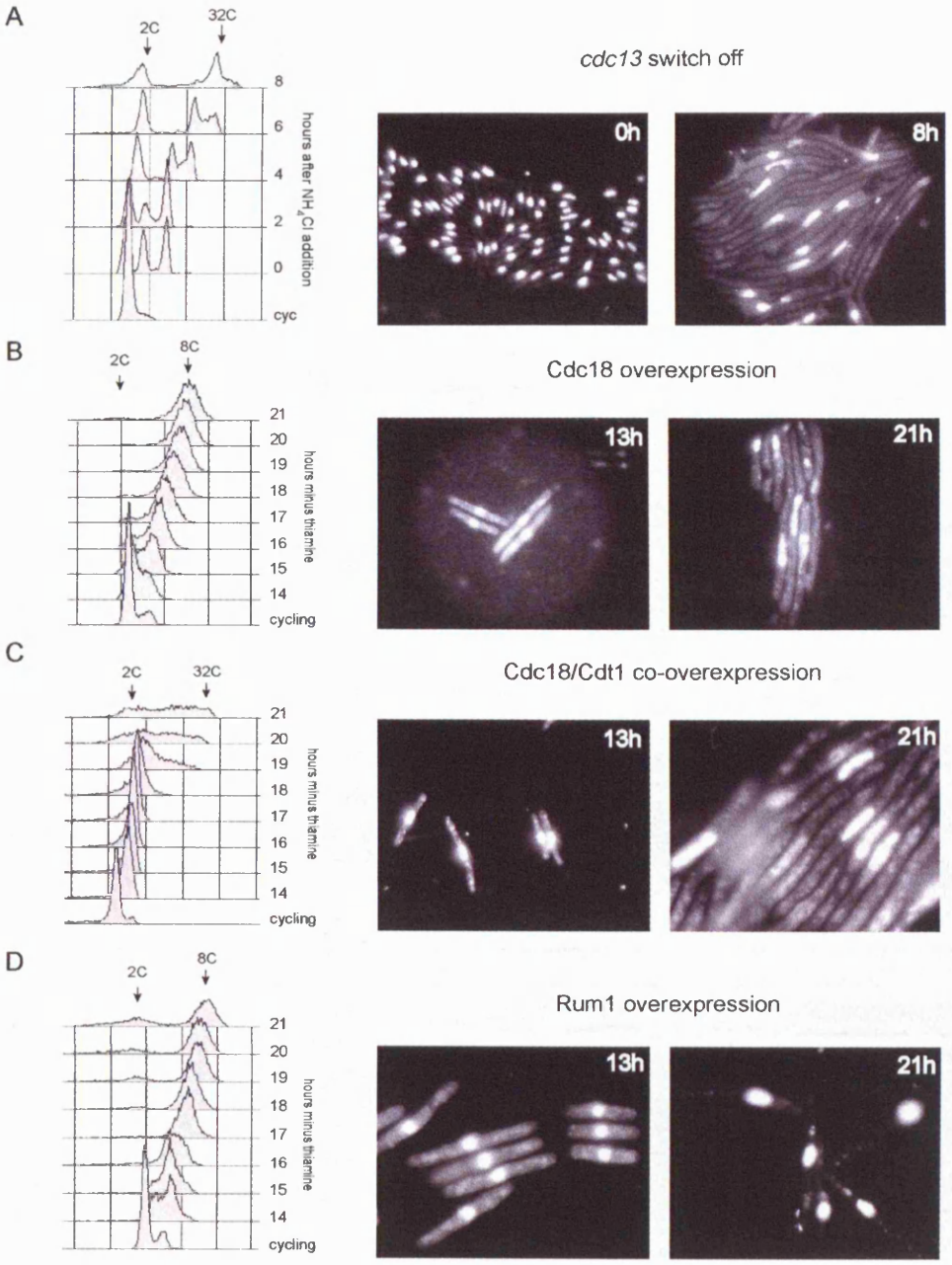

Figure 44: FACS Profiles and DAPI Stains of Re-replicating Cells
Flow cytometry profiles and DAPI stained cells are shown for the following: (A) Cdc13 s/o causes 32C DNA contents to accumulate in a single cell 8h after re-addition of nitrogen; DAPI stained cells 0h and 8h after release from nitrogen starvation. (B) Cdc18 o/e causes 8C DNA contents to accumulate in a single cell 18 – 21h after thiamine wash out; DAPI stained cells 13h and 21h after thiamine wash out. (C) Cdc18 and Cdt1 co-o/e causes up to 32C DNA contents to accumulate in a single cell 21h after thiamine wash out; DAPI stained cells 13h and 21h after thiamine wash out. (D) Rum1 o/e causes 8C DNA contents to accumulate in a single cell 18 - 21h after thiamine wash out; DAPI stained cells 13h and 21h after thiamine wash out.

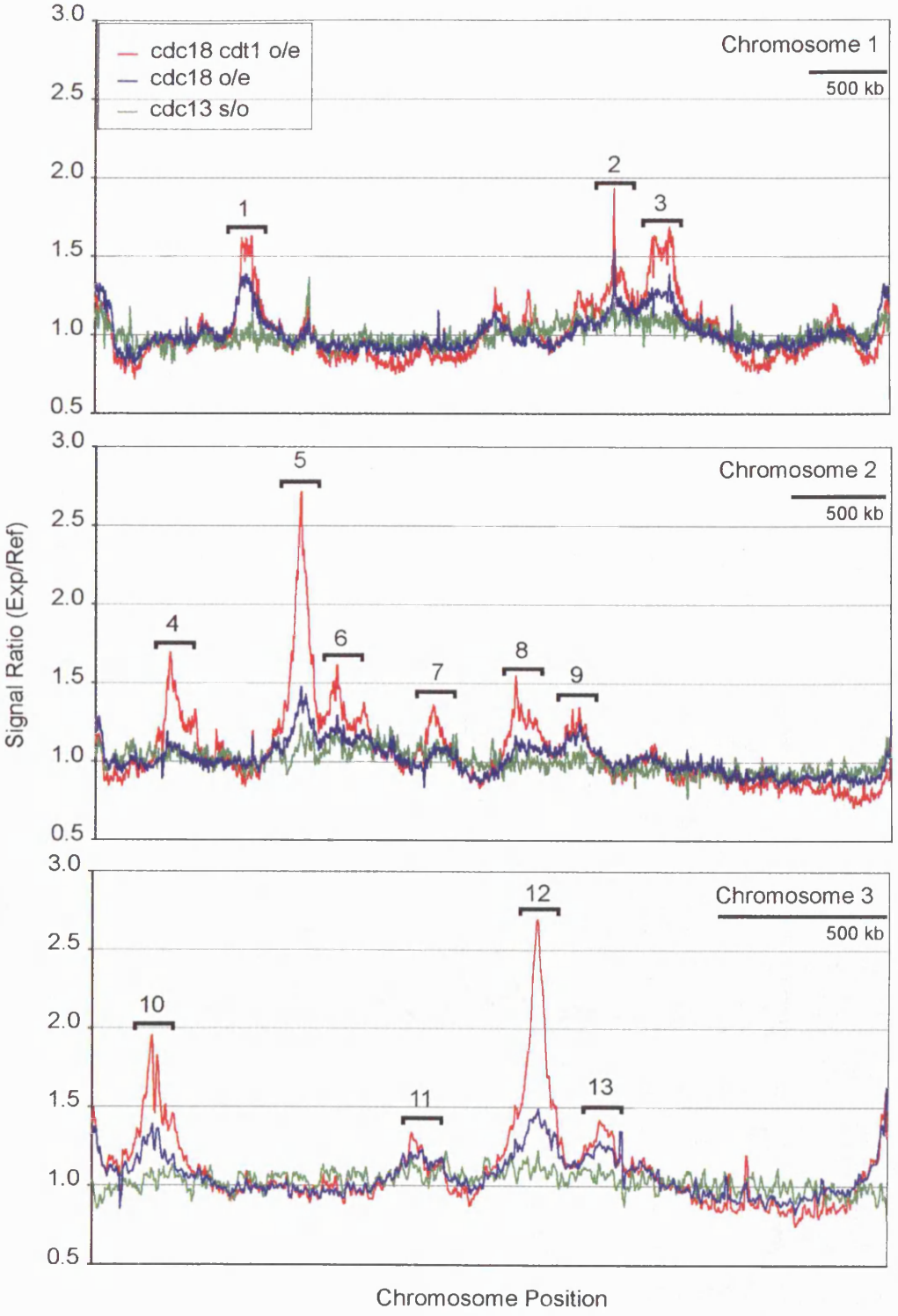

Figure 45: Replication Profiles of Different Re-replication Systems
A whole genome comparison of re-replication profiles from a Cdc18 o/e, cdc18/cdt1 co-o/e and a *cdc13* s/o is shown for the three fission yeast chromosomes. The peaks indicate regions that are amplified (Chromosomes One, Two, Three = top, middle, bottom diagrams). Peak numbers refer to ORI regions as specified in Table 11.

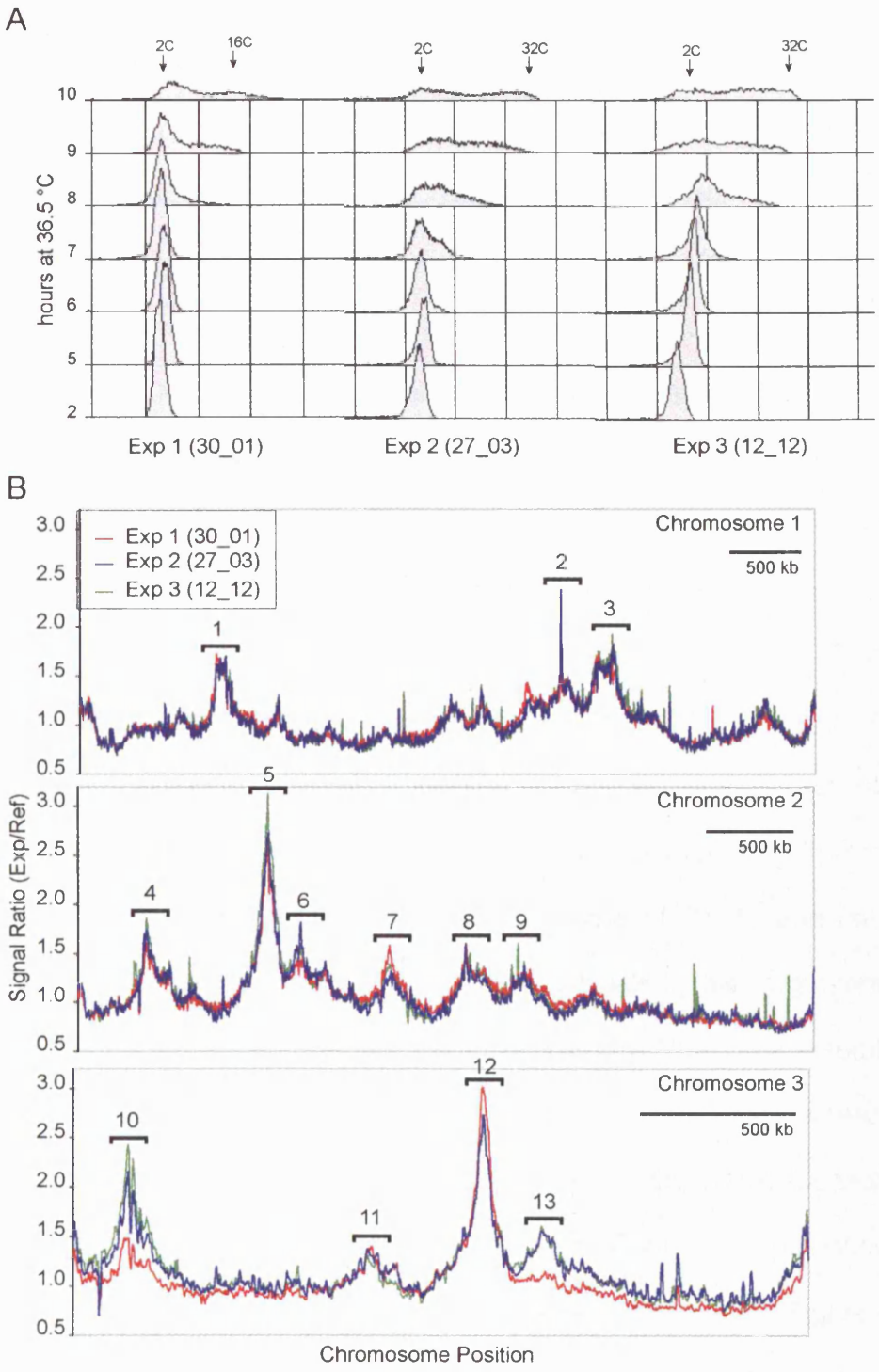

Figure 46: Over-amplification is mostly independent of Re-replication Efficiency
(A) FACS profiles of three experimental repeats (left to right) of the Cdc18/Cdt1 co-o/e experiment and (B) Re-replication profiles of the three experimental repeats shown in (A). Peak numbers refer to ORI regions as specified in Table 11.

Lower levels of amplification were also observed in the sub-telomeric regions of Chromosome One and Two, in regions adjacent to the rDNA repeats of Chromosome Three, and in regions flanking centromeres.

Next Rum1 was overexpressed from the *nmt1* promoter (see Methods) and cells accumulated 8C DNA content in a single cell after 18 h of induction (Figure 44D). Theoretically, Rum1 o/e should behave in a similar way to a *cdc13* s/o, as both have the effect to inactivate the mitotic kinase Cdc2/Cdc13. However, the re-replication profile of the Rum1 o/e resembled the Cdc18 o/e profile (Figure 48). The same regions were amplified to a similar extent in the two systems. It has been reported that Cdc18 levels increase significantly when Rum1 is o/e (Kominami and Toda, 1997; Yamano et al., 2004). Both proteins are degraded in S phase by the $SCF^{Pop1/Pop2}$ degradation complex. The competition of high levels of Rum1 with Cdc18 for $SCF^{Pop1/Pop2}$ binding leads to accumulation of Cdc18 in cells (Figure 47). Hence it is possible that the over-amplification in certain regions is the consequence of high levels of Cdc18 and not the inhibition of Cdc2/Cdc13 by high Rum1 levels. This argument is strengthened by the fact that the FACS profile of a Rum1 o/e resembles more the one of a Cdc18 o/e than a *cdc13* s/o (compare Figure 44A/B/D). It is interesting however, that regions adjacent to the rDNA repeats on Chromosome Three were not amplified in a Rum1 o/e, but showed significant amplification in a Cdc18 o/e (indicated by arrows in Figure 48). Another peak on Chromosome One (indicated by an arrow in Figure 48) is also much less amplified in Rum1 o/e. This suggests that re-replication and over-amplification from certain ORIs such as the ones found in rDNA

repeats is more efficient in the Cdc18 o/e background compared with the Rum1 o/e. I speculate that these ORIs require higher levels of Cdc18 to trigger significant over-amplification.

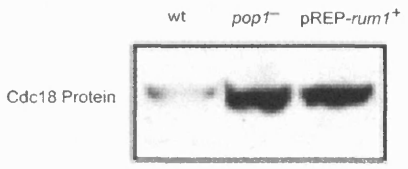

Figure 47: Cdc18 Protein Levels increase in a Rum1 o/e Background
This data was taken from (Yamano et al., 2004). Cdc18 protein levels during mitotic S phase are elevated when Rum1 was o/e in an SCF mutant (pop1-, second lane) and wildtype background (pREP-rum1⁺, third lane) compared with the control (wt, lane 1).

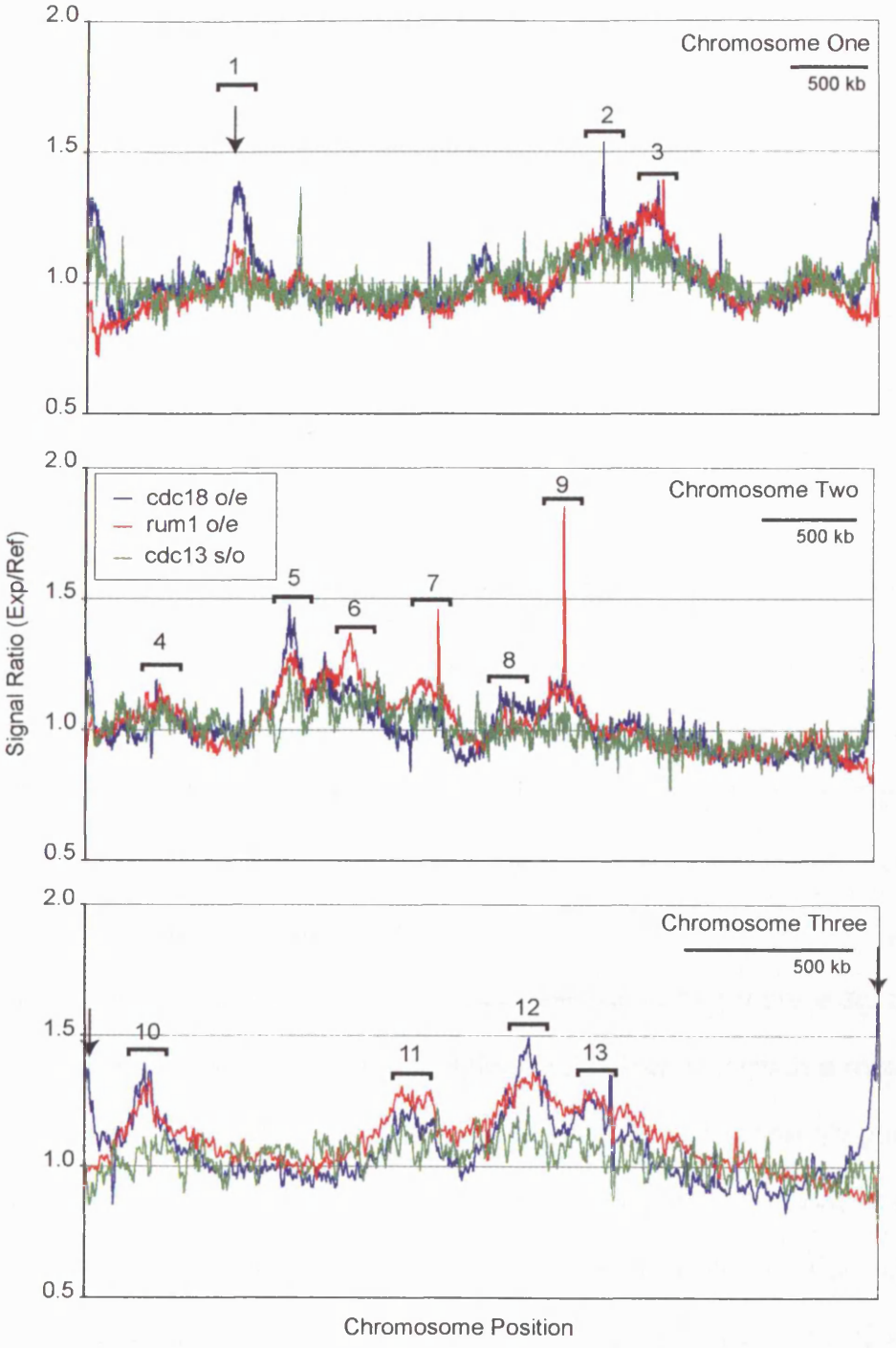

Figure 48: Re-replication Profiles of *cdc13* s/o, Cdc18 o/e and Rum1 o/e
Whole genome overlay of three different re-replication profiles from a *cdc13* s/o strain, a Cdc18 o/e strain and a Rum1 o/e strain. (Chromosomes One, Two, Three = top, middle, bottom diagrams). The regions that show significant differences in the Cdc18 and Rum1 o/e are indicated with arrows. Peak numbers refer to ORI regions as specified in Table 11.

4.2.2 Characterisation of Over-amplified Regions

Next, regions that were significantly (1.5fold) over-amplified in a Cdc18 Cdt1 co-o/e background were characterised further. A total of 57 ORIs were identified which mapped within these amplified regions (Table 11). The average inter-origin distance within the peaks in these regions was 25 kb that is about 20 % more dense than the rest of the genome. Average ORI efficiency was increased to 40 % compared with 29 % in the rest of the genome. For instance, as shown in Figure 49A/B, the two most over-amplified regions (region 5 and 12, around 96C) in the genome contained efficient ORIs with a tendency to cluster. The intergenic regions containing ORIs were found to be longer (2800 bp compared with 2088 bp in the rest of the genome) and often consisted of LTRs (Long Terminal Repeats). The average AT content was also higher, 76.9 % compared with 75.2 percent. ORIs that mapped to peaks of maximum amplification typically showed AT contents above 78 % and were also often more extreme with regard to other features. For example, ORI2040 which sits in a region that was amplified up to 3.41fold was located within a low complexity gene free region of 6143 bp and had an efficiency of 53 % and an AT content of 83.8 %. These ORIs were flanked by highly transcribed genes. For instance, housekeeping genes such as an alcohol dehydrogenase adh1, hexose transporters ght5 and ght6, and genes hta1, htb1 coding for histone subunits co-localised with over-amplified regions. ORI3049 mapped to a region of small ORFs (C622.03, C622.04) which probably do not code for proteins but are highly transcribed. ORI3056 is flanked by eight very efficiently transcribed genes (C13B11.02/03, 977.01 – 977.05 and adh1).

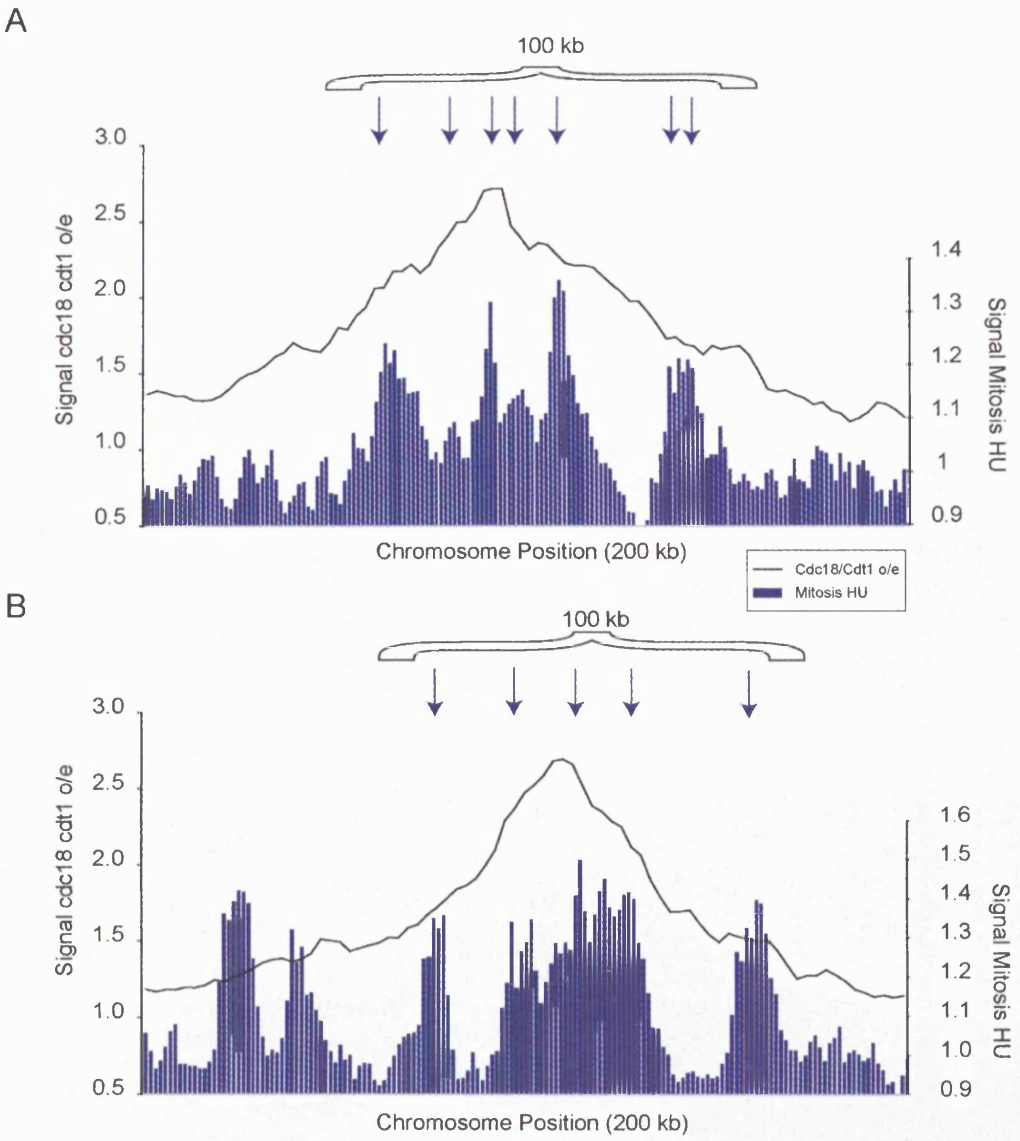

Figure 49: Amplified Regions contain efficient ORIs in Clusters
ORIs that were mapped in mitosis and map to the over-amplified regions are indicated by arrows. (A) 200 kb region from Chromosome Two. (B) 200 kb region from Chromosome Three. The average inter-origin distance in the two amplified regions was around 20 kb.

Peak Number	Origin	Chromosome Position	AT content (500 bp window)	Amplification Signal	% Efficiency	Intergenic Distance
1	1027	1021911	73.00	1.64	5	2838
	1028	1079985	78.40	1.68	57	3402
	1029	1087856	71.20	1.73	31	1686
	1030	1095332	74.80	1.45	44	1496
2	1109	3549172	77.20	1.42	59	3410
	1110	3575013	78.20	2.52	56	1421
	1111	3604381	73.40	1.42	20	2607
	1112	3636644	78.20	1.54	42	2105
3	1124	3860176	72.20	1.74	11	1045
	1125	3869814	81.40	1.76	45	7847
	1127	3893805	78.40	1.72	35	1455
	1128	3947976	76.60	1.82	73	2955
	1129	3987807	82.60	2.06	59	3978
	1130	4013740	75.80	1.8	31	1884
	1131	4064746	75.80	1.51	40	1619
	1132	4082746	77.80	1.32	61	1430
4	2015	520348	80.60	1.88	40	4423
	2016	569481	76.00	1.34	43	3366
	2017	592707	74.00	1.43	22	1993
5	2039	1255476	75.80	2.92	17	1256
	2040/2041	1268615	83.80	3.41	53	6143
	2042	1280407	78.60	2.67	58	1259
	2043	1309527	75.00	2.21	37	3130
	2044	1316300	75.00	2.2	29	1506
6	2045	1390459	75.20	1.42	41	1445
	2047	1444990	77.60	1.66	28	1992
	2048	1462321	75.80	1.7	41	4229
7	2064	2028284	80.80	1.4	30	3259
	2065	2036477	75.20	1.38	34	1175
	2066	2054052	76.20	1.34	30	2337
8	2080	2448059	77.80	1.58	21	3194
	2081	2525756	74.60	1.43	37	1267
	2082	2555034	81.00	1.52	27	1599
9	2091	2794668	80.20	1.26	44	1922
	2092	2799811	74.40	1.32	47	2081
10	3006	119903	78.20	1.36	64	2019
	3007	123154	78.60	1.36	50	2147
	3008	190170	73.40	1.93	29	2381
	3009	207534	82.60	2.49	52	5972
	3010	231433	78.60	2.35	30	4433
	3011	246552	75.80	1.88	14	922
	3012	253494	75.20	1.78	13	10242
	3014	287037	76.60	1.67	46	3168
	3015	314546	75.20	1.44	14	2057
11	3036	970246	78.80	1.35	45	8851
12	3045	1323040	76.00	1.37	52	1948
	3046	1343448	74.60	1.43	55	2646
	3047	1371089	76.40	1.89	48	4912

	3048	1398984	73.80	2.11	43	3495
	3049	1410248	78.60	2.75	57	1640
	3050	1418087	77.80	2.45	53	949
	3051	1449183	76.40	1.68	46	2228
	3053	1532669	76.80	1.25	45	2633
	3054	1556939	73.00	1.45	43	2249
13	3056	1595330	80.80	1.67	53	1223
	3057	1609474	78.80	1.49	52	2077
	Average		76.90	1.75	40	2800

Table 11: ORI Characteristics in Amplified Regions

In conclusion, DNA amplification in Cdc18/Cdt1 co-o/e occurs at ORIs which are used more efficiently, have above average AT content and are found in large intergenic regions. Efficient transcription in these regions may also enhance the likelihood that ORIs become competent for over-amplification of DNA.

4.2.3 Kinetics of Over-amplification

I then investigated the kinetics of re-replication. In order to compare results from the Cdc18 o/e and the Cdc18/Cdt1 co-o/e experiments, Cdc18 was also ectopically overexpressed in G_2 phase of the cell cycle. A comparison of the two flow cytometry profiles in Figure 50A shows that cells accumulated up to 4C DNA content in the Cdc18 o/e and up to 16C in the Cdc18/Cdt1 co-o/e experiment. In a control strain, cells arrested with 2C DNA content, as expected for G_2 cells, and there was no further increase in DNA content during the eight hour incubation at 36.5°C (Figure 50). It should be noted that the FACS peak in these cells drifted towards the right as they persisted in the block due to an auto fluorescence artefact as a consequence of cell elongation (Sazer and Sherwood, 1990). As can be seen from the increase in DNA content through time, most of re-replication took place in the final two hours of the time course in both

the Cdc18 oe and the Cdc18/Cdt1 co-o/e. DNA from cells harvested at 0, 4, 6, 8 and 10h into the G_2 block was differentially hybridised to microarrays with unreplicated DNA from the control cells blocked in G_2. Re-replication profiles of Chromosome Three are shown in Figure 50B/C for the two experiments. No DNA over-amplification could be seen at zero and four hours after temperature shift. By six hours significant peaks appeared in the amplified regions; the most amplified peak in the central part of the chromosome showed a further increase thereafter and reached a maximum by 10 h. The smaller peaks did not show much increase after six hours. This pattern was also observed on the other two chromosomes. No amplification was seen in regions flanking rDNA repeats by eight hours but a significant increase in signal to about 1.5fold was observed in the final two hours of the time course. This indicates that Cdc18 protein levels had to reach a certain threshold to cause significant over-amplification in the rDNA repeats. It also suggests that ORIs within some of the over-amplified regions of the genome have the potential to increase the degree of over-amplification from six hours onwards whereas others fail to do so. There are two possible explanations how this could come about. The first is that whole genome endo-reduplication ceases by six hours and only very few ORIs undergo an additional round of replication leading to an increase in amplification in these selected regions. Alternatively, endo-reduplication from ORIs could be accelerated in regions where signals do increase after six hours compared with ORIs in the rest of the genome, by increasing the frequency with which ORIs re-fire from one round of replication to the next (see Discussion).

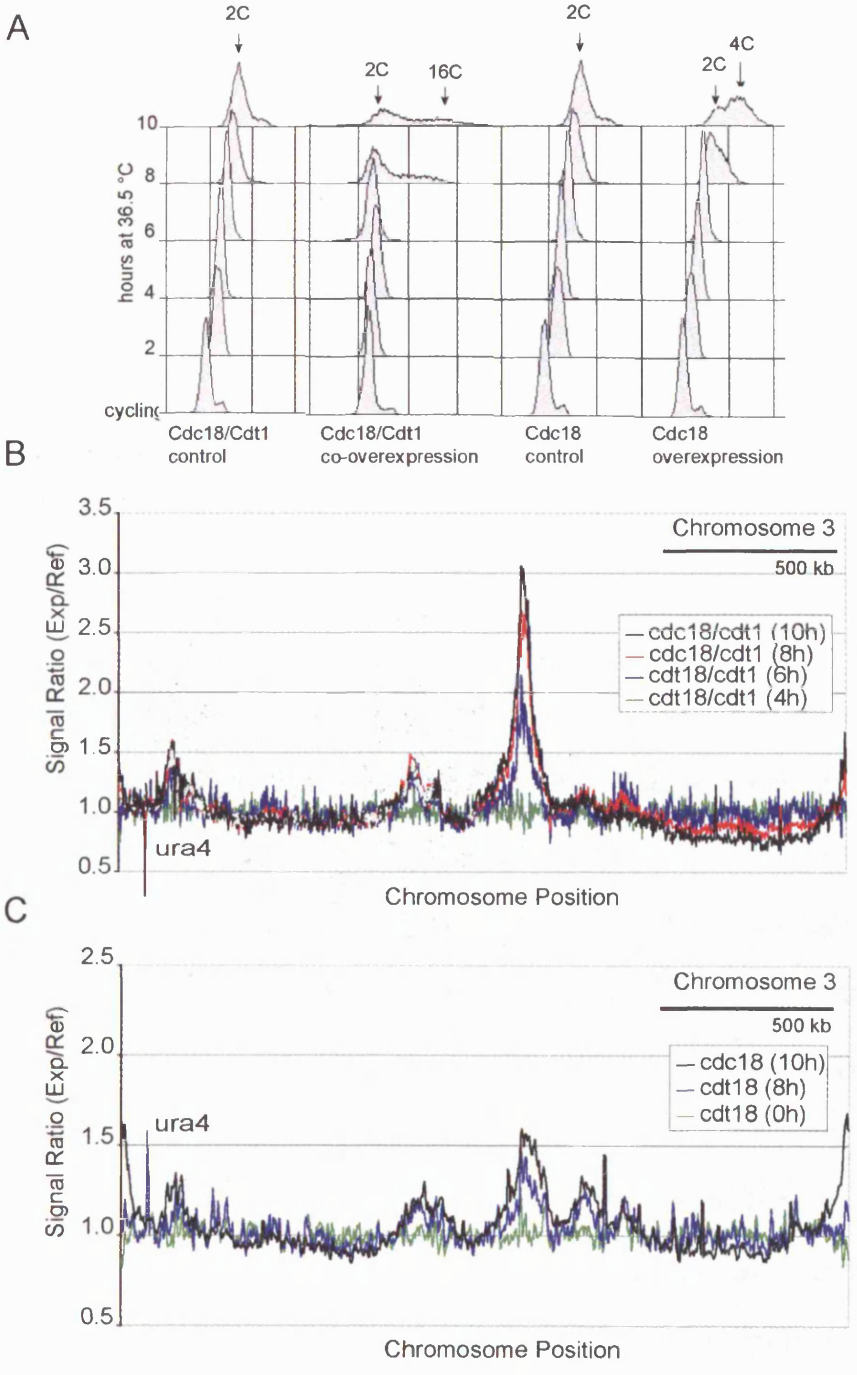

Figure 50: Re-replication Kinetics in a Cdc18 o/e and Cdc18 Cdt1 co-o/e System
(A) FACS profiles of a Cdc18 o/e (left panel) and a Cdc18 Cdt1 co-o/e time course. Chromosome Three re-replication profiles from a time course experiment of a Cdc18/Cdt1 co-o/e (B) and a cdc18 o/e (C). The *ura* gene is used as a genetic marker in the experimental strain and therefore results in artefactual signal ratios.

4.2.4 ORI firing in a Cdc13 endo-replication cycle

I also wanted to investigate whether the same set of ORIs was used in the *cdc13* s/o re-replication cycles as in a normal mitotic cell cycle. Endo-reduplication of DNA in the *cdc13* s/o background occurs in a semi-synchronous manner, leading to distinct peaks on the flow cytometry profiles (Figure 51A, left panel). However, as ORIs fire throughout the cell cycle, it is impossible to catch all ORIs at a particular time during the endo-reduplicating cycle. Therefore, re-replicating cells were blocked with 11mM HU, six hours after s/o. This is the time when a shift from 16C to 32C DNA content took place, as can be seen on the flow cytometry profile in Figure 51A (left panel). The increase in DNA content was much reduced in HU-treated cells (Figure 51A, right panel) compared with non-treated cells of the same culture, indicating that fork progression was slowed down due to depletion of dNTPs in the cells. Similar to the HU experiments in the normal mitotic and meiotic cell cycles, this should emphasise the positions in the genome where ORIs were activated in this particular endo-cycle. DNA from cells blocked for two hours in HU was analysed on microarrays. It should be pointed out that only ORF arrays were used for this analysis, reducing the resolution by about half compared with the ORI mapping experiments and that only one experiment (no repeats) was carried out. A comparison of the re-replication profile (500 kb) from the *cdc13* s/o and the replication profile from the mitotic HU experiment is shown in Figure 51B. Peaks that map to ORIs (indicated by arrows) co-localised in the two experiments with two exceptions. A similar pattern could be observed across the rest of the

genome. This indicates that essentially the same ORIs were used during the endo-reduplicating cell cycle of Cdc2/Cdc13 kinase-defective cells as in a normal mitotic cell cycle in the presence of HU.

A

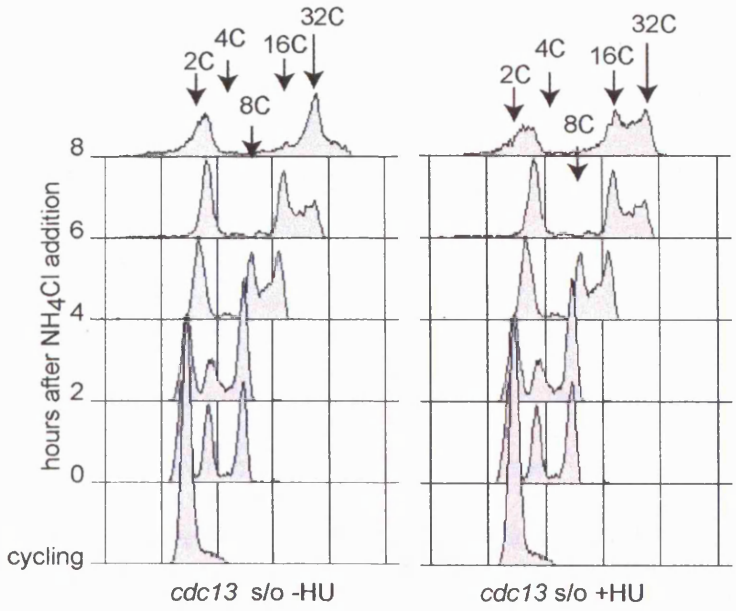

B

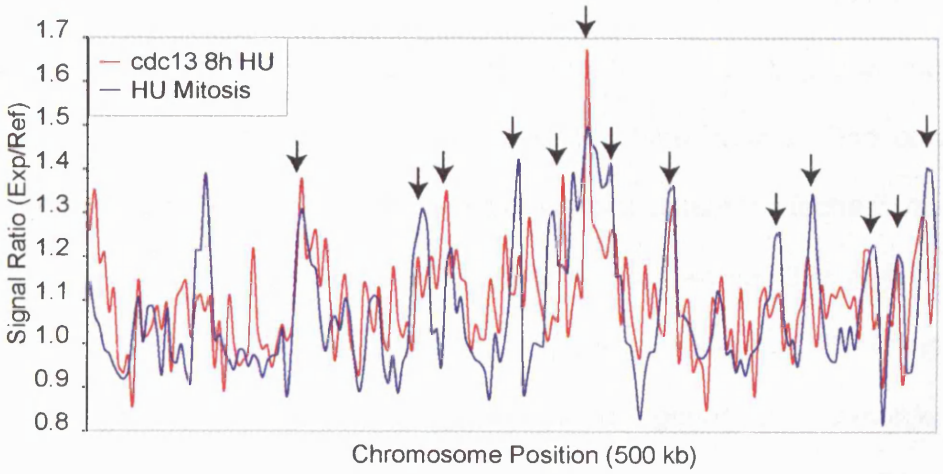

Figure 51: ORI firing in a *cdc13* s/o strain
(A) FACS profiles of a Cdc13 o/e experiment without HU (left panel) and in the presence of 11 mM HU (right panel); the FACS profiles up to 6h are equivalent in both panels (same FACS samples), HU was added at 6 h to an aliquot of the culture and a separate FACS sample was taken for the 8 h time point. (B) Overlay of re-replication profiles of a *cdc13* s/o HU experiment and the 90 minute time point of a mitotic S phase HU experiment

4.3 Discussion

In this chapter I found that endo-reduplication induced by removing the G_2/M CDK Cdc2/Cdc13 results in equal amplification of all parts of the genome. By contrast, o/e of the initiation factor Cdc18 or co-o/e with Cdt1 leads to greater amplification of certain segments, apparently breaking the rule that all genome regions are replicated only once in each S phase. The data indicates that the same ORIs as in normal mitotic cell cycles are used in the *cdc13* s/o endo-reduplication cycles. Peaks of over-amplified regions in the Cdc18/Cdt1 o/e re-replication profiles co-localise with ORIs of the mitotic cell cycle which show exceptional features. These ORIs are found in clusters, reminiscent of initiation zones, are more A+T-rich and efficient, map to large intergenic regions and are often surrounded by efficiently transcribed genes. I suggest that elevated levels of Cdc18 and Cdt1 act synergistically with these types of ORIs and that this interaction breaks the one replication per S phase rule. It is interesting that the kinetics of over-amplification changes during the time course. One can imagine that the re-firing of ORIs can arise via two different mechanisms or a combination of these. In one mechanism, the same ORI re-fires continuously, which is analogous to the "onion-skin" model of ORI firing that is also observed in amplification of chorion genes in *Drosophila* (Figure 52) (Osheim et al., 1988). The other mechanism involves the firing of different subsets of ORIs in each round of re-initiation.

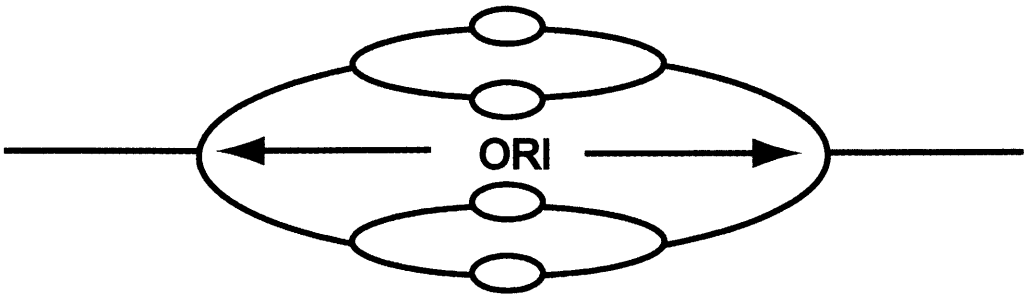

Figure 52: Onion Skin Model of Re-replication
ORIs re-fire during the same cell cycle in S-phase.

Figure 53 compares the microarray endo-reduplication profiles from an amplified region in *Drosophila* (Claycomb et al., 2004) and one from fission yeast. The shape of the two profiles looks broadly similar and the gradient of the graphs suggests the presence of onion skin structures which emanate from one or more ORIs that are located in the centre of the peak. These structures already form at the beginning of the endo-reduplication cycle at around six hours into the block in G_2 phase, as can be seen from the time course experiments. An increase in amplification could be observed in all regions within six to eight hours after temperature shift but only a subset of regions shows a further increase in signal ratios thereafter (8 to 10 hours). This indicates that the rate at which over-amplification takes place varies dependent on the region. Alternatively the increase in signal in these regions could be due to additional rounds of re-replication after bulk DNA synthesis has ceased, though this is unlikely given that DNA content only increases significantly on FACS profiles from eight to ten hours and therefore that bulk DNA replication must take place during this period. One possibility to account for differences in kinetics of over-amplification would be if some ORIs were more sensitive to de-

regulation upon accumulation of Cdc18/Cdt1 protein levels than others. This would result in a correlation of protein levels and the efficiency of over-amplification from these ORIs which could be explained by a greater affinity of these ORIs for Cdc18 and/or Cdt1 licensing factors (further discussions on this point, see chapter V).

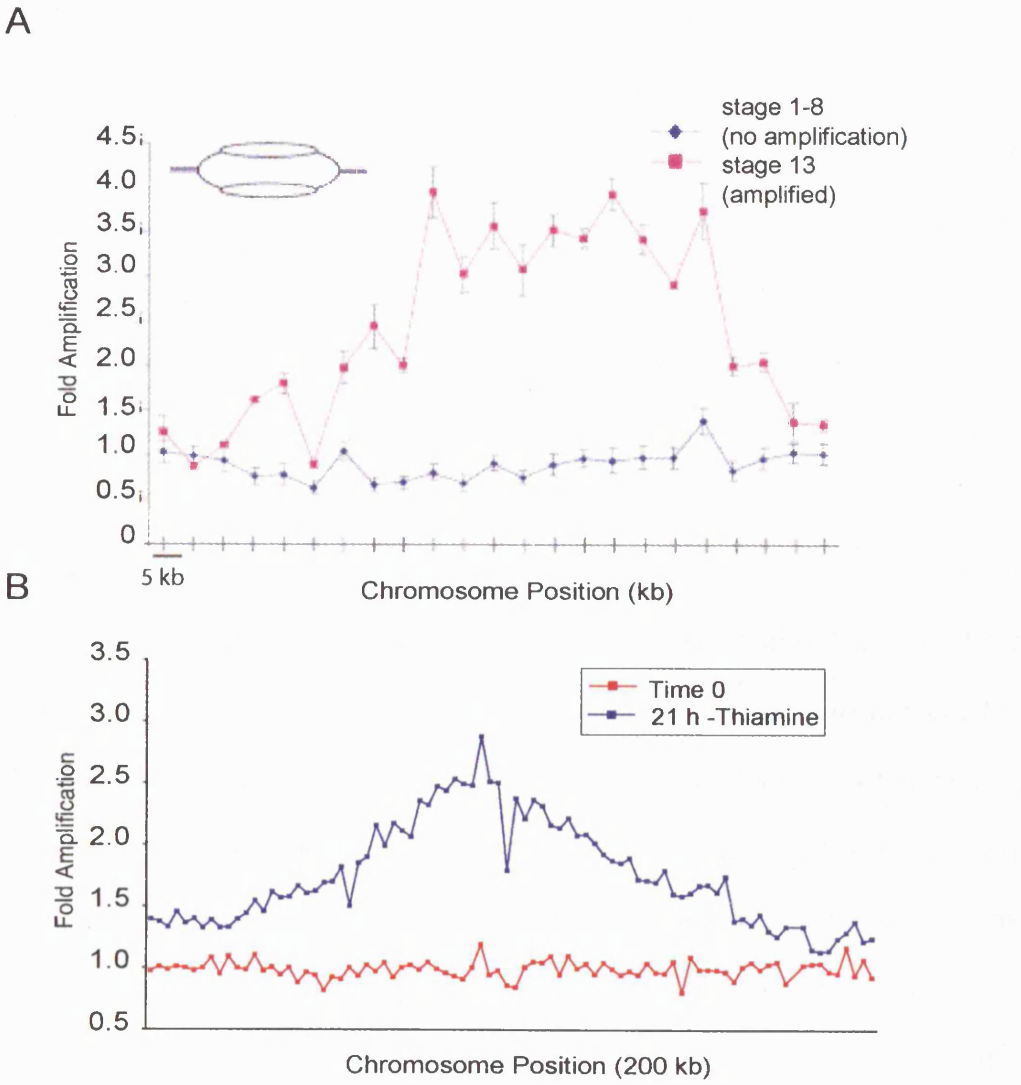

Figure 53: Comparison of amplified Region of *Drosophila* and Fission Yeast
The Drosophila plot was taken from (Claycomb et al., 2004). The fission yeast figure is data from a single experiment. The area shown in (B) corresponds to the central part of the amplified region number 5 on Chromosome Two as specified in table 11.

Another factor that could contribute to the difference in the kinetics of over-amplification in these regions may be the size of intergenic regions that contain putative over-amplifying ORIs. Presumably both Cdc18 and Cdt1 have to bind DNA in order to confer re-replication. The bigger an intergenic region, the more protein may be able to bind in the vicinity of ORIs. Intergenic size could be crucial for the maintenance of onion skin replication structures and perhaps synergistic action of Cdc18/Cdt1 complexes in closely spaced re-replicated DNA molecules could lead to a greater propensity of amplification in regions where more space is available for such interactions. It must be borne in mind, however, that the cultures in the Cdc18/Cdt1 o/e experiments were not well synchronised. The FACS profile of a Cdc18/Cdt1 co-o/e in Figure 44C shows a broad smear of DNA contents ranging from 2C to 32C which could be a consequence of the asynchrony of cells in the culture or incomplete rounds of re-replication (Yanow et al., 2001). In the case of the Cdc18 o/e (Figure 44B), the shift of broad but distinct peaks towards higher *C* DNA content was observed even though some of the DNA was over-amplified, which is consistent with a semi-synchronous culture where most cells were present within the same endo-reduplication cycle. The smear in the co-o/e experiment may be due to a combination of accelerated loss of the Cdt1 expression plasmid in a subset of cells during the time course rather than asynchrony in the culture. This possibility is strengthened by the fact that the degree of over-amplification did not correlate with the efficiency of re-replication in either system. Even if cells were completely

asynchronous, the kinetics of peaks in the different regions should be equally affected by the asynchrony, which was not the case as shown in the time course experiments.

The kinetics of re-replication upon Cdc18 o/e is different from that during Cdc18/Cdt1 co-o/e, as shown previously (Yanow et al., 2001). During Cdc18/Cdt1 co-o/e more rapid DNA re-replication was observed and the doubling time was reduced from two hours to thirty minutes. There are at least four ways this could come about: by an increase in the number of ORIs that fire simultaneously, which would reduce the amount of DNA synthesised by each replication fork; by increasing the frequency with which ORIs re-fire from one round of replication to the next; by inducing initiation from non-ORI regions, or by increasing the replication fork velocity. The efficiency of re-replicating ORIs could not be addressed in this study, as the synchrony of the culture was not adequate. However, as shown previously, the ratio of replication bubbles to passive replication forks was higher in the early stages of re-replication at *ars3001* when Cdc18 and Cdt1 were co-overexpressed than that observed in cells over-expressing Cdc18 alone, which suggests that ORI efficiency may be increased. The increase in amplification from eight to ten hours in some peaks but not others during the time course indicates that an increase in firing frequency takes place in selected regions when Cdt1 is co-o/e with Cdc18. It is possible that ORIs that co-localise with the centre of these peaks combine particular features such as high AT-contents and large intergenic regions, which accelerate endo-reduplication in these regions. It is likely that the same ORIs are used in both o/e situations (Cdc18 or

Cdc18/Cdt1) since the amplified peaks co-localise. Co-localisation of the central regions of amplified peaks with clusters of efficient ORIs also suggests that at least some of these ORIs are used in the re-replication cycles. Future studies using single molecule analysis should clarify these points. Finally, it is possible that high levels of Cdt1 could increase replication fork velocity. If this was the case, the shape and width of amplified peaks should be different in the two o/e systems. One would expect to see wider peaks in regions where replication fork velocity is increased unless cells encounter a replication fork barrier. However, the shape and extension of peaks was very similar in the two systems. Also Cdt1 has been shown not to be required for fork elongation (Maiorano et al., 2000; Nishitani et al., 2000). In conclusion, the data is consistent with an enhancement of Cdc18-induced re-replication by Cdt1 due to more rapid re-firing of the same ORIs. This effect may be limited to a restricted number of ORIs which combine particular features that allow re-replication to accelerate if high levels of Cdt1 are present in the cell.

Chapter V

Computational and Bioinformatic Analysis

5 Computational and Bioinformatic Analysis

5.1 Introduction

The only chromosomal eukaryotic ORIs known so far that consist of a consensus sequence essential for ORI activity are found in budding yeast (reviewed in (Cvetic and Walter, 2005). Fission yeast ORIs have been proposed to co-localise with A+T-rich islands which do not seem to contain a common consensus (Segurado et al., 2003; Dai et al., 2005). Similarly, the small number of metazoan ORIs that has been genetically studied also lack a consensus sequence (reviewed in (Aladjem and Fanning, 2004). A recent study suggested a G+C-rich consensus sequence which is associated with fission yeast ORIs and confers ORI activation in late S phase (Yompakdee and Huberman, 2004). The first aim of this chapter was to carry out sequence alignment for consensus sequence analysis across a significant number of fission yeast ORIs identified in Chapter Two.

A+T-rich islands in intergenic regions of fission yeast are thought to be genetic markers for ORIs (Segurado et al., 2003; Antequera, 2004; Dai et al., 2005). Fission yeast ORC binds to these regions via AT-hooks in its Orc4 subunit (Chuang and Kelly, 1999) and particular sequence patterns that are preferred binding sites have been identified by genetic analysis in a small number of ORIs (Kong and DePamphilis, 2001; Kong and DePamphilis, 2002). The second aim of this Chapter was therefore to identify AT-hook binding sequences in fission yeast ORIs to see whether

particular DNA sequence patterns in A+T-rich islands correlate with ORI efficiency.

ORIs in fission yeast preferentially localise between divergent transcription units upstream of promoter regions (Gomez and Antequera, 1999), which suggests that the processes of DNA replication and transcription may be functionally linked (Gilbert, 2002). No correlation between replication and transcription could be identified in budding yeast on a whole genome level (Raghuraman et al., 2001). This contrasts with findings in human and *Drosophila* where whole genomic analysis have shown a correlation between time of replication and the probability that a gene is expressed (Schubeler et al., 2002; MacAlpine et al., 2004; Woodfine et al., 2004; Woodfine et al., 2005). Hence, the third aim of this chapter was to look for possible correlations between transcription data and ORI utilisation.

5.2 Results

5.2.1 Sequence Specificity in ORIs

No consensus DNA sequence for ORIs has been identified in fission yeast. (Clyne and Kelly, 1995; Dubey et al., 1996; Kim and Huberman, 1998; Okuno et al., 1999). However, only a small number of ORIs have been analysed and it is possible that a loose consensus with a high redundancy of residues or conserved domains could have been missed in previous analyses. In the present study, a representative number of ORIs was chosen and sequence alignments were carried out using ClustalW to identify any consensus sequences for ORIs (Higgins and Sharp, 1988; Higgins and Sharp, 1989). I also investigated the presence of a "late

consensus sequence", which has been suggested to associate with ORIs that fire late during S phase (Yompakdee and Huberman, 2004).

5.2.1.1 Clustal Analysis for Consensus Sequences in Efficient ORIs and ORIs with low AT-contents

The sequence for ClustalW alignment was determined from A+T-rich islands that co-localised with ORIs from the microarray analysis. Analysis of four genetically and biochemically characterised ORI sequences (ars1, ars2004, ars3001, ars3002) indicated that binding of ORC to ORIs in fission yeast follows a pattern according to which the first protected region along the sequence always co-localises with the 500 bp window that consists of the highest AT-content (typically 75 %), and then more ORC binds further downstream or upstream of this sequence up to a distance where AT-content is no less than 63%. The average length of sequences selected with this procedure was 1724 bp. A clustalW alignment was then carried out for a subset of 50 ORIs that showed an above average efficiency of 48 % and more. This criterion was chosen because high efficiency could be a consequence of very strong interactions with initiation proteins mediated by a conserved consensus sequence. On visual inspection of the alignment, these ORIs did not show a significant consensus. The highest score (indicates the match in residues) in pair wise alignments for sequences with an average 1724 bp length was 24, which was not significant. I concluded that there was no consensus sequence between ORIs that were very efficiently used in fission yeast. Next I chose DNA sequences of 50 ORIs with AT-contents below average (< 72.6 %). There was no overlap between this and the previous set of

ORIs analysed for consensus sequence. These ORIs could potentially consist of a conserved consensus sequence that confers sufficient affinity for replication licensing factors without requiring the high AT-content that is typical of other fission yeast ORIs. Here again no significant consensus could be identified (score ≤19). I conclude that a consensus sequence is not essential for ORI specification in fission yeast. The fact that there was no overlap of ORIs in the two subsets chosen in this analysis suggests that ORI sequences with low AT-content do not confer high ORI efficiency, as already mentioned. All efficient ORIs had AT-contents above 74 %. Interestingly the sequences extracted for ORIs with low AT-contents were 2000 bp in length, about 300 bp longer than sequences for efficient ORIs. This suggests that elevated AT-contents over larger intergenic regions could compensate for shorter intergenic regions with high AT-contents for the specification of ORIs as previously suggested (Dai et al., 2005).

5.2.1.2 Late Consensus Sequence Analysis

A systematic search for the late ORI sequence identified in a previous study (Yompakdee and Huberman, 2004) was carried out. That study suggested that co-localisation of ORIs with the so-called "late consensus sequence" caused passive replication in a pARS element and generally late replication in fission yeast ORIs. For instance, three copies of the late consensus sequence were shown to map upstream of pARS727. ORI activity was not detected in a plasmid assay when the late sequences were present and pARS727 was not mapped in the present study in its chromosomal context. Upon deletion of these sequences pARS727 gained ORI activity and was activated early within S phase on plasmids.

Successive deletion of sequences suggested that late consensus sequences act synergistically (Yompakdee and Huberman, 2004).

The program fuzznuc from the EMBOSS software suite (see Methods) was used to systematically map 10 bp late consensus sequences which match the pattern (AG)(TG)(TG)GGGGGA(AT) across the genome. The sequence was searched in the forward and reverse direction on the coding and non-coding strand. In total 247 sequences were identified on the three chromosomes, amongst which were the three sequences previously shown to co-localise with pARS727 in the study cited. The average density of late consensus sequences on Chromosomes One and Two was 1/49 kb, and on Chromosome Three it was 1/63 kb. However, there was no correlation between late and early replicating segments of chromosomes and the density of late consensus sequences. To identify co-localisation of ORI and late consensus sequences, hits were first compared with positions of microarray ORIs. 47 ORIs co-localised with at least one late consensus sequence, specifically 21 on Chromosome One, 19 on Chromosome Two and 7 on Chromosome Three. Of these 47, a subset of 24 or 51 % (44% expected) could be termed late replicating ORIs given that they replicated in the second half (>76 minutes) of S phase (Table 12). These 24 have AT-contents typically above 74 % and should therefore possess the potential to replicate efficiently and hence early in S phase. Only two of those ORIs, ORI1070 and ORI2081 co-localised with three late consensus sequences similar to pARS727. As mentioned, pARS727 was not mapped in the present analysis, but it was found to co-localise with an A+T-rich island in the

bioinformatic analysis (Segurado et al., 2003). This failure to identify A+T-rich islands because of interaction with a late consensus sequence could also apply to other A+T-rich islands without significant ORI activity in the present study. Analysis of those showed that another 11 A+T-rich islands co-localised with at least one late consensus sequence (Table 12). AT2103 (corresponding to pARS727) and AT2069 both associated with three late consensus sequences. To summarise, I found that about 13 % (23/177) of ORIs that replicate late in S phase and an additional 11 A+T-rich islands that could not be identified as ORIs in their chromosomal context were associated with at least one late consensus sequence. However the % of early and late replicating ORIs associated with late consensus sequences was similar. Hence my results could not identify a correlation between the presence of late consensus sequences in ORIs and their time of replication and I can not support the existence of a defined "late consensus sequence" in ORIs of fission yeast.

ORI	AT-island	Consensus Sequence	Distance from AT-island Centre (bp)	AT-content (%)	Repli-cation Time (min)	Efficiency
ORI1005	na	TAGGGGGTTA	-1025	65.6	83	21
ORI1026	na	ATGGGGGGAT	-1471	71.4	77	5
ORI1027	AT1041	ATCCCCCAAT	2371	73	78	20
ORI1044	na	CAACCCCCTT	623	74.6	77	11
ORI1045	na	CCACCCCCTA	-1139	72.6	78	18
		AGTGGGGGAA	2177			
ORI1070	AT1075	AAGGGGGTTA	2818	76	80	35
		TTCCCCCCCC	5227			
ORI1073	na	GTTGGGGGAA	814	76	80	33
ORI1075	AT1080	TAACCCCCTT	407	75.6	78	33
ORI1076	AT1082	TTCCCCCAAC	3321	76.6	77	19
ORI1080	AT1086	TAGGGGGGTA	1121	74.6	78	5
ORI1092	na	CCACCCCCTT	993	72.8	77	19
ORI1136	AT1135	AAGGGGGGTA	-1371	76.6	77	42
ORI1155	AT1147	TTCCCCCCAC	-707	74	77	30
ORI1161	AT1150	AAGGGGGTGG	-4430	75.8	77	12
ORI2004	na	TTCCCCCCCC	1108	76.6	77	14

ORI2062	na	TTCCCCCCCC	861	73.8	79	28
ORI2068	AT2068/ pARS756	AGTGGGGGAT	-2170	79.4	81	25
		ATTGGGGGAA	2844			
ORI2081	na	ATCCCCCACC	283	74.6	78	37
		CAACCCCCTT	658			
ORI2094	AT2091	GTGGGGGGAA	1299	77	77	28
ORI2113	AT2112	GGTGGGGGAA	1093	75.2	78	23
ORI2131	na	CCACCCCCTA	-776	75.6	81	26
ORI2132	AT2129	GTTGGGGGAT	-692	77.8	80	na
ORI2134	na	TAACCCCCTT	612	73.8	78	12
ORI3019	AT3014	GTTGGGGGAT	1746	77.6	77	34
na	AT1012	CAACCCCCTT	-5661	76.6	na	na
na	AT1015	ATCCCCCCCC	1137	83.4	na	na
na	AT1026	GTGGGGGGAT	300	77.6	na	na
na	AT1034	AAGGGGGGTA	-1710	79.4	na	na
na	AT1059	TAACCCCCTT	-862	75.8	na	na
na	AT1087	GTGGGGGGAT	1064	75.4	na	na
		GTGGGGGGAA	1143			
na	AT1129	ATCCCCCACC	-4002	82.6	na	na
na	AT1171	ATCCCCCAAC	241	76	na	na
na	AT2067	AAGGGGGTGA	1383	73.6	na	na
		AAGGGGGTTA	-1081			
na	AT2069	AGTGGGGGAT	3031	74.2	na	na
		TTCCCCCAAT	3918			
		TTCCCCCCCC	1398			
na	pARS727/ AT2103	TTCCCCCACC	1419	76.6	na	na
		GTGGGGGGAT	1508			

Table 12: Late Consensus Sequences associated with ORIs and AT-rich Islands
The consensus sequence corresponds to the coding strand sequence. The – sign in the fourth column denotes direction along the chromosome (proximal, no sign is distal).

5.2.1.3 Mapping of AT-hook binding domains

Previous studies in fission yeast suggested that ORI efficiency is a function of percentage of AT-content (Segurado et al., 2003; Dai et al., 2005). Efficiency of ORI usage in mitosis was plotted against %AT-content of the relevant ORI region (Figure 54). The dot plot obtained was wedge shaped and displayed a correlation of approximately 38 %. This indicated that in order for ORIs to be used efficiently they need to have a high AT-content, but that a high AT-content is insufficient to define an efficient ORI. To determine what other properties of ORIs might be important for their efficiency, two sets of ORIs with AT-contents above 74 % in a 500 bp window were compared; one set contained ORIs used efficiently at 48 % or more (52 ORIs); a second set contained ORIs used inefficiently at 24 % or less (106 ORIs).

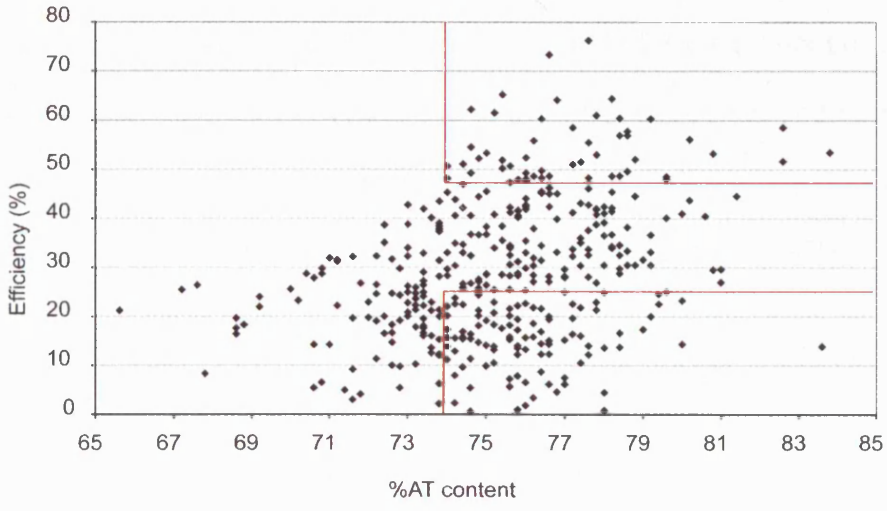

Figure 54: Correlation between % AT-content and ORI Efficiency
Mitotic ORI Efficiency for 401 ORIs was plotted against %AT-content. ORIs with AT-content higher than 74 % and with an efficiency lower than 24 % or 48 % and higher (indicated by the red lined boundaries) were further analysed for properties that could influence their efficiency.

The first criterion examined was presence of AT-hook binding sequences given that in fission yeast the ORC component Orc4 has 9 AT-hook motifs (Chuang and Kelly, 1999). This indicates that the presence of AT-hook domains embedded within a generally high A+T-rich region may be important for DNA replication. AT-hook binding sequences are asymmetric A+T-rich sequences consisting of $(AAAA/TTTT)_n$, $(AAAT/TTTA)_n$, and $(AATAAT/TTATTA)_n$ where n is greater than two (Okuno et al., 1999; Kong and DePamphilis, 2001; Takahashi and Masukata, 2001; Kong and DePamphilis, 2002), and with a spacing between the sequences of 4 – 8 nucleotides (Maher and Nathans, 1996). Binding occurs in a uni-directional manner on the T-rich strand (Kong and DePamphilis, 2002). A search algorithm was devised, using a combination of the aforementioned criteria to map AT-hook sequences and potential Orc4 binding sites in fission yeast ORIs. First genetically and biochemically analysed fission yeast ORIs ars1, ars2004, ars3001 and ars3002 were chosen to evaluate the search algorithm. An example of the input sequence and output results for ars2004 is shown in Figure 55. This algorithm managed to identify all previously characterised Orc4 binding domains in these ORIs.

ARS2004 Core Sequence

gccgtg**ttaaaaaaaattaaaaattaacaaaaaaaaaaaaaaaaaaaa**gagagacgaaagt
tatcgcaaacaaaaagaacttttattaatataactaattgcattaatgattgactcagtac
acaccacacaaatatattcacttaatttaattgttttaaaatgagtgtaaaatatctat
tggtataaccaattccatcacaattgctaattgaatggaatgatttgcataaaatgtttc
taacttaatttttttattcttttatgttcacgaatacaaatttatttttgttttaaaaa
acttcatttttctttgcttatcttttgggtagttttcggatccgtaatcccaacaaaatgc
caacccgtattgactaataagttcccgaaaatgtaagcaaaagatttcattgtaaaacaa
atgaattagctattaaaactgttatttaaatgttgtaagggttggtatgttatatataca
atctaagtctatgtaaagacttttttgaaagatcctactgtacagaattctccataattga
attcgtgacaagtactcataatatttgaaacttgtatattatttctgcgtataacctatc
tttatttttatttaatttttatttttttacttttatttttatttttatttttatttttttc

*The sequence in bold has been shown to bind ORC4 in vivo.

AT-Hook Binding Sequence Mapping Output

Map Start	Inter-Hook-Distance	AT-hook sequence
9	0	AAAA
13	0	AAAA
19	2	AAAA
29	6	AAAA
33	0	AAAA
37	0	AAAA
41	0	AAAA
71	26	AAAA
80	5	TTTA
130	46	AAAT
146	12	TTTT
155	5	TTTT
159	0	AAAA
170	7	AAAA
231	57	AAAA
249	14	TTTT
253	0	TTTA
260	3	TTTT
279	15	AAAT
286	3	TTTT
291	1	TTTT
296	1	AAAA
307	7	TTTT
322	11	TTTT
332	6	TTTT
354	18	AAAA
388	30	AAAA
399	7	AAAA
414	11	AAAA
419	1	AAAT
435	12	AAAA
445	6	TTTA
501	52	TTTT
601	96	TTTA
605	0	TTTT
611	2	TTTT
617	2	TTTT
622	1	TTTT
630	4	TTTA
634	0	TTTT
639	1	TTTT
644	1	TTTT
649	1	TTTT
654	1	TTTT

AT-Hook Binding Domain 1
ORC4 binding in vivo
7 asymmetric AT-hook sequences

AT-Hook Binding Domain 2
ORC4 binding in vivo
11 asymmetric AT-hook sequences

Figure 55: Characterisation of ARS2004 for AT-hook binding Domains
The core sequence (essential) and AT-hook binding domain mapping results for ARS2004. The "Map Start" column indicates the beginning of an AT-hook binding sequence, the distance between AT-hook sequences (column 2) was calculated by adding the length of the AT-hook sequence (typically 4 bp) to the respective Map Start and subtracting this from the Map Start of the next AT-hook sequence (e.g. for the second line this is [13 – (9+4)] = 0).

As with the ClustalW analysis, A+T-rich sequences that co-localised with ORIs were determined and the sequence that consisted of at least 63 % AT-content proximal and distal to the highest AT-content within the A+T-rich island was searched for potential Orc4 binding sites (as described in 5.2.1.1). These sites were defined as sequences that consist of at least five asymmetric AT-hook sequences without interference by more than two consecutive G or C residues and a maximum space between AT-hook sequences of 12 bp as there is evidence that GC residues and longer distances between AT-hooks could significantly reduce the affinity of HMG-I proteins such as Orc4 for DNA (Maher and Nathans, 1996; Chuang and Kelly, 1999). The number of potential Orc4 binding sites and the number and spacing of AT-hook sequences were scored within each binding site. On the basis of the results, ORIs were divided into strong or weak ones. The criteria used were derived from the structure and organisation of previously identified Orc4 binding domains in the above mentioned fission yeast ORIs, which all have been shown to be relatively efficient. Strong ORIs were ones with at least two putative Orc4 binding domains, where at least one consists of five or more asymmetric AT-hook sequences. This threshold criterion was met by 83 % of the efficient ORIs and 52 % of the inefficient ORIs. Clearly this criterion helped define efficient ORIs but is not a sufficient criterion on its own.

The 52 % inefficient ORIs (55 out of 106) were examined further, to determine if other characteristics could explain their inefficiency (Table 13). Interestingly, 34 of these 55 were relatively more efficient during pre-meiotic S phase. These 34 were used at least 1.4 fold more efficiently in

the meiotic cell cycle compared with the average ORI, than was the case during the mitotic cell cycle. Therefore these ORIs have the capacity to be more efficient in the meiotic cell cycle than in the mitotic cell cycle. This suggests that these ORIs could be specifically regulated such that they are efficient in pre-meiotic S phase but are at least partly repressed during mitotic S phase. For the remaining 21 ORIs which had good AT-hook binding domains, there were several other relevant factors which could have influenced their efficiency. For instance, five were near telomeres, two near the mating type locus and one (ORI2080) was part of an ORI cluster and was potentially subject to ORI interference. ORI2080 maps to a region where at least three initiation events occur in close proximity which includes ORI2079. This region consists of five A+T-rich islands with AT-contents above 72 % within an area of 17 kb. One of the initiation events, 1 kb proximal to ORI2080, although defined as a distinct peak was not mapped as ORI, because the signal ratio was below the threshold criteria. The efficiency from the three initiation events was 56% in total which would be that predicted from a correlation with an AT-content of 77.8%. This suggests that ORI interference could contribute to the low efficiency of ORI2080. ORI1076 consisted of a late consensus sequence which could have influenced its replication timing resulting in passive replication in late S phase in a significant percentage of cell cycles. Of the remaining 12 ORIs, eleven replicated late in mitosis and could be inefficient because of passive replication from adjacent ORIs. The results of the AT-hook analysis for inefficient ORIs are summarised in Table 14. In conclusion, I think that an efficient fission yeast ORI is one that is found

in an A+T-rich region and has good AT-hook binding domains. In addition efficiency in mitotic S phase can be reduced via specific regulation and chromosomal location.

ORI Number	*Classification*	ORI Number	*Classification*
ORI1008	TELOMERIC	ORI1003	AT-HOOK
ORI1014	TELOMERIC	ORI1007	AT-HOOK
ORI1178	TELOMERIC	ORI1009	AT-HOOK
ORI2108	TELOMERIC	ORI1023	AT-HOOK
ORI2129	TELOMERIC	ORI1044	AT-HOOK
ORI1049	LATE ACTIVATION	ORI1048	AT-HOOK
ORI1076	LATE ACTIVATION	ORI1051	AT-HOOK
ORI1098	LATE ACTIVATION	ORI1061	AT-HOOK
ORI2031	LATE ACTIVATION	ORI1062	AT-HOOK
ORI2059	LATE ACTIVATION	ORI1064	AT-HOOK
ORI2060	LATE ACTIVATION	ORI1065	AT-HOOK
ORI2075	LATE ACTIVATION	ORI1069	AT-HOOK
ORI2085	LATE ACTIVATION	ORI1071	AT-HOOK
ORI2093	LATE ACTIVATION	ORI1079	AT-HOOK
ORI2095	LATE ACTIVATION	ORI1080	AT-HOOK
ORI2098	LATE ACTIVATION	ORI1094	AT-HOOK
ORI1067	NONE	ORI1154	AT-HOOK
ORI2080	ORI INTERFERENCE	ORI1156	AT-HOOK
ORI2067	MATING TYPE	ORI1161	AT-HOOK
ORI2068	MATING TYPE	ORI1165	AT-HOOK
ORI1002	MEIOTIC INDUCTION	ORI1169	AT-HOOK
ORI1004	MEIOTIC INDUCTION	ORI2001	AT-HOOK
ORI1010	MEIOTIC INDUCTION	ORI2003	AT-HOOK
ORI1011	MEIOTIC INDUCTION	ORI2017	AT-HOOK
ORI1015	MEIOTIC INDUCTION	ORI2029	AT-HOOK
ORI1016	MEIOTIC INDUCTION	ORI2030	AT-HOOK
ORI1020	MEIOTIC INDUCTION	ORI2039	AT-HOOK
ORI1059	MEIOTIC INDUCTION	ORI2046	AT-HOOK
ORI1073	MEIOTIC INDUCTION	ORI2054	AT-HOOK
ORI1082	MEIOTIC INDUCTION	ORI2101	AT-HOOK
ORI1085	MEIOTIC INDUCTION	ORI2102	AT-HOOK
ORI1089	MEIOTIC INDUCTION	ORI2103	AT-HOOK
ORI1149	MEIOTIC INDUCTION	ORI2109	AT-HOOK
ORI1163	MEIOTIC INDUCTION	ORI2110	AT-HOOK
ORI1164	MEIOTIC INDUCTION	ORI2111	AT-HOOK
ORI1170	MEIOTIC INDUCTION	ORI2113	AT-HOOK
ORI1171	MEIOTIC INDUCTION	ORI2114	AT-HOOK
ORI1176	MEIOTIC INDUCTION	ORI2115	AT-HOOK
ORI1177	MEIOTIC INDUCTION	ORI2118	AT-HOOK
ORI2002	MEIOTIC INDUCTION	ORI2122	AT-HOOK
ORI2004	MEIOTIC INDUCTION	ORI2125	AT-HOOK
ORI2005	MEIOTIC INDUCTION	ORI2128	AT-HOOK
ORI2028	MEIOTIC INDUCTION	ORI2130	AT-HOOK

ORI2052	MEIOTIC INDUCTION	ORI2133	AT-HOOK
ORI2069	MEIOTIC INDUCTION	ORI2137	AT-HOOK
ORI2070	MEIOTIC INDUCTION	ORI2138	AT-HOOK
ORI2099	MEIOTIC INDUCTION	ORI3011	AT-HOOK
ORI2105	MEIOTIC INDUCTION	ORI3015	AT-HOOK
ORI2121	MEIOTIC INDUCTION	ORI3029	AT-HOOK
ORI2132	MEIOTIC INDUCTION	ORI3080	AT-HOOK
ORI2135	MEIOTIC INDUCTION	ORI3084	AT-HOOK
ORI2136	MEIOTIC INDUCTION		
ORI3012	MEIOTIC INDUCTION		
ORI3038	MEIOTIC INDUCTION		

Table 13: Classification of inefficient ORIs
ORIs that have >74 % AT-content and are <24% efficient were analysed for properties that could repress ORI efficiencies and classified accordingly ("AT-HOOK" indicates a weak AT-HOOK binding domain).

Classification (Inefficient ORIs)	Number of ORIs	% ORIs
Weak AT-Hook domains	51	48
Meiotically Induced	34	32
Telomeric	5	5
ORI Interference	1	1
Mating Type	2	2
Late Activation	12	11
Undefined	1	1
Total	106	100

Table 14: Summary of AT-hook Domain Analysis
Summary of Classification results from Table 13.

Next a subset of the 35 most efficient ORIs was chosen and their 95 potential Orc4 binding domains were analysed for an ORI consensus sequence using ClustalW (Higgins and Sharp, 1988; Higgins and Sharp, 1989). This alignment did not generate a consensus, suggesting that the Orc4 binding sequence is of a degenerate nature.

It has been shown that Xenopus ORC initiates DNA replication preferentially at sequences targeted by fission yeast ORC (Kong et al., 2003) suggesting that similar DNA sequences serve as ORC binding sites in metazoan cells. To investigate this, the same search algorithm as

above was used to look for ORC binding domains in five previously characterised metazoan ORIs: the human lamin B2 locus, the hamster DHFR locus, the *Drosophila* chorion amplification locus, the human c-myc locus, and the mammalian ß-globin locus (reviewed in (Aladjem and Fanning, 2004). This analysis identified 2 - 4 putative ORC binding domains in all of these ORIs, a number similar to that found in characterised fission yeast ORIs. Interestingly, in the human beta globin locus three previously identified auxiliary sequences essential for ORI function and located downstream and upstream of the core ORI sequence (Aladjem et al., 1998) were also associated with 2 – 4 putative ORC binding domains each. In total 13 potential ORC binding domains were identified in the 8 kb fragment of the human beta globin locus. In the *Drosophila* chorion amplification locus, one putative ORC binding site was identified in the ACE3 amplification control element and one in ori-ß. Like fission yeast ORIs, all characterised metazoan ORIs consist of AT-rich sequences. For example, two AT-rich islands with ~76% AT-residues (500 bp window) in the human ß-globin locus co-localise with the core ORI region and with an auxiliary element required for ORI function, respectively. This suggests that metazoan ORIs may share similarities with fission yeast ORIs and that the search algorithm developed here may be a useful approach to identify ORIs in metazoan organisms.

5.2.2 Consensus Sequences in Re-replicating ORIs

As shown in the previous chapter, ORIs that map to peaks in over-amplified regions have exceptional features, for instance very high AT-contents. Upon looking systematically for DNA regions which were 79 % or more AT-rich in a segment of at least 550 bp, only 27 were found throughout the whole genome and 19 of these were located in amplified regions. This suggests that there is a strong correlation between regions of the genome which are over-amplified and regions that consist of exceptionally high AT-contents. To see whether particular conserved sequence features make ORIs within amplified domains competent for re-replication and over-amplification of DNA, a ClustalW alignment was carried out across the AT-rich islands that map to 14 ORIs located at the centre of amplification peaks. No significant consensus sequence could be identified (score <=31). Next 57 ORIs found within amplified regions were examined for the presence of AT-hook binding domains. Eight ORIs were found that map to the peaks of amplification (ORI1110, 1129, 2040, 2080, 3009, 3012, 3049, 3056) and they contained 12 or more consecutive AT-hook binding sequences. ORI2048 has the strongest putative AT-hook binding domain which maps to an amplification peak (1.7fold amplification). This ORI has 22 consecutive sequences of a unidirectional AT-hook motif. It is also interesting that these Orc4 binding domains are often flanked by longer stretches of $(AT)_n$ residues, for instance in the sequence of ORI1129 (Figure 56). These are not common in other ORIs with comparable AT-content that were investigated for AT-hook domains and may potentiate the likelihood of over-amplification of DNA in a

Cdc18/Cdt1 o/e background. In conclusion, the data suggests that ORIs in amplified regions have particularly high AT-content and good AT-hook domains. Thus, the ability of high levels of Cdc18 and Cdt1 to break the rule ensuring that each DNA segment is replicated only once depends upon the presence of ORIs with high AT-content and with good AT-hook binding domains. AT-hook binding domains were also identified in metazoan amplification loci, the *Drosophila* chorion locus and the Chinese hamster DHFR locus. It has been shown that ORI ß in the DHFR locus is responsible for the 700 – 1000fold amplification of a 135 kb region in one hamster cell line (Milbrandt et al., 1981; Anachkova and Hamlin, 1989). Interestingly, a clustalW sequence alignment between the DNA sequence that binds ORC in ORI ß and the putative Orc4 binding site in fission yeast ORI1129, located at an amplification peak, revealed similarities in DNA sequence identity (Figure 56). This suggests that the phenomena of over-amplification in fission yeast and Metazoa could share similarities.

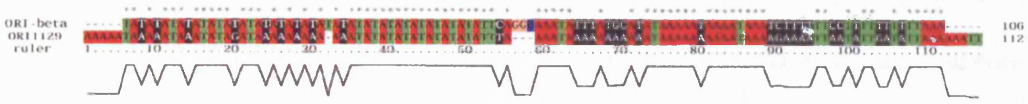

Figure 56: ORIs that confer DNA amplification may be structurally similar
The result of a ClustalW sequence alignment between fission yeast ORI1129 and the Chinese Hamster DHFR ORI ß is shown.

5.2.3 Correlation between Transcription and DNA Replication

A link between replication and transcription has been suggested in *Drosophila* (Schubeler et al., 2002). To identify any correlation between replication and transcription, ORI lists were compared with an excess of 200 lists of genes that are induced under various experimental conditions.

These lists were derived from unpublished data as well as published papers (http://www.sanger.ac.uk/PostGenomics/S_pombe/_publications/). The analysis was carried out for lists of genes induced in cell cycle, meiosis, mating, various stresses, starvation, RNAi mutants, silencing mutants and lists of genes that were expressed at high or low levels. There was no significant correlation with any of the lists suggesting that ORIs in fission yeast are randomly chosen across the genome. This is consistent with the stochastic model of ORI firing suggested in Chapter Three. To see whether there was any gene-specific correlation between transcription and early replication, the position of genes that were transcriptionally upregulated in S phase and genes required for DNA replication were compared with time of ORI activation (Rustici et al., 2004). Of the six proteins in the ORC complex, only Orc4 co-localises with an ORI that was activated early in S phase. Mcm3 and Mcm4 of the six protein Mcm2-7 complex also mapped to efficient early ORIs. Of the histone proteins which are all transcriptionally induced in S phase, histones H2A (C622.08c) and H2B (C622.09) mapped to a region that has a cluster of efficient early ORIs. No such co-localisation was seen for histones H3 and H4. DNA polymerase α and the cohesin rad21 were also located next to early replicating ORIs.

Subsequently genes which were induced in meiosis were analysed in more detail. 20 genes co-localised with ORIs, 13 of which were more efficient (>1.4fold) in meiosis than in mitosis. The most significant examples were meu13, meu11, meu4, spo20 and meu6. Only two of the remaining genes, meu31 and meu26, co-localised with ORIs that were

significantly repressed in meiosis. Three other genes induced in meiosis, mfr1/fzr1, meu14 and psy1, showed weak ORI activity in meiosis (around 4 %) and no activity in mitosis. These signals were below the threshold criteria and therefore no ORI was mapped to these regions. However, this increase in activity could be significant for regulation of the respective genes.

Next early and late replicating segments on all three chromosomes were investigated for the frequency of genes that were expressed at high or low levels. The analysis included a total of the 264 most efficiently and the 387 most inefficiently transcribed genes which were previously identified by measuring relative abundance of transcripts in cells. The density of these genes was similar in early and late replicating segments, 18.5 kb/gene and 20.2 kb/gene respectively. Inefficiently transcribed genes were almost as abundant in early replicating as in late replicating segments (55 and 45 %, respectively). However, late replicating segments contained only 33 % of highly expressed genes. Although this correlation is rather weak, I conclude that genes that are very efficiently transcribed are more likely to co-localise with DNA segments that are replicated early during mitotic S phase.

To summarise, no significant link between transcription and DNA replication could be established on a whole genome level. The link between genes that are upregulated in mitotic S phase and co-localisation with early replicating ORIs is weak. The correlation between genes that are induced in meiosis and ORIs that are relatively more efficient in meiosis than in mitosis is somewhat stronger and might be significant.

Finally, the most efficiently transcribed genes tend to co-localise with regions of DNA that are replicated early in mitotic S phase.

5.3 Discussion

The results in this chapter strongly support previous findings that fission yeast ORIs do not share a consensus sequence. Fission yeast ORIs compensate for the lack of consensus by a synergistic interaction of ORC molecules with A+T-rich sequence patterns. I have also shown that similar patterns are found in metazoan ORIs in regions that are protected by ORC. There was no significant correlation between transcriptional activity and the location of ORIs.

The analysis of efficiently utilised ORIs identified several characteristics. As indicated previously, ORIs should have high AT-content of at least 72 % over a 500 bp – 1000 bp segment. Efficient ORIs are associated with AT-content above 74 % and contain good AT-hook binding sequences. In fission yeast Orc4 contains AT-hook binding motifs which could preferentially target ORC to these efficient ORIs. These ORIs consist of three putative Orc4 binding domains on average with long stretches of asymmetric AT-hook binding sequences. This is consistent with the pattern seen in genetically characterised, efficient fission yeast ORIs. It is interesting that usually only two of the putative Orc4 binding domains were protected by Orc4 in these studies (Takahashi and Masukata, 2001). The third domain might function to bind other proteins or act as a DUE. This could facilitate helicase activity of the MCM complex and contribute to the increase in the efficiency of these ORIs (You et al., 2003; Masai et al., 2005). In vitro studies demonstrated that fission yeast

Orc4 protects 140 bp of ars1 DNA (Gaczynska et al., 2004) which would require a certain gap between two consecutive Orc4 binding sites. If the gap was too small, stearic hindrance would prevent Orc4 from binding to the domain with lower affinity. This is an alternative explanation for the fact that some putative AT-hook binding domains in characterised fission yeast ORIs are not associated with Orc4. Data from fission yeast, budding yeast and mammalian cells suggests that cellular concentrations of ORC molecules in eukaryotes are limited to one or two per ORI (DePamphilis, 2005). A limited pool of ORC would result in preferential binding of ORC to strong AT-hook binding domains because of their higher affinity for ORC in competition with weak binding sites. Although AT-hook binding domains co-localise with regions of high AT-content, usually only one AT-hook domain maps to the centre of AT-richness above 70 % in a 500 bp window. The second/third domain(s) map further upstream or downstream where percentage AT-content is below 70 %. Synergistic binding of multiple Orc4 molecules to the fission yeast ars2004 has been shown to be important for full ORI activity (Takahashi and Masukata, 2001). Co-operative binding of Orc4 would favour binding to ORIs with multiple strong AT-hook domains and result in high ORI usage, and thus high efficiency, compared with ORIs that have only one or very short and weak AT-hook domains. This is consistent with the results presented here and the large range of ORI efficiencies observed. Regions with high AT-content that lack strong Orc4 binding domains have weak ORI activity which explains why some A+T-rich islands have the propensity to function as ORIs whereas others fail to do so.

Some ORIs with high AT-contents and good potential AT-hook binding domains are not used efficiently during the mitotic S phase but are used more efficiently during pre-meiotic S phase. If these are located in more condensed chromatin regions, this may limit the efficiency of their utilisation, for instance in regions proximal to telomeres and the mating type locus. These regions were induced for ORI efficiency in meiosis, which indicates that some de-repression of the silencing effects occurred in the meiotic replication program.

Like fission yeast ORIs, all characterised metazoan ORIs consist of AT-rich sequences (Aladjem and Fanning, 2004). For example, two A+T-rich islands with ~76 % AT residues (500 bp window) in the human ß globin locus co-localised with the core ORI region, and an auxiliary element required for ORI function, respectively. I identified 2 – 4 putative ORC binding domains in five different metazoan ORIs within these A+T-rich islands, which is similar to the number of Orc4 binding domains observed in characterised fission yeast ORIs. Interestingly, in the human ß globin locus three previously identified auxiliary sequences essential for ORI function are also associated with 2 – 4 putative ORC binding domains. In total, 13 potential ORC binding domains were contained in the 8 kb fragment of this locus. In the Drosophila chorion amplification locus, one putative ORC binding site was identified in the ACE3 amplification control element and one in ori ß. Both of these and one in the lamin B2 locus co-localised with DNA sequences previously shown to be protected by ORC in vivo and in vitro (Austin et al., 1999; Abdurashidova et al., 2003; Stefanovic et al., 2003). In the hamster DHRF locus, two of the

three putative ORC binding domains in ori ß have been reported to bind ORC (Aladjem, 2004) and the third domain is required for DNA bending and binding of the RIP60 protein (Altman and Fanning, 2004), which contribute to ORI function. I conclude that biochemically and genetically characterised metazoan ORIs consist of AT-rich domains which can associate with ORC, and show a similar distribution to ones found in fission yeast. This suggests that the structure of metazoan ORIs bears resemblance to the structure of fission yeast ORIs.

I could not identify a genome-wide correlation between transcriptional and ORI activity in fission yeast. However, I found that ORIs flanked by genes that were transcriptionally induced in meiosis are often more efficient in meiosis than mitosis. I suggest that developmental regulation is involved in ORI specification in fission yeast such that a change in transcriptional activity might lead to a shift in ORI usage and result in changes of distribution patterns of ORIs in pre-meiotic S phase. Preferential co-localisation of highly expressed genes with regions that are replicated early during mitotic S phase suggests that transcriptional activity is implicated in the regulation of the temporal program of ORI activation.

Chapter VI

General Discussion

6 General Discussion

Prior to this study, a subset of ~ 45 fission yeast ORIs had been identified in fission yeast, four of which had been genetically and biochemically characterised in greater detail ((Gomez and Antequera, 1999; Segurado et al., 2003) and references therein). Data from those studies indicated that fission yeast ORIs were more similar to metazoan ORIs than ORIs identified in the distantly related budding yeast. According to those studies, fission yeast ORIs seemed to lack a defined sequence consensus and were characterised only by A+T-rich sequences located in intergenic regions. In this work, I have identified 401 efficient ORIs across the fission yeast genome and analysed these characteristics on a genome-wide level. In addition I identified a further 503 potential weaker ORIs and examined other features of fission yeast ORIs such as their structure, organisation in the genome, specification and utilisation in space and time. I will now discuss these features in the context of the published data.

6.1 ORI Characteristics in Fission Yeast

A wide range of inter-origin distances in different eukaryotic systems have been reported and it is unclear what contributes to these large differences (reviewed in (DePamphilis, 2005)). Budding yeast ORIs defined by a consensus DNA sequence, have been mapped throughout the genome with an inter-origin distance of ~35 kb (Raghuraman et al., 1997; Wyrick et al., 2001; Yabuki et al., 2002). A similar spacing of replicons has been observed in somatic cells of metazoan ORIs (Blumenthal et al., 1974; Hyrien et al., 1995; Maric et al., 1999; MacAlpine et al., 2004). By contrast,

ORI spacing in *Drosophila* and *Xenopus* embryonic cells has been found to be considerably less at 5 – 15 kb (reviewed in (Hyrien et al., 2003)). Those cells undergo a modified cell cycle without G_1 and G_2 (Gerhart et al., 1985; Miake-Lye and Kirschner, 1985) and have a very short S phase of four and 20 minutes respectively (reviewed in (Hyrien et al., 2003)). In human cells, results from an ARS assay suggested that replicons that could potentially act as ORIs are spaced on average at 10 kb intervals (Heinzel et al., 1991). The present analysis in fission yeast suggests that the spacing between efficient ORIs is 31 kb, whilst that between all potential ORIs, efficient and inefficient, is 14 kb. Several initiation zones in addition to the characterised ura4 locus (Dubey et al., 1994) were also identified, suggesting that initiation zones are a relatively common feature in fission yeast and not specific to metazoan cells (Gilbert, 2001). These data thus support the view that in eukaryotic organisms where ORIs are not defined by a clear consensus sequence (see later) there is a range of potential ORIs which operate with different efficiencies.

ORI specification and utilisation in eukaryotes is still not well understood and many reviews have attempted to interpret the data available from different model systems (DePamphilis, 1999; Todorovic et al., 1999; Bielinsky and Gerbi, 2001; Gilbert, 2001; Mechali, 2001; Bell and Dutta, 2002; Gerbi and Bielinsky, 2002; Biamonti et al., 2003; Aladjem and Fanning, 2004; Antequera, 2004; Weinreich et al., 2004; Cvetic and Walter, 2005). It seems that eukaryotic ORIs are sufficiently diverse in their structure, that general features for their specification have been difficult to define. The major questions thus remain, including the features,

if any, that specify a eukaryotic ORI and the parameters that determine how often an ORI is chosen in successive cell cycles.

It is interesting that during the mitotic cell cycle in fission yeast, an average of 74% of the genome is replicated by the 401 more efficient ORIs (average 29% efficiency), and only 26% by a further 503 less efficient potential ORIs (average 8% efficiency). This could mean that although there are some ORIs that are used very efficiently every 1 - 2 cell cycles, most operate at a lower rate only once every 3 - 5 cell cycles, and some which contribute overall only a minor part of total replication operate only once every 10 - 20 cell cycles. A similar mode of ORI firing seems to take place in human cells. A recent study which included the analysis of 400 initiation sites suggested that the majority of human DNA replication results from inefficient asynchronous ORIs that are distributed throughout the genome (reference within (Macalpine and Bell, 2005)). These data give strong support to the "continuum model" of ORI firing which was developed following an ARS analysis of 26 contiguous intergenic regions in a 60 kb segment of DNA in fission yeast (Dai et al., 2005). A total of 14 of these intergenic regions were found to contain potential ORIs and many of these regions were also identified as ORIs in the microarray analysis. The correlation between ORI efficiency and time of replication suggests that more efficient fission yeast ORIs tend to fire early in S phase whilst the less efficient ones tend to fire later. There may be a regionally regulated mechanism which monitors if ORIs in a particular region have fired and if not, ensures that less efficient nearby ORIs are fired so that the whole genome is replicated in a timely fashion. This could contribute to the

random completion problem of DNA replication in eukaryotes (Hyrien et al., 2003).

ORIs in fission yeast are not defined by a consensus sequence but I have identified further features which are important for ORI activity; some of these may be useful for identifying ORIs in multicellular eukaryotes. For example, ORIs are found to contain A+T-rich intergenic regions with a preference for sequences between divergently transcribed genes which therefore contain two promoter regions. This observation may support the view that the presence of transcription factor binding sites are important for ORI activity (reviewed in (Antequera, 2004)), but a further consideration is that there has to be sufficient space between the genes to contain an extended ORI. Generally, ORIs are found in larger intergenic regions and more efficient ORIs are found in particularly extended intergenic regions. ORIs are located between convergently transcribed genes but these are far larger than what is normal for these intergenic regions. I conclude that length of the intergenic region is important for ORI specification and that at least around 1 kb is required, although 2 kb is the average value. An earlier bioinformatic analysis (Segurado et al., 2003) based on 1 kb segments of DNA with a high AT content (≥ 72 %) was a good guide to ORI activity, but the data suggests that at least for some ORIs a less stringent requirement of a 0.5 kb segment (≥ 72 %) may be more appropriate.

Analysis of the more efficient ORIs has revealed the need for an AT content over 74% for a 500 bp segment and for good AT-hook binding sequences. The presence of these AT-hook binding domains could

preferentially target the ORC proteins. The idea that greater affinity for ORC to DNA sequences can increase the likelihood that an ORI is used is also supported by data from budding yeast (Wyrick et al., 2001). In that study the levels of ORC bound to ORIs show a positive correlation with relative efficiency. However, ORIs with high efficiencies seem to be more common in budding yeast compared with fission yeast and metazoans (Friedman et al., 1997; Yamashita et al., 1997). This suggests that the interaction between ORC and ORI is more specific in budding yeast, perhaps mediated by virtue of its strong consensus sequence which is not present in ORIs of fission yeast or other eukaryotic cells. This would also explain why a single ORC binding site suffices in budding yeast ORIs, whereas fission yeast and metazoan ORIs have been shown to require at least two ORC binding sites (reviewed in (Gilbert, 2001)). The data obtained from the AT-hook analysis confirmed this requirement for at least two strong AT-hook binding domains for Orc4 association in efficient ORIs of fission yeast. In heterochromatic regions such as the telomere and the mating type locus, the accessibility for ORC may have been compromised and this could explain the fact that ORIs with strong AT-hook binding domains generally exhibited low efficiencies in these regions (also see Discussion 6.2). Assuming that the specificity of ORC binding to DNA sequences is dependent on the ORC to DNA stoichiometry, an unrestricted supply of ORC could lead to activation of otherwise silent ORIs with weak AT-hook binding domains. This is consistent with the proposal that an increase in ORC protein levels in *Xenopus* oocytes could account for the high frequency of replication initiation events compared

with somatic cells where ORC pools are limiting (reviewed in (DePamphilis, 2005)). It would be interesting to put this model to a test in fission yeast by low level co-overexpression of ORC and other limiting replication initiation factors to see whether the frequency of ORI usage increases with a rise in these protein levels within the cell.

A search for AT-hook domains in five previously characterised metazoan ORIs found good AT-hook binding sequences located within A+T-rich islands in all these ORIs. Some of the identified sequences had been previously shown to be associated with ORC in vitro or in vivo, consistent with suggestions that fission yeast ORC targets similar DNA sequences as metazoan ORC do (DePamphilis, 2003; Kong et al., 2003; DePamphilis, 2005; Touchon et al., 2005). However, AT-hooks have not been identified in the ORC of any other model system. As has been suggested, mediator proteins such as HMG-I like proteins or proteins that have a high affinity for similar sequence patterns may be required to target metazoan ORC to AT-hook domains via their AT-hook protein motifs (Chuang and Kelly, 1999). For instance, it has recently been reported that the Ku70/Ku80, an abundant nuclear protein complex, associates specifically with human ORC subunits 2/3/4/6 at the lamin B2, beta globin and c-myc ORIs in a sequence specific manner and promotes replication initiation (Sibani et al., 2005; Sibani et al., 2005). The high accuracy with which ORC binding domains in metazoan ORIs were identified suggests that further refinement of a search algorithm based on the fission yeast data may be helpful to identify further ORC binding sites and ORIs in multicellular organisms.

6.2 Comparative Analysis of ORIs in Meiosis and Mitosis

Six ORIs have been mapped in pre-meiotic S phase of budding yeast (Collins and Newlon, 1994) and the same six were found also to operate during mitotic S phase. The current analysis, which provides the first genome-wide identification of ORIs during pre-meiotic S phase, also shows almost complete overlap between pre-meiotic and mitotic ORIs. Of the 401 efficient mitotic ORIs, 396 were used in pre-meiotic S phase and no ORIs were found that were specific to meiosis. However, ORI utilization was less efficient during pre-meiotic S phase at 16%, compared with the 29% observed during mitotic S phase. Replication fork velocities were also determined from the microarray analyses at 2.8 kb/min for mitotic S phase and 3.3 kb/min for pre-meiotic S phase. This means that less efficient utilization of ORIs is likely to explain why pre-meiotic S phase is extended compared with mitotic S phase. This could be a consequence of a higher dependence of replication on nucleotides or limiting pools of initiation proteins during pre-meiotic DNA replication. Unexpectedly, some ORIs were found to be significantly more efficient during pre-meiotic S phase than they were during mitotic S phase when compared with their respective S phase averages. Many of these 'meiotically induced' ORIs were found in particular segments of the genome, which suggests that these could be more condensed, including heterochromatic regions, and that they could be less available to DNA initiation factors during mitotic S phase. These regions could become de-condensed to be more available for recombination, thus providing access to initiation factors for more efficient replication during pre-meiotic S phase. It is interesting that this

analysis identified about the same number of ORIs active in the meiotic cell cycle as there are recombination events in meiosis in fission yeast (Munz et al., 1989). It is possible that recombination and DNA replication initiation share *cis* and *trans* acting factors. However, no significant ORI activity could be seen in the Mbs1 double strand break (DSB) locus. In fission yeast it has been shown that, although DSBs are required for recombination, DSB formation and recombination do not co-localise in contrast to budding yeast ((Cervantes et al., 2000) and references therein). Preventing DNA replication in budding yeast also prevents DSB formation in a replication checkpoint independent manner, suggesting a direct coupling of DNA replication and recombination in meiosis (Borde et al., 2000). Similar experiment in fission yeast showed that this link is established via DNA replication checkpoints independent of replication initiation proteins (Tonami et al., 2005). Interestingly a recombination hotspot has been identified in mammalian cells that overlaps with the beta globin ORI locus (Wall et al., 2003). The ß globin locus is associated with a DNA unwinding element (DUE) and the helical stability within such regions is particularly low and is inversely related to replication efficiency (Natale et al., 1992). It has been suggested that these regions may also be enhancers for recombination as DUEs may create accessible chromatin structure and thus be prone to DSB formation. Elements that could function as DUEs also exist in fission yeast ORIs (eg. ORI1129) and it is possible that co-localisation of ORIs and DSBs is facilitated by the existence of these functional *cis* acting elements.

The present analysis also found that some of the ORIs flanked by genes that are transcriptionally induced in meiosis are more efficient in pre-meiotic S phase, which may also reflect differences in the extent of chromatin condensation at those sites. This indicates that a change in transcriptional activity could lead to a shift of ORI usage and in changes in ORI efficiency, consistent with previous observations in budding yeast and metazoan cells (Gerbi and Bielinsky, 2002; Gilbert, 2002; Weinreich et al., 2004; Lin et al., 2005; Nieduszynski et al., 2005). The fact, that the same ORIs have been identified in meiosis and mitosis also indicates that ORI specification as such is not affected by the transcriptional program in fission yeast. Consistent with this, no global correlation was found between transcriptional activity and ORI efficiency during mitotic S phase. The mechanistic link between DNA replication and transcription seems to be a complex one and data from fission yeast and budding yeast shows ambiguous results: the deletion of promoter regions in fission yeast, such as the strong *nmt1* promoter, did not diminish nor decrease the activity of adjacent ORIs (Gomez and Antequera, 1999); in budding yeast, the B3 element which binds the transcription factor Abf1 in *ars1* normally increases the efficiency of ORI activation (Rao et al., 1994) but is inhibitory if placed next to *ars307* in the chromatin context (Kohzaki et al., 1999). These observations suggest that transcriptional activity is not generally required for ORI specification, but may be a factor in the differential regulation of ORI usage in different developmental programs of eukaryotic cells.

In conclusion, the same ORIs are used during mitotic and pre-meiotic S phase and so activating a different spectrum of ORIs is unlikely to be the explanation for the higher levels of recombination and differing chromosome segregation behaviour observed during meiosis in fission yeast.

6.3 ORI Behaviour in Re-replication Systems

In eukaryotes, cells maintain a strict control over S phase to make sure that DNA replication occurs only once per cell division cycle. A key element of this control is G_2/M cyclin dependent kinase activity which in fission yeast corresponds to the Cdc2/Cdc13 CDK (reviewed in (Nurse, 2002)). When this CDK is removed from cells they undergo re-replication without intervening mitosis (Hayles et al., 1994). Our microarray analyses have revealed that these endo-reduplication cycles lead to all regions of the genome being equally over replicated. Thus, this disturbance of the overall cell cycle regulator does not appear to affect the proper utilization of ORIs which ensure that all regions of the genome are replicated only once during each S phase. However, this is not the case when cells endo-reduplicate because they contain high levels of the initiation factors Cdc18 (Cdc6 in other organisms) and Cdt1. In this situation, the genome is not equally replicated, and some regions become amplified at least 3x more than the rest of the genome. These regions contain ORIs which are very efficient, with a high AT content and strong AT-hook binding regions. It appears that elevated levels of Cdc18 and Cdt1 interact synergistically with these types of ORIs and that this interaction breaks the one replication per S phase rule. It also suggests that understanding this

interaction will be important in revealing the molecular mechanism by which that rule is brought about. Over-amplification also occurs in the Chinese hamster DHFR ORI (Milbrandt et al., 1981; Anachkova and Hamlin, 1989). That ORI has a very similar structure to fission yeast ORI1129 which is located at the peak of a region amplified when Cdc18 and Cdt1 are overexpressed. It has been suggested recently that the DHFR gene regulates the activity of the amplifying ORI ß (Saha et al., 2004). ORIs located at the centre of amplified peaks in fission yeast were often surrounded by highly expressed genes, such as the histone genes. I speculate that the chromatin is in a particularly open conformation in these areas mediated by high levels of transcription, which may facilitate binding of *trans* regulatory molecules such as ORC as well as subsequent loading of pre-RCs. This open chromatin conformation may also be influenced by DUE elements [$(AT)_n$ residues] which are present both the amplifying fission yeast ORI1129 and the DHFR ORI ß (Altman and Fanning, 2004; Schroll and Heintz, 2004). Local amplification in fission yeast could therefore depend on the combination of several parameters: overexpression of *trans* acting factors such as Cdc18 and Cdt1; *cis* acting amplification enhancer sequences; low complexity of intergenic regions, and high transcriptional activity. Fission yeast has a much greater propensity to de-regulate replication initiation and re-replicate DNA than budding yeast (reviewed in (Feng and Kipreos, 2003)). Simultaneous inactivation of three mechanisms that interfere with replication initiation is necessary to achieve 3C to 4C DNA contents in budding yeast compared with up to 128C DNA contents in fission yeast by manipulation of just one

mechanism. I have shown that the presence of strong AT-hook binding *cis* acting sequences is probably important to confer re-replication to fission yeast ORIs. Developmental gene amplification is frequently observed in regions that consist of complex ORI structures and are classified as initiation zones (Tower, 2004). Similar ORI structure and clustering of ORIs and the formation of initiation zones were found at the over amplified regions identified in this analysis. Budding yeast ORIs lack complex binding domains (the ACS is only 11 – 17 bp long) which might account for the lack of efficient re-replication. The budding yeast ORI usually only consists of one ORC binding site in relatively small intergenic regions (reviewed in (Gilbert, 2001)). The larger intergenic spaces and multiple ORC binding sites in fission yeast and metazoan ORIs provides more opportunity for binding of protein complexes and thus greater flexibility in ORI regulation. The molecules that are required for replication initiation and involved in DNA re-replication are differentially controlled in different model organisms (reviewed in (Feng and Kipreos, 2003). Cdt1 is an important negative regulator to prevent re-replication (Arias and Walter, 2005; Li and Blow, 2005; Maiorano et al., 2005). In contrast to fission yeast, where Cdt1 is degraded during S phase by proteolysis, the ortholog of Cdt1 in budding yeast, Tah11/Sid2, is exported from the nucleus to the cytoplasm after pre-RC formation, thus separating the two initiators, Cdc6 and Cdt1 (reviewed in (Takeda and Dutta, 2005)). Mammalian cells have in addition a negative regulator of Cdt1, Geminin, and similar to Tah11/Sid2 in budding yeast, Cdc6 is exported from the nucleus which separates the two proteins and would prevent re-replication and local DNA

amplification. It is possible that this differential way of Cdt1 regulation causes fission yeast to be more prone to re-replication and amplification of its DNA during mitotic S phase, as both Cdc18/Cdc6 and Cdt1 accumulate in the nucleus. Whether amplification is due to faster re-initiation in an amplifying locus or a last additional round of endoreplication, when the rest of the genome has ceased to replicate, is not clear. The peak of amplification in a Cdc18 and Cdt1 co-overexpression increases drastically in the late stages of re-replication, which suggests that the latter model applies. However, although re-replication was initiated from G_2 of the cell cycle in this case, induction from the *nmt1* promoter could be variable and introduce a certain degree of asynchrony. More work is needed to determine the physical nature of the amplified loci and the mechanisms involved in local DNA amplification. It has been suggested that the structure of the DHFR ORI locus is similar to the one in the developmentally regulated chorion amplification locus in *Drosophila* (Tower, 2004). Therefore, the phenomena of over-amplification and the one replication per S phase rule may share similarities between fission yeast and the metazoa.

Recent whole genome studies in different model systems have provided a great wealth of information. Integration of results from DNA replication profiling, transcription profiling, mutant studies on chromatin remodelling factors and protein binding (ChiP/CHIP) will greatly contribute to and enhance our understanding of the interaction of these mechanisms in future studies.

Chapter VII

Materials and Methods

7 Materials and Methods

7.1 Methods, Strains and Growth Conditions

7.1.1 Nomenclature for gene names, proteins, integrants and plasmids

The gene nomenclature in this thesis is the following (see Table 15): For fission yeast genes, the name of the gene is in lower case letters and italicised (e.g. *cdc2*). The wildtype allele is designated by a + sign (e.g. *cdc2+*). The mutant form of the gene is in lower case and italicised, with an allele number when specified (e.g. *pat1-114*). For proteins encoded by genes the first letter is in upper case and the rest of the gene name in lower case (e.g. Cdc18). Budding yeast wildtype genes are in upper case letters and italicised (e.g. *CDC6*). The mutant form of the gene is in lower case letters and italicised, with an allele number when specified (e.g. *cdc28-4*). The first letter of the protein encoded by the gene is in upper case and the rest of the gene name in lower case (e.g. Cdc6). When referring to homologous genes or proteins in fission yeast and budding yeast, the two names are separated by a forward slash (e.g. *cdc2/CDC28*). For genes and proteins in Metazoa, the same nomenclature convention used for fission yeast was applied. The mating type is indicated either as h^+ or h^-.

Genotype	Origin	Number
wildtype 975 h^+ and 972 h^-	CCL Collection	41/1
HM248 his2 ade6-210 Ch16	CCL Collection	
cdc25-22 HM248 his2 ade6-210 Ch16 h⁻	This study	
cdc25-22 h⁻	CCL Collection	7
pat1-114/pat1-114 ade-M210/ade6-M216 h⁺/h⁺	CCL Collection	2159
nmt1-cdc18+ leu 1-32 h-	CCL Collection	1803
leu1-32 ade6-704 pREP3x (sup3-5) rum1+	CCL Collection	1152
cdc25-22 leu1-32 nmt1-cdc18+ ura4D-18 pREP4-cdt1+ h⁻	CCL Collection	3613
cdc13Δ::ura4+ ade6-704 leu1-32 ura4-D18 pREP45-cdc13+(sup3-5) h⁻	CCL Collection	1414
cdc25-22 cdc13Δ::ura4+ ade6-704 leu1-32 ura4-D18 pREP45-cdc13+(sup3-5) h⁻	CCL Collection	1930

Table 15: Fission Yeast Strains used in this Thesis
CCL stands for **C**ell **C**ycle **L**aboratory (CRUK, Lincoln's Inn Fields, London)

Genes expressed from plasmids are marked by a small "p" and the name of the plasmid appear in front of the gene name. The name of the plasmid reflects the strength of the promoter used (e.g. *pREP4-cdt1+)*. There are three version of the nmt promoter, which can be ordered by strength: REP4>REP42>REP82. Plasmids containing the *ura4* gene as a marker use the numbers 4, 42, and 82, plasmids containing the gene *leu1* as marker use the numbers 1, 3, 41, 81, which can be ordered by strength: REP1=REP3>REP41>REP81. pREP45 plasmids contain the *sup3-5* marker (adenine deficiency suppressor) and the medium strength nmt promoter. Genes integrated into the chromosome under the nmt promoter are designated by nmt followed by the strength of that promoter, the nmt1 used in this study is the strongest promoter. The nmt promoter is repressed in cells grown in media containing 5 µg/ml thiamine. To induce

full expression form the nmt promoter, cultures were grown in minimal medium containing thiamine until logarithmic growth, filtered and washed three times with medium lacking thiamine, then re-suspended and grown in the absence of thiamine. Full induction of this promoter takes ~15 hours.

7.1.2 Methods

7.1.2.1 Fluorescence Activated Cell Sorting Analysis (FACS)

Between 2x106 and 2x107 cells were fixed in 70% ethanol/dH2O and stored at 4°C. To process cell samples for FACS, cells were washed twice with 5mls of 70 % ethanol (to remove growth medium). This was followed by two washes with 2 ml of 50mM Sodium Citrate [HOC (COONa) (CH2COONa)2.2H2O]. Cells were then resuspended in 0.5ml of 50mM Sodium Citrate containing 0.1 mg/ml RNaseA and incubated at 37°C for at least two hours. 0.5ml of Na3Citrate containing 2 μg/ml of propidium iodide was then added and cells were sonicated for 15 to 30 seconds at setting 6 in a Soniprep 150 sonicator (MSE, Crawley, Surrey, UK). Analysis was carried out using a Becton Dickinson FACScan as previously described (Sazer and Sherwood, 1990).

7.1.2.2 Cell number determination

Cell number was determined using a Coulter counter, Z series (Beckman Coulter, Inc., Buckinghamshire, UK). Cells were fixed by adding 1.6 ml of formal saline solution (0.9% saline, 3.7% formaldehyde) to 0.4 ml of cell culture and stored at 4°C. Before processing for cell number, 18 ml of

Isoton solution was added and cells were sonicated for 30 seconds as described above, and then counted.

7.1.2.3 Visualisation of nuclei by DAPI staining

Cells were fixed in 70% ethanol/H_2O and stored at 4°C. Cells were then re-hydrated in water, heat fixed on a slide and mounted in 1 μg/ml of DAPI (4',6-diamidino-2-phenylindole) in 50% glycerol/H_2O. Photographs were taken using a Hamamatsu camera (Hamamatsu Photonics UK LTD, Hertfortshire, UK).

7.1.3 Experimental Design

Standard strains, media and methods were used (Moreno et al., 1991). Strains used were derived from the wildtype strains 972 h^- and 975 h^+ (Hayles and Nurse, 1992). Minichromosome CH16 strain *HM248* (Niwa et al., 1989) was crossed with *cdc25-22*. Cells were grown to exponential growing phase and blocked in G_2 by temperature shift from 25°C to 36.5°C for 3.5 hours and harvested. Minichromosome CH16 loss was determined as previously described (Niwa et al., 1989). *cdc25-22*^{ts} cells were synchronised in the mitotic cell cycle as follows: haploid cells were grown in Edinburgh minimal medium (EMM) at 25°C to a density of $1.6x10^6$/ml. The culture was shifted to the restrictive temperature of 36.5° C for 3.5 hours to block cells in G_2. Cells were released back into the cell cycle at 25°C with or without addition of 11 mM HU (HU) (Sigma-Aldrich, UK). Samples for DNA extraction were taken at time 0 and at 5 - 10 minute intervals during the synchronous S phase and at 90 minutes into the HU block, respectively. As a reference for all timepoints of the *cdc25-*

22^{ts} block/release and the minichromosome CH16 experiment, 2C DNA from cells blocked in G_2 of the cell cycle was used (time 0). Synchronous meiosis was induced as follows: *pat1-114^{ts}/pat1-114^{ts} ade-M210/ade6-M216 h$^+$/h$^+$* diploid cells were grown to a density of $8x10^6$/ml in EMM at 25°C and then re-suspended in EMM without *NH_4Cl* (EMM-N) at $2.7x10^6$/ml and incubated for 14 hours at 25°C. Meiosis was started by shifting to 34°C in the presence of 0.05 % *NH_4Cl*, with or without 11 mM HU. Samples for DNA extraction were taken at time 0 after nitrogen starvation and at 5 min intervals during the synchronous pre-meiotic S phase and at 3 hours and 4 hours into the HU block. As a reference for the *pat1-114^{ts}* experiments, diploid pat1-114 nitrogen starved cells from the same culture blocked in G_1 of the cell cycle with 2C DNA content were used (time 0). Re-replication was induced as follows: Multiple integrant *nmt1*-cdc18+ (Nishitani and Nurse, 1995) cells were grown at 32°C in EMM supplemented with adenine and uridine in the presence of 5 μg/ml thiamine. To o/e Cdc18 from G_2 phase of the cell cycle, Cdc18 was ectopically expressed in *cdc25-22* cells arrested in G_2 from the multiple integrant *nmt1*-cdc18+. Cells were grown at the permissive temperature of 25 °C in EMM in the presence of 5 μg/ml thiamine. The nmt1 promoter was induced by washing cells three times and re-suspending in EMM. To ensure that the inducible *cdc18* was expressed only once all cells had arrested in G_2, the nmt1 promoter was de-repressed for 11 hours at 25°C before shifting the culture to 36.5°C. Samples for DNA extraction were taken at 0, 8 and 10 hours into the G_2 block. *cdc25-22 nmt1-cdc18+ pREP4-Cdt1+* (Yanow et al., 2001) were grown at 25° with 5 μg/ml

thiamine. Expression from the nmt1 promoters was induced as for *nmt1-cdc18+* and cells were shifted to the restrictive temperature of 36.5 °C after 11 hours induction. Samples for DNA extraction were taken at 4, 6, 8 and 10 hours after temperature shift. *cdc13Δ ura4+ ade6-704 leu1-32 ura4-D18 pREP45-cdc13+(sup3-5) h⁻* cells were grown at 32°C in EMM supplemented with leucine. Cells were washed twice and re-suspended in EMM without *NH_4Cl* (EMM-N) plus 5 μg/ml thiamine at $2x10^6$ cells/ml. After 15 hour nitrogen starvation, 5 mg/ml NH_4Cl and leucine were added and samples for DNA extraction taken at 4, 6 and 8 hours into re-replication. The reference for all re-replication experiments were cdc25-22 cells blocked in G_2 for 3.5 hours with 2C DNA content. The mitotic and meiotic time course as well as the HU experiments for ORI mapping were carried out at least in duplicate. Re-replication experiments for Cdc18 o/e, Cdc18/Cdt1 co-o/e and *cdc13* s/o were also carried out at least in duplicate for the late timepoints (10 hours); time course experiments including early time-points were not repeated.

7.2 Microarray Design

The microarrays used were of two types: ORF arrays with gene specific probes and intergenic arrays with probes covering all non-coding regions. ORF microarrays were designed as described (Lyne et al., 2003). The intergenic microarrays were developed using similar approaches as follows: for intergenic regions larger than 2 kb, more than one PCR probe was produced, and the average probe length was ~1 kb. The two microarrays cover all three chromosomes of the genome with 10400 PCR-

based probes, which include control spots. All probes are printed in duplicate on the arrays. The ORF array consists of 5265 unique probes, which are 200 – 500 bp in length. The intergenic array is made up of 5135 unique probes which are 1.25 – 2 kb in size. A summary of the number and distribution of probes is shown in Table 16, which contains only probes used in this analysis, after elimination of probes that served as controls. The interprobe distance is on average 1.26 kb and equivalent to the average maximum resolution of the microarray analysis. The arrays do not cover the rDNA repeats proximal to the telomeres on Chromosome Three (1.2 Mb in total) and core sequences of the three centromeres (29kb on Chromosome One, 50kb on Chromosome Two, and 67kb on Chromosome Three). Chromosome Two also lacks subtelomeric regions; a 5kb fragment from the distal end of the chromosome and a 25kb fragment from the proximal end of the chromosome are not covered. The mating type locus is covered by a total of 17 probes.

	Number of ORF Probes	Number of intergenic Probes	Total Number of Probes	Sequence Covered (kb)	Interprobe distance centre to centre (kb)
Chromosome One	2245	2322	4567	5550	1.22
Chromosome Two	1818	1658	3476	4460	1.28
Chromosome Three	901	886	1787	2369	1.33
Total	4964	4866	9830	12379	1.26

Table 16: Distribution of Microarray Probes
The table summarises the number and the distribution of ORF and intergenic probes on the three chromosomes which were used as a basis for our microarray analysis to generate DNA replication profiles.

7.3 DNA Preparation and Microarray Processing

A maximum of 10^9 cells were harvested by filtration and washed once with 50 ml of ice-cold buffer (50 mM MOPS pH 7.2, 150 mM potassium acetate, 2 mM magnesium chloride) with 0.1 % sodium azide, then washed again with 50 ml of buffer alone. Genomic DNA was purified from cells as described (Wu and Gilbert, 1995). DNA yield and quality was determined by gel-electrophoresis and spectrophotometry and 600 ng of DNA was labelled according to (Fiegler et al., 2003). The size distribution of purified labelled DNA fragments was between 200 to 1000 nucleotides (Figure 57), consistent with the results from the supplier of the Random Primer Labelling kit (Stratagene, La Jolla, California, USA). The purified experimental DNA was mixed with the corresponding reference DNA (Cy3/Cy5 or vice versa) for differential hybridisation. DNA was precipitated with 1/10 volume of 3M NaAc pH 5.2 and 3 volumes of 100 % ethanol at –70°C for 30 minutes. Samples were centrifuged for 15 minutes at 14k rpm in a microcentrifuge and the pellet was washed with 100 µl 70 % Ethanol (4 °C), dried and resuspended in 70 µl of hybridisation buffer [5xSSC, 6 x Denhardt's: (1x Denhardt's solution is 0.02% Ficoll, 0.02% polyvinylpyrrolidone, and 0.02% bovine serum albumin), 60 mM TrisHCl pH7.6, 0.12% sarcosyl ($CH_3(CH_2)_{10}CON(CH_3)CH_2COONa$), 48 % formamide; filter sterilised]. An aliquot of 30 µl was hybridised to the microarrays at 49 °C in a Grant Boekel hybridisation oven for approximately 16 hours. Slides were washed and stored in the dark for scanning. A detailed protocol for hybridisation and slide washing is available at this URL: (http://www.sanger.ac.uk/PostGenomics/S_pombe/).

Two independent time course experiments were carried out for both mitosis and meiosis and DNA from cells taken in 5 to 10 minute intervals during S phase was used for hybridisation. DNA samples from re-replication experiments were hybridised at least in duplicate. A so called dye swap was carried out, where the Cy5/Cy3 dyes for labelling were swapped between experimental and reference samples in the repeat experiments.

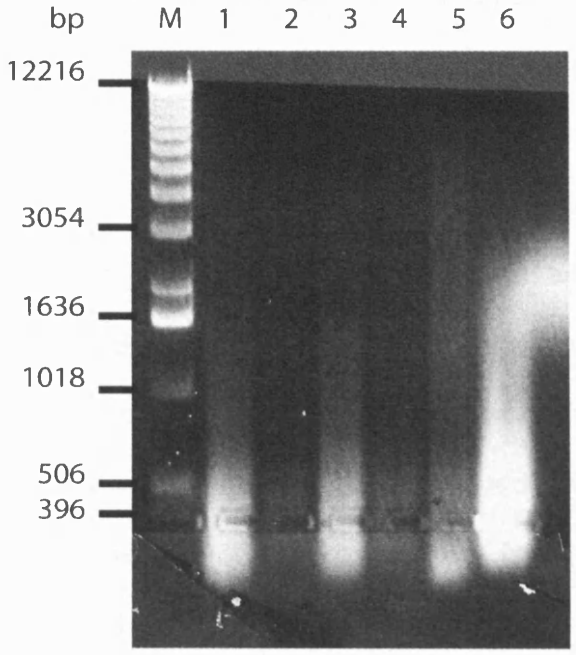

Figure 57: Size distribution of random primer labelled genomic DNA.
The Prime-It® II Random Primer Labelling Kit (Stratagene, La Jolla, California, USA) was used to label genomic DNA. The size distribution of labelled DNA in six different labelling reactions is shown; 10 µl of labelling reaction were loaded in lanes 1 – 5, 20 µl in lane 6. The labelled DNA is typically 200 – 1000 bp in length.

7.4 Data Acquisition and Analysis

Data acquisition, processing and normalisation were as described by (Lyne et al., 2003). The analysis is based on the genome sequence of

April 2004. This and current pombe sequence data can be obtained at the following URL: (http://www.sanger.ac.uk/Projects/S_pombe/).

7.4.1 Processing of Raw Data

Microarray slides were scanned using the software application Genepix Pro V4.0/5.0 in conjunction with the Genepix 4000/4100 Series scanner (Molecular Devices Corporation, Sunnyvale, California, USA). Signals from the two dyes (experimental/reference) were independently scanned in two channels; after a pre-scan signals were adjusted so that the ratio in both channels was well balanced across the range of the signals. Scanned images were saved as ".TIFF" files for further analysis. Figure 58A shows part of a typical microarray image before analysis in Genepix. The image was first aligned with a ".GAL" file which contained the geographic information for all the probes on the array including probe names and positions of probes on the microarray. This file also consisted of information of probes that should not be included for further analysis, for instance probes where PCR products had failed or probes which corresponded to controls that should be eliminated. Spots that showed signals below a certain threshold were marked as absent. The microarray image was then visually inspected for any abnormal or bad spots or misalignments that needed to be corrected. A typical microarray image after this analysis is shown in Figure 58B. Logistic curves for replication kinetics in the time course experiments were fitted using XlFit 4.0 (ID Business Solutions Ltd, Surrey, UK) and used to determine scaling factors for microarray signals. Microarray signals were normalised using a PERL script that was specifically designed for the microarrays used in this

analysis (Lyne et al., 2003). The normalisation script can be downloaded from the following URL: http://www.sanger.ac.uk/PostGenomics/S_pombe/software/. Signal ratios were corrected so that the "median of ratios" equalled 1 across the array. This was done by calculating the signal ratio for central spots in a sliding window (33 x 33 spots) assuming that the median of ratio equalled 1. The reason for this procedure was to account for spatial artefacts across the microarray slide. For time course experiments the "median of ratios" for each experimental time point were adjusted according to the scaling factors determined from the logistic curves. Replicate spots on the arrays were averaged in this analysis and the normalised data was written to an output file.

A

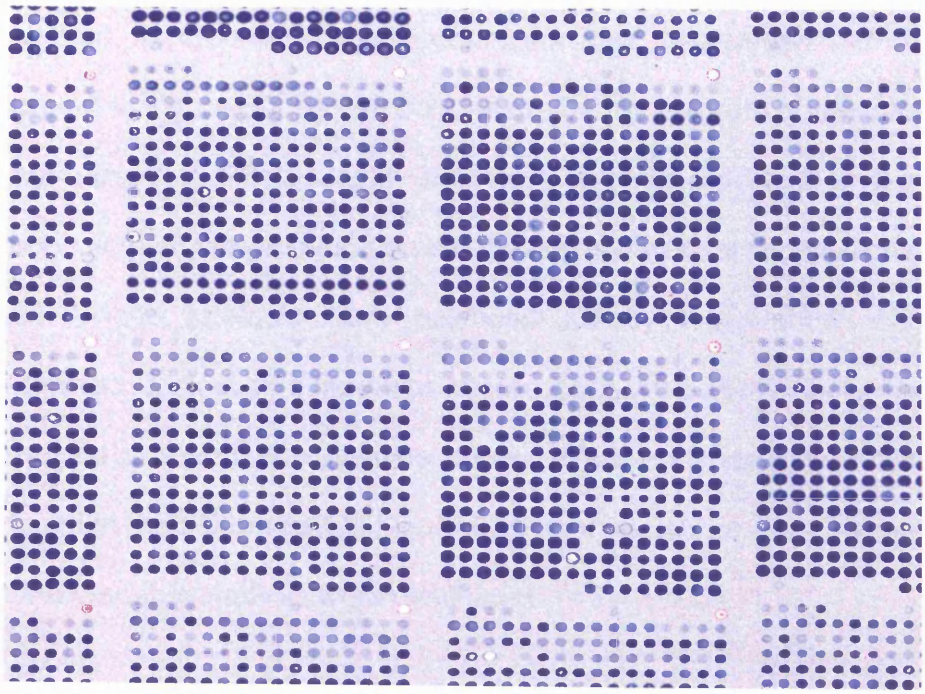

B

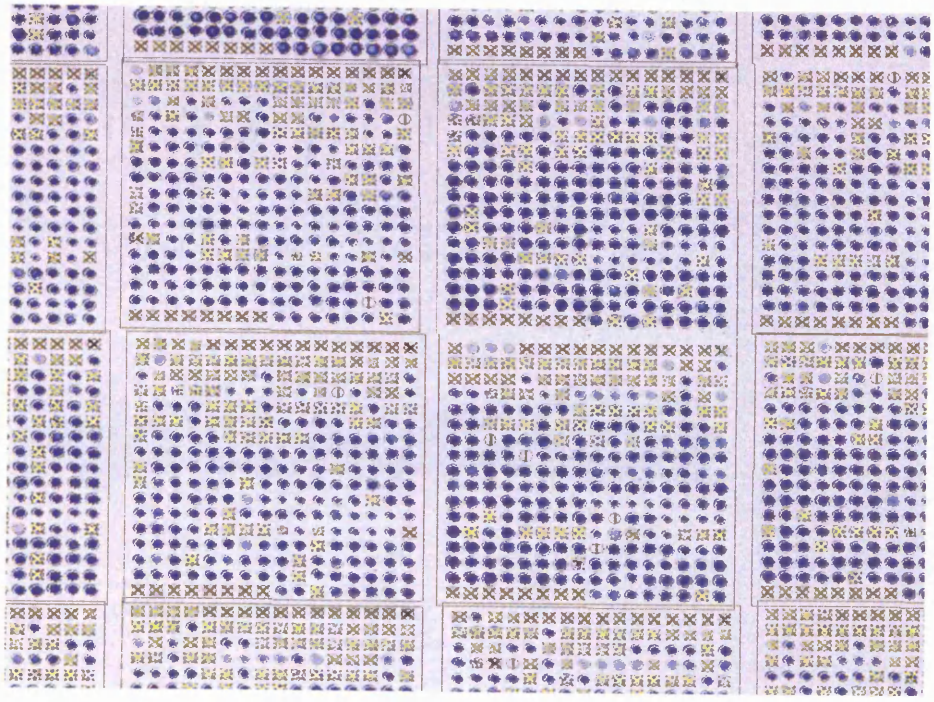

Figure 58: Processing of Microarray Raw Data in Genepix
(A) Microarrays as they appear in Genepix after scanning. (B) Microarrays after elimination of spots that should not be included in the final analysis.

7.4.2 Processing of Normalised Data

The result of a normalisation procedure for one microarray chip is demonstrated in Figure 59. As can be seen in the top diagram of the data before normalisation, differences in slide surface could lead to a shift in signal ratios across a large region on the microarray (from array position 0 – 10000). These artefacts were balanced out by the normalisation procedure which took such differences into account. Also all the spots that should not be included (for instance spots with low standard deviation values found in the bottom half of Figure 59A) and spots that were marked "bad" in the Genepix analysis were eliminated.

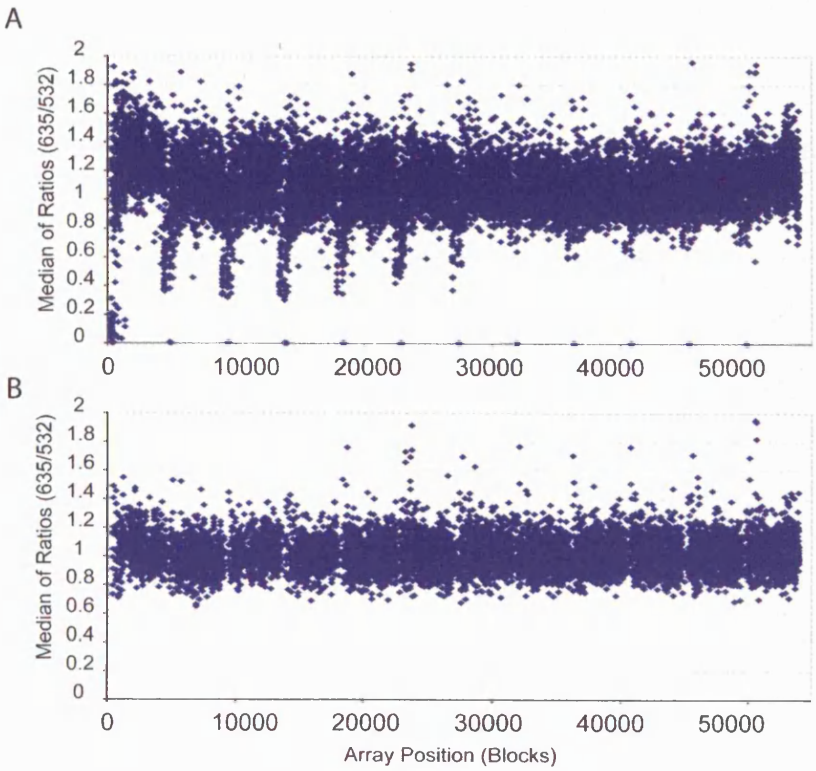

Figure 59: Data from one Microarray Experiment before and after Normalisation
This figure shows data from one microarray slide before (A) and after (B) normalisation of signal ratios.

The normalisation script produced an output file with a protocol of certain normalisation parameters, an example of which is shown in Figure 60. Apart from parameters used for normalisation, it also produced information on spots that were marked in the Genepix analysis and the number of spots that were discarded because they did not qualify the threshold for the standard deviation (50 % of pixels >2 standard deviations) between the local background signal from the microarray and the signal from the spot. The most important information in the file was on the correlation of signals between two replicate spots (coefficient of variation or CV value). Replicate spots that deviated by more than 30 % were listed and could be examined and if necessary eliminated from further analysis. The average deviation between replicate spots in this particular experiment was 2.6 %, which gave an indication of the reproducibility of signals from replicate probes.

Using script: C:\Perl\March_April2004_Analysis_Microarray_data\local_normal_scale22.pl (v 1.26).
Analysing file: C:/Perl/March_April2004_Analysis_Microarray_data/131202_030103_170103HUdata2003/13_12_02_files/CH_334_90min.gpr at 11:29 on 06 May 2004.
Using gene list file: C:/Perl/March_April2004_Analysis_Microarray_data/ORF_genelist_for_normalisation.txt.

Columns per block: 16.
Rows per block: 16.
Blocks per array: 4.

Ratio: 532/635.
File type: GenePix version 4.

Masked spot information:

Number of masked spots: 212.
Number of not found spots: 34.
Number of spots flagged bad by user: 1264.
Number of marginal spots: 0.

Using background SD cut-offs.

Using upper background cut-off: 95.
Using lower background cut-off: 50.

Number of spots discarded: 804.

Not using spot diameter cut-off.

Not using bacterial controls.

Normalisation parameters:

Using normalisation window size of: 16.
Using maximum normalisation window of: 24.
Using normalisation block size of: 400.
Using initial block size of: 600.

Using scale factor of 1.
Genes with only marginal spots:

There are no marginal genes.

Overall array signals:

Total signal experiment: 44602609.
Total signal control: 44520396.
Ratio of total signals: 1.00185.

Replicate spot information:

Zero spots: 205.
One spot: 18.
Two spots: 4763.
More than two spots: 278.

Average % CV: 2.6391.

Genes with CVs higher than 30%:

Gene	Spots	% CV	Max. ratio
c31g5.07	4	37.655	1.9772

Figure 60: Protocol/Output of a Normalisation Analysis

Normalised signals were imported into the microarray analysis application GeneSpring (Agilent Technologies UK Limited, Cheshire, UK). Here probes were matched with the chromosomal co-ordinates and any patterns across the genome could be visualised. This software also consisted of tools for further statistical analysis. Normalised and scaled signals were exported from GeneSpring into Microsoft Excel and data from intergenic microarrays and ORF microarrays was combined. To normalise for any dye bias, signal ratios of all time points during the time courses and HU experiments were divided by signals obtained from self/self hybridisations of a sample at time 0 (either G_1 block or G_2 block) from the same culture. For the mitotic and meiotic time courses, a sigmoid curve of signal ratio against time was fitted for each probe using the regression analysis in XlFit 4.0. The time at which 50 % of each probe was replicated was determined and plotted against chromosome position. Excel pivot tables and graphs were used to construct the replication profiles for all experiments. Replication profiles for the time course experiment were constructed from a moving average over 5 probes; all other plots were constructed from moving averages over 3 probes. These plots were used to identify ORIs across the genome.

7.4.3 Mapping and Characterisation of ORIs

The threshold for mapping ORIs in the HU experiments was defined from the background noise as follows. The background noise of the self/self hybridisation (G_2 blocked cells) followed a normal distribution Figure 61. The likelihood that signals reached a certain threshold above 1 was

calculated using statistical analysis (Table 16). This reached a value of 0 for a moving average of three probes and a threshold of 1.15. The likelihood that three probes with signals above 1.1 fold in a moving average were next to each other on the chromosome was $5x10^{-8}$. This was considered a threshold that was strict enough not to pick up any false negatives across the genome. Consequently, peaks were only considered for ORI mapping if three consecutive probes had signal ratios above 1.1 in a moving average. It should be pointed out, that this moving average was constructed from three experimental repeats in mitosis and two experimental repeats in meiosis, which decreased the signal/noise ratio even further.

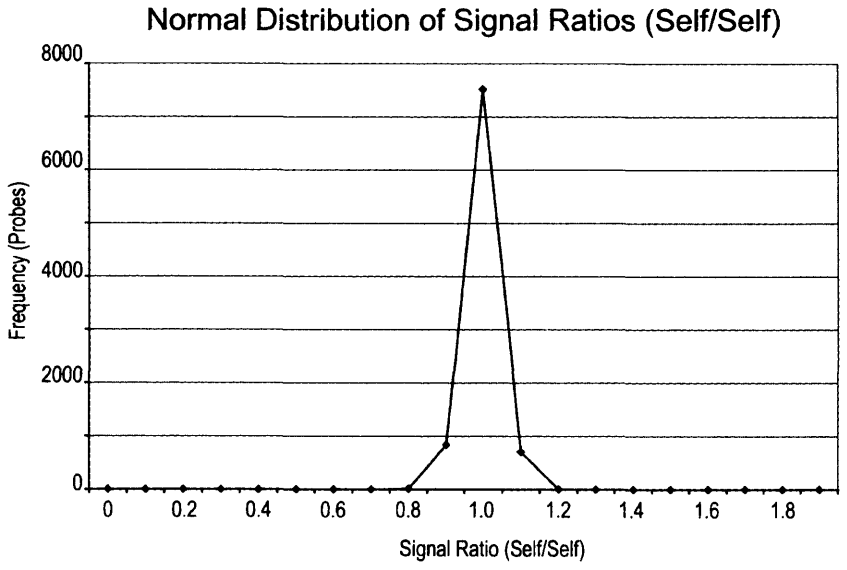

Figure 61: Normal Distribution of Signal Ratios in a Self/Self hybridisation

	Self/Self	Self/Self Moving Average
Mean Signal	0.998919291	0.998656468
Standard deviation	0.038948011	0.025552698
P value Signal >1.1	0.472504020	0.003653530
P value Signal >1.15	0.005240420	0.000000160
P value Signal >1.20	0.000012150	0.000000000

Table 17: Statistics on background noise of Self/Self hybridisation

For the time course experiments, peaks for ORI mapping were identified that replicated at least three minutes faster than the surrounding regions and were defined by a minimum of five contiguous probes. Data from two experimental repeats in mitosis and meiosis, respectively, were used to determine the position of ORIs.

The efficiency of ORIs in the microarray analysis was calculated from the averaged data of two experimental repeats in the HU experiments. The time of replication was determined from the moving average of two experimental repeats. The efficiency of ORIs from published 2D gel data was determined from the signals of bubble and Y-arcs using the software NIH Image (http://rsb.info.nih.gov/nih-image/Default.html), by dividing the signal of the bubble arc by the total signal of bubble- and Y-arc.

The size of replication bubbles was determined from the width of peaks of the replication profiles from HU experiments. The width was measured from the chromosome position between the first probe and the last probe that had signal ratios above 1 within a particular peak.

7.5 Computational Tools and Bioinformatics Analysis

The analysis of intergenic sequences is based on genome annotations as of May 2005. Current genome annotation status can be viewed on the Sanger Institute website for Pombe Functional Genomics (http://www.sanger.ac.uk/Projects/S_pombe/). A custom made Perl script was used to extract information for intergenic regions from genome annotations. A Perl script (Woodfine et al., 2004) was used to assess the optimal segmentation for replication timing analysis across the genome. Genespring was used to construct the whole genome replication origin map and figures to show distribution of induction/repression of ORIs in pre-meiotic S phase. ClustalW (http://www.ebi.ac.uk/clustalw/) was used to carry out sequence alignments. Custom build Perl scripts were used to extract ORI sequences from the *S. pombe* genome sequence for AT-hook analysis as well as to map AT-hook binding domains onto *S. pombe* and metazoan ORIs (available upon request). The programs "freak", "dreg" and "fuzznuc" from the EMBOSS suite (http://www.es.embnet.org/Doc/EMBOSS/index.html) were used for mapping AT-hook sequences, the calculation of % AT/GC content and the mapping of the late ORI sequence respectively. Sequences from the following Genbank (http://www.ncbi.nlm.nih.gov/Genbank/index.html) accession numbers were used for analysis of metazoan ORIs: U01317 between 61110bp – 63754bp (Human ß globin locus), X00364 (Human c-myc locus), AE003554 from CG6511 to Cp15 (*Drosophila* chorion amplification locus), M94363 (Human lamin B2 locus), Y09885 (Hamster DHFR locus). A+T-rich islands that were closely spaced were grouped for

comparative analysis with microarray ORIs if two or more A+T-rich islands co-localised with a single peak on the replication profiles.

Appendix

DNA Replication Origin Lists

Chromosome 1

ORI Number	5' Gene	3' Gene	Map Position	%AT-content (500 bp)	Efficiency Mitosis	Efficiency Meiosis	Replication Time Mitosis (mins)	Replication Time Meiosis (mins)
ORI1001	c1f8.04c	isp3: meu4	95650	73.8	2	17	80	122
ORI1002	c11d3.02c	c11d3.05	113896	75.6	15	12	79	121
ORI1003	c11d3.07c	c11d3.13	125773	75.8	13	11	78	121
ORI1004	chs1	aps1	200654	80	23	18	78	119
ORI1005	c24b11.12c	c806.01	230958	65.6	21	8	83	120
ORI1006	cid14	c12g12.11c	326001	76.8	33	8	78	122
ORI1007	c630.05	c630.08c	358454	74.8	15	12	78	121
ORI1008	c630.15	c630.12	366626	79.4	23	8	80	119
ORI1009	c31a2.04c	c31a2.08	398386	74.4	15	11	81	122
ORI1010	c13c5.06c	gaf2	438359	76.6	6	10	80	122
ORI1011	c24h6.10c	c24h6.08	473245	76.6	12	11	80	121
ORI1012	pcu3	pb21f2.02	492530	78.4	33	10	77	120
ORI1013	c227.15	c227.17c	528878	73.8	12	16	73	121
ORI1014	c2f7.13c	c2f7.15	563188	76.6	19	10	77	119
ORI1015	c3h8.08c	sec14	606263	75.8	1	5	78	122
ORI1016	c1d4.03c	c1d4.09c	648545	77.6	12	16	81	121
ORI1017	c22f3.03c	c1296.01c	707806	72	23	12	77	119
ORI1018	c1296.01c	c1296.04	713564	79.2	33	16	79	118
ORI1019	c1296.04	c1296.06	718467	74	51	19	79	117
ORI1020	c16c9.01c	c16c9.03	794734	78	14	19	80	119
ORI1021	c2g11.15c	c521.03	844635	76.8	40	22	76	118
ORI1022	c23g3.03	c23g3.06	876779	74.4	27	8	77	118
ORI1023	c23g3.06	c23g3.08c	881992	75.8	19	11	77	117

ORI1024	c22h12.05c	c1687.02	903324	77.2	51	13	74	117
ORI1025	byr4	atp2	966458	78	41	4	78	119
ORI1026	c222.14c	csn3	978693	71.4	5	14	77	120
ORI1027	c139.01c	c139.03	1021911	73	20	10	78	119
ORI1028	c1a6.04c	c1a6.07	1079985	78.4	57	17	74	114
ORI1029	c1a6.07	lag1	1087856	71.2	31	13	74	115
ORI1030	c30d11.15c	rpl38-2	1095332	74.8	44	13	73	115
ORI1031	c56f8.07	c56f8.10	1140949	72	20	4	78	120
ORI1032	esc1	c22a12.01c	1157904	73.8	20	12	77	118
ORI1033	bip	c22a12.17c	1188295	73.8	38	16	74	116
ORI1034	c22a12.17c	rad31: uba4	1196479	78.2	49	17	74	116
ORI1035	cut6	c56e4.06c	1256615	76.4	60	8	76	118
ORI1036	pb17e12.03	rpl37	1274662	74.8	26	12	76	119
ORI1037	pb17e12.07c	pb17e12.11	1282094	74	28	14	76	119
ORI1038	c57a10.04	c57a10.07	1374919	73.4	17	4	79	122
ORI1039	ura3	c20g8.02	1389465	74	33	12	77	121
ORI1040	c3a12.01	c3a12.03c	1423569	75	46	2	77	119
ORI1041	cwf2	cam1	1443033	77.8	42	17	74	118
ORI1042	c3a12.13c	vps53	1446276	77.8	27	14	74	115
ORI1043	c9.05	c9.09	1475607	76	48	19	76	116
ORI1044	c9.10	c5d6.13	1488975	74.6	11	13	77	117
ORI1045	c5d6.07c	c5d6.05	1504720	72.6	18	2	78	117
ORI1046	c5d6.04	c5d6.02c	1509647	76.2	32		73	117
ORI1047	c23h4.19	c23h4.17c	1575911	73.8	37	4	76	120
ORI1048	vps41	p27g11.07c	1619927	74.4	17	2	81	125
ORI1049	c343.11c	c343.20	1665010	75	14	10	77	118
ORI1050	c664.02c	rps16-2	1709162	74.2	35	7	76	115
ORI1051	c664.08c	c664.10	1720871	74.8	25	10	75	116
ORI1052	c664.13	cmk1	1735182	78.2	37	25	74	115
ORI1053	c1002.14	c1002.17c	1828654	79.2	30	25	74	115

ORI1054	c1002.17c	c1399.05c	1835520	78.2	45	18	76	115
ORI1055	p11e10.01	pb1a10.02	1860354	71.6	32	8	77	118
ORI1056	wis4: wak1: wik1	oxa1sp1	1974689	75.6	34	17	77	118
ORI1057	cdt2	c607.06c	2041332	76.6	27	14	79	120
ORI1058	c3c7.08c	cal1: cnx1	2085622	70.6	14	4	79	124
ORI1059	obr1	c25a8.01c	2099786	76.4	12	10	80	121
ORI1060	ufd2	c23c11.01	2134196	68.6	20	10	79	122
ORI1061	c23c11.03	ppa	2139643	77	7	11	81	122
ORI1062	pap1	c18g6.01c	2208023	76.4	14	6	76	119
ORI1063	c18g6.05c	mra1	2230761	73.2	22	2	77	118
ORI1064	c18g6.13	rps7	2242648	76.2	16		76	117
ORI1065	rps7	byr3	2246254	74	20	11	76	117
ORI1066	byr3	c13d6.04c	2249969	76.4	34	6	75	117
ORI1067	c4g9.04c	b8647-3	2262439	74.2	16	6	76	118
ORI1068	pep8	c4g9.15	2280762	78	30	8	74	117
ORI1069	c13g7.05	c13g7.09c	2311243	74.4	22	14	79	121
ORI1070	c13g7.12c	c13g7.13c	2319383	76	35	5	80	120
ORI1071	c6c3.06c	c6c3.07	2336134	76.6	15	4	77	122
ORI1072	c6c3.08	c6c3.09	2340871	78	25	11	77	120
ORI1073	c15f9.01c	c6b12.02c	2403808	76	7	14	80	123
ORI1074	c6b12.04c	c6b12.09	2424146	73.8	6	5	77	120
ORI1075	c6b12.14c	tif212: tif22	2442981	75.6	33	4	78	119
ORI1076	c32a11.01	c19a8.15	2453555	76.6	20	4	77	120
ORI1077	c23h3.03c	c23h3.04	2498995	73.2	18	0	78	121
ORI1078	prs1	tif33	2580709	75.6	31	14	75	117
ORI1079	c7d4.14c	c7d4.09c	2618996	75.8	8	10	78	120
ORI1080	c7d4.03c	hcs	2640885	74.6	5	7	78	120
ORI1081	c4f8.04	c644.02	2673222	70.8	30	5	79	123
ORI1082	pb2b4.04c	pb2b4.06	2721295	75.6	22	16	76	119
ORI1083	c6f6.05	c6f6.11c	2747243	73.8	15	13	78	119

ORI1084	c6f6.12	c6f6.16c	2760855	78.2	34	13	75	117
ORI1085	cki3	dlc1	2785948	74.2	24	18	78	119
ORI1086	c1805.15c	c1b2.02c	2805245	72.4	35	8	75	116
ORI1087	c1b2.03c	nda4: mcm5	2815685	71.6	3	6	76	116
ORI1088	c8f11.04	c8f11.06	2862544	77	25	12	76	119
ORI1089	cunk4.16c	cunk4.14	2882186	76.4	0	8	77	118
ORI1090	c513.02	c513.04	2913696	73	34	23	75	119
ORI1091	pb24d3.06c	pb24d3.09c	2961052	79.6	48	11	75	116
ORI1092	pb1a11.01	pb1a11.04c	2984146	72.8	19	5	77	117
ORI1093	pac2	c31g5.15	3011870	78.2	41	16	74	114
ORI1094	rps10-1	c1786.04	3026197	77.2	16	7	76	113
ORI1095	bgs2: meu21	c24c9.08	3060522	77.4	36	12	76	116
ORI1096	c688.07c	c688.10	3126859	76	42	16	77	118
ORI1097	scn1	sak1	3145188	78.6	33	28	76	117
ORI1098	c3g9.01	alm1	3185366	76	23	11	77	116
ORI1099	c6g9.01c	c6g9.04	3245826	76	44	24	74	115
ORI1100	c6g9.10c	c6g9.13c	3270677	76.2	38	22	75	116
ORI1101	pb1e7.10	pb1e7.07	3300554	77.6	14	5	77	115
ORI1102	pb1e7.04c	pb1e7.02c	3319241	77.8	42	23	76	113
ORI1103	rps4-3	p32a8.03c	3404719	77.6	43	24	75	115
ORI1104	p32a8.02	rpl5	3410586	76.4	50	25	76	114
ORI1105	pkl1: klp1	c3a11.11c	3443353	76	42	24	74	115
ORI1106	c3a11.07	kms1	3462181	70.6	28	N.A.	76	N.A.
ORI1107	c328.08c	c16e8.01	3496579	75.8	29	28	75	113
ORI1108	c16e8.12c	c16e8.14c	3526148	73.4	42	1	75	115
ORI1109	c1b1.03c	car1: sod1	3549172	77.2	59	N.A.	75	N.A.
ORI1110	c17a2.08c	c17a2.12	3575013	80.2	56	19	74	105
ORI1111	c17g6.03	cpp1	3604381	73.4	20	7	78	114
ORI1112	c1142.04	vps32: snf7	3636644	78.2	42	22	74	114
ORI1113	c15a10.05c	c15a10.07	3689496	73.2	24	12	74	116

ORI1114	c15a10.09c	c15a10.11	3701094	78	39	46	73	113
ORI1115	vps29	c15e1.09	3730356	73.6	21	16	74	113
ORI1116	p7g5.01	lys1	3738683	78.4	60	31	74	113
ORI1117	rpl10-2	centromere	3750632	73.8	39	22	68	113
ORI1118	p7g5.06	centromere	3755290	76.4	45	17	68	118
ORI1119	centromere	centromere	3769666	75	10	5	74	115
ORI1120	centromere	c1556.01c	3785857	74.4	51	27	70	114
ORI1121	c1f12.02c	c1f12.05	3807392	73	26	N.A.	78	N.A.
ORI1122	srs2	c4h3.08	3835350	74	45	28	72	113
ORI1123	c4h3.12c	c1071.01c	3849194	75.4	50	27	74	115
ORI1124	c1071.03c	c1071.06	3860176	72.2	11	7	74	108
ORI1125	pma1	c1071.11	3869814	81.4	45	22	77	105
ORI1126	c1071.11	rlc1	3879937	77.6	56	28	75	107
ORI1127	c926.07c	fas1	3893805	78.4	35	22	77	113
ORI1128	c2f3.14c	c2f3.15	3947976	76.6	73	28	74	110
ORI1129	pb18e9.05c	c27e2.01	3987807	82.6	59	17	76	109
ORI1130	c27e2.04c	c27e2.07	4013740	75.8	31	30	73	113
ORI1131	pcy1: cpy1	its3	4064746	75.8	40	35	73	112
ORI1132	c23a1.03	cmk2	4082746	77.8	61	23	73	110
ORI1133	c26h5.07c	tif51	4132305	75.8	42	10	76	115
ORI1134	isp7	c25b8.16	4181429	78.8	30	19	76	114
ORI1135	c25b8.19c	c694.01c	4190182	71.2	22	33	79	113
ORI1136	c1f7.12	c21e11.05c	4248673	76.6	42	18	77	114
ORI1137	c2c4.07c	c2c4.10c	4270629	77.6	46	31	74	114
ORI1138	nuf2	c27f1.06c	4321507	79.2	60	23	75	116
ORI1139	c29e6.05c	c29e6.07	4409027	77.4	30	14	76	115
ORI1140	c9e9.01	leu2	4434135	74.4	33	13	78	116
ORI1141	c17c9.11c	tim13	4478518	75.6	28	22	76	115
ORI1142	c17c9.06	lys7	4488604	72.6	25	18	76	117
ORI1143	mei2	c27d7.06	4512848	72.4	20	27	78	115

ORI1144	c27d7.10c	ssm4	4528716	77.6	33	29	76	114
ORI1145	c12b10.01c	c12b10.03	4570339	73	25	18	79	120
ORI1146	c12b10.05	c12b10.07	4580433	69.2	24		79	123
ORI1147	c12b10.14c	c12b10.16c	4596825	73	23	18	80	120
ORI1148	c1093.03	dhc1	4614134	72.6	10	16	81	123
ORI1149	c144.01	apl5	4653201	75.6	7	7	81	121
ORI1150	klp8	c144.16	4679455	67.8	8	7	83	124
ORI1151	sec18	pex7	4718057	70.8	29	14	78	119
ORI1152	c458.03	c458.06	4734781	78.2	34	6	75	120
ORI1153	c11h11.01	mam2	4774379	79.6	25	18	77	121
ORI1154	pam1	c22f8.09	4796492	75.8	14	14	78	121
ORI1155	c4f10.07c	c4f10.10c	4842540	74	30	10	77	118
ORI1156	c4f10.10c	c4f10.12	4850084	75.8	22	6	75	118
ORI1157	c4f10.19c	grx1	4869244	73	39	17	72	118
ORI1158	pb8e5.07c	pb8e5.10	4920297	75	26	30	77	115
ORI1159	c1b3.02c	c1b3.06c	4929375	72.6	15	23	77	115
ORI1160	c1b3.16c	c1b3.18c	4959274	78	42	18	76	115
ORI1161	c1952.04c	rad1	4972122	75.8	12	17	77	115
ORI1162	c22e12.01	c22e12.04	5019237	75.6	41	23	76	114
ORI1163	c22e12.12	c22e12.16c	5041297	77.2	20	17	75	114
ORI1164	rpl30-2	ubc14	5093020	75.6	20	18	79	117
ORI1165	c29a4.05	c29a4.03c	5135533	74	16	17	77	114
ORI1166	c26f1.13c	c26f1.11	5151779	77.6	38	39	76	114
ORI1167	gpm1	pda1	5173237	68.8	18	10	78	116
ORI1168	mek1	c14c4.05c	5229322	76	30	16	78	116
ORI1169	c14c4.10c	atp1	5247966	76	13	8	81	117
ORI1170	rpl22	p8a3.05	5314068	78	1	20	81	121
ORI1171	rad2	c3g6.09c	5388638	76.4	17	22	77	117
ORI1172	c29b12.10c	c29b12.13	5431795	75.4	36	12	76	118
ORI1173	c1039.01	c1039.03	5445146	76.4	31	12	77	116

ORI1174	c922.01	c922.03	5469961	76.6	28	19	79	119
ORI1175	c922.04	c922.06	5478510	76	33	7	80	118
ORI1176	c869.10c	c869.05c	5496463	78	4	13	80	122
ORI1177	c186.09	telomere	5552999	75	0	4	85	123
ORI1178	c186.09	telomere	5562992	83.6	0		85	124

Chromosome 2

ORI Number	5' ORF/Gene	3' ORF/Gene	Map Position (central)	AT-content (500bp)	Efficiency Mitosis	Efficiency Meiosis	Replication Time Mitosis (mins)	Replication Time Meiosis (mins)
ORI2001	pb10d8.03	pb10d8.07c	96664	74.6	15	11	76	122
ORI2002	c359.03c	c359.06	122104	77	6	12	77	122
ORI2003	c1683.01	c1683.04	140017	78.4	14	8	77	121
ORI2004	c1683.04	c1683.07	149849	76.6	14	19	77	121
ORI2005	c800.02	tub1: atb2: alp2	259149	75.4	18	18	80	116
ORI2006	c800.10c	c800.13	277815	75	38	33	75	116
ORI2007	c1773.03c	c1773.04	289557	70.4	29	7	76	116
ORI2008	c1773.13	c1773.16c	316784	77.8	39	28	76	115
ORI2009	c1773.17c	p26c9.03c	326417	76	48	25	76	113
ORI2010	c1271.08c	c1271.05c	361327	72.2	19	37	68	117
ORI2011	idi1	c106.17c	410396	77.8	41	31	76	115
ORI2012	pho4	c428.04	448811	74.8	28	14	76	118
ORI2013	meu6	c428.10	460215	73.2	0	2	79	118
ORI2014	c1685.05	rps29	513899	75	44	25	76	112
ORI2015	rps29	c1685.12c	520348	80.6	40	24	74	112
ORI2016	c354.08c	c354.10	569481	76	43	24	76	111
ORI2017	c354.15	c839.01	592707	74	22	7	74	114
ORI2018	rpl8-3: rpk5-b: rpkd4	cta3	606100	75.8	28	28	74	110
ORI2019	c839.17c	c115.02c	636352	75.4	38	19	76	114
ORI2020	c947.13	c947.11c	649766	73.6	16	6	75	116
ORI2021	c947.05c	c947.01	675594	81	30	20	75	115
ORI2022	c947.01	pj4664.02	684848	74.2	41	16	74	114
ORI2023	ubc4	mei3	719835	69.2	22	23	78	114
ORI2024	c119.18	rti1	746380	75.2	62	20	76	115

ORI2025	c119.15	c577.04	753427	72.2	32	19	76	117
ORI2026	c530.11c	c530.13	821603	75.4	65	16	73	114
ORI2027	c36.02c	c36.04	844438	78	37	18	76	114
ORI2028	rad3	tor2	916120	77	15	17	81	121
ORI2029	c646.07c	c646.10c	939885	74	11	13	79	121
ORI2030	orc5	p35g2.01c	957659	77.4	16	6	78	120
ORI2031	c146.08c	c146.12	1020611	74	14	7	80	120
ORI2032	ubi4	c337.10c	1049111	68.6	16	7	80	120
ORI2033	c337.12	c337.19	1060371	73.2	26	11	80	118
ORI2034	c1709.04c	c1709.20	1109650	76.2	27	30	76	114
ORI2035	mis12	wis1: spc2	1142614	77.2	41	24	73	105
ORI2036	c409.09c	meu18	1158217	75.4	29	22	73	111
ORI2037	c409.16c	c409.18	1170877	73.2	21	8	78	117
ORI2038	c651.01c	c651.04	1241936	72.6	32	17	76	111
ORI2039	c651.07	c651.10	1255476	75.8	17	19	75	112
ORI2040	c651.12c	c3d6.01	1265693	83.8	53		75	104
ORI2041	c3d6.01	rps25-1	1272086	71.2	32	27	75	104
ORI2042	c3d6.04c	c3d6.07	1280407	78.6	58	23	74	111
ORI2043	c30b4.03c	c30b4.04c	1309527	75	37	17	77	113
ORI2044	c30b4.04c	c30b4.07c	1316300	75	29	28	76	109
ORI2045	c8d2.16c	c8d2.18c	1390459	75.2	41	24	77	114
ORI2046	apl3:pi033	pi030	1430119	74.4	16	8	77	115
ORI2047	pi026	prp5: cwf1: pi024	1444990	77.6	28	22	75	113
ORI2048	pi019	git5	1462321	75.8	41	35	76	112
ORI2049	c83.11	c83.12	1531979	71.6	20	18	76	115
ORI2050	c83.18c	atf1: mts1: sss1: gad7.b	1546892	75.6	51	59	72	111
ORI2051	c28f2.11	c21b10.13c	1591200	73.6	13	25	80	106
ORI2052	centromere	c21b10.13c	1649764	79.2	20	23	76	115
ORI2053	c21b10.09	c21b10.07	1657459	73	32	18	78	113
ORI2054	c21b10.06c	nrf1	1665029	74	17	14	78	114

ORI2055	c19c2.10	c2f12.15c	1703662	74.6	41	28	74	114
ORI2056	klp5	rep2	1716509	72.6	17	12	74	113
ORI2057	c11g11.05	c18h10.01	1767813	73.4	27	10	76	114
ORI2058	sce3	c18h10.05	1780518	74.4	26	43	76	113
ORI2059	c18h10.17c	c18h10.20c	1808035	74.8	20	11	77	115
ORI2060	c3h7.09	c3h7.07c	1870662	76.4	9	1	82	121
ORI2061	c16e9.11c	c16e9.13	1941513	75.8	42	20	75	114
ORI2062	c16e9.16c	c1e8.01	1954646	73.8	28	25	79	111
ORI2063	c1e8.03c	c1e8.05	1967649	73.4	18	12	76	114
ORI2064	p23a10.11c	p23a10.14c	2028284	80.8	30	19	75	110
ORI2065	p23a10.14c	p23a10.16	2036477	75.2	34	4	75	114
ORI2066	c29a3.05	c29a3.09c	2054052	76.2	30	27	77	115
ORI2067	c29a3.16	c29a3.17	2071513	77.4	10	5	79	116
ORI2068	matmc: c23g7.09	c23g7.10c	2117792	79.4	25	14	81	108
ORI2069	rpp2-2	matmi: c1711.01	2132132	77.4	22	19	75	113
ORI2070	matmi: c1711.01	c1711.03	2138165	75.2	18	24	76	114
ORI2071	c1711.10c	c1711.15c	2160529	73.2	25	1	77	116
ORI2072	c17g9.04c	c17g9.06c	2179483	71.8	27	16	76	116
ORI2073	rps24-2	pyr1	2188311	74.2	30	14	79	115
ORI2074	cut2	c14c8.03	2207960	72.2	25	2	79	118
ORI2075	c15c4.03	c21h7.02	2250479	74.8	18		77	117
ORI2076	c12d12.05c	ubl1	2318450	79	32	14	76	117
ORI2077	ubl1	c24c6.02	2322258	71	32	22	75	116
ORI2078	c19g7.10c	c19g7.15	2375361	71	14	N.A.	81	N.A.
ORI2079	c21d10.09c	c21d10.07	2433487	73.4	22	6	76	117
ORI2080	c21d10.05c	c12c2.11	2448059	77.8	21	5	78	114
ORI2081	hba1: caf1	alp4	2525756	74.6	37	5	78	117
ORI2082	c29a10.07	c29a10.09c	2555034	81	27	1	78	119
ORI2083	cad1: hmt2	c25b2.01	2594005	78.4	29	4	76	122
ORI2084	c25b2.01	c25b2.03	2602416	67.2	25	6	76	121

ORI2085	c25b2.10	c6b1.04	2627249	75.6	6	1	80	123
ORI2086	c3e7.05c	c3e7.09	2674878	73.2	10	6	78	122
ORI2087	c4f6.07c	c4f6.09	2702668	75	29	7	76	119
ORI2088	c18a7.02c	dim1: c336.02	2737244	75.6	34	8	75	117
ORI2089	c336.14c	c685.05	2775733	72.8	5	16	78	117
ORI2090	rec14	gpx1	2790075	72.8	30	11	75	115
ORI2091	gpx1	pch1	2794668	80.2	44	22	75	115
ORI2092	pch1	rum1	2799811	74.4	47	24	77	111
ORI2093	rps23-2	p4h10.17c	2904150	83.6	14	5	80	117
ORI2094	c1703.12	top1	2943267	77	28	7	77	119
ORI2095	fib	rhp23	2987796	74.8	21		78	120
ORI2096	c13e7.04	c13e7.07	3053100	77	30	7	78	120
ORI2097	c30d10.15	tor1	3071838	72.8	10	7	78	122
ORI2098	c30d10.02	c1778.02	3099581	79	17	7	79	120
ORI2099	sep1	c4c3.03	3139049	74.2	13	12	78	122
ORI2100	rpl29	sec23b	3178150	79.2	37	14	77	120
ORI2101	c21.07c	c19f8.05	3235165	78.4	17	8	78	119
ORI2102	c20f10.02c	c20f10.04c	3289316	77.2	23	4	75	118
ORI2103	c17d1.02	c17d1.06	3336269	76.4	22	11	77	121
ORI2104	c11c11.12	c3b8.13c	3365078	75.6	34	8	78	121
ORI2105	c4b4.02c	smg1	3419511	80	14	18	77	120
ORI2106	smg1	ght2	3425794	80	41	7	75	120
ORI2107	c2g2.14	pop1	3466351	73	21	6	79	119
ORI2108	chr2.1451.2	chr2.1451.5	3493494	75.2	21	6	79	117
ORI2109	abp1	exg1	3515615	75	19	4	76	119
ORI2110	c887.08	c887.11	3557798	76.2	3	8	79	121
ORI2111	c16d10.03	c16d10.06	3604074	75.2	10	16	80	121
ORI2112	c317.01	p8b7.02	3636659	79.6	40	16	74	118
ORI2113	p8b7.14c	dbp2	3662010	75.2	23	1	78	120
ORI2114	p8b7.21	p8b7.24c	3684548	76.2	19	6	78	122

ORI2115	mcm7	c25d12.06	3723346	76	16	5	77	122
ORI2116	ykt6	c31f10.03	3755812	72.4	17	14	77	118
ORI2117	sar1	c31f10.08	3765712	77.2	34	8	75	119
ORI2118	c21c3.02c	c21c3.04c	3805136	74.6	16	12	75	118
ORI2119	c21c3.10c	rps19-1	3818601	73.8	31	17	76	115
ORI2120	c21c3.16c	c21c3.19	3828136	73.4	16	8	77	117
ORI2121	c23e6.01c	c23e6.03c	3841588	74.8	24	17	76	119
ORI2122	c1604.19c	c1604.15	3901442	76.8	5	11	80	121
ORI2123	c1604.10	c1604.07	3918898	77.2	32	10	78	118
ORI2124	c1677.02	thi2: nmt2	3940396	77.4	35	19	77	120
ORI2125	c3b9.16c	c3b9.19	4021258	77.8	23	12	75	119
ORI2126	c215.02	gpd1	4032048	74.6	27	6	78	119
ORI2127	c1861.04c	c1861.08c	4145557	75.2	25	8	77	119
ORI2128	c14f5.07	c3f6.01c	4179176	74.4	10	12	83	119
ORI2129	c3f6.05	c342.02	4202081	75.6	16	2	78	120
ORI2130	c16g5.07c	c16g5.10	4228981	74.2	8	5	81	121
ORI2131	top3	rps3	4238357	75.6	26	2	81	121
ORI2132	c16a3.04	c16a3.02c	4296568	77.8	0	5	80	122
ORI2133	c244.02c	c1539.01c	4362959	75.6	18	8	79	123
ORI2134	c1539.04	c1539.07c	4373377	73.8	12	16	78	123
ORI2135	c1289.13c	c8e4.07c	4416477	74.6	1	5	79	124
ORI2136	c8e4.06	c8e4.02c	4438381	77.8	0	5	80	123
ORI2137	pho1	pb2b2.01	4454665	76.8	0	17	79	125
ORI2138	pb2b2.03c	pb2b2.08	4470382	76	2	18	79	124

Chromosome 3

ORI Number	5' ORF/Gene	3' ORF/Gene	Map Position (central)	AT-content (500bp)	Efficiency Mitosis	Efficiency Meiosis	Replication Time Mitosis (mins)	Replication Time Meiosis (mins)
ORI3001	c1884.01	meu3	37347	74.8	37	39	71	115
ORI3002	c757.03c	cta1	54097	70	26	22	72	113
ORI3003	c757.09c	c757.12	69049	72.2	26	13	76	111
ORI3004	c757.11c	c757.13	75798	76.6	45	23	75	102
ORI3005	c330.02	c330.03c	108693	73.4	25	14	72	113
ORI3006	pmp20	c330.07c	119903	78.2	64	27	72	106
ORI3007	c330.07c	alg11: gmd3	123154	78.6	50	31	73	113
ORI3008	c1235.05c	c1235.07	190170	73.4	29	22	74	112
ORI3009	c1235.12c	ght5	207534	82.6	52	27	71	110
ORI3010	c548.06c	c794.01c	231433	78.6	31	18	74	109
ORI3011	wtf4	c794.04c	246552	75.8	14	17	72	113
ORI3012	c794.04c	c794.14	253494	75.2	13	14	76	114
ORI3013	c794.15	c553.11c	280769	68.6	18	16	74	114
ORI3014	c553.10	c553.08c	287037	76.6	46	16	73	112
ORI3015	c553.02	c736.05	314546	75.2	14	7	75	115
ORI3016	c736.09c	c736.11	331518	73.4	33	14	76	116
ORI3017	c594.07c	c1682.01	369948	77.4	43	27	73	113
ORI3018	C1682.12c	rpl19-2	398033	76	49	13	74	114
ORI3019	aph1	c364.06	472234	77.6	34	4	77	114
ORI3020	C970.06	mob2	506572	75.2	25	23	76	113
ORI3021	rad16: rad10: rad20: swi9	prp11	519272	74.6	62	28	73	110
ORI3022	P31B10.02	P31B10.05	532057	73.4	18	8	73	116
ORI3023	c962.05	c1672.01	558383	70.8	7	36	75	114
ORI3024	sap1	C1672.05c	566770	77.6	48	31	74	104

ORI3025	C1672.05c	tfa2	574432	74.8	52	31	74	108
ORI3026	ung1	c1183.07	607185	74.4	35	8	74	115
ORI3027	c1183.09c	wtf7	615662	70.6	5	11	74	115
ORI3028	c31h12.06	c5e4.05c	641699	78.6	38	24	76	109
ORI3029	C16C4.03	C16C4.05	667789	76.2	22	12	76	115
ORI3030	bfr1: hba2	wee1	720250	75.6	47	22	76	112
ORI3031	c1020.10	C1020.08	765301	78.4	30	27	76	113
ORI3032	ctr4	c1393.11	820551	75	53	23	73	112
ORI3033	c63.08c	prp28	854530	76.8	64	39	72	112
ORI3034	cdc21: mcm4	C24B10.05	906049	73.6	23	N.A.	77	N.A.
ORI3035	c24b10.18	c24b10.20	935300	75.4	52	20	74	112
ORI3036	c1795.13	sum3: ded1: slh3: moc2	970246	78.8	45	22	75	112
ORI3037	C1795.08c	map2	986920	74.6	49	N.A.	76	N.A.
ORI3038	c1259.02c	c1259.06	1040367	74.2	2	5	79	117
ORI3039	c1259.12c	chk1: rad27	1058659	71.8	4	12	76	114
ORI3040	chk1: rad27	meu27: b8647-6	1061951	67.6	26	22	79	111
ORI3041	meu27: b8647-6	centromere	1065271	73.4	26		79	111
ORI3042	centromere	C4B3.17	1144065	73	23	23	77	107
ORI3043	c550.04c	c550.05	1194523	73.6	40	25	75	116
ORI3044	c645.08c	c645.10	1253167	76.2	56	20	74	115
ORI3045	C1322.14c	C132.01c	1323040	76	52	20	70	114
ORI3046	C338.19	pof3	1343448	74.6	55	27	73	113
ORI3047	mms2	ags1: mok1	1371089	76.4	48	19	71	109
ORI3048	c1281.06c	wtf11	1398984	73.8	43		73	113
ORI3049	C622.04	hta1	1410248	78.6	57	51	69	112
ORI3050	c622.10c	C622.12c	1418087	77.8	53	43	72	112
ORI3051	C61.03	C11E10.01	1449183	76.4	46	22	72	112
ORI3052	c584.10c	c584.12	1512633	76.2	28	20	74	114
ORI3053	C584.01c	C584.03c	1532669	76.8	45	24	71	113
ORI3054	C1753.05	C162.10	1556939	73	43	7	75	115

ORI3055	C162.07	c162.05	1577814	74.4	42	23	74	113
ORI3056	adh1: adh	C777.01c	1595330	80.8	53	29	72	110
ORI3057	gtr2	C777.08c	1609474	78.8	52	24	70	112
ORI3058	c663.10	c663.16c	1658253	72.8	24	8	79	116
ORI3059	C417.06c	C417.08	1685737	76.2	49	36	74	111
ORI3060	C417.08	C417.09c	1691448	78.4	49	23	73	113
ORI3061	cyc1	inv1	1721086	77.6	76	31	73	108
ORI3062	inv1	C191.13	1727074	76.6	49	20	73	109
ORI3063	C1450.10c	C1450.12	1753652	74	48	27	75	109
ORI3064	ret2	c285.14	1818815	75.6	42	19	72	113
ORI3065	gut2	c1223.04c	1843891	77.4	52	23	76	113
ORI3066	C1223.10c	C1223.13	1868681	74.8	27		74	113
ORI3067	ssp1: c297.03	c737.02c	1885003	71.6	9	7	77	116
ORI3068	c74.02c	c74.04	1931752	74.8	46	20	75	113
ORI3069	c18.06c	rpc53	1968761	73.8	38	19	72	114
ORI3070	c18.09c	C18.10	1975681	73.8	21	18	72	115
ORI3071	wtf6	c1739.01	2023101	70.2	23	6	72	115
ORI3072	c1739.04c	c1739.05	2035798	75.8	48	28	69	112
ORI3073	wtf3	pb1c11.01	2068592	76	25	6	76	108
ORI3074	rps20	c576.17c	2105031	77	28	22	78	113
ORI3075	c576.17c	pku70	2116626	74.6	32	11	73	114
ORI3076	C126.12	C126.13c	2140697	72.4	24	22	77	116
ORI3077	C830.08c	C830.11c	2201606	77	54	30	69	113
ORI3078	c1919.05	c1919.07	2219921	71.2	11	10	73	116
ORI3079	C1840.08c	lsm8	2277636	78.2	32	2	72	118
ORI3080	c965.06	c965.10	2299922	74.2	23	10	73	120
ORI3081	C1494.05c	c1494.07	2339523	73.4	24	6	74	121
ORI3082	c70.05c	tmp1: tmp	2364264	74.8	27	12	74	117
ORI3083	c1827.02c	c1827.05c	2382536	79.6	49	20	71	114
ORI3084	c569.05c	c569.02c	2427531	75.8	24	27	74	116

ORI3085	c569.02c	c569.01c	2434890	72.4	39	22	74	117

Bibliography

Abdurashidova, G., Danailov, M. B., Ochem, A., Triolo, G., Djeliova, V., Radulescu, S., Vindigni, A., Riva, S., and Falaschi, A. (2003). Localization of proteins bound to a replication origin of human DNA along the cell cycle. Embo J *22*, 4294-4303.

Adachi, Y., Usukura, J., and Yanagida, M. (1997). A globular complex formation by Nda1 and the other five members of the MCM protein family in fission yeast. Genes Cells *2*, 467-479.

Aggarwal, B. D., and Calvi, B. R. (2004). Chromatin regulates origin activity in Drosophila follicle cells. Nature *430*, 372-376.

Aladjem, M. I. (2004). The mammalian beta globin origin of DNA replication. Front Biosci *9*, 2540-2547.

Aladjem, M. I., and Fanning, E. (2004). The replicon revisited: an old model learns new tricks in metazoan chromosomes. EMBO Rep *5*, 686-691.

Aladjem, M. I., Rodewald, L. W., Kolman, J. L., and Wahl, G. M. (1998). Genetic dissection of a mammalian replicator in the human beta-globin locus. Science *281*, 1005-1009.

Alexandrow, M. G., and Hamlin, J. L. (2004). Cdc6 chromatin affinity is unaffected by serine-54 phosphorylation, S-phase progression, and overexpression of cyclin A. Mol Cell Biol *24*, 1614-1627.

Alter, O., and Golub, G. H. (2004). Integrative analysis of genome-scale data by using pseudoinverse projection predicts novel correlation between DNA replication and RNA transcription. Proc Natl Acad Sci U S A *101*, 16577-16582.

Altman, A. L., and Fanning, E. (2004). Defined sequence modules and an architectural element cooperate to promote initiation at an ectopic mammalian chromosomal replication origin. Mol Cell Biol *24*, 4138-4150.

Anachkova, B., and Hamlin, J. L. (1989). Replication in the amplified dihydrofolate reductase domain in CHO cells may initiate at two distinct sites, one of which is a repetitive sequence element. Mol Cell Biol *9*, 532-540.

Anglana, M., Apiou, F., Bensimon, A., and Debatisse, M. (2003). Dynamics of DNA replication in mammalian somatic cells: nucleotide pool modulates origin choice and interorigin spacing. Cell *114*, 385-394.

Antequera, F. (2003). Structure, function and evolution of CpG island promoters. Cell Mol Life Sci *60*, 1647-1658.

Antequera, F. (2004). Genomic specification and epigenetic regulation of eukaryotic DNA replication origins. Embo J *23*, 4365-4370.

Antequera, F., and Bird, A. (1999). CpG islands as genomic footprints of promoters that are associated with replication origins. Curr Biol *9*, R661-667.

Antunes, D. F., Kim, S. M., Huberman, J. A., and de Morais, M. A., Jr. (2003). Motifs in Schizosaccharomyces pombe ars3002 important for replication origin activity in Saccharomyces cerevisiae. Plasmid *50*, 113-119.

Aparicio, O. M., Stout, A. M., and Bell, S. P. (1999). Differential assembly of Cdc45p and DNA polymerases at early and late origins of DNA replication. Proc Natl Acad Sci U S A *96*, 9130-9135.

Aparicio, O. M., Weinstein, D. M., and Bell, S. P. (1997). Components and dynamics of DNA replication complexes in S. cerevisiae: redistribution of MCM proteins and Cdc45p during S phase. Cell *91*, 59-69.

Araki, H., Leem, S. H., Phongdara, A., and Sugino, A. (1995). Dpb11, which interacts with DNA polymerase II(epsilon) in Saccharomyces cerevisiae, has a dual role in S-phase progression and at a cell cycle checkpoint. Proc Natl Acad Sci U S A *92*, 11791-11795.

Araki, M., Wharton, R. P., Tang, Z., Yu, H., and Asano, M. (2003). Degradation of origin recognition complex large subunit by the anaphase-promoting complex in Drosophila. Embo J *22*, 6115-6126.

Arias, E. E., and Walter, J. C. (2005). Replication-dependent destruction of Cdt1 limits DNA replication to a single round per cell cycle in Xenopus egg extracts. Genes Dev *19*, 114-126.

Asano, M., and Wharton, R. P. (1999). E2F mediates developmental and cell cycle regulation of ORC1 in Drosophila. Embo J *18*, 2435-2448.

Austin, R. J., Orr-Weaver, T. L., and Bell, S. P. (1999). Drosophila ORC specifically binds to ACE3, an origin of DNA replication control element. Genes Dev *13*, 2639-2649.

Aves, S. J., Tongue, N., Foster, A. J., and Hart, E. A. (1998). The essential schizosaccharomyces pombe cdc23 DNA replication gene shares structural and functional homology with the Saccharomyces cerevisiae DNA43 (MCM10) gene. Curr Genet *34*, 164-171.

Baber-Furnari, B. A., Rhind, N., Boddy, M. N., Shanahan, P., Lopez-Girona, A., and Russell, P. (2000). Regulation of mitotic inhibitor Mik1 helps to enforce the DNA damage checkpoint. Mol Biol Cell *11*, 1-11.

Bartek, J., Lukas, C., and Lukas, J. (2004). Checking on DNA damage in S phase. Nat Rev Mol Cell Biol *5*, 792-804.

Baum, B., Nishitani, H., Yanow, S., and Nurse, P. (1998). Cdc18 transcription and proteolysis couple S phase to passage through mitosis. Embo J *17*, 5689-5698.

Baumeister, W., Walz, J., Zuhl, F., and Seemuller, E. (1998). The proteasome: paradigm of a self-compartmentalizing protease. Cell *92*, 367-380.

Beach, D., Durkacz, B., and Nurse, P. (1982). Functionally homologous cell cycle control genes in budding and fission yeast. Nature *300*, 706-709.

Beall, E. L., Bell, M., Georlette, D., and Botchan, M. R. (2004). Dm-myb mutant lethality in Drosophila is dependent upon mip130: positive and negative regulation of DNA replication. Genes Dev *18*, 1667-1680.

Beall, E. L., Manak, J. R., Zhou, S., Bell, M., Lipsick, J. S., and Botchan, M. R. (2002). Role for a Drosophila Myb-containing protein complex in site-specific DNA replication. Nature *420*, 833-837.

Bell, S. P., and Dutta, A. (2002). DNA replication in eukaryotic cells. Annu Rev Biochem *71*, 333-374.

Bell, S. P., and Stillman, B. (1992). ATP-dependent recognition of eukaryotic origins of DNA replication by a multiprotein complex. Nature *357*, 128-134.

Benito, J., Martin-Castellanos, C., and Moreno, S. (1998). Regulation of the G1 phase of the cell cycle by periodic stabilization and degradation of the p25rum1 CDK inhibitor. Embo J *17*, 482-497.

Biamonti, G., Paixao, S., Montecucco, A., Peverali, F. A., Riva, S., and Falaschi, A. (2003). Is DNA sequence sufficient to specify DNA replication origins in metazoan cells? Chromosome Res *11*, 403-412.

Bielinsky, A. K., and Gerbi, S. A. (2001). Where it all starts: eukaryotic origins of DNA replication. J Cell Sci *114*, 643-651.

Biermann, E., Baack, M., Kreitz, S., and Knippers, R. (2002). Synthesis and turn-over of the replicative Cdc6 protein during the HeLa cell cycle. Eur J Biochem *269*, 1040-1046.

Biswas-Fiss, E. E., Khopde, S. M., and Biswas, S. B. (2005). The Mcm467 complex of Saccharomyces cerevisiae is preferentially activated by autonomously replicating DNA sequences. Biochemistry *44*, 2916-2925.

Blow, J. J., and Dutta, A. (2005). Preventing re-replication of chromosomal DNA. Nat Rev Mol Cell Biol *6*, 476-486.

Blow, J. J., Gillespie, P. J., Francis, D., and Jackson, D. A. (2001). Replication origins in Xenopus egg extract Are 5-15 kilobases apart and are activated in clusters that fire at different times. J Cell Biol *152*, 15-25.

Blumenthal, A. B., Kriegstein, H. J., and Hogness, D. S. (1974). The units of DNA replication in Drosophila melanogaster chromosomes. Cold Spring Harb Symp Quant Biol *38*, 205-223.

Boddy, M. N., Furnari, B., Mondesert, O., and Russell, P. (1998). Replication checkpoint enforced by kinases Cds1 and Chk1. Science *280*, 909-912.

Bonatti, S., Simili, M., and Abbondandolo, A. (1972). Isolation of temperature-sensitive mutants of Schizosaccharomyces pombe. J Bacteriol *109*, 484-491.

Borde, V., Goldman, A. S., and Lichten, M. (2000). Direct coupling between meiotic DNA replication and recombination initiation. SciBorde, V

Goldman, A S

Lichten, Mence *290*, 806-809.

Bosl, W. J., and Li, R. (2005). Mitotic-exit control as an evolved complex system. Cell *121*, 325-333.

Brewer, B. J., and Fangman, W. L. (1991). Mapping replication origins in yeast chromosomes. Bioessays *13*, 317-322.

Broach, J. R., Li, Y. Y., Feldman, J., Jayaram, M., Abraham, J., Nasmyth, K. A., and Hicks, J. B. (1983). Localization and sequence analysis of yeast origins of DNA replication. Cold Spring Harb Symp Quant Biol *47 Pt 2*, 1165-1173.

Broek, D., Bartlett, R., Crawford, K., and Nurse, P. (1991). Involvement of p34cdc2 in establishing the dependency of S phase on mitosis. Nature *349*, 388-393.

Brondello, J. M., Boddy, M. N., Furnari, B., and Russell, P. (1999). Basis for the checkpoint signal specificity that regulates Chk1 and Cds1 protein kinases. Mol Cell Biol *19*, 4262-4269.

Brown, G. W., Jallepalli, P. V., Huneycutt, B. J., and Kelly, T. J. (1997). Interaction of the S phase regulator cdc18 with cyclin-dependent kinase in fission yeast. Proc Natl Acad Sci U S A *94*, 6142-6147.

Brown, G. W., and Kelly, T. J. (1998). Purification of Hsk1, a minichromosome maintenance protein kinase from fission yeast. J Biol Chem *273*, 22083-22090.

Caddle, M. S., and Calos, M. P. (1994). Specific initiation at an origin of replication from Schizosaccharomyces pombe. Mol Cell Biol *14*, 1796-1805.

Castro, A., Bernis, C., Vigneron, S., Labbe, J. C., and Lorca, T. (2005). The anaphase-promoting complex: a key factor in the regulation of cell cycle. Oncogene *24*, 314-325.

Celniker, S. E., Sweder, K., Srienc, F., Bailey, J. E., and Campbell, J. L. (1984). Deletion mutations affecting autonomously replicating sequence ARS1 of Saccharomyces cerevisiae. Mol Cell Biol *4*, 2455-2466.

Cervantes, M. D., Farah, J. A., and Smith, G. R. (2000). Meiotic DNA breaks associated with recombination in S. pombe. Mol Cell *5*, 883-888.

Chakraborty, T., Yoshinaga, K., Lother, H., and Messer, W. (1982). Purification of the E. coli dnaA gene product. Embo J *1*, 1545-1549.

Chen, Y., and Sanchez, Y. (2004). Chk1 in the DNA damage response: conserved roles from yeasts to mammals. DNA Repair (Amst) *3*, 1025-1032.

Chuang, R. Y., Chretien, L., Dai, J., and Kelly, T. J. (2002). Purification and characterization of the Schizosaccharomyces pombe origin recognition complex: interaction with origin DNA and Cdc18 protein. J Biol Chem *277*, 16920-16927.

Chuang, R. Y., and Kelly, T. J. (1999). The fission yeast homologue of Orc4p binds to replication origin DNA via multiple AT-hooks. Proc Natl Acad Sci U S A *96*, 2656-2661.

Claycomb, J. M., Benasutti, M., Bosco, G., Fenger, D. D., and Orr-Weaver, T. L. (2004). Gene amplification as a developmental strategy: isolation of two developmental amplicons in Drosophila. Dev Cell *6*, 145-155.

Claycomb, J. M., and Orr-Weaver, T. L. (2005). Developmental gene amplification: insights into DNA replication and gene expression. Trends Genet *21*, 149-162.

Clyne, R. K., and Kelly, T. J. (1995). Genetic analysis of an ARS element from the fission yeast Schizosaccharomyces pombe. Embo J *14*, 6348-6357.

Clyne, R. K., and Kelly, T. J. (1997). Identification of autonomously replicating sequence (ARS) elements in eukaryotic cells. Methods *13*, 221-233.

Cobb, J. A., Shimada, K., and Gasser, S. M. (2004). Redundancy, insult-specific sensors and thresholds: unlocking the S-phase checkpoint response. Curr Opin Genet Dev *14*, 292-300.

Collins, I., and Newlon, C. S. (1994). Chromosomal DNA replication initiates at the same origins in meiosis and mitosis. Mol Cell Biol *14*, 3524-3534.

Cook, J. G., Chasse, D. A., and Nevins, J. R. (2004). The regulated association of Cdt1 with minichromosome maintenance proteins and Cdc6 in mammalian cells. J Biol Chem *279*, 9625-9633.

Correa-Bordes, J., Gulli, M. P., and Nurse, P. (1997). p25rum1 promotes proteolysis of the mitotic B-cyclin p56cdc13 during G1 of the fission yeast cell cycle. Embo J *16*, 4657-4664.

Correa-Bordes, J., and Nurse, P. (1995). p25rum1 orders S phase and mitosis by acting as an inhibitor of the p34cdc2 mitotic kinase. Cell *83*, 1001-1009.

Coue, M., Kearsey, S. E., and Mechali, M. (1996). Chromotin binding, nuclear localization and phosphorylation of Xenopus cdc21 are cell-cycle dependent and associated with the control of initiation of DNA replication. Embo J *15*, 1085-1097.

Coux, O., Tanaka, K., and Goldberg, A. L. (1996). Structure and functions of the 20S and 26S proteasomes. Annu Rev Biochem *65*, 801-847.

Coverley, D., Laman, H., and Laskey, R. A. (2002). Distinct roles for cyclins E and A during DNA replication complex assembly and activation. Nat Cell Biol *4*, 523-528.

Coverley, D., Pelizon, C., Trewick, S., and Laskey, R. A. (2000). Chromatin-bound Cdc6 persists in S and G2 phases in human cells, while soluble Cdc6 is destroyed in a cyclin A-cdk2 dependent process. J Cell Sci *113 (Pt 11)*, 1929-1938.

Cvetic, C., and Walter, J. C. (2005). Eukaryotic origins of DNA replication: could you please be more specific? Semin Cell Dev Biol *16*, 343-353.

Dai, J., Chuang, R. Y., and Kelly, T. J. (2005). DNA replication origins in the Schizosaccharomyces pombe genome. Proc Natl Acad Sci U S A *102*, 337-342.

Del Bene, F., Tessmar-Raible, K., and Wittbrodt, J. (2004). Direct interaction of geminin and Six3 in eye development. Nature *427*, 745-749.

Delgado, S., Gomez, M., Bird, A., and Antequera, F. (1998). Initiation of DNA replication at CpG islands in mammalian chromosomes. Embo J *17*, 2426-2435.

Delidakis, C., and Kafatos, F. C. (1989). Amplification enhancers and replication origins in the autosomal chorion gene cluster of Drosophila. Embo J *8*, 891-901.

Delmolino, L. M., Saha, P., and Dutta, A. (2001). Multiple mechanisms regulate subcellular localization of human CDC6. J Biol Chem *276*, 26947-26954.

DePamphilis, M. L. (1993). Origins of DNA replication in metazoan chromosomes. J Biol Chem *268*, 1-4.

DePamphilis, M. L. (1999). Replication origins in metazoan chromosomes: fact or fiction? Bioessays *21*, 5-16.

DePamphilis, M. L. (2003). Eukaryotic DNA replication origins: reconciling disparate data. Cell *114*, 274-275.

DePamphilis, M. L. (2003). The 'ORC cycle': a novel pathway for regulating eukaryotic DNA replication. Gene *310*, 1-15.

DePamphilis, M. L. (2005). Cell cycle dependent regulation of the origin recognition complex. Cell Cycle *4*, 70-79.

Diffley, J. F. (2004). Regulation of early events in chromosome replication. Curr Biol *14*, R778-786.

Diffley, J. F., and Cocker, J. H. (1992). Protein-DNA interactions at a yeast replication origin. Nature *357*, 169-172.

Diffley, J. F., Cocker, J. H., Dowell, S. J., Harwood, J., and Rowley, A. (1995). Stepwise assembly of initiation complexes at budding yeast replication origins during the cell cycle. J Cell Sci Suppl *19*, 67-72.

Diffley, J. F., Cocker, J. H., Dowell, S. J., and Rowley, A. (1994). Two steps in the assembly of complexes at yeast replication origins in vivo. Cell *78*, 303-316.

Diffley, J. F., and Stillman, B. (1989). Similarity between the transcriptional silencer binding proteins ABF1 and RAP1. Science *246*, 1034-1038.

Dijkwel, P. A., and Hamlin, J. L. (1995). The Chinese hamster dihydrofolate reductase origin consists of multiple potential nascent-strand start sites. Mol Cell Biol *15*, 3023-3031.

Dijkwel, P. A., Vaughn, J. P., and Hamlin, J. L. (1994). Replication initiation sites are distributed widely in the amplified CHO dihydrofolate reductase domain. Nucleic Acids Res *22*, 4989-4996.

Dijkwel, P. A., Wang, S., and Hamlin, J. L. (2002). Initiation sites are distributed at frequent intervals in the Chinese hamster dihydrofolate reductase origin of replication but are used with very different efficiencies. Mol Cell Biol *22*, 3053-3065.

Dimitrova, D. S., and Gilbert, D. M. (1999). The spatial position and replication timing of chromosomal domains are both established in early G1 phase. Mol Cell *4*, 983-993.

Donaldson, A. D. (2005). Shaping time: chromatin structure and the DNA replication programme. Trends Genet *21*, 444-449.

Donovan, S., Harwood, J., Drury, L. S., and Diffley, J. F. (1997). Cdc6p-dependent loading of Mcm proteins onto pre-replicative chromatin in budding yeast. Proc Natl Acad Sci U S A *94*, 5611-5616.

Doree, M., and Hunt, T. (2002). From Cdc2 to Cdk1: when did the cell cycle kinase join its cyclin partner? J Cell Sci *115*, 2461-2464.

Drury, L. S., Perkins, G., and Diffley, J. F. (1997). The Cdc4/34/53 pathway targets Cdc6p for proteolysis in budding yeast. Embo J *16*, 5966-5976.

Drury, L. S., Perkins, G., and Diffley, J. F. (2000). The cyclin-dependent kinase Cdc28p regulates distinct modes of Cdc6p proteolysis during the budding yeast cell cycle. Curr Biol *10*, 231-240.

Dubey, D. D., Kim, S. M., Todorov, I. T., and Huberman, J. A. (1996). Large, complex modular structure of a fission yeast DNA replication origin. Curr Biol *6*, 467-473.

Dubey, D. D., Zhu, J., Carlson, D. L., Sharma, K., and Huberman, J. A. (1994). Three ARS elements contribute to the ura4 replication origin region in the fission yeast, Schizosaccharomyces pombe. Embo J *13*, 3638-3647.

Dunphy, W. G., Brizuela, L., Beach, D., and Newport, J. (1988). The Xenopus cdc2 protein is a component of MPF, a cytoplasmic regulator of mitosis. Cell *54*, 423-431.

Dutta, A., and Bell, S. P. (1997). Initiation of DNA replication in eukaryotic cells. Annu Rev Cell Dev Biol *13*, 293-332.

Edgar, B. A., and Orr-Weaver, T. L. (2001). Endoreplication cell cycles: more for less. Cell *105*, 297-306.

Elsasser, S., Chi, Y., Yang, P., and Campbell, J. L. (1999). Phosphorylation controls timing of Cdc6p destruction: A biochemical analysis. Mol Biol Cell *10*, 3263-3277.

Esposito, R. E., and Klapholz, S. (1981). Meiosis and Scospore Development (Strathern, J.N., Jones, E.W. and Broach, J.R., eds.). Cold Spring Harbor Laboratory, Cold Spring Harbor, New York, 211 - 287.

Fantes, P. (1979). Epistatic gene interactions in the control of division in fission yeast. Nature *279*, 428-430.

Featherstone, C., and Russell, P. (1991). Fission yeast p107wee1 mitotic inhibitor is a tyrosine/serine kinase. Nature *349*, 808-811.

Feng, H., and Kipreos, E. T. (2003). Preventing DNA re-replication--divergent safeguards in yeast and metazoa. Cell Cycle *2*, 431-434.

Feng, L., Hu, Y., Wang, B., Wu, L., and Jong, A. (2000). Loss control of Mcm5 interaction with chromatin in cdc6-1 mutated in CDC-NTP motif. DNA Cell Biol *19*, 447-457.

Fiegler, H., Carr, P., Douglas, E. J., Burford, D. C., Hunt, S., Scott, C. E., Smith, J., Vetrie, D., Gorman, P., Tomlinson, I. P., and Carter, N. P. (2003). DNA microarrays for comparative genomic hybridization based on DOP-PCR amplification of BAC and PAC clones. Genes Chromosomes Cancer *36*, 361-374.

Fisher, D., and Nurse, P. (1995). Cyclins of the fission yeast Schizosaccharomyces pombe. Semin Cell Biol *6*, 73-78.

Fisher, D. L., and Nurse, P. (1996). A single fission yeast mitotic cyclin B p34cdc2 kinase promotes both S-phase and mitosis in the absence of G1 cyclins. Embo J *15*, 850-860.

Forsburg, S. L. (2004). Eukaryotic MCM proteins: beyond replication initiation. Microbiol Mol Biol Rev *68*, 109-131, table of contents.

Forsburg, S. L., and Nurse, P. (1991). Cell cycle regulation in the yeasts Saccharomyces cerevisiae and Schizosaccharomyces pombe. Annu Rev Cell Biol *7*, 227-256.

Fox, M. E., and Smith, G. R. (1998). Control of meiotic recombination in Schizosaccharomyces pombe. Prog Nucleic Acid Res Mol Biol *61*, 345-378.

Friedman, K. L., Brewer, B. J., and Fangman, W. L. (1997). Replication profile of Saccharomyces cerevisiae chromosome VI. Genes Cells *2*, 667-678.

Friedman, K. L., Diller, J. D., Ferguson, B. M., Nyland, S. V., Brewer, B. J., and Fangman, W. L. (1996). Multiple determinants controlling activation of yeast replication origins late in S phase. Genes Dev *10*, 1595-1607.

Fujita, M., Kiyono, T., Hayashi, Y., and Ishibashi, M. (1996). hCDC47, a human member of the MCM family. Dissociation of the nucleus-bound form during S phase. J Biol Chem *271*, 4349-4354.

Fujita, M., Yamada, C., Tsurumi, T., Hanaoka, F., Matsuzawa, K., and Inagaki, M. (1998). Cell cycle- and chromatin binding state-dependent phosphorylation of human MCM heterohexameric complexes. A role for cdc2 kinase. J Biol Chem *273*, 17095-17101.

Fujita, M. Q., Yoshikawa, H., and Ogasawara, N. (1989). Structure of the dnaA region of Pseudomonas putida: conservation among three bacteria, Bacillus subtilis, Escherichia coli and P. putida. Mol Gen Genet *215*, 381-387.

Furnari, B., Blasina, A., Boddy, M. N., McGowan, C. H., and Russell, P. (1999). Cdc25 inhibited in vivo and in vitro by checkpoint kinases Cds1 and Chk1. Mol Biol Cell *10*, 833-845.

Fuss, H., Dubitzky, W., Downes, C. S., and Kurth, M. J. (2005). Mathematical models of cell cycle regulation. Brief Bioinform *6*, 163-177.

Gaczynska, M., Osmulski, P. A., Jiang, Y., Lee, J. K., Bermudez, V., and Hurwitz, J. (2004). Atomic force microscopic analysis of the binding of the Schizosaccharomyces pombe origin recognition complex and the spOrc4 protein with origin DNA. Proc Natl Acad Sci U S A *101*, 17952-17957.

Gautier, J., Norbury, C., Lohka, M., Nurse, P., and Maller, J. (1988). Purified maturation-promoting factor contains the product of a Xenopus homolog of the fission yeast cell cycle control gene cdc2+. Cell *54*, 433-439.

Gavin, K. A., Hidaka, M., and Stillman, B. (1995). Conserved initiator proteins in eukaryotes. Science *270*, 1667-1671.

Gerbi, S. A., and Bielinsky, A. K. (2002). DNA replication and chromatin. Curr Opin Genet Dev *12*, 243-248.

Gerbi, S. A., Strezoska, Z., and Waggener, J. M. (2002). Initiation of DNA replication in multicellular eukaryotes. J Struct Biol *140*, 17-30.

Gerhart, J., Wu, M., Cyert, M., and Kirschner, M. (1985). M-phase promoting factors from eggs of Xenopus laevis. Cytobios *43*, 335-347.

Gilbert, D. M. (2001). Making sense of eukaryotic DNA replication origins. Science *294*, 96-100.

Gilbert, D. M. (2001). Nuclear position leaves its mark on replication timing. J Cell Biol *152*, F11-15.

Gilbert, D. M. (2002). Replication timing and metazoan evolution. Nat Genet *32*, 336-337.

Gilbert, D. M. (2002). Replication timing and transcriptional control: beyond cause and effect. Curr Opin Cell Biol *14*, 377-383.

Gomez, M., and Antequera, F. (1999). Organization of DNA replication origins in the fission yeast genome. Embo J *18*, 5683-5690.

Gould, K. L., and Nurse, P. (1989). Tyrosine phosphorylation of the fission yeast cdc2+ protein kinase regulates entry into mitosis. Nature *342*, 39-45.

Grallert, B., and Nurse, P. (1996). The ORC1 homolog orp1 in fission yeast plays a key role in regulating onset of S phase. Genes Dev *10*, 2644-2654.

Gregan, J., Lindner, K., Brimage, L., Franklin, R., Namdar, M., Hart, E. A., Aves, S. J., and Kearsey, S. E. (2003). Fission yeast Cdc23/Mcm10 functions after pre-replicative complex formation to promote Cdc45 chromatin binding. Mol Biol Cell *14*, 3876-3887.

Hansen, K. R., Burns, G., Mata, J., Volpe, T. A., Martienssen, R. A., Bahler, J., and Thon, G. (2005). Global effects on gene expression in fission yeast by silencing and RNA interference machineries. Mol Cell Biol *25*, 590-601.

Hartwell, L. H., Culotti, J., Pringle, J. R., and Reid, B. J. (1974). Genetic control of the cell division cycle in yeast. Science *183*, 46-51.

Hatton, K. S., Dhar, V., Brown, E. H., Iqbal, M. A., Stuart, S., Didamo, V. T., and Schildkraut, C. L. (1988). Replication program of active and inactive multigene families in mammalian cells. Mol Cell Biol *8*, 2149-2158.

Hayles, J., Fisher, D., Woollard, A., and Nurse, P. (1994). Temporal order of S phase and mitosis in fission yeast is determined by the state of the p34cdc2-mitotic B cyclin complex. Cell *78*, 813-822.

Hayles, J., and Nurse, P. (1992). Genetics of the fission yeast Schizosaccharomyces pombe. Annu Rev Genet *26*, 373-402.

Hayles, J., and Nurse, P. (1995). A pre-start checkpoint preventing mitosis in fission yeast acts independently of p34cdc2 tyrosine phosphorylation. Embo J *14*, 2760-2771.

Heinzel, S. S., Krysan, P. J., Tran, C. T., and Calos, M. P. (1991). Autonomous DNA replication in human cells is affected by the size and the source of the DNA. Mol Cell Biol *11*, 2263-2272.

Hendrickson, M., Madine, M., Dalton, S., and Gautier, J. (1996). Phosphorylation of MCM4 by cdc2 protein kinase inhibits the activity of the minichromosome maintenance complex. Proc Natl Acad Sci U S A *93*, 12223-12228.

Hereford, L. M., and Hartwell, L. H. (1974). Sequential gene function in the initiation of Saccharomyces cerevisiae DNA synthesis. J Mol Biol *84*, 445-461.

Higgins, D. G., and Sharp, P. M. (1988). CLUSTAL: a package for performing multiple sequence alignment on a microcomputer. Gene *73*, 237-244.

Higgins, D. G., and Sharp, P. M. (1989). Fast and sensitive multiple sequence alignments on a microcomputer. Comput Appl Biosci *5*, 151-153.

Hofmann, J. F., and Beach, D. (1994). cdt1 is an essential target of the Cdc10/Sct1 transcription factor: requirement for DNA replication and inhibition of mitosis. Embo J *13*, 425-434.

Homesley, L., Lei, M., Kawasaki, Y., Sawyer, S., Christensen, T., and Tye, B. K. (2000). Mcm10 and the MCM2-7 complex interact to initiate DNA synthesis and to release replication factors from origins. Genes Dev *14*, 913-926.

Hopwood, B., and Dalton, S. (1996). Cdc45p assembles into a complex with Cdc46p/Mcm5p, is required for minichromosome maintenance, and is essential for chromosomal DNA replication. Proc Natl Acad Sci U S A *93*, 12309-12314.

Humphrey, T., and Pearce, A. (2005). Cell cycle molecules and mechanisms of the budding and fission yeasts. Methods Mol Biol *296*, 3-29.

Hyrien, O., Marheineke, K., and Goldar, A. (2003). Paradoxes of eukaryotic DNA replication: MCM proteins and the random completion problem. Bioessays *25*, 116-125.

Hyrien, O., Maric, C., and Mechali, M. (1995). Transition in specification of embryonic metazoan DNA replication origins. Science *270*, 994-997.

Hyrien, O., and Mechali, M. (1993). Chromosomal replication initiates and terminates at random sequences but at regular intervals in the ribosomal DNA of Xenopus early embryos. Embo J *12*, 4511-4520.

Iino, Y., Hiramine, Y., and Yamamoto, M. (1995). The role of cdc2 and other genes in meiosis in Schizosaccharomyces pombe. Genetics *140*, 1235-1245.

Ina, S., Sasaki, T., Yokota, Y., and Shinomiya, T. (2001). A broad replication origin of Drosophila melanogaster, oriDalpha, consists of AT-rich multiple discrete initiation sites. Chromosoma *109*, 551-564.

Ishiai, M., Dean, F. B., Okumura, K., Abe, M., Moon, K. Y., Amin, A. A., Kagotani, K., Taguchi, H., Murakami, Y., Hanaoka, F., *et al.* (1997). Isolation of human and fission yeast homologues of the budding yeast origin recognition complex subunit ORC5: human homologue (ORC5L) maps to 7q22. Genomics *46*, 294-298.

Ishimi, Y. (1997). A DNA helicase activity is associated with an MCM4, -6, and -7 protein complex. J Biol Chem *272*, 24508-24513.

Ishimi, Y., and Komamura-Kohno, Y. (2001). Phosphorylation of Mcm4 at specific sites by cyclin-dependent kinase leads to loss of Mcm4,6,7 helicase activity. J Biol Chem *276*, 34428-34433.

Ishimi, Y., Komamura-Kohno, Y., You, Z., Omori, A., and Kitagawa, M. (2000). Inhibition of Mcm4,6,7 helicase activity by phosphorylation with cyclin A/Cdk2. J Biol Chem *275*, 16235-16241.

Izumi, M., Yanagi, K., Mizuno, T., Yokoi, M., Kawasaki, Y., Moon, K. Y., Hurwitz, J., Yatagai, F., and Hanaoka, F. (2000). The human homolog of

Saccharomyces cerevisiae Mcm10 interacts with replication factors and dissociates from nuclease-resistant nuclear structures in G(2) phase. Nucleic Acids Res *28*, 4769-4777.

Izumi, M., Yatagai, F., and Hanaoka, F. (2001). Cell cycle-dependent proteolysis and phosphorylation of human Mcm10. J Biol Chem *276*, 48526-48531.

Izumi, M., Yatagai, F., and Hanaoka, F. (2004). Localization of human Mcm10 is spatially and temporally regulated during the S phase. J Biol Chem *279*, 32569-32577.

Jacob, F., and Brenner, S. (1963). [On the regulation of DNA synthesis in bacteria: the hypothesis of the replicon.]. C R Hebd Seances Acad Sci *256*, 298-300.

Jallepalli, P. V., and Kelly, T. J. (1997). Cyclin-dependent kinase and initiation at eukaryotic origins: a replication switch? Curr Opin Cell Biol *9*, 358-363.

Jallepalli, P. V., Tien, D., and Kelly, T. J. (1998). sud1(+) targets cyclin-dependent kinase-phosphorylated Cdc18 and Rum1 proteins for degradation and stops unwanted diploidization in fission yeast. Proc Natl Acad Sci U S A *95*, 8159-8164.

Jares, P., and Blow, J. J. (2000). Xenopus cdc7 function is dependent on licensing but not on XORC, XCdc6, or CDK activity and is required for XCdc45 loading. Genes Dev *14*, 1528-1540.

Jeon, Y., Bekiranov, S., Karnani, N., Kapranov, P., Ghosh, S., Macalpine, D., Lee, C., Hwang, D. S., Gingeras, T. R., and Dutta, A. (2005). Temporal profile of replication of human chromosomes. Proc Natl Acad Sci U S A *102*, 6419-6424.

Johnston, L. H., and Barker, D. G. (1987). Characterisation of an autonomously replicating sequence from the fission yeast Schizosaccharomyces pombe. Mol Gen Genet *207*, 161-164.

Johnston, L. H., Masai, H., and Sugino, A. (2000). A Cdc7p-Dbf4p protein kinase activity is conserved from yeast to humans. Prog Cell Cycle Res *4*, 61-69.

Kalejta, R. F., and Hamlin, J. L. (1996). Composite patterns in neutral/neutral two-dimensional gels demonstrate inefficient replication origin usage. Mol Cell Biol *16*, 4915-4922.

Kamimura, Y., Tak, Y. S., Sugino, A., and Araki, H. (2001). Sld3, which interacts with Cdc45 (Sld4), functions for chromosomal DNA replication in Saccharomyces cerevisiae. Embo J *20*, 2097-2107.

Kearsey, S. (1984). Structural requirements for the function of a yeast chromosomal replicator. Cell *37*, 299-307.

Kearsey, S. (2002). Surveying genome replication. Genome Biol *3*, REVIEWS1016.

Kearsey, S. E., and Labib, K. (1998). MCM proteins: evolution, properties, and role in DNA replication. Biochim Biophys Acta *1398*, 113-136.

Kearsey, S. E., Montgomery, S., Labib, K., and Lindner, K. (2000). Chromatin binding of the fission yeast replication factor mcm4 occurs during anaphase and requires ORC and cdc18. Embo J *19*, 1681-1690.

Kelly, T. J., and Brown, G. W. (2000). Regulation of chromosome replication. Annu Rev Biochem *69*, 829-880.

Kelly, T. J., Martin, G. S., Forsburg, S. L., Stephen, R. J., Russo, A., and Nurse, P. (1993). The fission yeast cdc18+ gene product couples S phase to START and mitosis. Cell *74*, 371-382.

Kihara, M., Nakai, W., Asano, S., Suzuki, A., Kitada, K., Kawasaki, Y., Johnston, L. H., and Sugino, A. (2000). Characterization of the yeast Cdc7p/Dbf4p complex purified from insect cells. Its protein kinase activity is regulated by Rad53p. J Biol Chem *275*, 35051-35062.

Kim, S. M., Dubey, D. D., and Huberman, J. A. (2003). Early-replicating heterochromatin. Genes Dev *17*, 330-335.

Kim, S. M., and Huberman, J. A. (1998). Multiple orientation-dependent, synergistically interacting, similar domains in the ribosomal DNA replication origin of the fission yeast, Schizosaccharomyces pombe. Mol Cell Biol *18*, 7294-7303.

Kim, S. M., and Huberman, J. A. (2001). Regulation of replication timing in fission yeast. Embo J *20*, 6115-6126.

Kim, S. M., Zhang, D. Y., and Huberman, J. A. (2001). Multiple redundant sequence elements within the fission yeast ura4 replication origin enhancer. BMC Mol Biol *2*, 1.

Kishimoto, T., Kuriyama, R., Kondo, H., and Kanatani, H. (1982). Generality of the action of various maturation-promoting factors. Exp Cell Res *137*, 121-126.

Kitamura, K., Maekawa, H., and Shimoda, C. (1998). Fission yeast Ste9, a homolog of Hct1/Cdh1 and Fizzy-related, is a novel negative regulator of cell cycle progression during G1-phase. Mol Biol Cell *9*, 1065-1080.

Kleckner, N. (1996). Meiosis: how could it work? Proc Natl Acad Sci U S A *93*, 8167-8174.

Kohzaki, H., Ito, Y., and Murakami, Y. (1999). Context-dependent modulation of replication activity of Saccharomyces cerevisiae autonomously replicating sequences by transcription factors. Mol Cell Biol *19*, 7428-7435.

Kominami, K., and Toda, T. (1997). Fission yeast WD-repeat protein pop1 regulates genome ploidy through ubiquitin-proteasome-mediated degradation of the CDK inhibitor Rum1 and the S-phase initiator Cdc18. Genes Dev *11*, 1548-1560.

Kong, D., Coleman, T. R., and DePamphilis, M. L. (2003). Xenopus origin recognition complex (ORC) initiates DNA replication preferentially at sequences targeted by Schizosaccharomyces pombe ORC. Embo J *22*, 3441-3450.

Kong, D., and DePamphilis, M. L. (2001). Site-specific DNA binding of the Schizosaccharomyces pombe origin recognition complex is determined by the Orc4 subunit. Mol Cell Biol *21*, 8095-8103.

Kong, D., and DePamphilis, M. L. (2002). Site-specific ORC binding, pre-replication complex assembly and DNA synthesis at Schizosaccharomyces pombe replication origins. Embo J *21*, 5567-5576.

Kroll, K. L., Salic, A. N., Evans, L. M., and Kirschner, M. W. (1998). Geminin, a neuralizing molecule that demarcates the future neural plate at the onset of gastrulation. Development *125*, 3247-3258.

Kubota, Y., Takase, Y., Komori, Y., Hashimoto, Y., Arata, T., Kamimura, Y., Araki, H., and Takisawa, H. (2003). A novel ring-like complex of Xenopus proteins essential for the initiation of DNA replication. Genes Dev *17*, 1141-1152.

Kukimoto, I., Igaki, H., and Kanda, T. (1999). Human CDC45 protein binds to minichromosome maintenance 7 protein and the p70 subunit of DNA polymerase alpha. Eur J Biochem *265*, 936-943.

Kumagai, H., Sato, N., Yamada, M., Mahony, D., Seghezzi, W., Lees, E., Arai, K., and Masai, H. (1999). A novel growth- and cell cycle-regulated protein, ASK, activates human Cdc7-related kinase and is essential for G1/S transition in mammalian cells. Mol Cell Biol *19*, 5083-5095.

Labbe, J. C., Lee, M. G., Nurse, P., Picard, A., and Doree, M. (1988). Activation at M-phase of a protein kinase encoded by a starfish homologue of the cell cycle control gene cdc2+. Nature *335*, 251-254.

Labib, K., Diffley, J. F., and Kearsey, S. E. (1999). G1-phase and B-type cyclins exclude the DNA-replication factor Mcm4 from the nucleus. Nat Cell Biol *1*, 415-422.

Ladenburger, E. M., Keller, C., and Knippers, R. (2002). Identification of a binding region for human origin recognition complex proteins 1 and 2 that coincides with an origin of DNA replication. Mol Cell Biol *22*, 1036-1048.

Lander, E. S., Linton, L. M., Birren, B., Nusbaum, C., Zody, M. C., Baldwin, J., Devon, K., Dewar, K., Doyle, M., FitzHugh, W., *et al.* (2001). Initial sequencing and analysis of the human genome. Nature *409*, 860-921.

Langan, T. A., Gautier, J., Lohka, M., Hollingsworth, R., Moreno, S., Nurse, P., Maller, J., and Sclafani, R. A. (1989). Mammalian growth-associated H1 histone kinase: a homolog of cdc2+/CDC28 protein kinases controlling mitotic entry in yeast and frog cells. Mol Cell Biol *9*, 3860-3868.

Leatherwood, J., Lopez-Girona, A., and Russell, P. (1996). Interaction of Cdc2 and Cdc18 with a fission yeast ORC2-like protein. Nature *379*, 360-363.

Lee, D. G., and Bell, S. P. (1997). Architecture of the yeast origin recognition complex bound to origins of DNA replication. Mol Cell Biol *17*, 7159-7168.

Lee, J. K., and Hurwitz, J. (2000). Isolation and characterization of various complexes of the minichromosome maintenance proteins of Schizosaccharomyces pombe. J Biol Chem *275*, 18871-18878.

Lee, J. K., and Hurwitz, J. (2001). Processive DNA helicase activity of the minichromosome maintenance proteins 4, 6, and 7 complex requires forked DNA structures. Proc Natl Acad Sci U S A *98*, 54-59.

Lee, J. K., Moon, K. Y., Jiang, Y., and Hurwitz, J. (2001). The Schizosaccharomyces pombe origin recognition complex interacts with multiple AT-rich regions of the replication origin DNA by means of the AT-hook domains of the spOrc4 protein. Proc Natl Acad Sci U S A *98*, 13589-13594.

Lee, M. G., and Nurse, P. (1987). Complementation used to clone a human homologue of the fission yeast cell cycle control gene cdc2. Nature *327*, 31-35.

Lei, M., Kawasaki, Y., Young, M. R., Kihara, M., Sugino, A., and Tye, B. K. (1997). Mcm2 is a target of regulation by Cdc7-Dbf4 during the initiation of DNA synthesis. Genes Dev *11*, 3365-3374.

Li, A., and Blow, J. J. (2005). Cdt1 downregulation by proteolysis and geminin inhibition prevents DNA re-replication in Xenopus. Embo J *24*, 395-404.

Li, C. J., and DePamphilis, M. L. (2002). Mammalian Orc1 protein is selectively released from chromatin and ubiquitinated during the S-to-M transition in the cell division cycle. Mol Cell Biol *22*, 105-116.

Li, F., Chen, J., Izumi, M., Butler, M. C., Keezer, S. M., and Gilbert, D. M. (2001). The replication timing program of the Chinese hamster beta-globin locus is established coincident with its repositioning near peripheral heterochromatin in early G1 phase. J Cell Biol *154*, 283-292.

Li, F., Chen, J., Solessio, E., and Gilbert, D. M. (2003). Spatial distribution and specification of mammalian replication origins during G1 phase. J Cell Biol *161*, 257-266.

Liang, C., and Stillman, B. (1997). Persistent initiation of DNA replication and chromatin-bound MCM proteins during the cell cycle in cdc6 mutants. Genes Dev *11*, 3375-3386.

Lilly, M. A., and Duronio, R. J. (2005). New insights into cell cycle control from the Drosophila endocycle. Oncogene *24*, 2765-2775.

Lin, H. B., Dijkwel, P. A., and Hamlin, J. L. (2005). Promiscuous initiation on mammalian chromosomal DNA templates and its possible suppression by transcription. Exp Cell Res *308*, 53-64.

Lindner, K., Gregan, J., Montgomery, S., and Kearsey, S. E. (2002). Essential role of MCM proteins in premeiotic DNA replication. Mol Biol Cell *13*, 435-444.

Lindsay, H. D., Griffiths, D. J., Edwards, R. J., Christensen, P. U., Murray, J. M., Osman, F., Walworth, N., and Carr, A. M. (1998). S-phase-specific activation of Cds1 kinase defines a subpathway of the checkpoint response in Schizosaccharomyces pombe. Genes Dev *12*, 382-395.

Linskens, M. H., and Huberman, J. A. (1990). The two faces of higher eukaryotic DNA replication origins. Cell *62*, 845-847.

Liu, E., Li, X., Yan, F., Zhao, Q., and Wu, X. (2004). Cyclin-dependent kinases phosphorylate human Cdt1 and induce its degradation. J Biol Chem *279*, 17283-17288.

Liu, G., Malott, M., and Leffak, M. (2003). Multiple functional elements comprise a Mammalian chromosomal replicator. Mol Cell Biol *23*, 1832-1842.

Loebel, D., Huikeshoven, H., and Cotterill, S. (2000). Localisation of the DmCdc45 DNA replication factor in the mitotic cycle and during chorion gene amplification. Nucleic Acids Res *28*, 3897-3903.

Loog, M., and Morgan, D. O. (2005). Cyclin specificity in the phosphorylation of cyclin-dependent kinase substrates. Nature *434*, 104-108.

Lu, L., and Tower, J. (1997). A transcriptional insulator element, the su(Hw) binding site, protects a chromosomal DNA replication origin from position effects. Mol Cell Biol *17*, 2202-2206.

Lundgren, K., Walworth, N., Booher, R., Dembski, M., Kirschner, M., and Beach, D. (1991). mik1 and wee1 cooperate in the inhibitory tyrosine phosphorylation of cdc2. Cell *64*, 1111-1122.

Luo, L., and Kessel, M. (2004). Geminin coordinates cell cycle and developmental control. Cell Cycle *3*, 711-714.

Lygerou, Z., and Nurse, P. (1999). The fission yeast origin recognition complex is constitutively associated with chromatin and is differentially modified through the cell cycle. J Cell Sci *112 (Pt 21)*, 3703-3712.

Lyne, R., Burns, G., Mata, J., Penkett, C. J., Rustici, G., Chen, D., Langford, C., Vetrie, D., and Bahler, J. (2003). Whole-genome microarrays of fission yeast: characteristics, accuracy, reproducibility, and processing of array data. BMC Genomics *4*, 27.

Macalpine, D. M., and Bell, S. P. (2005). A genomic view of eukaryotic DNA replication. Chromosome Res *13*, 309-326.

MacAlpine, D. M., Rodriguez, H. K., and Bell, S. P. (2004). Coordination of replication and transcription along a Drosophila chromosome. Genes Dev *18*, 3094-3105.

Madine, M. A., Khoo, C. Y., Mills, A. D., Musahl, C., and Laskey, R. A. (1995). The nuclear envelope prevents reinitiation of replication by regulating the binding of MCM3 to chromatin in Xenopus egg extracts. Curr Biol *5*, 1270-1279.

Maher, J. F., and Nathans, D. (1996). Multivalent DNA-binding properties of the HMG-1 proteins. Proc Natl Acad Sci U S A *93*, 6716-6720.

Maiorano, D., Krasinska, L., Lutzmann, M., and Mechali, M. (2005). Recombinant Cdt1 induces rereplication of G2 nuclei in Xenopus egg extracts. Curr Biol *15*, 146-153.

Maiorano, D., Moreau, J., and Mechali, M. (2000). XCDT1 is required for the assembly of pre-replicative complexes in Xenopus laevis. Nature *404*, 622-625.

Maiorano, D., Rul, W., and Mechali, M. (2004). Cell cycle regulation of the licensing activity of Cdt1 in Xenopus laevis. Exp Cell Res *295*, 138-149.

Marahrens, Y., and Stillman, B. (1992). A yeast chromosomal origin of DNA replication defined by multiple functional elements. Science *255*, 817-823.

Marheineke, K., and Hyrien, O. (2004). Control of replication origin density and firing time in Xenopus egg extracts: role of a caffeine-sensitive, ATR-dependent checkpoint. J Biol Chem *279*, 28071-28081.

Maric, C., Levacher, B., and Hyrien, O. (1999). Developmental regulation of replication fork pausing in Xenopus laevis ribosomal RNA genes. J Mol Biol *291*, 775-788.

Marston, A. L., and Amon, A. (2004). Meiosis: cell-cycle controls shuffle and deal. Nat Rev Mol Cell Biol *5*, 983-997.

Martin-Castellanos, C., Blanco, M. A., de Prada, J. M., and Moreno, S. (2000). The puc1 cyclin regulates the G1 phase of the fission yeast cell cycle in response to cell size. Mol Biol Cell *11*, 543-554.

Masai, H., Miyake, T., and Arai, K. (1995). hsk1+, a Schizosaccharomyces pombe gene related to Saccharomyces cerevisiae CDC7, is required for chromosomal replication. Embo J *14*, 3094-3104.

Masai, H., You, Z., and Arai, K. (2005). Control of DNA Replication: Regulation and Activation of Eukaryotic Replicative Helicase, MCM. IUBMB Life *57*, 323-335.

Masuda, T., Mimura, S., and Takisawa, H. (2003). CDK- and Cdc45-dependent priming of the MCM complex on chromatin during S-phase in Xenopus egg extracts: possible activation of MCM helicase by association with Cdc45. Genes Cells *8*, 145-161.

Masui, Y., and Markert, C. L. (1971). Cytoplasmic control of nuclear behavior during meiotic maturation of frog oocytes. J Exp Zool *177*, 129-145.

Masumoto, H., Muramatsu, S., Kamimura, Y., and Araki, H. (2002). S-Cdk-dependent phosphorylation of Sld2 essential for chromosomal DNA replication in budding yeast. Nature *415*, 651-655.

Masumoto, H., Sugino, A., and Araki, H. (2000). Dpb11 controls the association between DNA polymerases alpha and epsilon and the autonomously replicating sequence region of budding yeast. Mol Cell Biol *20*, 2809-2817.

Mata, J., Lyne, R., Burns, G., and Bahler, J. (2002). The transcriptional program of meiosis and sporulation in fission yeast. Nat Genet *32*, 143-147.

Maundrell, K., Hutchison, A., and Shall, S. (1988). Sequence analysis of ARS elements in fission yeast. Embo J *7*, 2203-2209.

Maundrell, K., Wright, A. P., Piper, M., and Shall, S. (1985). Evaluation of heterologous ARS activity in S. cerevisiae using cloned DNA from S. pombe. Nucleic Acids Res *13*, 3711-3722.

McCune, H. J., and Donaldson, A. D. (2003). DNA replication: telling time with microarrays. Genome Biol *4*, 204.

McFarlane, R. J., Carr, A. M., and Price, C. (1997). Characterisation of the Schizosaccharomyces pombe rad4/cut5 mutant phenotypes: dissection of DNA replication and G2 checkpoint control function. Mol Gen Genet *255*, 332-340.

McGarry, T. J., and Kirschner, M. W. (1998). Geminin, an inhibitor of DNA replication, is degraded during mitosis. Cell *93*, 1043-1053.

Mechali, M. (2001). DNA replication origins: from sequence specificity to epigenetics. Nat Rev Genet *2*, 640-645.

Melendy, T., and Li, R. (2001). Chromatin remodeling and initiation of DNA replication. Front Biosci *6*, D1048-1053.

Melixetian, M., and Helin, K. (2004). Geminin: a major DNA replication safeguard in higher eukaryotes. Cell Cycle *3*, 1002-1004.

Mendez, J., and Stillman, B. (2000). Chromatin association of human origin recognition complex, cdc6, and minichromosome maintenance proteins during the cell cycle: assembly of prereplication complexes in late mitosis. Mol Cell Biol *20*, 8602-8612.

Mendez, J., and Stillman, B. (2003). Perpetuating the double helix: molecular machines at eukaryotic DNA replication origins. Bioessays *25*, 1158-1167.

Meselson, M., and Stahl, F. W. (1958). The replication of DNA. Cold Spring Harb Symp Quant Biol *23*, 9-12.

Miake-Lye, R., and Kirschner, M. W. (1985). Induction of early mitotic events in a cell-free system. Cell *41*, 165-175.

Mihaylov, I. S., Kondo, T., Jones, L., Ryzhikov, S., Tanaka, J., Zheng, J., Higa, L. A., Minamino, N., Cooley, L., and Zhang, H. (2002). Control of DNA replication and chromosome ploidy by geminin and cyclin A. Mol Cell Biol *22*, 1868-1880.

Milbrandt, J. D., Heintz, N. H., White, W. C., Rothman, S. M., and Hamlin, J. L. (1981). Methotrexate-resistant Chinese hamster ovary cells have amplified a 135-kilobase-pair region that includes the dihydrofolate reductase gene. Proc Natl Acad Sci U S A *78*, 6043-6047.

Miller, M. E., and Cross, F. R. (2001). Cyclin specificity: how many wheels do you need on a unicycle? J Cell Sci *114*, 1811-1820.

Mimura, S., Masuda, T., Matsui, T., and Takisawa, H. (2000). Central role for cdc45 in establishing an initiation complex of DNA replication in Xenopus egg extracts. Genes Cells *5*, 439-452.

Mimura, S., and Takisawa, H. (1998). Xenopus Cdc45-dependent loading of DNA polymerase alpha onto chromatin under the control of S-phase Cdk. Embo J *17*, 5699-5707.

Mitchison, J. M. (1970). Methods in cell physiology (ed D M Prescott) *4*, 131.

Mitchison, J. M., and Creanor, J. (1971). Further measurements of DNA synthesis and enzyme potential during cell cycle of fission yeast Schizosaccharomyces pombe. Exp Cell Res *69*, 244-247.

Miyake, S., and Yamashita, S. (1998). Identification of sna41 gene, which is the suppressor of nda4 mutation and is involved in DNA replication in Schizosaccharomyces pombe. Genes Cells *3*, 157-166.

Moon, K. Y., Kong, D., Lee, J. K., Raychaudhuri, S., and Hurwitz, J. (1999). Identification and reconstitution of the origin recognition complex from Schizosaccharomyces pombe. Proc Natl Acad Sci U S A *96*, 12367-12372.

Moore, J. D., Kirk, J. A., and Hunt, T. (2003). Unmasking the S-phase-promoting potential of cyclin B1. Science *300*, 987-990.

Moreno, S., Hayles, J., and Nurse, P. (1989). Regulation of p34cdc2 protein kinase during mitosis. Cell *58*, 361-372.

Moreno, S., Klar, A., and Nurse, P. (1991). Molecular genetic analysis of fission yeast Schizosaccharomyces pombe. Methods Enzymol *194*, 795-823.

Moreno, S., and Nurse, P. (1994). Regulation of progression through the G1 phase of the cell cycle by the rum1+ gene. Nature *367*, 236-242.

Moreno, S., Nurse, P., and Russell, P. (1990). Regulation of mitosis by cyclic accumulation of p80cdc25 mitotic inducer in fission yeast. Nature *344*, 549-552.

Munz, P., Wolf, K., Kholl, J., and Leupold, U. (1989). Genetics Overview. In Molecular Biology of the Fission Yeast. A. Nasim, P. Young, and B.F. Johnson, eds. San Diego: Academic Press, 1 - 30.

Murakami, H., and Nurse, P. (1999). Meiotic DNA replication checkpoint control in fission yeast. Genes Dev *13*, 2581-2593.

Murakami, H., and Nurse, P. (2000). DNA replication and damage checkpoints and meiotic cell cycle controls in the fission and budding yeasts. Biochem J *349*, 1-12.

Murakami, H., and Nurse, P. (2001). Regulation of premeiotic S phase and recombination-related double-strand DNA breaks during meiosis in fission yeast. Nat Genet *28*, 290-293.

Murray, A. W. (2004). Recycling the cell cycle: cyclins revisited. Cell *116*, 221-234.

Muzi-Falconi, M., and Kelly, T. J. (1995). Orp1, a member of the Cdc18/Cdc6 family of S-phase regulators, is homologous to a component of the origin recognition complex. Proc Natl Acad Sci U S A *92*, 12475-12479.

Nakajima, R., and Masukata, H. (2002). SpSld3 is required for loading and maintenance of SpCdc45 on chromatin in DNA replication in fission yeast. Mol Biol Cell *13*, 1462-1472.

Nakajo, N., Yoshitome, S., Iwashita, J., Iida, M., Uto, K., Ueno, S., Okamoto, K., and Sagata, N. (2000). Absence of Wee1 ensures the meiotic cell cycle in Xenopus oocytes. Genes Dev *14*, 328-338.

Nasmyth, K., and Nurse, P. (1981). Cell division cycle mutants altered in DNA replication and mitosis in the fission yeast Schizosaccharomyces pombe. Mol Gen Genet *182*, 119-124.

Nasmyth, K., Nurse, P., and Fraser, R. S. (1979). The effect of cell mass on the cell cycle timing and duration of S-phase in fission yeast. J Cell Sci *39*, 215-233.

Natale, D. A., Schubert, A. E., and Kowalski, D. (1992). DNA helical stability accounts for mutational defects in a yeast replication origin. Proc Natl Acad Sci U S A *89*, 2654-2658.

Newlon, C. S., Collins, I., Dershowitz, A., Deshpande, A. M., Greenfeder, S. A., Ong, L. Y., and Theis, J. F. (1993). Analysis of replication origin function on chromosome III of Saccharomyces cerevisiae. Cold Spring Harb Symp Quant Biol *58*, 415-423.

Newlon, C. S., and Theis, J. F. (1993). The structure and function of yeast ARS elements. Curr Opin Genet Dev *3*, 752-758.

Newlon, C. S., and Theis, J. F. (2002). DNA replication joins the revolution: whole-genome views of DNA replication in budding yeast. Bioessays *24*, 300-304.

Nguyen, V. Q., Co, C., Irie, K., and Li, J. J. (2000). Clb/Cdc28 kinases promote nuclear export of the replication initiator proteins Mcm2-7. Curr Biol *10*, 195-205.

Nieduszynski, C. A., Blow, J. J., and Donaldson, A. D. (2005). The requirement of yeast replication origins for pre-replication complex proteins is modulated by transcription. Nucleic Acids Res *33*, 2410-2420.

Nishitani, H., and Lygerou, Z. (2002). Control of DNA replication licensing in a cell cycle. Genes Cells *7*, 523-534.

Nishitani, H., and Lygerou, Z. (2004). DNA replication licensing. Front Biosci *9*, 2115-2132.

Nishitani, H., Lygerou, Z., Nishimoto, T., and Nurse, P. (2000). The Cdt1 protein is required to license DNA for replication in fission yeast. Nature *404*, 625-628.

Nishitani, H., and Nurse, P. (1995). p65cdc18 plays a major role controlling the initiation of DNA replication in fission yeast. Cell *83*, 397-405.

Nishitani, H., Taraviras, S., Lygerou, Z., and Nishimoto, T. (2001). The human licensing factor for DNA replication Cdt1 accumulates in G1 and is destabilized after initiation of S-phase. J Biol Chem *276*, 44905-44911.

Niwa, O., Matsumoto, T., Chikashige, Y., and Yanagida, M. (1989). Characterization of Schizosaccharomyces pombe minichromosome deletion derivatives and a functional allocation of their centromere. Embo J *8*, 3045-3052.

Nougarede, R., Della Seta, F., Zarzov, P., and Schwob, E. (2000). Hierarchy of S-phase-promoting factors: yeast Dbf4-Cdc7 kinase requires prior S-phase cyclin-dependent kinase activation. Mol Cell Biol *20*, 3795-3806.

Nurse, P., and Bissett, Y. (1981). Gene required in G1 for commitment to cell cycle and in G2 for control of mitosis in fission yeast. Nature *292*, 558-560.

Nurse, P., and Thuriaux, P. (1980). Regulatory genes controlling mitosis in the fission yeast Schizosaccharomyces pombe. Genetics *96*, 627-637.

Nurse, P., Thuriaux, P., and Nasmyth, K. (1976). Genetic control of the cell division cycle in the fission yeast Schizosaccharomyces pombe. Mol Gen Genet *146*, 167-178.

Nurse, P. M. (2002). Nobel Lecture. Cyclin dependent kinases and cell cycle control. Biosci Rep *22*, 487-499.

Nyberg, K. A., Michelson, R. J., Putnam, C. W., and Weinert, T. A. (2002). Toward maintaining the genome: DNA damage and replication checkpoints. Annu Rev Genet *36*, 617-656.

O'Connell, M. J., Raleigh, J. M., Verkade, H. M., and Nurse, P. (1997). Chk1 is a wee1 kinase in the G2 DNA damage checkpoint inhibiting cdc2 by Y15 phosphorylation. Embo J *16*, 545-554.

Ogawa, Y., Takahashi, T., and Masukata, H. (1999). Association of fission yeast Orp1 and Mcm6 proteins with chromosomal replication origins. Mol Cell Biol *19*, 7228-7236.

Okayama, H., Nagata, A., Jinno, S., Murakami, H., Tanaka, K., and Nakashima, N. (1996). Cell cycle control in fission yeast and mammals: identification of new regulatory mechanisms. Adv Cancer Res *69*, 17-62.

Okishio, N., Adachi, Y., and Yanagida, M. (1996). Fission yeast Nda1 and Nda4, MCM homologs required for DNA replication, are constitutive nuclear proteins. J Cell Sci *109 (Pt 2)*, 319-326.

Okuno, Y., McNairn, A. J., den Elzen, N., Pines, J., and Gilbert, D. M. (2001). Stability, chromatin association and functional activity of mammalian pre-replication complex proteins during the cell cycle. Embo J *20*, 4263-4277.

Okuno, Y., Okazaki, T., and Masukata, H. (1997). Identification of a predominant replication origin in fission yeast. Nucleic Acids Res *25*, 530-537.

Okuno, Y., Satoh, H., Sekiguchi, M., and Masukata, H. (1999). Clustered adenine/thymine stretches are essential for function of a fission yeast replication origin. Mol Cell Biol *19*, 6699-6709.

Olsson, T., Ekwall, K., and Ruusala, T. (1993). The silent P mating type locus in fission yeast contains two autonomously replicating sequences. Nucleic Acids Res *21*, 855-861.

Orr-Weaver, T. L., Johnston, C. G., and Spradling, A. C. (1989). The role of ACE3 in Drosophila chorion gene amplification. Embo J *8*, 4153-4162.

Osheim, Y. N., Miller, O. L., Jr., and Beyer, A. L. (1988). Visualization of Drosophila melanogaster chorion genes undergoing amplification. Mol Cell Biol *8*, 2811-2821.

Owens, J. C., Detweiler, C. S., and Li, J. J. (1997). CDC45 is required in conjunction with CDC7/DBF4 to trigger the initiation of DNA replication. Proc Natl Acad Sci U S A *94*, 12521-12526.

Pacek, M., and Walter, J. C. (2004). A requirement for MCM7 and Cdc45 in chromosome unwinding during eukaryotic DNA replication. Embo J *23*, 3667-3676.

Parker, L. L., Atherton-Fessler, S., and Piwnica-Worms, H. (1992). p107wee1 is a dual-specificity kinase that phosphorylates p34cdc2 on tyrosine 15. Proc Natl Acad Sci U S A *89*, 2917-2921.

Pasero, P., Bensimon, A., and Schwob, E. (2002). Single-molecule analysis reveals clustering and epigenetic regulation of replication origins at the yeast rDNA locus. Genes Dev *16*, 2479-2484.

Patel, P. K., Arcangioli, B., Baker, S. P., Bensimon, A., and Rhind, N. (2005). DNA Replication Origins Fire Stochastically in Fission Yeast. Mol Biol Cell, in press.

Pelizon, C., Madine, M. A., Romanowski, P., and Laskey, R. A. (2000). Unphosphorylatable mutants of Cdc6 disrupt its nuclear export but still support DNA replication once per cell cycle. Genes Dev *14*, 2526-2533.

Perkins, G., Drury, L. S., and Diffley, J. F. (2001). Separate SCF(CDC4) recognition elements target Cdc6 for proteolysis in S phase and mitosis. Embo J *20*, 4836-4845.

Peters, C. W., Sippel, A. E., Vingron, M., and Klempnauer, K. H. (1987). Drosophila and vertebrate myb proteins share two conserved regions, one of which functions as a DNA-binding domain. Embo J *6*, 3085-3090.

Petersen, B. O., Lukas, J., Sorensen, C. S., Bartek, J., and Helin, K. (1999). Phosphorylation of mammalian CDC6 by cyclin A/CDK2 regulates its subcellular localization. Embo J *18*, 396-410.

Philpott, A., and Yew, P. R. (2005). The Xenopus cell cycle: an overview. Methods Mol Biol *296*, 95-112.

Quinn, L. M., Herr, A., McGarry, T. J., and Richardson, H. (2001). The Drosophila Geminin homolog: roles for Geminin in limiting DNA replication, in anaphase and in neurogenesis. Genes Dev *15*, 2741-2754.

Raghuraman, M. K., Brewer, B. J., and Fangman, W. L. (1997). Cell cycle-dependent establishment of a late replication program. Science *276*, 806-809.

Raghuraman, M. K., Winzeler, E. A., Collingwood, D., Hunt, S., Wodicka, L., Conway, A., Lockhart, D. J., Davis, R. W., Brewer, B. J., and Fangman, W. L. (2001). Replication dynamics of the yeast genome. Science *294*, 115-121.

Raleigh, J. M., and O'Connell, M. J. (2000). The G(2) DNA damage checkpoint targets both Wee1 and Cdc25. J Cell Sci *113 (Pt 10)*, 1727-1736.

Rao, H., Marahrens, Y., and Stillman, B. (1994). Functional conservation of multiple elements in yeast chromosomal replicators. Mol Cell Biol *14*, 7643-7651.

Rape, M., and Kirschner, M. W. (2004). Autonomous regulation of the anaphase-promoting complex couples mitosis to S-phase entry. Nature *432*, 588-595.

Reeves, R. (2001). Molecular biology of HMGA proteins: hubs of nuclear function. Gene *277*, 63-81.

Remus, D., Beall, E. L., and Botchan, M. R. (2004). DNA topology, not DNA sequence, is a critical determinant for Drosophila ORC-DNA binding. Embo J *23*, 897-907.

Rowles, A., Tada, S., and Blow, J. J. (1999). Changes in association of the Xenopus origin recognition complex with chromatin on licensing of replication origins. J Cell Sci *112 (Pt 12)*, 2011-2018.

Rowley, A., Cocker, J. H., Harwood, J., and Diffley, J. F. (1995). Initiation complex assembly at budding yeast replication origins begins with the recognition of a bipartite sequence by limiting amounts of the initiator, ORC. Embo J *14*, 2631-2641.

Rowley, A., Dowell, S. J., and Diffley, J. F. (1994). Recent developments in the initiation of chromosomal DNA replication: a complex picture emerges. Biochim Biophys Acta *1217*, 239-256.

Russell, P., and Nurse, P. (1986). cdc25+ functions as an inducer in the mitotic control of fission yeast. Cell *45*, 145-153.

Rustici, G., Mata, J., Kivinen, K., Lio, P., Penkett, C. J., Burns, G., Hayles, J., Brazma, A., Nurse, P., and Bahler, J. (2004). Periodic gene expression program of the fission yeast cell cycle. Nat Genet *36*, 809-817.

Saha, P., Chen, J., Thome, K. C., Lawlis, S. J., Hou, Z. H., Hendricks, M., Parvin, J. D., and Dutta, A. (1998). Human CDC6/Cdc18 associates with Orc1 and cyclin-cdk and is selectively eliminated from the nucleus at the onset of S phase. Mol Cell Biol *18*, 2758-2767.

Saha, S., Shan, Y., Mesner, L. D., and Hamlin, J. L. (2004). The promoter of the Chinese hamster ovary dihydrofolate reductase gene regulates the activity of the local origin and helps define its boundaries. Genes Dev *18*, 397-410.

Saka, Y., and Yanagida, M. (1993). Fission yeast cut5+, required for S phase onset and M phase restraint, is identical to the radiation-damage repair gene rad4+. Cell *74*, 383-393.

Sakaguchi, J., and Yamamoto, M. (1982). Cloned ural locus of Schizosaccharomyces pombe propagates autonomously in this yeast assuming a polymeric form. Proc Natl Acad Sci U S A *79*, 7819-7823.

Santocanale, C., and Diffley, J. F. (1998). A Mec1- and Rad53-dependent checkpoint controls late-firing origins of DNA replication. Nature *395*, 615-618.

Sawyer, S. L., Cheng, I. H., Chai, W., and Tye, B. K. (2004). Mcm10 and Cdc45 cooperate in origin activation in Saccharomyces cerevisiae. J Mol Biol *340*, 195-202.

Sazer, S., and Sherwood, S. W. (1990). Mitochondrial growth and DNA synthesis occur in the absence of nuclear DNA replication in fission yeast. J Cell Sci *97 (Pt 3)*, 509-516.

Schroll, A. L., and Heintz, N. H. (2004). Chemical footprinting of structural and functional elements of dhfr oribeta during the CHOC 400 cell cycle. Gene *332*, 139-147.

Schubeler, D., Scalzo, D., Kooperberg, C., van Steensel, B., Delrow, J., and Groudine, M. (2002). Genome-wide DNA replication profile for Drosophila melanogaster: a link between transcription and replication timing. Nat Genet *32*, 438-442.

Schulte, D., Burkhart, R., Musahl, C., Hu, B., Schlatterer, C., Hameister, H., and Knippers, R. (1995). Expression, phosphorylation and nuclear localization of the human P1 protein, a homologue of the yeast Mcm 3 replication protein. J Cell Sci *108 (Pt 4)*, 1381-1389.

Schwacha, A., and Bell, S. P. (2001). Interactions between two catalytically distinct MCM subgroups are essential for coordinated ATP hydrolysis and DNA replication. Mol Cell *8*, 1093-1104.

Schwob, E. (2004). Flexibility and governance in eukaryotic DNA replication. Curr Opin Microbiol *7*, 680-690.

Segurado, M., de Luis, A., and Antequera, F. (2003). Genome-wide distribution of DNA replication origins at A+T-rich islands in Schizosaccharomyces pombe. In EMBO Rep,pp. 1048-1053.

Segurado, M., Gomez, M., and Antequera, F. (2002). Increased recombination intermediates and homologous integration hot spots at DNA replication origins. Mol Cell *10*, 907-916.

Shinomiya, T., and Ina, S. (1991). Analysis of chromosomal replicons in early embryos of Drosophila melanogaster by two-dimensional gel electrophoresis. Nucleic Acids Res *19*, 3935-3941.

Sibani, S., Price, G. B., and Zannis-Hadjopoulos, M. (2005). Decreased origin usage and initiation of DNA replication in haploinsufficient HCT116 Ku80+/- cells. J Cell Sci *118*, 3247-3261.

Sibani, S., Price, G. B., and Zannis-Hadjopoulos, M. (2005). Ku80 Binds to Human Replication Origins Prior to the Assembly of the ORC Complex. Biochemistry *44*, 7885-7896.

Sivakumar, S., Porter-Goff, M., Patel, P. K., Benoit, K., and Rhind, N. (2004). In vivo labeling of fission yeast DNA with thymidine and thymidine analogs. Methods *33*, 213-219.

Smith, L. D., and Ecker, R. E. (1971). The interaction of steroids with Rana pipiens Oocytes in the induction of maturation. Dev Biol *25*, 232-247.

Spradling, A. C. (1981). The organization and amplification of two chromosomal domains containing Drosophila chorion genes. Cell *27*, 193-201.

Stefanovic, D., Stanojcic, S., Vindigni, A., Ochem, A., and Falaschi, A. (2003). In vitro protein-DNA interactions at the human lamin B2 replication origin. J Biol Chem *278*, 42737-42743.

Stern, B., and Nurse, P. (1996). A quantitative model for the cdc2 control of S phase and mitosis in fission yeast. Trends Genet *12*, 345-350.

Stern, B., and Nurse, P. (1997). Fission yeast pheromone blocks S-phase by inhibiting the G1 cyclin B-p34cdc2 kinase. Embo J *16*, 534-544.

Stern, B., and Nurse, P. (1998). Cyclin B proteolysis and the cyclin-dependent kinase inhibitor rum1p are required for pheromone-induced G1 arrest in fission yeast. Mol Biol Cell *9*, 1309-1321.

Stillman, B. (2005). Origin recognition and the chromosome cycle. FEBS Lett *579*, 877-884.

Stinchcomb, D. T., Struhl, K., and Davis, R. W. (1979). Isolation and characterisation of a yeast chromosomal replicator. Nature *282*, 39-43.

Su, T. T., and O'Farrell, P. H. (1997). Chromosome association of minichromosome maintenance proteins in Drosophila mitotic cycles. J Cell Biol *139*, 13-21.

Sugimoto, N., Tatsumi, Y., Tsurumi, T., Matsukage, A., Kiyono, T., Nishitani, H., and Fujita, M. (2004). Cdt1 phosphorylation by cyclin A-dependent kinases negatively regulates its function without affecting geminin binding. J Biol Chem *279*, 19691-19697.

Sun, W. H., Coleman, T. R., and DePamphilis, M. L. (2002). Cell cycle-dependent regulation of the association between origin recognition proteins and somatic cell chromatin. Embo J *21*, 1437-1446.

Sunkara, P. S., Wright, D. A., and Rao, P. N. (1979). Mitotic factors from mammalian cells: a preliminary characterization. J Supramol Struct *11*, 189-195.

Sveiczer, A., Csikasz-Nagy, A., Gyorffy, B., Tyson, J. J., and Novak, B. (2000). Modeling the fission yeast cell cycle: quantized cycle times in wee1- cdc25Delta mutant cells. Proc Natl Acad Sci U S A *97*, 7865-7870.

Sveiczer, A., Tyson, J. J., and Novak, B. (2004). Modelling the fission yeast cell cycle. Brief Funct Genomic Proteomic *2*, 298-307.

Szostak, J. W., Orr-Weaver, T. L., Rothstein, R. J., and Stahl, F. W. (1983). The double-strand-break repair model for recombination. Cell *33*, 25-35.

Tada, S., Li, A., Maiorano, D., Mechali, M., and Blow, J. J. (2001). Repression of origin assembly in metaphase depends on inhibition of RLF-B/Cdt1 by geminin. Nat Cell Biol *3*, 107-113.

Takahashi, T., and Masukata, H. (2001). Interaction of fission yeast ORC with essential adenine/thymine stretches in replication origins. Genes Cells *6*, 837-849.

Takahashi, T., Ohara, E., Nishitani, H., and Masukata, H. (2003). Multiple ORC-binding sites are required for efficient MCM loading and origin firing in fission yeast. Embo J *22*, 964-974.

Takayama, Y., Kamimura, Y., Okawa, M., Muramatsu, S., Sugino, A., and Araki, H. (2003). GINS, a novel multiprotein complex required for chromosomal DNA replication in budding yeast. Genes Dev *17*, 1153-1165.

Takeda, D. Y., and Dutta, A. (2005). DNA replication and progression through S phase. Oncogene *24*, 2827-2843.

Takeda, T., Ogino, K., Matsui, E., Cho, M. K., Kumagai, H., Miyake, T., Arai, K., and Masai, H. (1999). A fission yeast gene, him1(+)/dfp1(+), encoding a regulatory subunit for Hsk1 kinase, plays essential roles in S-phase initiation as well as in S-phase checkpoint control and recovery from DNA damage. Mol Cell Biol *19*, 5535-5547.

Takeda, T., Ogino, K., Tatebayashi, K., Ikeda, H., Arai, K., and Masai, H. (2001). Regulation of initiation of S phase, replication checkpoint signaling, and maintenance of mitotic chromosome structures during S phase by Hsk1 kinase in the fission yeast. Mol Biol Cell *12*, 1257-1274.

Tanaka, S., and Diffley, J. F. (2002). Interdependent nuclear accumulation of budding yeast Cdt1 and Mcm2-7 during G1 phase. Nat Cell Biol *4*, 198-207.

Tanaka, T., Knapp, D., and Nasmyth, K. (1997). Loading of an Mcm protein onto DNA replication origins is regulated by Cdc6p and CDKs. Cell *90*, 649-660.

Tercero, J. A., Labib, K., and Diffley, J. F. (2000). DNA synthesis at individual replication forks requires the essential initiation factor Cdc45p. Embo J *19*, 2082-2093.

Todorovic, V., Falaschi, A., and Giacca, M. (1999). Replication origins of mammalian chromosomes: the happy few. Front Biosci *4*, D859-868.

Tonami, Y., Murakami, H., Shirahige, K., and Nakanishi, M. (2005). A checkpoint control linking meiotic S phase and recombination initiation in fission yeast. Proc Natl Acad Sci U S A *102*, 5797-5801.

Touchon, M., Nicolay, S., Audit, B., Brodie Of Brodie, E. B., d'Aubenton-Carafa, Y., Arneodo, A., and Thermes, C. (2005). Replication-associated strand asymmetries in mammalian genomes: Toward detection of replication origins. Proc Natl Acad Sci U S A *102*, 9836-9841.

Tower, J. (2004). Developmental gene amplification and origin regulation. Annu Rev Genet *38*, 273-304.

Uchiyama, M., Arai, K., and Masai, H. (2001). Sna41goa1, a novel mutation causing G1/S arrest in fission yeast, is defective in a CDC45 homolog and interacts genetically with polalpha. Mol Genet Genomics *265*, 1039-1049.

Vas, A., Mok, W., and Leatherwood, J. (2001). Control of DNA rereplication via Cdc2 phosphorylation sites in the origin recognition complex. Mol Cell Biol *21*, 5767-5777.

Vashee, S., Cvetic, C., Lu, W., Simancek, P., Kelly, T. J., and Walter, J. C. (2003). Sequence-independent DNA binding and replication initiation by the human origin recognition complex. Genes Dev *17*, 1894-1908.

Vaughn, J. P., Dijkwel, P. A., and Hamlin, J. L. (1990). Replication initiates in a broad zone in the amplified CHO dihydrofolate reductase domain. Cell *61*, 1075-1087.

Vogelauer, M., Rubbi, L., Lucas, I., Brewer, B. J., and Grunstein, M. (2002). Histone acetylation regulates the time of replication origin firing. Mol Cell *10*, 1223-1233.

Wall, J. D., Frisse, L. A., Hudson, R. R., and Di Rienzo, A. (2003). Comparative linkage-disequilibrium analysis of the beta-globin hotspot in primates. Am J Hum Genet *73*, 1330-1340.

Walworth, N., Davey, S., and Beach, D. (1993). Fission yeast chk1 protein kinase links the rad checkpoint pathway to cdc2. Nature *363*, 368-371.

Weinreich, M., Palacios DeBeer, M. A., and Fox, C. A. (2004). The activities of eukaryotic replication origins in chromatin. Biochim Biophys Acta *1677*, 142-157.

Weinreich, M., and Stillman, B. (1999). Cdc7p-Dbf4p kinase binds to chromatin during S phase and is regulated by both the APC and the RAD53 checkpoint pathway. Embo J *18*, 5334-5346.

White, E. J., Emanuelsson, O., Scalzo, D., Royce, T., Kosak, S., Oakeley, E. J., Weissman, S., Gerstein, M., Groudine, M., Snyder, M., and Schubeler, D. (2004). DNA replication-timing analysis of human chromosome 22 at high resolution and different developmental states. Proc Natl Acad Sci U S A *101*, 17771-17776.

Whittaker, A. J., Royzman, I., and Orr-Weaver, T. L. (2000). Drosophila double parked: a conserved, essential replication protein that colocalizes with the origin recognition complex and links DNA replication with mitosis and the down-regulation of S phase transcripts. Genes Dev *14*, 1765-1776.

Williamson, D. H., Johnston, L. H., Fennell, D. J., and Simchen, G. (1983). The timing of the S phase and other nuclear events in yeast meiosis. Exp Cell Res *145*, 209-217.

Wilmes, G. M., and Bell, S. P. (2002). The B2 element of the Saccharomyces cerevisiae ARS1 origin of replication requires specific sequences to facilitate pre-RC formation. Proc Natl Acad Sci U S A *99*, 101-106.

Wohlgemuth, J. G., Bulboaca, G. H., Moghadam, M., Caddle, M. S., and Calos, M. P. (1994). Physical mapping of origins of replication in the fission yeast Schizosaccharomyces pombe. Mol Biol Cell *5*, 839-849.

Wohlschlegel, J. A., Dhar, S. K., Prokhorova, T. A., Dutta, A., and Walter, J. C. (2002). Xenopus Mcm10 binds to origins of DNA replication after Mcm2-7 and stimulates origin binding of Cdc45. Mol Cell *9*, 233-240.

Wood, V., Gwilliam, R., Rajandream, M. A., Lyne, M., Lyne, R., Stewart, A., Sgouros, J., Peat, N., Hayles, J., Baker, S., *et al.* (2002). The genome sequence of Schizosaccharomyces pombe. Nature *415*, 871-880.

Woodfine, K., Beare, D. M., Ichimura, K., Debernardi, S., Mungall, A. J., Fiegler, H., Collins, V. P., Carter, N. P., and Dunham, I. (2005). Replication timing of human chromosome 6. Cell Cycle *4*, 172-176.

Woodfine, K., Fiegler, H., Beare, D. M., Collins, J. E., McCann, O. T., Young, B. D., Debernardi, S., Mott, R., Dunham, I., and Carter, N. P. (2004). Replication timing of the human genome. Hum Mol Genet *13*, 191-202.

Wright, A. P., Maundrell, K., and Shall, S. (1986). Transformation of Schizosaccharomyces pombe by non-homologous, unstable integration of plasmids in the genome. Curr Genet *10*, 503-508.

Wu, J. R., and Gilbert, D. M. (1995). Rapid DNA preparation for 2D gel analysis of replication intermediates. Nucleic Acids Res *23*, 3997-3998.

Wu, J. R., and Gilbert, D. M. (1996). A distinct G1 step required to specify the Chinese hamster DHFR replication origin. Science *271*, 1270-1272.

Wu, J. R., and Gilbert, D. M. (1997). The replication origin decision point is a mitogen-independent, 2-aminopurine-sensitive, G1-phase event that precedes restriction point control. Mol Cell Biol *17*, 4312-4321.

Wu, J. R., Keezer, S. M., and Gilbert, D. M. (1998). Transformation abrogates an early G1-phase arrest point required for specification of the Chinese hamster DHFR replication origin. Embo J *17*, 1810-1818.

Wuarin, J., Buck, V., Nurse, P., and Millar, J. B. (2002). Stable association of mitotic cyclin B/Cdc2 to replication origins prevents endoreduplication. Cell *111*, 419-431.

Wyrick, J. J., Aparicio, J. G., Chen, T., Barnett, J. D., Jennings, E. G., Young, R. A., Bell, S. P., and Aparicio, O. M. (2001). Genome-wide distribution of ORC and MCM proteins in S. cerevisiae: high-resolution mapping of replication origins. Science *294*, 2357-2360.

Yabuki, N., Terashima, H., and Kitada, K. (2002). Mapping of early firing origins on a replication profile of budding yeast. Genes Cells *7*, 781-789.

Yamada, Y., Nakagawa, T., and Masukata, H. (2004). A novel intermediate in initiation complex assembly for fission yeast DNA replication. Mol Biol Cell *15*, 3740-3750.

Yamaguchi, S., Murakami, H., and Okayama, H. (1997). A WD repeat protein controls the cell cycle and differentiation by negatively regulating Cdc2/B-type cyclin complexes. Mol Biol Cell *8*, 2475-2486.

Yamamoto, M., Iami, Y., and Watanabe, Y. (1997). The Molecular and Cellular Biology of the Yeast Saccharomyces (pringle, J.R., Broach, J.R. and Jones, E.W., eds). Cold Spring Harbor Laboratory, Cold Spring Harbor, New York, 1035 - 1106.

Yamano, H., Kominami, K., Harrison, C., Kitamura, K., Katayama, S., Dhut, S., Hunt, T., and Toda, T. (2004). Requirement of the SCFPop1/Pop2 Ubiquitin Ligase for Degradation of the Fission Yeast S Phase Cyclin Cig2. J Biol Chem *279*, 18974-18980.

Yamashita, M., Hori, Y., Shinomiya, T., Obuse, C., Tsurimoto, T., Yoshikawa, H., and Shirahige, K. (1997). The efficiency and timing of initiation of replication of multiple replicons of Saccharomyces cerevisiae chromosome VI. Genes Cells *2*, 655-665.

Yang, X., Gregan, J., Lindner, K., Young, H., and Kearsey, S. E. (2005). Nuclear distribution and chromatin association of DNA polymerase alpha-primase is affected by TEV protease cleavage of Cdc23 (Mcm10) in fission yeast. BMC Mol Biol *6*, 13.

Yanow, S. K., Lygerou, Z., and Nurse, P. (2001). Expression of Cdc18/Cdc6 and Cdt1 during G2 phase induces initiation of DNA replication. Embo J *20*, 4648-4656.

Yasuda, S., and Hirota, Y. (1977). Cloning and mapping of the replication origin of Escherichia coli. Proc Natl Acad Sci U S A *74*, 5458-5462.

Yompakdee, C., and Huberman, J. A. (2004). Enforcement of late replication origin firing by clusters of short G-rich DNA sequences. J Biol Chem *279*, 42337-42344.

You, Z., Ishimi, Y., Mizuno, T., Sugasawa, K., Hanaoka, F., and Masai, H. (2003). Thymine-rich single-stranded DNA activates Mcm4/6/7 helicase on Y-fork and bubble-like substrates. Embo J *22*, 6148-6160.

You, Z., Komamura, Y., and Ishimi, Y. (1999). Biochemical analysis of the intrinsic Mcm4-Mcm6-mcm7 DNA helicase activity. Mol Cell Biol *19*, 8003-8015.

Young, J. A., Schreckhise, R. W., Steiner, W. W., and Smith, G. R. (2002). Meiotic recombination remote from prominent DNA break sites in S. pombe. Mol Cell *9*, 253-263.

Young, M. R., and Tye, B. K. (1997). Mcm2 and Mcm3 are constitutive nuclear proteins that exhibit distinct isoforms and bind chromatin during specific cell cycle stages of Saccharomyces cerevisiae. Mol Biol Cell *8*, 1587-1601.

Zeng, Y., Forbes, K. C., Wu, Z., Moreno, S., Piwnica-Worms, H., and Enoch, T. (1998). Replication checkpoint requires phosphorylation of the phosphatase Cdc25 by Cds1 or Chk1. Nature *395*, 507-510.

Zhang, Y., Yu, Z., Fu, X., and Liang, C. (2002). Noc3p, a bHLH protein, plays an integral role in the initiation of DNA replication in budding yeast. Cell *109*, 849-860.

Zhu, W., Chen, Y., and Dutta, A. (2004). Rereplication by depletion of geminin is seen regardless of p53 status and activates a G2/M checkpoint. Mol Cell Biol *24*, 7140-7150.

Zou, L., and Stillman, B. (1998). Formation of a preinitiation complex by S-phase cyclin CDK-dependent loading of Cdc45p onto chromatin. Science *280*, 593-596.

Zou, L., and Stillman, B. (2000). Assembly of a complex containing Cdc45p, replication protein A, and Mcm2p at replication origins controlled by S-phase cyclin-dependent kinases and Cdc7p-Dbf4p kinase. Mol Cell Biol *20*, 3086-3096.